New insights into the role of oxidized histone H3 in heterochromatin

Gemma Serra Bardenys

DOCTORAL THESIS / 2019

Thesis supervisor:

Dra. Sandra Peiró Sales

Department of Experimental and Health Sciences

UNIVERSITAT POMPEU FABRA

A la mare, el pare i l'Anna

“Que tot està per fer i tot és possible”

Miquel Martí I Pol

Abstract

Oxidation of histone H3 (H3K4ox) by lysyl oxidase-like 2 (LOXL2) is important in triple-negative breast cancer (TNBC) cells to generate compacted heterochromatin regions. However, the molecular mechanisms by which it establishes chromatin compaction have not yet been characterized. In this thesis, we found that LOXL2 interacts with RUVBL1, RUVBL2, BAF53A, and DMAP1, which are proteins that form complexes involved in the exchange of the histone variant H2A.Z. Genome-wide experiments showed that H2A.Z, RUVBL2, and H3K4ox colocalize in heterochromatin regions in TNBC cells. Moreover, we demonstrated that oxidation of histone H3 is linked to DDB1 recruitment to chromatin and the ubiquitination of H2A through RBX1. Interestingly, the interplay between these series of events is required to maintain H3K4ox-enriched heterochromatin regions. Loss of H3K4ox decreases the levels of H3K9me3 and alters chromatin compaction, thereby compromising the oncogenic properties of TNBC cells. Our data revealed a direct link between H3K4ox maintenance, chromatin compaction, and tumorigenic capacities and suggest novel potential targets for cancer therapy.

Resum

L'oxidació de la histona H3 (H3K4ox) per la lisil-oxidasa 2 (LOXL2) és important en les cèl·lules de càncer de mama triple-negatives (TNBC) per generar regions d'heterocromatina compactades. Tot i així, els mecanismes moleculars mitjançant els quals s'estableix la compactació de la cromatina encara no han estat caracteritzats. En aquesta tesi, hem demostrat que la LOXL2 interacciona amb RUVBL1, RUVBL2, BAF53A i DMAP1, proteïnes que formen complexes implicats en l'intercanvi de la variant d'histona H2A.Z. Experiments de seqüenciació del genoma van demostrar que l'H2A.Z, el RUVBL2 i la H3K4ox co-localitzen a les regions d'heterocromatina a les cèl·lules TNBC. A més, hem trobat que l'oxidació de la histona H3 està associada amb el al reclutament de DDB1 a la cromatina i a la ubiqüitinació de l'H2A a través de RBX1. Curiosament, la interacció entre aquesta sèrie d'esdeveniments és necessària per mantenir les regions heterocromatina enriquides amb H3K4ox. La pèrdua d'H3K4ox disminueix els nivells de H3K9me3 i altera la compactació de la cromatina, tot comprometent les propietats oncogèniques de les cèl·lules TNBC. Les nostres dades revelen una relació directa entre el manteniment de l'H3K4ox, la compactació de la cromatina i les capacitats tumorigèniques, així com suggereixen noves dianes potencials per a la teràpia contra el càncer.

Table of contents

Figure index

Introduction

Results

Discussion

Concluding remarks

Annex

Table index

Introduction

Materials and methods

Annex

Abbreviations

3C: chromosome conformation capture

3D: three-dimensional

53BP1: p53-binding protein 1

ACTL6A: actin like 6a

AEBP2: adipocyte enhancer-binding protein 2

ANP32E: acidic nuclear phosphoprotein 32 family member E

ATAC: assay for transposase-accessible chromatin

ATM: ataxia telangiectasia mutated

ATP: adenosine triphosphate

BAF53: BAF Complex 53 KDa Subunit

bp: DNA base pairs

BRCA1: breast cancer gene 1

BSA: bovine serum albumin

BTP: bromothenylpteridine

CAF-1: chromatin assembly factor 1

CDH1: E-cadherin gene

CDW: CUL4–DDB1-associated WDR (WD40 repeat domain) proteins

CHAF1B: chromatin assembly factor 1 Subunit B

cHC: constitutive heterochromatin

ChIP-Seq: ChIP sequencing

ChIP: Chromatin Immunoprecipitation

CRL4s: CUL4-RING E3 ubiquitin ligases

CRLs: cullin-ring ligases

CSC: cancer stem cell

CT: control

CTCF: CCCTC-binding factor

CUL: cullin

DAPI: 4',6-diamidino-2-phenylindole

DAXX: death domain associated protein

DBRs: differentially bound regions

DCAF: DDB1–CUL4-associated factors

DDB1/2: damage specific DNA binding protein 1/2

DDR: DNA damage response

DMAP1: DNA methyltransferase 1 associated protein 1

DNA: deoxyribonucleic acid

DNMT: DNA methyltransferase

DSB: DNA double-strand Breaks

DTBP: dimethyl 3,3'-dithiobispropionimidate

DTT: dithiothreitol

DUB: de-ubiquitin enzymes

DWD: DDB1-binding WD40

EDTA: ethylenediaminetetraacetic acid

EED: embryonic ectoderm development

EMT: epithelial-to-mesenchymal transition

ER: estrogen receptor

EZH1/2: enhancer of zeste homolog 1/2

FBS: fetal bovine serum

fHC: facultative heterochromatin

GEO: gene expression omnibus

GFP: green fluorescent protein

GO: gene ontology

H3K4ox: oxidized histone H3

HAT: Histone acetyltransferase

HDAC: histone deacetylase

HECT: homologous to E6-AP carboxy terminus

HER-2: human epidermal growth factor receptor 2

Hi-C: high-throughput sequencing of chromosome conformation capture

HIRA: histone cell cycle regulator

HMGN2: High mobility group nucleosomal binding domain 2

HMT: histone methyltransferase

HP1: heterochromatin protein 1

HPRT: hypoxanthine

hr: hour

HTM: high-throughput microscopy

IgG: immunoglobulin

IL-33: interleukin 33

IP: immunoprecipitation

JARID2: jumonji and AT-rich interaction domain containing 2

KD: knockdown

LADs: lamina-associated domains

LC-MS/MS: liquid chromatography-tandem mass spectrometry

lock: large organized chromatin k9-modifications

LOX: lysyl oxidase

LOXL1-4: lysyl oxidase-like 1-4

LSD1: lysine-specific histone demethylase 1

LTQ: lysyl tyrosylquinone

MBT: malignant brain tumor

MET: mesenchymal-to-epithelial transition

min: minutes

MLL3: histone-lysine N-methyltransferase 2C

MMR: mismatch repair

MNase: micrococcal nuclease

mRNA: messenger ribonucleic acid

MS: mass spectrometry

MTT: 3-(4,5-Dimethylthiazol-2-yl)-2,5-diphenyltetrazolium bromidefor

ncRNA: non-coding RNA

p53: tumor protein p53

PARP: poly (ADP-ribose) polymerase

PBS: *phosphate buffered* saline

PcG: polycomb group

PCR: polymerase chain reaction

PDX: patient-derived Xenograft

PEI: polyethylenimine polymer

PFA: *paraformaldehyde*

PHF1: PHD finger protein 1

PMSF: phenylmethylsulfonyl fluoride

PR: progesterone receptor

PRC1/2: polycomb repressive complex 1/2

PRMT: protein arginine methyltransferases

PTM: post-translational modification

qRT-PCR: real-time polymerase chain reaction

RbAp46/RBBP7: retinoblastoma-binding protein p46/7

RbAp48/RBBP4: retinoblastoma-binding protein p46/4

RBX1 (or ROC1): RING-box protein 1

RCC1: regulator of chromosome condensation 1

RING: really interesting new gene

RNA: ribonucleic acid

RNAPII: RNA polymerase II

RNF: RING Finger Protein 8

RUVBL1/2: RuvB-Like AAA ATPase 1/2

SAGA: Spt-Ada-Gcn5-Acetyl transferase

SD: standard deviation

SDS-PAGE: sodium dodecyl sulfate polyacrylamide gel electrophoresis

SET7/9: SET domain containing lysine methyltransferase 7

shRNA: short hairpin RNA

SMA: smooth muscle actin

SNAIL1: zinc finger protein SNAI1 (Snail family transcriptional repressor 1)

SRCAP: Snf-2 related CREB-binding protein activator protein

SRCR: scavenger receptor cysteine-rich

STAT3: signal transducer and activator of transcription 3

SUV39H1/2: suppressor of variegation 3-9 Homolog 1/2

SUZ12: suppressor of zeste 12

SWR1: Swi2/Snf2-related ATPase homolog (*S. Cerevisiae*)

TAD: topologically associated domain

TAF10: TATA-box binding protein associated factor 10

TAP: tandem affinity purification

TBS-T: tris buffer saline-tween

TBS: tris buffer saline

TGF-β: transforming growth factor beta

TGS: tris-glycine-SDS

TIP60: histone acetyltransferase KAT5

TMR: tetramethylrhodamine

TNBC: triple-negative breast cancer

TRIM37: tripartite motif containing 37

TSS: transcription start site

TWIST: twist family BHLH transcription homeobox

WDR: WD40 repeat domain

WT: wild type

ZEB: zinc finger E-Box binding homeobox

INTRODUCTION

1. Chromatin structure and organization

1.1. Nucleosomes as chromatin unit

Eukaryotic cells have around two meters of DNA that must be packaged into a small nucleus. However, within this context, selective and coordinated accessibility has to be maintained to regulate fundamental processes such as transcription, DNA replication, and repair. To achieve this, DNA is highly condensed in a dynamic nucleoprotein complex termed chromatin, which has several levels of organization.

The basic unit of chromatin is the **nucleosome**, which consists of 147 base pairs of DNA wrapped around an octamer of histone proteins. This histone core comprises two copies of each of H2A, H2B, H3, and H4, forming one $(H3/H4)_2$ tetramer and two H2A-H2B histone dimers[1-3] (Figure I1).

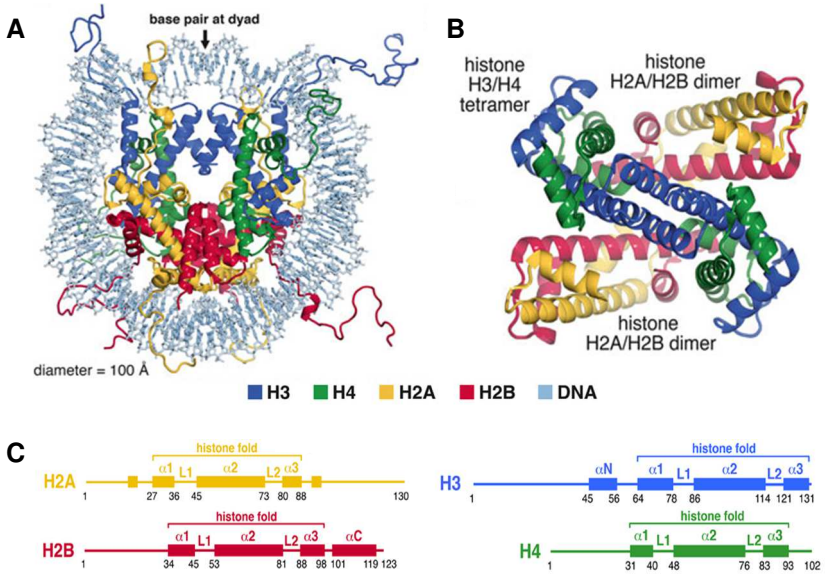

Figure I1. Nucleosome core particle structure and the histone-fold heterodimers. A) Nucleosome core particle structure. Histones and DNA are depicted in cartoon and sticks representations, respectively, and colored as shown in legend. **B)** The histone-fold octamer in cartoon representation from an orthogonal profile view. **C)** Schemes of core histones with secondary structure elements indicated. Adapted from[3,4].

Histones are small proteins formed by a central α-helical region flanked by extensions referred as “tails” that protrude away from the nucleosome core. These “tails” can have post-translational modifications (PTM) and can adopt flexible structures that bind to intranucleosomal DNA, neighboring nucleosomes, and/or nuclear factors.

One striking feature of nucleosomes is the presence of a special cavity known as the “**acidic patch**”. It is located on both sides of the nucleosome surface and is formed by eight acidic residues, six from H2A (E56, E61, E64, D90, E91, and E92) and two from H2B (E102 and E110)[3,5]. This region, in contrast to the overall positive charge of histones, has the unique feature of being negatively charged (Figure I2). It interacts with the H4 tail of the neighboring nucleosomes to regulate internucleosome interactions and is important for the binding of numerous chromatin factors, such as RCC1, Sir3, IL-33, HMGN2, PRC1, the SAGA complex, and Set8 methyltransferase[5].

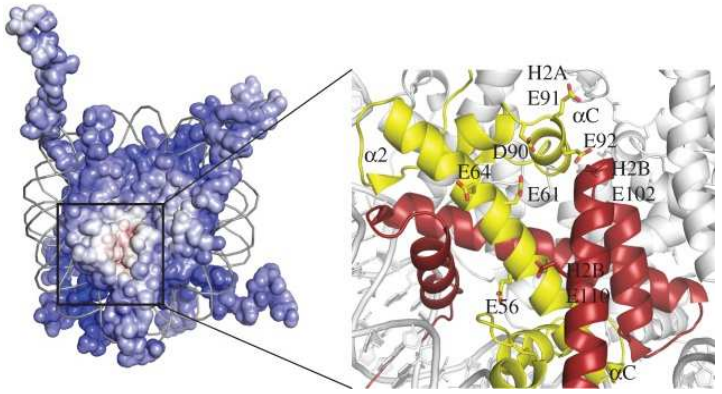

Figure I2. The nucleosome and its acidic patch. Electrostatic potential view of the nucleosome surface (left) and close-up view of the acidic patch (right). Histone H2A is shown in yellow (α2- and αC-helices) and H2B, in red (α1- and αC-helices). The eight residues that make up the acidic patch are labelled[5].

Another member of the nucleosome subunit is the **linker histone H1 or H5** (in avian), which binds to the entry or exit sites of the DNA on the surface of the nucleosome core particle. Linker histones are structurally

and functionally distinct from the four core histones, and at least 11 different subtypes have been described in mammals[6-8]. They are broadly distributed across the genome and have several functions, including influencing nucleosome spacing on DNA, regulating specific gene expression[9], and stabilizing DNA wrapped around the nucleosome and higher-order chromatin structures[10].

Nucleosomes are repeating building blocks of chromatin connected by **"linker" DNA**, which ranges in length from 20 to 90 bp and varies among different species and tissues[11]. These unfolded nucleosomal arrays form a primary chromatin structure of 10 nm diameter that was originally described as "**beads on a string**"[12]. However, it is well known that this is not a uniform and regular structure as was first believed; instead, many different variations can occur in the composition of nucleosomes (see Section 2).

1.2. Chromatin assembly and genome organization

Classically, it was thought that this 10 nm fiber of chromatin first folds into a 30 nm fiber and then sequentially into higher-order stages of condensation following a hierarchical model. However, new microscopy approaches and genome-wide chromosome conformation capture (3C)-related studies have questioned this organization. Alternative models that involve a less-ordered three-dimensional (3D) organization of chromatin have been proposed[13,14].

Although the 30 nm fiber has been extensively studied *in vitro*, evidences of its existence *in vivo* are limited. Several studies demonstrate that this structure probably is not formed in most mammalian cells, and that it can only be found in particular biological contexts with heterochromatic transcriptional repression and compaction[14-16].

Alternatively, the "**polymer melt**" model has been proposed to explain chromatin organization inside the nucleus of mammalian cells, where nucleosomes are highly concentrated and irregularly spaced. In this model, chromatin is described as a highly disordered state with dynamic

movement in which fibers interdigitate with one another and are irregularly folded.

In this context, frequent looping interactions between regions that are not linear neighbors can take place, thus generating series of chromatin globules. These structures can in turn associate with each other in highly compacted states that ultimately form different **chromosomes**[14,17]. Chromosomes are thread-like structures with two chromatids located as an X shape that can only be observed in the cell nucleus during cell division. During interphase, they are decondensed and distributed over chromosome territories[18] where each chromosome occupies its own distinct region in the nucleus.

In the recent years, the development of the 3C technique and its high-throughput modifications, which include the 4C, 5C, and Hi-C methods, have shown that genomes can be distinguished between two major **compartments**, termed A and B, mainly depending on the activity of the genomic regions. While the A compartment is generally gene-rich, transcriptionally active, and accessible, the B compartment represents a more repressed environment with fewer genes[19].

At the same time, inside chromosomal compartments, chromatin is organized in megabase-sized domains that display high internal contact frequencies called "**topological associated domains**" or **TADs**. These domains are structural and functional entities that correlate with coordinated gene expression, histone modifications, or DNA replication timing, and their boundaries are enriched for insulator proteins such as CTCF, active transcription marks, and repetitive elements[20].

Interestingly, although TADs are conserved between different cell types and even species, they are organized into **sub-TADs** domains or chromatin loops that undergo more dynamic changes in cell-type specific rearrangements[21]. Interactions between these TADs as well as the strength of TAD borders are tightly regulated by architectural proteins such as CTCF. Hence, genome architecture and the dynamic folding of chromatin is crucial for regulating gene expression and can impact many biological functions; indeed, alterations in these folding units are associated with multiple diseases and cancer[22,23].

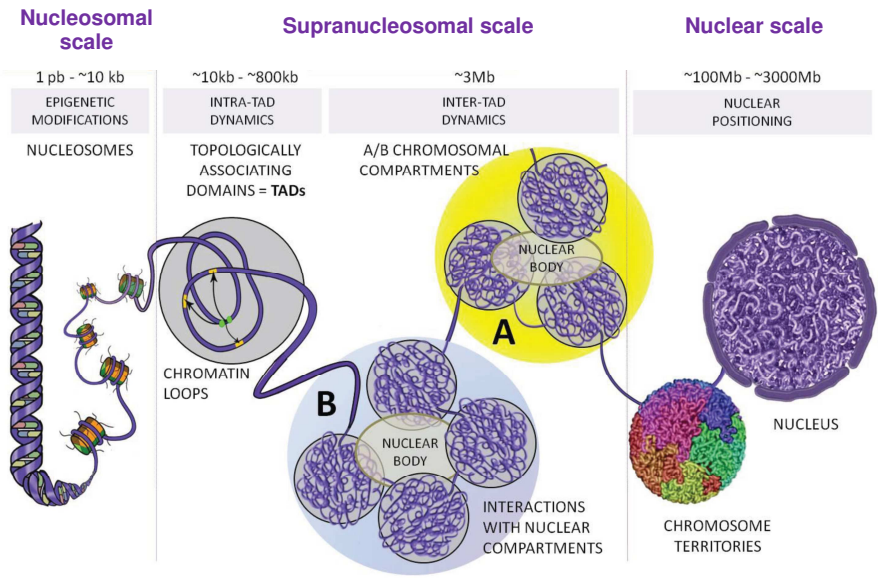

Figure I3. Genome organization in mammals. Schematic representation showing the different levels of organization including the nucleosome scale (chromatin fibers), the supranucleosome scale (chromatin loops, TADS, and A/B chromosome compartments) and the nuclear scale (chromosome territories). Adapted from [24].

In addition to the 3D organization, the radial **position** of genes **within the nucleus** can also affect transcription. Genomic regions that interact with the nuclear lamina form lamin-associated domains (LADs) that are characterized by low gene density and transcriptional repression[25]. In contrast, transcription inside the nucleus can be spatially organized in nuclear structures called "transcriptional factories"[26] or euchromatin-associated lamin B1 domains (eLADs)[23]. However, gene expression and nuclear positioning are not necessarily dependent on each other, as relocation of genes through the nucleus is not always sufficient for changing gene expression and also depends on chromatin condensation[27,28].

Finally, some recent studies show that it could also be the other way around: that is, the transcription machinery regulates genome organization. It is still unclear what is cause and what is consequence, but it seems that the spatial organization of the genome and transcription can indeed modulate each other[29].

2. Epigenetics

Epigenetics refers to the study of mitotically and meiotically heritable changes in gene function and expression that cannot be explained by changes in DNA sequence. In this way, although all cells in an organism contain the same genetic information, different gene expression patterns in different cell types can be achieved. In response to development or environment stimuli, epigenetic modifications lead to inheritable and non-inheritable changes in the chromatin state that affect gene expression and consequently determine cell lineage, function, and fate[30,31]. These mechanisms involve several chemically and structurally modifications of DNA and/or its associated proteins that do not alter the primary sequence of DNA.

First, histone proteins are key elements in epigenetic regulation. On the one hand, canonical histones of the nucleosome core have diversified into a range of **histone variants** with distinct properties that can be incorporated at a certain time and location. On the other hand, the amino acid chains of histones can be **post-translationally modified** in many different ways. Thus, considering that each nucleosome contains two copies of each histone, there is a huge amount of possible variations that can regulate their stability and dynamics, the recruitment of chromatin enzymes, and compaction into higher-order chromatin structures[13,32]. Given its relevance for this thesis, these epigenetic mechanisms are explained in more detail in a separate section (Sections 2.1 and 2.2).

Besides histones, **DNA** can be covalently modified by the addition of a **methyl group** to the fifth carbon of the cytosine residue (5-methyl-cytosine, 5mC). This mechanism is associated with epigenetic silencing and is fundamental for gene regulation and cell differentiation[33].

On the other hand, epigenetics also includes **structural alterations** mediated by chromatin remodeling complexes and architectural proteins that shift nucleosome conformation and affect inter and intrachromosomal interactions, thereby bringing linearly distant regions together[34,35].

Finally, **non-coding RNAs** (ncRNAs) create transcripts that are not translated into proteins and also participate in the epigenetic regulatory network by interacting with histone-modifying complexes or DNA methyltransferases[36].

2.1. Histone modifications

PTM of histones is a well-studied epigenetic mechanism that plays essential roles in regulating many fundamental biological processes. Since the field appeared, an increasing number of histone modifications have been described, including acetylation, methylation, phosphorylation, sumoylation, and ubiquitination[37]. These modifications can occur on many different residues in both the tails and the central globular domains of core histone proteins. Moreover, they can be of different forms depending on the residues; for instance, methylation can be found in a mono-, di-, or trimethyl state for lysines, and mono- or di- (asymmetric or symmetric) for arginines[38,39] (Figure I4).

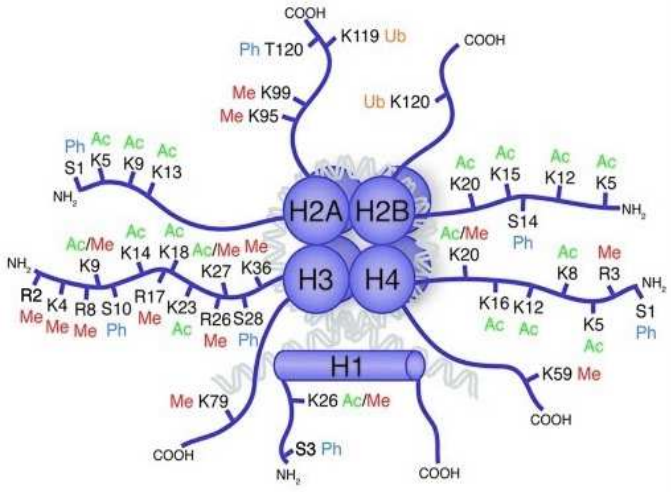

Figure I4. Histone PTMs in histone tails. Schematic representation of a nucleosome with the following PTMs on the N- and C-terminal histone tails: acetylation (Ac), methylation (Me), phosphorylation (Ph), and ubiquitination (Ub)[40].

Histone PTMs are widely distributed throughout the whole genome and operationally can modulate chromatin regulation by two mechanisms: direct structural perturbation or regulation of chromatin factor binding.

On the one hand, histone PTMs can influence the **overall chromatin structure** by affecting both their interactions with DNA or the adjacent nucleosomes as well as their binding to histone chaperones. Different modifications can have different consequences. For instance, acetylation and phosphorylation reduce the positive charge density of histone tails, thereby disrupting electrostatic interactions with DNA and promoting chromatin accessibility. In contrast, neutral modifications such as methylation do not alter charge and have less-direct effects. Other PTMs, such as ubiquitination, can add a large molecule to histones and induce a change in the overall conformation of the nucleosome[39,41].

Additionally, histone PTMs act as **docking sites for proteins** called "histone readers" (Figure I5). These proteins recognize modified histones through specific recognition domains, such as bromodomains and chromodomains, that bind to acetylated and methylated lysine residues, respectively[42-44]. Their recruitment to specific genomic regions can be modulated by non-coding RNA (ncRNA), binding partners, or conformational changes[42,45]. These readers, in turn, recruit other components of the nuclear signaling machinery that exert different effects on the chromatin structure and function[42].

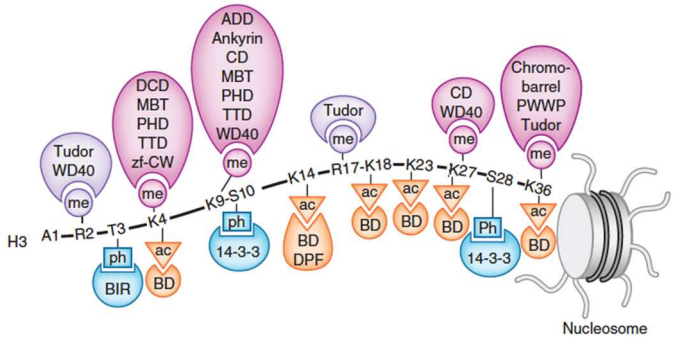

Figure I5. Readers of histone PTMs. PTMs of N-terminal H3 tail, including methylation (me), phosphorylation (ph), and acetylation (ac), are recognized by different domains of readers[45].

2.1.1. Histone modifying enzymes: readers, writers, and erasers

Regulation of PTMs is a highly dynamic process that involves different types of epigenetic regulators: readers, writers, and erasers (Figure I6). **Epigenetic writers** are proteins that modify amino acid residues on histone tails. Some examples are histone acetyltransferases (HATs), histone methyltransferases (HMTs), and protein arginine methyltransferases (PRMTs); **epigenetic readers** are proteins that specifically recognize these epigenetic marks; and **epigenetic erasers,** such as histone deacetylases (HDACs), lysine demethylases (KDMs), and phosphatases, remove histones modifications[39,46].

Interestingly, chromatin-associating complexes often contain multiple readers within one or several subunits and simultaneously recognize several PTMs; in this way, the overall binding is enhanced by multiple weak interactions, and it is possible to ensure a finely-tuned regulation. Moreover, positive and negative feedback loops between them can be established to reinforce or inhibit histone modifications, thus allowing the maintenance of robust chromatin states[42,47].

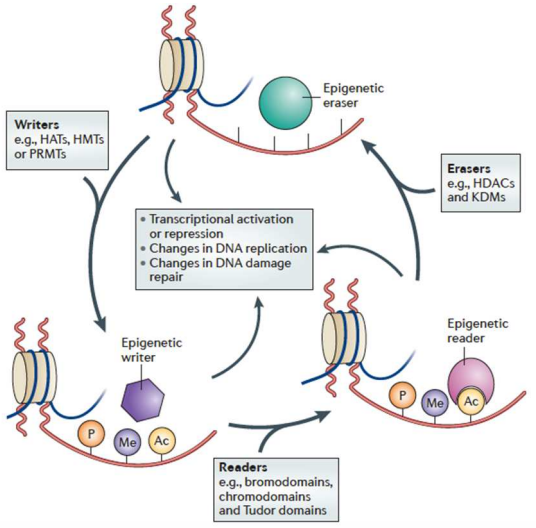

Figure I6. Epigenetic writers, readers and erasers. Epigenetic regulation is a dynamic process that involves readers, writers, and erasers (see text). In this way, histone modifications regulate various DNA-dependent processes, including transcription, DNA replication, and DNA repair[48].

2.1.2. Histone modification cross-talk

Histone modifications can positively or negatively affect other modifications either in *cis*, on the same histone molecule, or in *trans*, either between histone molecules or across nucleosomes.

This crosstalk can occur through different mechanisms. A modification can depend on another one or, in contrast, can be antagonistic, such as in situations where several modification pathways compete for the same site. Further, protein binding to a particular modification can be disrupted by an adjacent modification, while some modifications can cooperate to recruit specific factors[42,49].

Histone modifications can also cooperate with DNA methylation to promote or inhibit protein binding to histone modifications as well as to non-histone proteins[50].

2.2. Histone variants

The canonical histones of the nucleosome core can be replaced by histone variants that change their features and so confer new properties to chromatin. So far, several histone variants have been identified in humans: eight of H2A, six of H3, and two of H2B. While variants of histone H2A and H3 are ubiquitous, those of H2B are only expressed in testes. No histone variants of H4 have been identified yet (Figure I7).

Canonical histones are encoded by multiple genes mainly organized in clusters and deposited on DNA during replication, when new nucleosomes are formed[51]. In contrast, histone variants are only encoded by one or two genes located in different chromosomes and are mostly incorporated throughout the cell cycle[52], in a replication-independent manner. In this way, it is possible to control precisely the time and the location of each histone variant.

While canonical histone genes do not have introns, the histone variant ones undergo splicing, which allows alternative splice isoforms to exist. At the protein level, histone variants differ from their canonical equivalents in part by the amino acid sequences, but they can also be post-translationally modified.

Altogether, there is a wide diversity of histones that can form the nucleosomes[52,53].

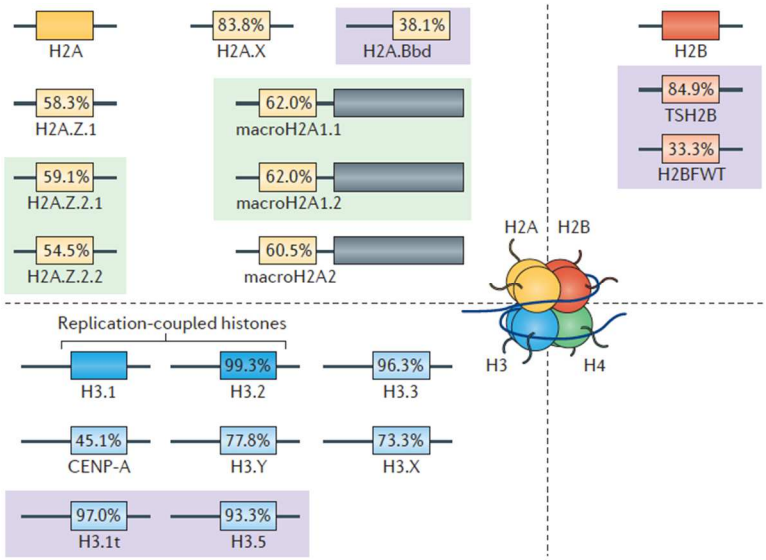

Figure I7. Variants of human core histones. Schematic representation of variants of histone H2A (yellow), H2B (orange), and H3 (blue); so far, no histone variants have been described for H4 (green). Rectangles represent core regions and lines flexible histone tails. Light purple boxes highlight testis-specific histone variants and light green boxes the alternative splice isoforms. Percentages of amino acid sequence conservation relative to their respective canonical histones are indicated. CENP-A, histone H3-like centromeric protein A; H2BFWT, histone H2B type wild-type; TSH2B, testis-specific histone H2B [52].

Incorporation of histone variants is regulated by histone chaperones that control nucleosome formation and stability[54] as well as some chromatin remodelers[35]. These last ones use ATP to slide or eject assembled nucleosomes and are able to exchange H2A–H2B dimers for histone variant dimers. The resulting nucleosomes containing histone variants can be homotypic, with two copies of the histone variant, or heterotypic, with one copy of the histone variant[53].

Similar to histone PTMs, histone variants exert their function in chromatin through different mechanisms, such as by influencing nucleosome structure or stability and thus chromatin organization, or by regulating the recruitment of interacting proteins, chromatin-modifying enzymes, or readers of post-translational modifications[52].

3. Chromatin classification into euchromatin and heterochromatin

Eukaryotic genomes can be partitioned into distinct functional and structural chromatin domains with different accessibility, patterns of histone modifications, nuclear organization, and chromatin-associated proteins.

In 1928, Heitz defined two major environments, called **heterochromatin** and **euchromatin** depending on the differential staining of chromatin at interphase[55]. Since then, this classification has been widely used, and many studies have better characterized the organization and function of these two genomic domains (Figure I8). However, we have to keep in mind that despite being the most common one, this classical division nonetheless is a simplistic view, and finer classifications of chromatin diversity can be done[56-59].

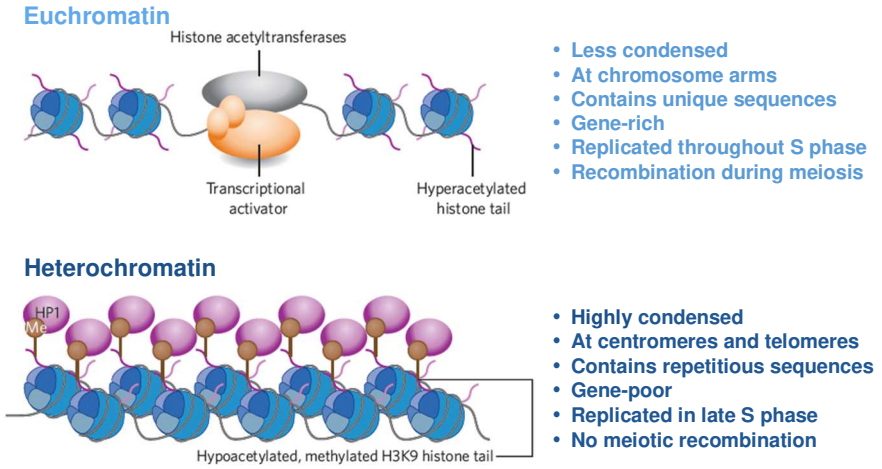

Figure I8. General properties of euchromatin and heterochromatin regions. Main characteristics of each type of chromatin are listed, although there are some exceptions in each case. Heterochromatin features listed are representative of pericentromeric heterochromatin. Adapted from [60]

3.1. Euchromatin

Euchromatin is typically slightly condensed, accessible, and enriched in active genes. It is generally located in chromosome arms, replicates throughout the S-phase, and undergoes recombination during meiosis[60,61].

Although its distribution is not homogeneous, euchromatin regions are enriched with certain histone modifications. Promoters of active genes[62,63] contain high levels of H3 and H4 acetylation as well as hypermethylation of H3 at K4 (H3K4me3). On the other hand, gene bodies are enriched in acetylation of H3 and H4[64], H2B ubiquitination (H2B120ub)[65], trimethylation of H3 at K79 (H3K79me3)[66], and in K36 (H3K36me3), which peak toward the 3′ end of the gene[67]. Finally, acetylation of H3 at K27 (H3K27ac) and monomethylation of H3 at K4 (H3K4me1) are the predominant histone modifications in the nucleosomes around enhancer elements[68,69].

3.2. Heterochromatin

In contrast to euchromatin, heterochromatin is highly condensed, inaccessible, contain mostly inactive genes, and is replicated in late S-phase. It can be further categorized into two classes, **constitutive** and **facultative** heterochromatin[61,70].

Contrary to what it was initially thought, there is now strong evidence that heterochromatin has important functions. It plays a structural role flanking the chromosome centromeres and is required for sister chromatid cohesion and correct assembly of kinetochores[71,72]. Further, it is important to keep unexpressed genes and repetitive sequences in a silent state, thereby preventing them from self-duplication or recombination that produce genome instability[61,73,74].

Although it might seem contradictory, heterochromatin regions can also be transcribed, and this is in fact important for its formation in several organisms. However, transcription levels in these regions are low, and the resulting transcripts are not protein-coding genes[60,75], but rather ncRNAs important for the recruitment of silencing factors[73,76].

In fission yeast, ncRNAs mediate their effect through RNA interference (RNAi) processes in which small RNA molecules reduce the activity of specific regions of DNA[73,76,77]. However, in mammals, very little evidence exists for RNAi in heterochromatin establishment, and other mechanisms may play a more important role. For instance, ncRNAs regulate the localization of HP1α at pericentromeric heterochromatin[78] as well as heterochromatin formation by recruiting SUV39H1 to stay attached for longer periods of time[79,80].

3.2.1. Facultative heterochromatin (fHC)

Facultative heterochromatin can be defined as transcriptionally silent chromatin regions that retains the potential to decondense and allow transcription in certain spatial and temporal contexts, such as developmental states, specific cell cycle stages, or nuclear localization changes.[61,81]

fHC formation and distinctive molecular signatures

fHC is formed through a combination of many different mechanisms. It can be regulated by the recruitment of histone modifying enzymes, DNA methyltransferases (DNMTs), ATP-dependent chromatin remodelers, trans-acting factors (such as PcG, G9a, HP1, CTCF, MBT, and PARP-1), ncRNAs, the nuclear localization signal, and by incorporation of chromatin components such as macroH2A or the linker histone H1. In addition to its structural role in higher order chromatin, H1 can also be recruited by trans-acting factors in restricted chromatin regions, exerting a regulatory function[82].

Probably the best-known mark of fHC is methylation of lysine 27 on histone H3 (H3K27me3) by the Polycomb repressive complex 2 (PRC2)[83], a multiprotein complex formed by EZH1/2 (catalytic subunits), SUZ12, EED, RbAp46/48, AEBP2, Polycomb-like proteins (PCLs), and JARID2. Exactly how mammalian PRC2 is recruited to chromatin is not clear; it has been suggested that several mechanisms work together, including interactions of the PRC2 components with DNA, ncRNAs, histones, and histone PTMs[84].

The mechanism of action by which PRC2 mediates gene silencing is recruitment of further regulatory factors through H3K27me3. Promoters marked with H3K27me3 are still accessible to the binding of transcription factors as well as RNA polymerase, but they remain inactive or paused[85,86]. In addition, H3K27me3 provides a signal for recruiting PRC1. PRC1 mediates gene repression either through the incorporation of H2AK119ub1, via its ubiquitin ligases RING1A or RING1B, or by mechanisms independent of its enzymatic activity[84,87]. In addition, PRC2 can also interact with other proteins, such as DNMTs and HDACs, which contribute to its functions [87].

Despite being mainly associated with constitutive heterochromatin (see the next section), **H3K9me2/3** are also involved in fHC formation. These histone modifications are catalyzed by the family of proteins of SET-domain–containing methyltransferases. Among their components, **SUV39H1/2** and **SETDB1** mediate the incorporation of H3K9me2 and H3K9me3[86,88,89], whereas **G9a** mainly exists as a G9a-GLP (G9a-like protein) heteromeric complex of H3K9me1 and H3K9me2[90,91].

Finally, several studies have shown that H3K27me3 and H3K9me3 can colocalize in the genome regions, suggesting that there could be a crosstalk between these two pathways[92-94]. Indeed, both modifications can cooperate, as PRC2-dependent H3K27me3 can stabilize HP1 binding to H3K9me3[92].

In addition to the repressive histone marks, hypoacetylation of histones through the action of histone deacetylases (**HDACs**) is also a general feature of fHC[81].

Establishment of fHC at various genomic regions

fHC is very heterogeneous and may adopt a wide range of chromatin condensation states (Figure I9).

First, fHC can involve **entire chromosomal regions**. In mammals, some imprinted autosomal genes are only expressed from one of the two parental alleles, and one randomly-chosen X chromosome of females is stably silenced[81,95,96] (see Figure I9).

Second, fHC also regulates **long-range silencing**. On the one hand, large domains of more than 100 kb that contain clusters of genes, such as *HOX*, are regulated by the recruitment of PRC2 and its interaction with DNMTs and PRC1; this is important during mammalian development[97]. On the other hand, some megabase-scale domains of fHC enriched in H3K9me2/3[86] also exist: (I) Large organized chromatin K9-modifications (LOCKs) contain H3K9me2 and are linked to the repression of specific genes; they are regulated by the histone methyltransferase G9a, highly conserved between human and mouse and specific for certain differentiation states[98]. (II) Large domains of H3K9me3 known as differentially bound regions **(**DBRs) are found in differentiated human cells to form a barrier to transcription factors, thereby avoiding reprograming to a pluripotent state; however, it is unclear which methyltransferase (SUV39H1/2, SETDB1, or G9a) is most responsible for regulating them[86,99,100]. (III) Lamina-associated domains (LADs) are regions of chromatin in contact to the nuclear lamina, which are typically 0.1 to 10 Mb in size. They are linked to transcriptional silencing and decorated with the histone marks H3K9me2/3. Although the vast majority of LADs do not change in different cell types (constitutive LADs), some differ between cell types as well as during differentiation and cancer (facultative LADs)[101]. Interestingly, LOCKs and LADs mark similar genomic locations[98].

Finally, fHC can be stablished **locally in restricted regions,** such as in promoters of euchromatin, through many different mechanisms[61,81,88,102,103] (Figure I9). Interestingly, there is a particular case in which H3K27me3 coincides with H3K4me3, creating so-called “bivalent genes”. These genes are involved in development and differentiation processes and, as their name suggests, are characterized by having both activating and repressing marks in a way that they are transcriptionally poised. At certain time, these chromatin modifications can change to only H3K4me3 or only H3K27me3 if a gene is expressed or repressed, respectively[104,105].

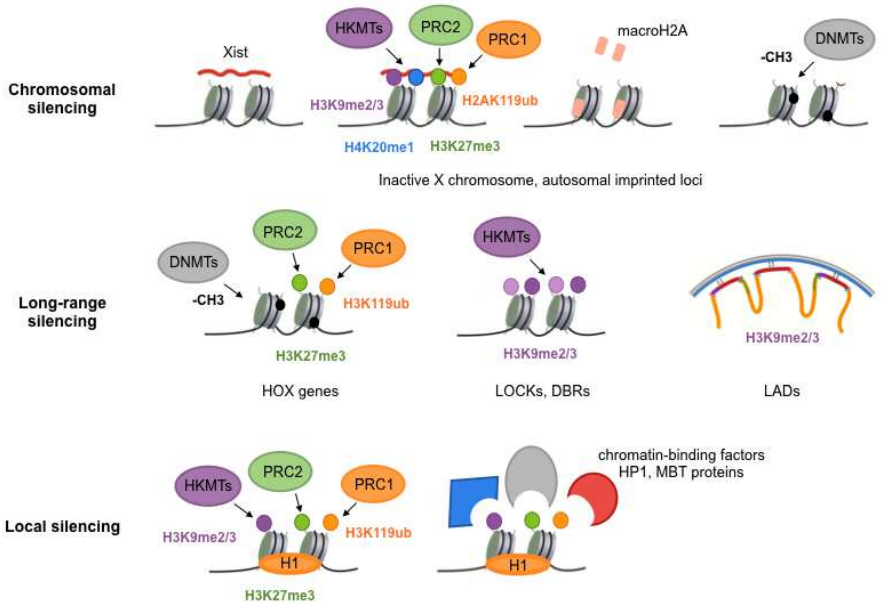

Figure I9. Establishment of fHC at various genomic regions and molecular signatures. fHC can cover an entire chromosome (e.g. inactive X), span large genomic distances (e.g. *HOX* genes, LOCKs DBRs, and LADs), or be restricted to certain regulatory regions (e.g. promoters). Depending on the context, different mechanisms are involved in its formation, promoting a condensed chromatin state. During chromosome X inactivation, the initiating factor for heterochromatin formation is a ncRNA termed XIST. This is followed by histone PTM (H4K20me1 and H3K27me3). Finally, late events include the histone variant macroH2A and DNA methylation. The establishment of long-range silencing is regulated by PRC1, PRC2, and DNMTs, as well as by the SET methyltransferases G9a, SUV39H1, and SETDB1. In restricted regions, fHC is created by the incorporation of histone variants, histone H1, histone modifying enzymes (PRC1/2, G9a, SETB1, and SUV39H1/2), PTMs (H3K27me3 and H3K9me2/3), and the recruitment of trans-acting factors (HP1, L3MBTL1, and MBT). Adapted from [81]

3.2.2. Constitutive heterochromatin (cHC)

Constitutive heterochromatin includes permanently silenced and highly compacted genomic regions that contain repetitive DNA sequences including tandem repeats forming clusters called satellites and transposable elements (DNA transposons, LTR-endogenous retroviral elements, non-LTR autonomous retrotransposons). These regions are mainly found at **telomeres, centromeric, and pericentromeric regions** as well as in ribosomal regions and different loci along the chromosome[106,107].

In most metazoans, telomeres are formed by conserved, repeated short DNA motif (5′-TTAGGG-3′) with H3K9me3 bound by conserved protein machineries that protect chromosomal ends from being recognized as double-strand breaks. In contrast, pericentromeres show a variable organization between species or even chromosomes of the same species, suggesting that their functions do not depend on a specific DNA motif [107].

In organisms ranging from fission yeast to human, constitutive heterochromatin domains are marked with extensive methylation of histone H3 at lysine 9, with both **H3K9me2** and **H3K9me3**[73,86]. In this type of heterochromatin regions, these posttranslational modifications are mainly regulated by the evolutionary conserved histone methyltransferases **SUV39H1** and **SUV39H2**, known as Su(var)3-9 in *Drosophila melanogaster* and Clr4 in *Sacharomyces pombe*[89,108,109]. In all species, this enzyme has a similar organization with two characteristic domains, a **SET-domain** in the C-terminal part and a **chromodomain (CD)** in the N-terminal part. The first one contains the catalytic activity and uses a *S*-adenosyl methionine as a methyl donor to methylate histone H3 in lysine 9. The latter allows SUV39H1 to bind to the product of its own reaction, H3K9me2/3, which is important for the methyltransferase activity and creates a positive feedback loop that controls heterochromatin formation[73,110,111].

Histone methylation also serves as a “molecular anchor” to recruit **heterochromatin protein 1 (HP1)**, a reader of H3K9me3 and another key element for heterochromatin formation. In mammals, three different

isoforms have been identified, **HP1α**, **HP1β,** and **HP1γ**. Despite having the same main domains, they interact with different proteins and work in different genomic regions[61,112].

HP1 proteins contain a N-terminal **chromodomain** that selectively bind to H3 methylated at K9, and a C-terminal **chromoshadow domain (CSD)** that is involved in its dimerization. The formation of this CDS dimer creates a platform to recruit effector proteins that are involved in the maintenance and spreading of heterochromatin. These two mentioned regions are separated by a **"hinge" domain** that contributes to HP1 localization and interacts with DNA, RNA, and chromatin (Figure I10) [113-115].

The binding and function of HP1 to chromatin can be modulated either by its association with many other proteins[116] or by characteristics of the chromatin, such as the presence of the histone variant H2A.Z. In particular, recent studies suggest that H2A.Z could work as a functional substitute for H3K9me3, as it is able to enhance HP1 binding similar to this histone modification[117].

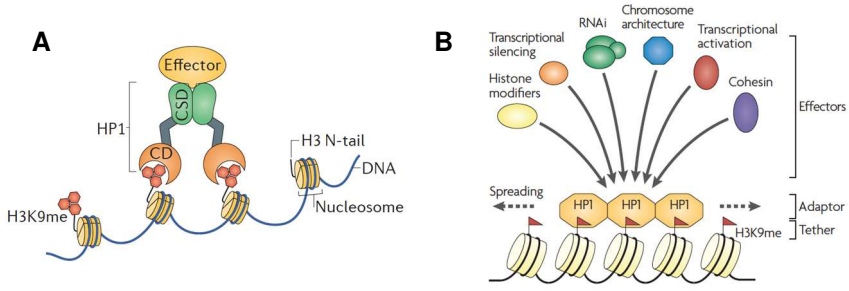

Figure I10. HP1α and the establishment of heterochromatin. A) Depiction of a HP1 dimer bound to nucleosomes modified with H3K9me; chromodomain (CD) and chromoshadow domains (CSD) are shown. **B)** The platform produced by the CSD dimer enables recruitment of effector proteins. Adapted from [73,113]

Another hallmark of cHC is the enrichment in the levels of **H4K20me2/3**, although their function still remains unclear. These histone modifications are incorporated by **SUV420H1/2** enzymes (also called KMT5B/C) that

are targeted to chromatin through their interaction with HP1 isoforms. The induction of H4K20me2/3 requires H3K9me3, suggesting a sequential mechanism to establish H3K9 and H4K20 trimethylation in these regions[118].

In addition, global hypoacetylation is also a prominent histone feature. It is regulated by **HDACs** and their absence leads to the loss of epigenetic marks such as H3K9me3 and H4K20me1[107,119].

Finally, some histone variants such as H3.3[120] and H2A.Z[121] are also crucial for formation of centromeric and pericentromeric heterochromatin (see Section 6.2).

3.2.3. Heterochromatin spreading

One key feature of heterochromatin is that it can **spread into neighboring regions** independently of the DNA sequence. Interestingly, this established state can be maintained through cell division.

This process has been well characterized in *Drosophila* (termed position-effect variegation) and in yeast, the genome of which contain large heterochromatic regions[73,113,122]. In humans, these mechanisms are less defined, but it has also been described that large heterochromatin domains exist, such as in developmental genes during the differentiation[86,99,100,122] or in the inactivation of the mammalian X chromosome[73,123].

Once nucleated in a particular location, the interconnection among readers and writers of heterochromatin form a positive feedback loop that extends the heterochromatin domains and represses the nearby sequences[73,113] (Figure I11a). In addition, these feedback mechanisms can act both locally on adjacent nucleosomes and over greater distances by random collisions between chromatin domains that are spatially closer[123,124].

The most well-established and conserved example is the one that involves **SUV39H1** and **HP1**. During heterochromatin formation, first SUV39H1 methylates H3K9 and then HP1 recognizes it. SUV39H1 is

able to bind to H3K9me3, and it interacts with HP1α to maintain the methyltransferase in chromatin, thus mediating H3K9me2/3 incorporation in the adjacent nucleosomes and propagating heterochromatin[110,125]. Moreover, this mechanism cooperates with others, including those involving ncRNAs, HDACs, and DNA methylation that allow a more robust gene repression[73,123,126,127]. For instance, SUV39H1 is able to interact with the DNA methyltransferases DNMT1 and DNMT3a[129].

On the other hand, **PRC2-mediated H3K27me3** can also be linked to a mechanism of heterochromatin spread. The EED subunit of PRC2 can bind to H3K27me3**,** thereby enhancing the activation of the methyltransferase activity of PRC2 (Ezh2 SET domain) and leading to further methylation of H3K27[128]. However, it is not clear if heterochromatin spreading involves the same mechanism of sliding (tracking along the chromatin) as for SUV39H1 and HP1α; alternative models have been proposed, such as the local diffusion of PCR2 to nearby sites and/or the formation of chromosome loops[123,129].

Finally, as spreading of heterochromatin is stochastic, it must be tightly controlled to avoid erroneous silencing. Hence, several mechanisms exist to **establish boundaries** (Figure I11b). Spreading can be restricted by the presence of features opposing heterochromatin, such as ongoing transcription, nucleosome-free regions or histone modifications that affect nucleosome stability. Additionally, it can also be restricted by regulating turnover of histones, RNAs or through nuclear structures such as CTCF and nuclear pore components[73,122].

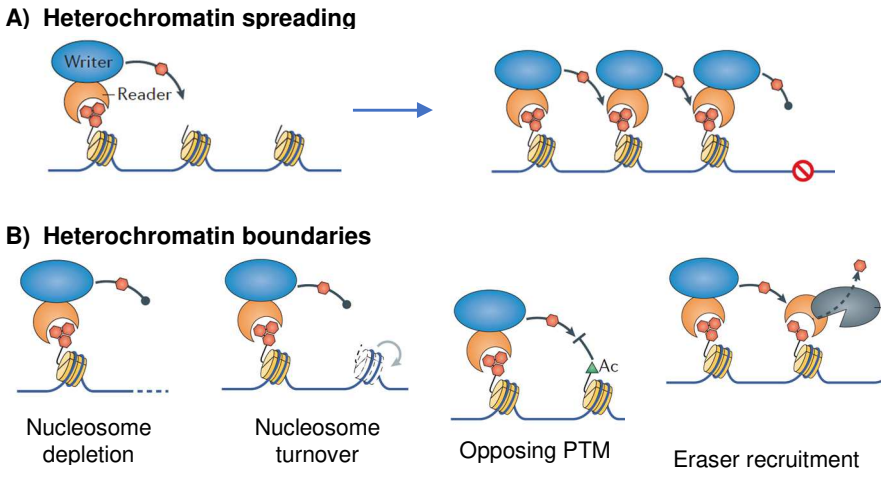

Figure I11. The regulation of heterochromatin spreading. A) A model for the expansion of HC domains through the reader–writer coupling**. B)** Mechanisms that restrict HC spreading include: factors that promote nucleosome depletion and turnover, adjacent expressed transcription units, and recruited erasers. Ac, acetylation**.** Adapted from[73]

Chromatin and epigenetics have an important impact in human health and disease. In particular, it is now well known that epigenetic dysregulation is a common feature of most cancers. Thus, understanding the mechanisms that regulate chromatin dynamics and genome organization during cancer progression is crucial for the development of new therapies. Epigenetics provides a new opportunity for therapeutic intervention, and over the last years, some drugs directed at epigenetic modulators have already entered in clinical development[130].

4. Cancer

Cancer is a leading cause of mortality worldwide. Many different types have been described, with carcinoma the most prevalent form. This type of cancer arises in epithelial tissues, and include colorectal, breast, prostate, and lung cancer, among others[131].

4.1. General insight

Cancer is a multistep process in which normal cells evolve progressively to a neoplasic state that is characterized by the acquisition of a set of malignant traits. These capacities include unlimited replicative potential, tissue invasion and metastasis, sustained angiogenesis, self-sufficient growth, reprogramming of energy metabolism as well as the evasion of apoptosis, immune destruction, and growth suppressors. These are known as the "**hallmarks of cancer**" and are shared by all types of cancer, even when these differ in terms of cellular morphology, growth, genetic lesions, prognosis, or therapeutic response[132].

Frequently, cancers display high **tumor heterogeneity**, both spatial (across different regions of the primary tumor and/or metastatic sites) and temporal (in the molecular makeup of cancer cells during tumor progression as a result of selective pressure). Genetic and epigenetic alterations lead to the appearance of cells with different molecular signatures, malignant capacities, and levels of sensitivity to treatment[133,134]. Although several hypotheses have been proposed to explain this diversity, the majority of contemporary studies use the **clonal evolution model[133]**. In this model, tumor initiation is stochastic and begins when a cell is transformed and acquire malignant capacities and a growth advantage. Genomic instability in the expanding population then creates additional diversity that is subjected to selection pressure, resulting in heterogeneous subpopulations with increased genetic abnormalities[135]. Within this context, tumor evolution can be linear or branched. The first one involves sequential acquisition of mutations that are advantageous, with sequential clones competing with the ancestral ones.

Alternatively, in a branched evolution, multiple genetically distinct populations emerge from a common ancestral clone with certain subclonal populations diverging from the common ancestor before others. Many solid tumors adopt a branched pattern of evolution[133].

Among tumoral cells, there is a group of **cancer stem cells (CSCs)** that have the ability to self-renew and initiate tumors; they also express markers typical of normal stem cells. Although this population represent a small fraction, they are critical drivers of cancer progression. CSCs are more resistant to radiation and chemotherapeutic treatments and may show certain forms of tumor dormancy, remaining latent but with the ability to regenerate a tumor after long times (which can be decades, depending on the cancer type)[132,136].

Furthermore, it is important to point out that cancer cannot be understood only as a homogenous group of malignant cells. Within a tumor, cancer cells are constantly interacting with their **microenvironment** (cell types of the parenchyma and stroma) that influence tumor growth, and this microenvironment evolves during tumor progression to enable primary, invasive, and metastatic growth[132]. On the other hand, the immune system also plays a crucial role in cancer. Interestingly, immune cells have dichotomous roles: they can work as a barrier to tumor formation and progression as well as promote these effects, contributing to multiple hallmark capabilities. Hence, in recent years, immunotherapy has become a promising strategy to fight cancer.

Within cancer pathogenesis, **metastasis** is responsible for as much as 90% of cancer-associated mortality. Metastasis is the end of a process in which cancer cells in primary tumors execute the following sequence of steps to disseminate to distant organs. They locally invade the surrounding extracellular matrix and stromal cell layers, intravasate into the microvasculature of the lymph and blood systems, survive the transport through the bloodstream, and are arrested at distant organ sites. Then, they extravasete into the parenchyma of these tissues, survive in the foreign microenvironments and form micrometastases, and finally colonize distant organ sites, forming a macroscopic secondary tumor[136,137].

In carcinomas, cancer cells tend to be organized tightly bound with each other through cell-cell junctions, as in normal epithelial tissues. However, when a tumor progress, some cells liberate themselves from these associations, acquire the ability to migrate, and invade and degrade the basement membranes moving to adjacent stromal compartments. Once they have survived in the circulation and reach a distal organ, colonization at the metastatic site is the rate-limiting step of the process. This is extremely inefficient, and most cancer cells that successfully translocate to a secondary site die. For successful colonization, cells must adapt and acquire mitogenic stimulation from the growth factors, cells, and cytokines present in the new microenvironment[136-138].

It is now well known that each cancer type has a certain **tropism** to form metastases in a subset of target organs. However, it is still not clear if this is due to restrictions imposed by the vasculature or rather involves specific mechanisms of interactions between the circulating tumor cells (CTCs) and certain tissues[137].

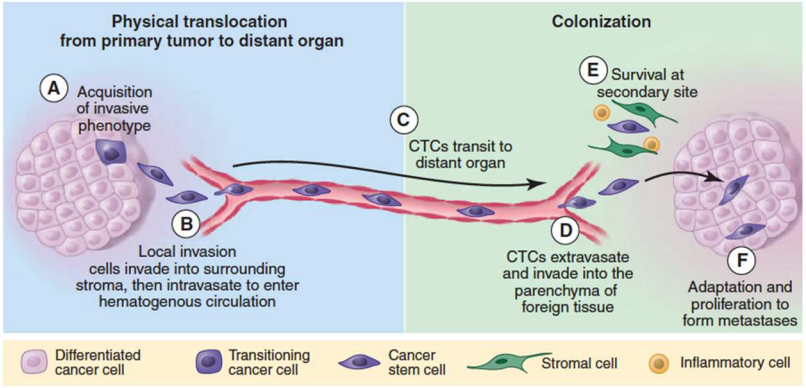

Figure I12. The metastatic cascade. Metastasis can be understood as a process that occurs in two major phases: (i) physical translocation of cancer cells from the primary tumor to a distant organ (shown in blue) and (ii) colonization of the translocated cells within that organ (shown in green). The different steps are indicated with a brief summary**.** CTC, circulating tumor cells [136].

4.1.1. Epithelial-to-mesenchymal transition

The epithelial-to-mesenchymal transition (EMT) is a process in which epithelial cells convert to mesenchymal ones through a cascade of biological events (Figure I13).

In a typical epithelial layer, epithelial cells show apical-basal polarity and establish robust intercellular adhesions through structures, such as tight junctions, desmosomes, and hemi-desmosomes. During EMT, these cell-cell junctions are deconstructed, cystoskeleton is reorganized, and cells acquire a mesenchymal phenotype with an elongated morphology and invasive capacities. In addition, mesenchymal cells express high levels of intermediate filament protein vimentin, smooth muscle actin, and extracellular matrix components, such as fibronectin and collagen precursors; also, integrins and matrix metalloproteinases (MMPs) that will allow contact with the extracellular matrix and its degradation[139-141].

The transition between these two types of cells involve changes in gene expression patterns in a way that epithelial genes, such as E-cadherin, must be repressed and the mesenchymal ones activated. This switch in the transcriptional program is mediated by the **SNAIL, TWIST and ZEB** families of **transcription factors** that are tightly regulated at transcriptional, translational, and posttranslational levels by other proteins or noncoding RNAs[139-141]. These master regulators are activated early in EMT and show distinct expression profiles and contributions to the process, depending on the cell type or tissue. Moreover, these transcription factors collaborate with epigenetic regulators that contribute to their function. For instance, SNAIL1 induces repressive histone modifications at the CDH1 promoter through the recruitment of HDAC1/2 (which deacetylates histone H3 and H4)[142], LSD1 (removes di- and tri-methyl marks of H3K4)[143], PRC2 (trimethylates H3K27)[144], SUV39H1 (trimethylates H3K9)[145], G9a (dimethylates H3K9)[146], and LOXL2 (deaminates H3K4me3)[147].

Despite having conserved characteristics, EMT is a very complex process that can be activated by several intrinsic and extrinsic factors. Depending on the context, cells can have **different modes of EMT** and adopt different intermediates states. In addition, the inverse process,

known as the mesenchymal-to-epithelial transition (MET), can also take place[140,141].

EMT is essential during embryonic development but is also aberrantly activated in pathological conditions, such as fibrosis and cancer148. Although its exact function in cancer is a matter of active debate, it is known that cancer cells frequently undergo partial or transient EMT. This process is linked to a lot of malignant features of cancer cells, such as the acquisition of stem-cell properties, immune evasion, chemoresistance, altered metabolism, and blocked senescence. In addition, EMT and MET are also involved in all the steps of metastasis: invasion, dissemination, extravasation, and metastatic colonization[140,141].

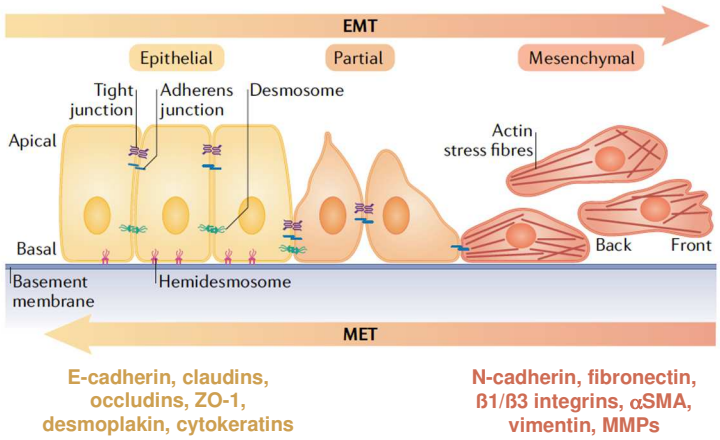

Figure I13. Epithelial-to-mesenchymal transition (EMT). During EMT, epithelial cells lose cell-cell junctions concomitantly with the repression of epithelial markers and cytoskeleton reorganization. In the end, they express mesenchymal genes and acquire new properties, such the ability to migrate and invade. Cells have different modes of EMT and adopt different intermediates states. Mesenchymal-to-epithelial transition (MET) is the inverse process[149]. ZO: Zonula occludens; SMA: smooth muscle actin; MMPs: matrix metalloproteinases.

4.2. Breast cancer

The female human breast is a tube-alveolar gland that undergoes extensive remodeling and differentiation during a woman's lifetime: hormonal changes during each menstrual cycle induce waves of proliferation in the mammary epithelium, whereas pregnancy leads to extensive ductal branching and alveogenesis[134,150-152].

The glandular tissue that makes up the breast consists of a stratified epithelium with two different cell populations that can be distinguished immunohistochemically. The **luminal epithelial cells** form the inner layer and are involved in milk production during lactation; they express keratins 7, 8, 18, and 19, and/or the estrogen and progesterone receptors (ER/PR). The outer layer is formed by **basal or myoepithelial cells** that provide structural support and are involved in the milk ejection during lactation; they express keratins 5, 6, 14, 17, and/or smooth muscle actin (SMA) and/or p63[134,150,151]. Finally, **mammary stem cells** have the ability to self-renew and are important for maintaining tissue homeostasis. They give rise to several populations of progenitors that eventually differentiate to the different cell types of the breast epithelium.

Breast cancers arise from the transformation of normal breast cells that progress from a premalignant disease (for instance hyperplasia or ductal carcinoma in situ) to invasive carcinoma and metastasis, mainly to the lungs, brain, bone, and liver[137,151]. They are a complex and highly heterogeneous group of tumors that show distinct molecular signatures, prognoses, and therapeutic responses.

Recently, the development of gene-expression profiling methods has allowed breast cancer to be classified into five main distinct molecular subtypes[152-155]. It has been suggested that the different subtypes might be the result of the arrest of stem progenitors in different stages of development[150,156] (Figure I14).

- **Normal-like:** seems to represent samples with low tumor cell content and more normal tissue components. These tumors are small and have good prognosis. However, some groups have questioned if this subtype represents cancerous tissue.

- **Luminal A**: characterized by the expression of luminal markers and being estrogen-receptor and/or progesterone-receptor positive and HER2/neu negative. Luminal A cancers are low-grade, tend to grow slowly and have the best prognosis.

- **Luminal B**: characterized by the expression of luminal markers and being estrogen-receptor and progesterone-receptor positive. They can be either HER2/neu positive or negative and in general grow faster than luminal A and their prognosis is slightly worse.

- **HER-2/neu.** This type of breast cancer is estrogen-receptor and progesterone receptor negative, but they show overexpression of HER-2/neu. Tumors tend to grow faster than in luminal cancers and may have a worse prognosis.

- **Basal-like:** characterized by the expression of genes usually found in the basal or myoepithelial cells of the human breast. In addition, the vast majority of them are classified as **triple-negative**, as they lack expression of estrogen-receptor, progesterone-receptor and HER2. They are highly aggressive and with high metastasis recurrence. It is important to point out that although there are similarities and many cancers show both basal and triple-negative phenotypes, the terms are not interchangeable; there are some basal-like tumors that show expression of ER, PR or HER-2 and few triple-negative tumors that do not express basal markers[157].

Currently several cancer cell lines have been stablished as models of the disease. Despite not being fully representative in terms of reproducing the heterogeneity of the clinical samples and the same phenotype as the breast tumor *in vivo*, so far many of them reflect the characteristics of the molecular profiling subtypes described. However, there are some rare histopathological types that still lack relevant models[158].

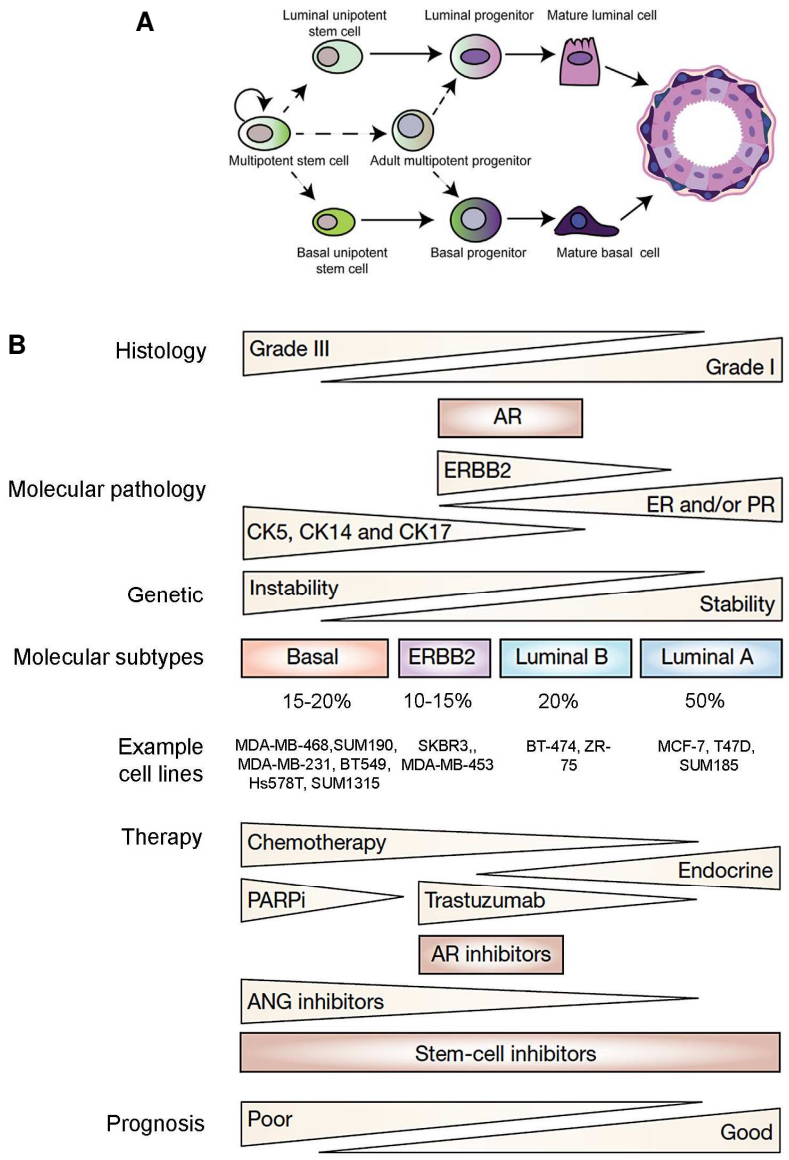

Figure I14. Mammary cell hierarchy and classification of breast cancer subtypes. A) Schematic representation of stem-cell hierarchy and the generation of the different cell linages in the breast epithelium. **B)** Molecular classification of breast cancer subtypes and summary of the characteristics of each group. ANG, angiogenesis; AR, androgen receptor; CK, cytokeratin; ER, estrogen receptor; ERBB2 (HER2), erythroblastic leukemia viral oncogene homolog 2; PARPi, poly (ADP-ribose) polymerase inhibitors; PR, progesterone receptor.Adapted from[151,152]

4.2.1. Triple-negative breast cancer (TNBC)

Triple-negative breast cancers (TNBC) account approximately from 15 to 20% of all women with breast cancer[159]. This type of breast cancer can, in turn, be classified in different subtypes, including **two basal-like (BL1 and BL2)**, **mesenchymal (M), mesenchymal-stem like (MSL), immunomodulatory and a luminal androgen receptor** subtype[160]. The MSL group includes a previously well-defined subgroup known as **claudin-low,** which is characterized by presenting a downregulation of claudin-3 and claudinin-4, high enrichment for EMT markers and stem cell-like features, such as CD44+ CD24–/low phenotype[161].

It is now known that the EMT pathway is involved in the pathogenesis of these breast cancers, where some cells show mesenchymal phenotype and display gene-expression patterns consistent with this process[160,162].

TNBC are usually high-grade, difficult to detect for their rapid growth and more likely to metastasize. In addition, patients with this type of cancer show a sharp decrease in survival curves. Less than 30% of women with metastatic TNBC survive 5 years, and almost all die despite being treated with chemotherapy. Moreover, relapse rates are higher during the first years following surgery[157,163].

So far, effective therapies have been developed for the other types of breast cancer. Luminal A and B can be treated with hormone therapy because they have estrogen and progesterone receptors, whereas the HER-2 positive can be treated with the humanized monoclonal antibody trastuzumab[157].

However, TNBCs do not show expression of recognized therapeutic targets, so that there is no specific target therapy for them. The other mentioned therapies are not useful, and chemotherapy is the only approved systemic treatment that can improve the outcome in TNBC patients. Currently, the treatment options are few and, although they are effective in some patients, the response rates in general are poor and lack durability. More research needs to be done to better understand the molecular basis of TNBC and to identify new targets to develop effective treatments[150,157].

4.3. Genomic instability, cancer, and heterochromatin

A major feature of cancer is **genome instability**, which refers to an increased tendency of alterations in the genome during cell division[164]. Cancer cells accumulate and tolerate thousands of mutations[165].

In human cancers, the major form of genomic instability is the chromosomal instability (CIN), characterized by abnormal chromosome structures and numbers (amplifications, rearrangements and copy number alterations), but there is also microsatellite instability or increased frequency of base pair mutations[164].

Normally, cells are constantly exposed to endogenous and exogenous sources of DNA damage, but they have evolved several mechanisms to combat it, collectively known as the DNA damage response (DDR) pathway. It involves signal sensors, transducers and effectors that work for repairing the DNA damage or, in cases in which it is maintained, trigger apoptosis or cellular senescence[165,166]. However, cancer cells frequently show alterations in the members of this pathway, leading to the accumulation of DNA damage without compromising cell integrity and replication. In this way, during cancer progression, cells constantly accumulate heritable genetic variations, and the ones that provide an advantage for cells to proliferate and survive more effectively are favored by natural selection[167,168].

In hereditary cancers, genomic instability results from **mutations in DNA repair genes and cell-cycle check point genes**. One of the best-known examples is the deleterious germline mutation of the *BRCA-1* and *BRCA-2* genes, which encode two proteins involved in the repair of DNA double-strand breaks (DSBs) by homologous recombination and predispose women to develop breast and ovarian cancer[164,169]. These tumors usually show loss of heterozygosity of the wild-type allele, resulting in a lack of BRCA-1 functionality and leading in most cases to a triple-negative and/or basal-like phenotype[157].

In contrast, in sporadic cancers, the molecular basis of genomic instability is much less well-defined. The most probable model that has been proposed is the **oncogene-induced DNA replication stress**

model[164,170]. According to this model, genomic instability is a functional capability of cancer *per se* that results from oncogenic-induced DNA damage. Most oncogenes deregulate cell cycle progression, compromising DNA replication and producing the collapse of DNA replication forks, a state known as **DNA replication stress** that leads the formation of **DNA DSBs**. Thus, precancerous lesions tend to accumulate DNA DSBs, genomic instability and the activation of the DNA damage response as compared to normal tissue[170-172].

However, there are some **tumor suppressive barriers** that counteract them to limit the growth of the lesion, such as the activation of p53 in order to direct these cells to apoptosis or cellular senescence (irreversible form of cell cycle arrest)[171,173]. Afterwards, the breach of this barrier by various mechanisms, mainly mutations in p53 or ATM as well as in other proteins involved in the DDR, allow cells to become a cancerous lesion. In fact, apoptosis and senescence are abundant in precancerous lesions, but become eroded during tumor progression[164,168,170].

Increasing evidence has shown that chromatin structure and accessibility plays a crucial role in the accumulation of DNA damage and the regulation of DDR, which is particularly interesting in the context of cancer. First, in response to DNA damage, the surrounding chromatin must be reorganized to allow proper repair. This involves several chromatin-related complexes and incorporation of histone modifications, which allow access to the damage and facilitate the processing and repackage the repaired DNA[174-176].

Moreover, several studies have suggested that **heterochromatin** could be a barrier to DDR, affecting the accessibility of the DNA repair complexes and the transduction of the response[172,177-181]. Accordingly, genome sequencing studies have shown that mutation rates in cancer genomes depend on the chromatin organization, showing increased rates in heterochromatin as compared to euchromatin[182,183].

Furthermore, DNA mismatch repair (MMR) is more efficient in euchromatic genomic regions than in heterochromatin, and as such,

accumulates more mutations[184]. However, the relationship between chromatin accessibility and mutation rates has recently been questioned. In skin tumors, a knockout of G9a, a methyltransferase involved in H3K9me2, increases chromatin accessibility but does not affect the mutational burden. Thus, chromatin compaction might not be the only determinant of mutation rates in cancer cells, and the effects might be different depending on the cancer type and the chromatin modifier that is altered[185]. On the other hand, oncogene-expressing transformed cells and human tumors have also been found to have high levels of heterochromatic markers compared to the normal tissues.

In this way, cells that are continually exposed to oncogene-induced DNA replication stress restrain the DDR signaling and hinder its access to DNA-damage sensors and associated DDR factors. In addition, this heterochromatin state does not affect the expression of proliferative genes and is maintained or even increased during cancer progression in human tumors[172] (Figure I15).

In tumor cells, alteration of heterochromatin components such as SUV39H1 or HP1 α, or treatment with inhibitors of HDACs, lead to an increase of DDR signaling and consequently compromise cell survival. Thus, the use of drugs that regulate chromatin accessibility represents an attractive strategy to more specifically attack cancer cells characterized by high levels of heterochromatin but with a higher probably of having less effects on normal cells. In addition, these drugs could also be used as chemo- or radio-sensitizers to increase the effectiveness of these standard genotoxic treatments[172,186].

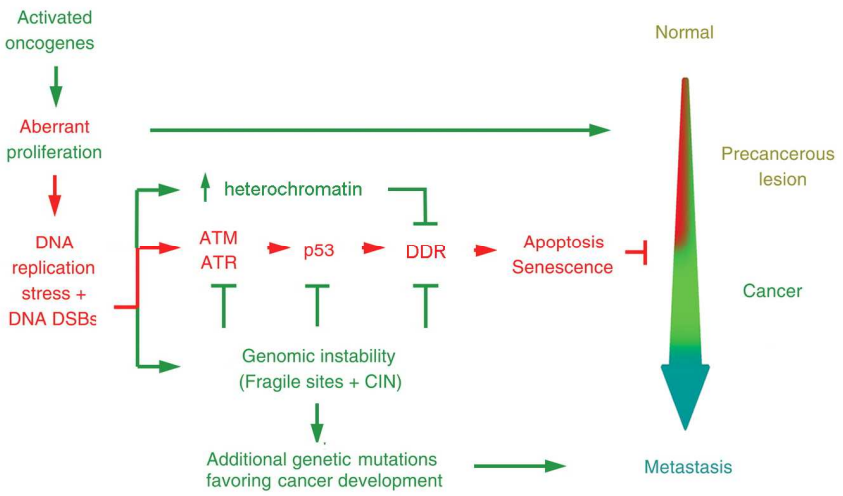

Figure I15. Oncogene-induced DNA damage model for cancer development and the role of heterochromatin. Genomic instability and tumor suppression are consequences of oncogene-induced DNA replication stress present at the beginning of cancer development. Some human tumors display an induction of heterochromatin that is linked to a restriction of the DDR signaling and the maintenance of genome instability favoring tumor progression. Adapted from[170,172].

5. Lysyl oxidase-like 2 (LOXL2)

5.1. LOX family of proteins

The lysyl oxidase (LOX) family of proteins comprises five different amine oxidase enzymes, LOX and four LOX–like proteins (LOXL1–4). These proteins catalyse the oxidation of the amino group located in the ε-position of lysine and hydroxylysine residues, generating an aldehyde group. To perform the reaction, they require two cofactors, copper and quinone[187]. The resulting aldehyde groups are highly reactive and can spontaneously condense with other residues to generate intra- and inter-molecular crosslinks[188].

All members of the LOX family share a **highly conserved carboxyl (C)-terminal domain** that contains all the elements required for its catalytic activity: a His-X-His-X-His copper-binding motif, residues for

the formation of the lysine tyrosylquinone (LTQ) cofactor, and a cytokine receptor-like domain (CRL)[189,190].

In contrast, the **amino-terminal regions** are very **different** between the members of the family. LOX and LOXL1 proteins contain pro-sequences and are secreted as inactive pro-enzymes that are cleaved extracellularly for their activation by metalloproteinases, such as bone morphogenetic protein 1 (BMP-1)[191,192]. Alternatively, LOXL2, LOXL3, and LOXL4 contain four scavenger receptor cysteine-rich (SRCR) domains that appear to have a role in protein-protein interactions as seen for other proteins, and thus modulate its catalytic activity[193,194] (Figure I16).

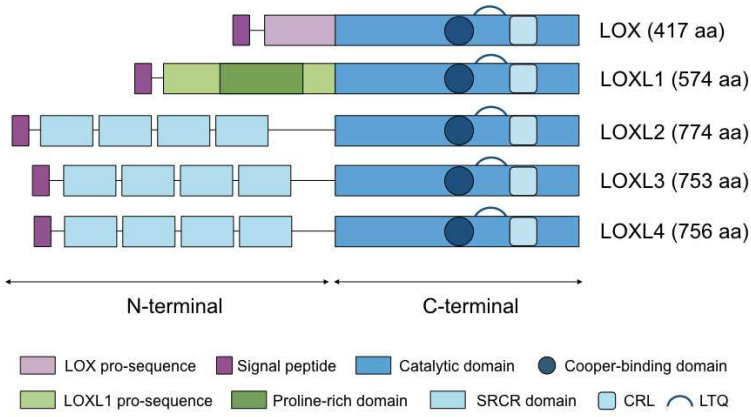

Figure I16. LOX family of proteins. Schematic representation of the five members of the LOXL family of proteins structure. SRCR, scavenger receptor cysteine-rich domain; LTQ, lysine tyrosylquinone domain; CRL, cytokine receptor-like.

The expression of the members of LOX family of proteins is tightly controlled during normal development and in the adult tissues, suggesting that each member may have individual and specific functions[195].

The LOX family of proteins was first described to be involved in covalent crosslinking of collagens and elastin in the extracellular matrix, which is important for maintaining the tensile strength and structural integrity of many tissues[193,196]. However, there is now strong evidence that these proteins also have many other **intracellular roles,** including the regulation of cell signaling pathways and nuclear-related functions such as transcription[193,194,197]. For instance, LOX protein can oxidize residues in histones H1, H2, and H3[198,199] as well as fibroblast growth factor 2 (FGF2)[200], being important for maintaining chromosome stability and regulating chromosome condensation[201]. On the other hand, LOXL2 also oxidizes histones (see Section 5.3)[147] as well as other non-histone proteins such as TAF10. This last example is important for maintaining the pluripotent capacity of embryonic stem cells, as oxidized TAF10 is released from the promoters, inactivating pluripotency genes[202]. Finally, LOXL3 oxidizes STAT3 in the nucleus; in this way, LOXL3 inhibits STAT3 dimerization and the transcription of target genes, thereby regulating negatively the differentiation of Th17 and Treg cells in inflammatory response[203].

5.2. LOXL2 in cancer

Altered expression and/or activity of the LOX family of proteins has been linked to numerous diseases, including fibrotic disorders[204], cardiovascular diseases[205], and, in particular, cancer[193]. Here we will focus on LOXL2 and its role in regulating tumorigenesis and cancer metastasis.

Several studies have shown that LOXL2 can regulate tumour cell survival, chemoresistance, cell adhesion, motility, and invasion. It can also remodel the tumour microenvironment and has even been proposed to have a possible role in the formation of the pre-metastatic niche. Interestingly, for this, both its intra- and its extracellular functions are involved[190,193,197,206].

In particular, LOXL2 has been considered to be a key regulator in human breast tumorigenesis and therefore is a promising therapeutic target for this type of cancer. LOXL2 is upregulated in various breast

cancer cells and patient-derived xenografs (PDXs), promoting invasiveness *in vitro* and *in vivo*. For instance, while it is almost absent in poorly invasive and non-metastatic MCF-7 breast cancer cells, it is highly expressed in MDA-MB-231, MDA-MB-435, and 4T1I, which are more invasive and metastatic[207-210]. In MDA-231 cells, it interacts with numerous co-repressors and is involved in the repression of epithelial genes, maintaining a mesenchymal phenotype[147]. Moreover, its expression is associated with poor outcome and lower survival rates of breast cancer patients[211]. Interestingly, immunohistochemical analyses have revealed an association between perinuclear localization of LOXL2 and aggressiveness of basal-like carcinoma[212].

Finally, it is well known that LOXL2 promotes EMT. It regulates the repression of E-cadherin via a dual mechanism: its interaction with the transcription factor SNAIL1, which prevents its degradation by GSK3β; and by incorporating the repressive histone modification H3K4ox into the CDH1 promoter[147,213]. This last function is also important for regulating chromatin reorganization during this process[78] (see Section 5.3). Furthermore, it has also been described that EMT inducers, such as hypoxia and TGFß, promote LOXL2 expression[214,215].

5.3. LOXL2 as a new epigenetic writer

Previous work in our group has described **LOXL2 as a histone modifying enzyme** that specifically oxidizes trimethylated lysine 4 in histone H3 *in vitro* and *in vivo*. In this reaction, first an alcohol is produced by the nucleophilic attack of a water-derived OH to the Cε of the lysine and the release of the $N(CH_3)_3$. Then, this alcohol is rapidly oxidized by the internal redox cofactor lysine-tyrosilquinone (LTQ) to aldehyde, generating a new modification in the histone tail of H3 referred as H3K4ox[147] (Figure I17).

It has been demonstrated that LOXL2 has a preference for H3K4me3 over H3K4me1 or H3K4me2 as substrates. However, unpublished data from our laboratory show that recombinant LOXL2 can also oxidize an unmethylated H3 peptide tail *in vitro*, although to a lesser extent.

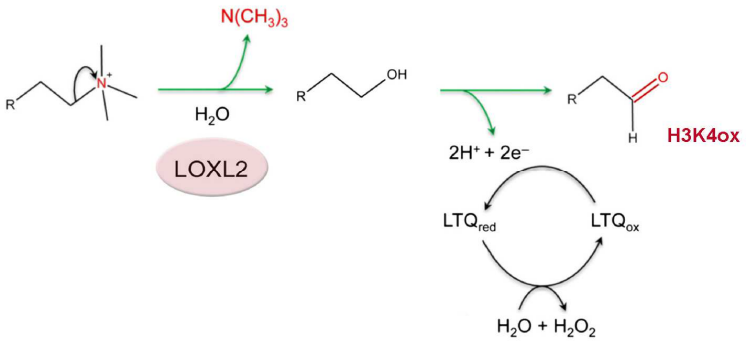

Figure I17. LOXL2 oxidizes H3K4me3. Schematic diagram of the chemical mechanism model for LOXL2 deamination of H3K4me3. The removal of an amino group on the lysine produces an intermediate alcohol that is rapidly oxidized to an aldehyde group, generating H3K4ox. Adapted from[147]

This new histone modification has been linked to the **repression of E-cadherin gene** (CDH1) at the onset of the epithelial-to-mesenchymal transition (EMT), when LOXL2 is recruited to its promoter together with the SNAIL1 transcription factor[147,213]. In addition, it is also involved in the **down-regulation of pericentromeric heterochromatin transcription** during this process, which allows a transient release of HP1α from heterochromatin foci and a chromatin reorganization required for completing the EMT[78].

LOXL2 activity as a histone-modifying enzyme has also been observed in premalignant lesions in a human head and neck squamous cell carcinoma (HNSCC) model. In this context, LOXL2 negatively regulate Notch1 binding to its promoter reducing methylation levels of H3K4me3 and subsequent RNA polymerase II recruitment in the proximal region[216].

A recent study in our lab has demonstrated that LOXL2 and H3K4ox levels are higher in **TNBC** cell lines and PDXs as compared with luminal breast cancer cells. Genome-wide analyses have demonstrated that this new histone modification is mainly located in heterochromatin, where it regulates chromatin compaction. This is important for protecting cancer cells from the activation of the DNA-damage response pathway

and suggests that targeting LOXL2 could be a way to sensitize TNBC cells to conventional therapy[210].

However, it is still not well defined which is the molecular mechanism through which this histone modification can induce chromatin compaction, or how such high levels of H3K4ox can be maintained in these metastatic cells. Thus, in this thesis, we will address these questions by analyzing both LOXL2 partners and H3K4ox readers, focusing on their role in heterochromatin formation and function.

In the next two sections, we will introduce the involved proteins and their functions.

6. RUVBL1/2 proteins and the incorporation of the histone variant H2A.Z

6.1. RUVBL1/2 proteins

RUVBL1 and RUVBL2 are ATP-binding proteins that belong to the AAA+ (ATPase-associated with diverse cellular activities) family of ATPases. Among other names, they can also be referred as Rvb1/Rvb2, Pontin/Reptin, TIP49/TIP48, TIP49A/TIP49B, ECP54/ECP51, INO80H/INO80J, and TIH1/TIH2.

Human RUVBL1 and RUVBL2 share 43% sequence identity and 65% sequence similarity[217]. Based on their X-ray structures, their sequence can be divided into three different domains: (I) an N-terminal alpha-beta-alpha subdomain of the AAA+ domain that adopts a Rossman fold and is separated in two halves by domain II; (II) an insertion domain, unique to RUVBL1/2 among the AAA+ proteins, which mediates DNA/RNA binding and oligomerization of RUVBL1/2; and (III) a C-terminal all-alpha subdomain of the AAA+ domain[217-219] (Figure I18).

The AAA+ domain contain several regions important for ATPase function. In domain I, there is the **Walker A motif** that binds and orients the γ-phosphate for ATP hydrolysis. Within domain III, the **Walker B**

motif is responsible for ATP hydrolysis, and the **sensor domains I and II** discern whether the protein is bound to the di- or tri-nucleotide. Additionally, there is an **arginine finger (Arg)** that extends into the ATPase site of the neighboring subunits when they form a hexamer, allowing the coordination of ATP hydrolysis between them [217-219].

Comparison of the crystal structures of RUVBL1 and RUVBL2 show that both the oligomerization dynamics and the distribution of the charges of the surface are different between them, suggesting that they can have different mechanisms or affinities for binding to DNA or other proteins[217].

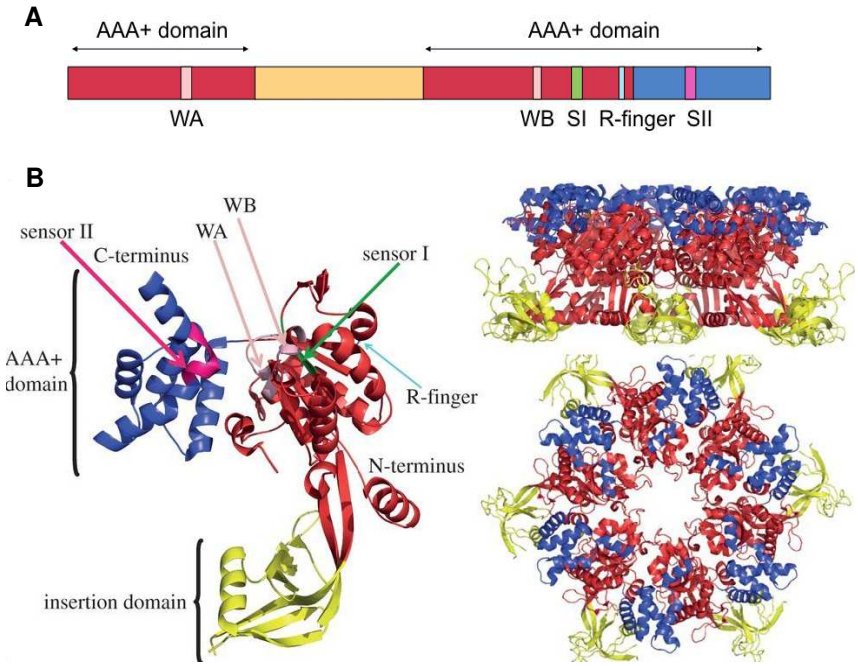

Figure I18. Overview of RUVBL1/2 structure. A) Schematic representation of human RUVBL1. In red, the N-terminal αβα subdomain of the AAA+ domain; in blue, the C-terminal all-α subdomain of the AAA+ domain; in yellow, the insertion domain. Conserved motifs with the AAA+ domain are also represented: WA, Walker A; WB, Walker B; SI, Sensor I; SII, sensor II; R-finger, arginine finger. **B)** On the left-hand side, the crystal structure of human RUVBL1 monomer. On the right-hand side, the top and side views of human RUVBL1 hexamer. Colors indicate the same structures as in *A)*. Adapted from[219]

RUVBL1/2 can exist as monomers, homo- or hetero-hexamers, as well as a dodecamer of two hexameric rings. These various oligomeric states can be modulated by the insertion domain as well as their interactions with other nucleosomes and modifications of protruding H3 tails (PTM)[219,220]. In addition, they can have different localizations, be post-translationally modified, and interact with many proteins and nucleoproteins[221,222].

Altogether, this allows them to participate in different cellular pathways depending on their context. They can work together or antagonistically, and not all their functions require the ATPase domain[223,224]. In addition, RUVBL1/2 are involved in the formation of several complexes, such as the telomerase or the INO80 subfamily of chromain remodellers. Although they are not transcription factors themselves, they can modulate the transcriptional activity of MYC, ß-catenin, E2F1, RNA polymerase II, and PRC2, among others. They also collaborate in the phosphoinositide 3-kinase related kinase (PIKK) pathway, the small nucleolar RNA (snoRNA) biogenesis machinery, and regulation of chromatin decondensation[225]. In this way, they regulate many cellular functions such as DNA damage response and repair, cell cycle progression, mitotic division, replication, apoptosis, and transcriptional activation or repression.

Interestingly, functional studies have demonstrated that RUVBL1/2 also play important roles in cancer, by regulating the expression of oncogenes and metastasis suppressor genes and/or promoting cell invasion and metastasis[224,226,227]. They have been identified as overexpressed in multiple cancer types, such as in hepatocellular carcinoma, colorectal, breast, lung, gastric, esophageal, pancreatic, kidney, bladder, lymphatic, and leukemia. For this reason, they are proving to be biomarkers for cancer diagnosis and/or prognosis as well as putative targets for the development of new therapeutic anticancer drugs[228].

6.1.1. RUVBL2 in chromatin remodeling complexes

Chromatin remodeling complexes are necessary for regulating nucleosome dynamics and composition. They can slide nucleosomes along the DNA, exposing new sites for protein binding, add or remove covalent modifications on histone tails, or alter chromatin composition by exchanging canonical histones for histone variants[229]. Consequently, they modulate the accessibility of different proteins and other cofactors to the DNA.

Several studies have demonstrated that RUVBL1/2 are part of several chromatin remodeling complexes, working like chaperones and regulating their formation and activity[219].

Here we will focus on the human chromatin remodeling complexes of the **INO80 subfamily** that regulate the deposition of the histone variant H2A.Z[230-232] (Table 1). Their function is important for controlling transcription (both activation and repression)[219,224] and replication[233,234], and for maintaining genome integrity. Recruitment of these complexes and a tightly-regulated H2A.Z deposition are required for reorganizing the chromatin structure surrounding DSBs, so that the repair machinery can process the damage[174,234,235].

INO80

The INO80 complex can be found in yeast, flies, and humans. It acts as a nucleosome spacing factor and mediates the removal of the histone variant H2A.Z from the wrong locations[219,224,232]. In this complex, RUVBL1/2 are required for the incorporation of the protein Arp5, which is essential for its chromatin-remodelling activity[236].

SRCAP complex

RUVBL1/2 are integral subunits of Snf-2 related CREB-binding protein activator protein (SRCAP) complex and its homologs SWR1-C in yeast and Tip60 (Domino) in *Drosophila*.

These complexes are involved in the exchange of H2A-H2B dimers for H2A.Z-H2B in specific locations of the genome[231,237-240]. The deposition of this histone variant by this complex can be regulated by histone acetylation[241-243].

Three-dimensional structure of SWR1-C obtained by electron microscopy have demonstrated that, in this complex, RUVBL1/2 form an hexameric ring that acts as a platform for the assembly of its functional modules; their structural role may also be important for a proper coordination of the nucleosome and the H2A.Z-H2B dimer and therefore for its exchange[244].

TIP60/p400

This complex is present only in higher organisms, but it shares several subunits with two separate yeast complexes, the SWR1 (previously mentioned) and NuA4. Thus, it integrates the function of both complexes at the same time. First, similar to NuA4, it is a histone acetyltransferase that mediates the acetylation of histones and other cellular proteins. Second, it is involved in the exchange of the histone variant H2A.Z; it contains the ATPase p400, the homolog protein of SWR1 and SRCAP proteins, as well as other components of SWR1/SRCAP complexes, such as Ruvbl1/2 or ARPs[243,245-247].

In fact, several pieces of evidence in yeast illustrate the functional link between these two complexes. Fist, both SWR1-C and NuA4 share four subunits (Act1, Arp4, Swc4, and Yafp), suggesting that they could act as a docking platform to chromatin[243]. In addition, the association of the SWR1 complex in chromatin and H2A.Z exchange in these regions require a proper function of NuA4 complex and acetylation of H4[241,248]. Finally, H2A.Z can also be acetylated by NuA4 once it has been deposited by SWR1-C; this is required for maintaining H2A.Z in heterochromatin boundaries and avoid heterochromatin spread to euchromatic domains[249,250].

RUVBL1/2 are required for a proper assembly and function of the TIP60 complex. They act as molecular adaptors and avoid the inhibitory effect of p400 as well as maintain the heat stability and function of histone acetylation. RUVBL1/2 are redundant in this function, and their contribution to TIP60 activity is independent of their ATPase activity[251,252].

INO80		
Yeast	**Fly**	**Human**
Ino80	dIno80	hIno80
Rvb1, Rvb2	Reptin, Pontin	RUVBL1, RUVBL2
Arp4,5,8, Act1	dArp5,8, dActin	BAF53a, Arp5,8
Ies2		hIes2
Ies6		hIes6
Taf14		
Ies1, Ies3-5, Nhp10	**Pho**	**Amida, NFRKB, MCRS1, FLJ90652, FLJ20309**

Yeast SWR1	**Human SRCAP**	**Yeast NuA4**	**Human TIP60/p400**	**Fly Tip60**
Swr1	SRCAP		P400	Domino
Rvb1, Rvb2	RUVBL1, RUVBL2		RUVBL1, RUVBL2	Reptin, Pontin
Arp4,6, Act1	BAF53a, Arp6	Arp4, Act1	BAF53a, Actin	BAP55, Act87E
Yaf9	GAS41	Yaf9	GAS41	dGAS41
Swc4/Eaf2	DMAP1	Swc4/Eaf2	DMAP1	dDMAP1
Swc2/Vps72	YL-1		YL-1	dYL-1
Bdf1			Brd8/TRCp120	dBrd8
H2AZ, H2B	H2AZ, H2B			H2Av, H2B
Swc6/Vps71	ZnF-HIT1			
		Tra1	TRRAP	dTra1
		Esa1	Tip60	dTIP60
		Eaf3	MRG15, MRGX	dMRG15
		Eaf6	FLJ11730	dEaf6
		Eaf7	MRGBP	dMRGBP
		Epl1	EPC1, EPC-like	E(Pc)
		Yng2	ING3	dING3
Swc3,5,7		Eaf5, Eaf1/ Vid21		

Table I1. Chromatin remodeling complexes of the INO80 family. Homologous subunits are lightly shaded, and the unique subunits are darkly shaded. Adapted from [247]

6.2. The histone variant H2A.Z

H2A.Z is a histone variant that represents about 5–10% of total cellular H2A. It is highly conserved between species (~90% sequence identity) and is essential for the viability of many organisms, such as *Tetrahymena thermophila*, *Drosophila*, *Xenopus leavis,* and *Mus musculus*[253,254].

In vertebrates, two different isoforms of H2A.Z exist, H2A.Z.1 and H2A.Z.2, encoded by two different genes named *H2AFZ* and *H2AFV*, respectively. Although at the protein level they only differ by three amino acids, knock-out studies suggest that they are not redundant, and some isoform-specific effects have already been described[255,256]. In addition, a third isoform, H2A.Z.2.2, has also been identified. It is an alternative splicing variant of H2A.Z.2 and, uniquely, it has a shorter C-terminus that destabilizes nucleosomes both *in vitro* and *in vivo*[257,258].

It is important to point out that most studies for H2A.Z do not distinguish between the different isoforms, and especially the studies that use antibody-based approaches, as until recently there were no specific antibodies for each isoform. However, in general, what is commonly referred as H2A.Z is the isoform H2A.Z.1.

As previously mentioned, incorporation of this histone variant is mediated by the SRCAP and TIP60 complexes, and its removal, by the INO80 complex[230-232]. However, other subcomplexes can also regulate H2A.Z exchange. ANP32E mediates its removal[259] and a small complex that contains only RUVBL1/2, BAF53, DMAP1, and actin but lacks the catalytic subunits p400 and SRCAP can catalyze its incorporation *in vitro*[260].

H2A.Z can form both heterotypic (H2A-H2A.Z) and homotypic (H2A.Z-H2A.Z) nucleosomes *in vivo*. However, the functional differences between these two types of nucleosomes are still not fully understood[261-263].

Compared to the canonical H2A, H2A.Z shares only ~60% sequence identity with canonical H2A and can also be post-translationally modified[53,253]. These PTMs might be important for its function; for instance, acetylation of H2A.Z is found at the 5′ regions of active genes in yeast and vertebrates[264], whereas its monoubiquitylation distinguishes the fraction associated with facultative heterochromatin[265].

Structurally, H2A.Z presents different features as compared to canonical H2A. There are some differences in loop L1 (important for interactions between the two H2A/H2A.Z-H2B dimers) and the C-terminal docking domain (important for interactions between H2A.Z and the H3-H4 tetramer). It has been suggested that this could affect the stability (with highly controversial results) and sliding of nucleosomes to different positions. Within the C-terminal docking domain, two acidic residues in H2A.Z (Asp and Ser) subtly **extend the acidic patch region,** which alters the nucleosome surface as compared to that of the canonical H2A[53,253,266] (Figure I19). This region is involved in protein binding and in establishing contacts with neighboring nucleosomes. Hence, H2A.Z has been postulated to be able to regulate chromatin fiber folding through this region, leading to gene repression; *in vitro* experiments show that H2A.Z promotes HP1α-mediated intramolecular folding of nucleosomal arrays but inhibits their intermolecular association[267-269].

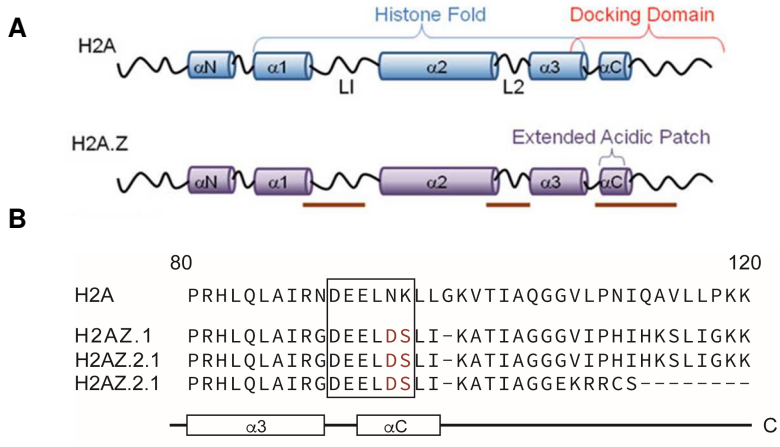

Figure I19. The histone variant H2A.Z and the canonical H2A. **A)** Schematic diagram of the secondary structures of histone H2A and H2A variants. The red bars below the H2A.Z mark the regions that are most divergent from H2A). **B)** Amino acid sequences of the C-terminal docking domain of human H2A and H2A.Z variants. The box indicates the region which contains the aminoacids that contribute to the acidic patch; in red, the two residues that extend this region in all the H2A.Z isoforms. α-helices are represented by cylinders; L1: loop 1; L2: loop 2. Adapted from[53,266,268]

It is now well known that in many species H2A.Z has an important role in regulating transcription. This histone variant is located in the promoters of genes occupying nucleosomes surrounding the TSS (transcription start site) and it can activate, repress or poise inducible genes for activation[53,241,246,270,271]. Besides, it regulates multiple steps of transcription, both initiation (by recruiting RNA Pol II to promoters) and elongation[272,273]. It has also been described that it is enriched at enchancers and gene regulatory elements[271].

On the other hand, several studies have linked H2A.Z to heterochromatin formation and gene silencing in different organisms and cell types.

It is located in pericentromeric heterochromatin of mouse cells colocalizing with HP1α from the early embryo[121]. Moreover, it is necessary for centromer function; the lack of H2A.Z leads to chromosome segregation defects, improper heterochromatin formation and loss of centromere cohesion[274,275]. In yeast, H2A.Z is enriched near telomeres and regulates boundaries between euchromatin and heterochromatin to prevent heterochromatin spread[276-278]. In *Drosophila*, it is involved in the establishment of heterochromatin being required for the subsequent acetylation of H4K12, H3K9 methylation and HP1 recruitment[279].

Regarding facultative heterochromatin, H2A.Z can be located in promoters of developmental genes that are repressed by polycomb complexes[270] as well as cover large regions on the body of non-transcribed genes enriched in H3K9me2[271]. Furthermore, when H2A.Z is monoubiquitylated, it is incorporated on the inactive X chromosome in human female cells and this modification seems to distinguish its association with facultative heterochromatin[265].

Altogether, the incorporation of the histone variant H2A.Z is essential in multiple cellular processes such as transcriptional regulation, chromosome segregation, cell cycle progression and DNA damage response. Interestingly, several studies have reported that it is overexpressed in some types of cancer such as breast, melanoma, prostate and hepatocellular carcinoma affecting the gene expression programs[52]. Furthermore, the SRCAP and Tip60/p400 complexes involved in its deposition can also be found deregulated.

7. CUL4-RING E3 ubiquitin ligases and H2AK119ub

7.1. CRL4s: the CUL4-RING E3 ubiquitin ligases

Ubiquitination of proteins can regulate many cellular processes altering their functions or promoting their degradation by the proteasome. This pathway consists of a cascade of three activities: the **E1 enzyme**, involved in the ATP-dependent activation of ubiquitin, the **E2 ubiquitin-conjugating enzyme**, which transfers the ubiquitin to the substrate, and the **E3 ubiquitin ligase,** that selects the substrate and brings it close to E2 enzyme[280-282].

In higher eukaryotes, two families of E3 ligases have been identified, the HECT (homologous to E6-AP carboxy terminus) and the RING (really interesting new gene) domain ligases. The latter is the most prevalent and, as the name states, its members contain a RING domain; this is a type of zinc binding domain with 40-60 residues of a motif rich in cysteines and histidines involved in the binding to the E2 enzyme[280-282].

One of the most well-conserved group of E3 ligases is the **cullin-RING ligases (CRLs**). These enzymes are multiprotein complexes formed by several subunits: a **RING protein** that binds to the E2 enzyme, a **cullin** which acts as a scaffold protein, an **adaptor or linker protein** and the **substrate-receptor** that specifically recognizes the substrate[280-282].

Remarkably, several RING proteins (RBX1, RBX2 and in certain complexes RING1B) and cullins (in mammals CUL1, CUL2, CUL3, CUL4A, CUL4B, CUL5, and CUL7) exist. Taking into account that they can associate with different adaptors and receptors, it is possible to generate a huge amount of distinct E3 ligases that regulate the ubiquitination of many different substrates [280-282] (Figure I20).

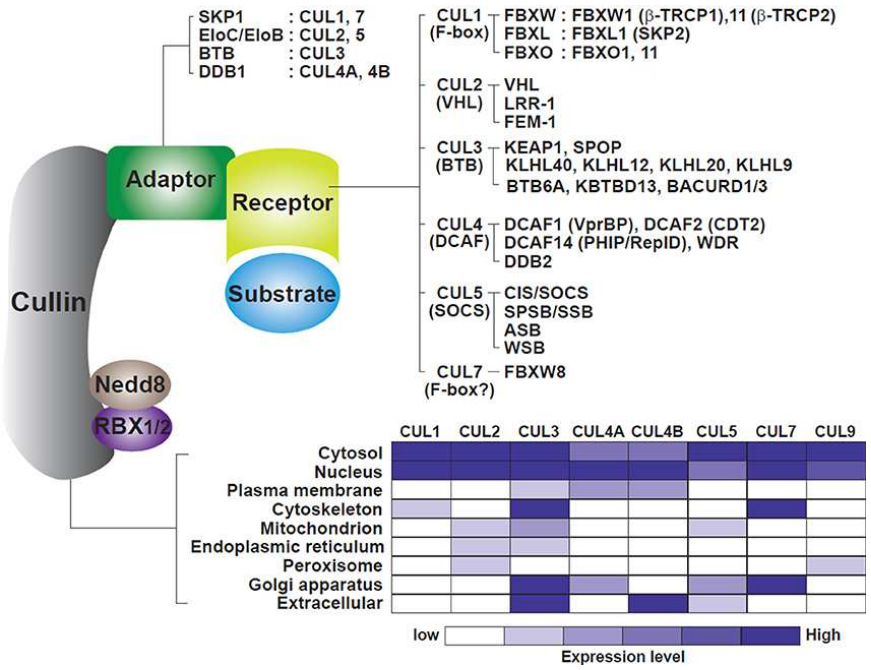

Figure I20. Cullin-RING ligase complexes (CRLs). Schematic diagram of the diversity of CRLs complexes. In general, they are composed by a RING finger protein (RBX1/2), a cullin scaffold protein (CUL1, -2, -3, -4A, -4B, -5, -7, -9), adaptors (SKP1, EloC/EloB, BTB, DDB1), and many different receptors that recognize the substrate (indicated in the image). The bottom part of the table depicts the cellular localization of the cullins[282].

Here, we will focus on the complexes termed **CUL4-RING E3 ubiquitin ligases (CRL4s),** which contain the core components RING protein **RBX1** (or **ROC1**), the cullin **CUL4,** and the adaptor protein **DDB1**. *Schizosaccharomyces pombe*, *C. elegans*, *Drosophila*, and *Arabidopsis* only have one cullin 4, but mammals have two different proteins, **CUL4A**

and **CUL4B**. Despite sharing 83% sequence identity, CUL4A and -4B have different substrates and are not entirely redundant. Interestingly, CUL4B, unlike CUL4A and other cullins, carries a nuclear localization signal (NLS) in its N-terminus that allows its nuclear localization[280,281,283,284].

In these complexes, cullins do not directly bind to the substrate, but use the adaptor **DDB1**. This protein was first discovered as the larger subunit of the heterodimeric UV-damaged DNA binding (UV-DDB) protein complex, which is important for regulating DNA damage repair. However, subsequent studies have demonstrated that beyond this function, it is also a key element in protein ubiquitination and is part of many CUL4-E3 ligases[280,285].

This linker protein DDB1 interacts with multiple **WD40 proteins**, the substrate receptors that eventually recognize the substrate. They can be referred to as DDB1-binding WD40 (**DWD**), DDB1–CUL4-associated factors (**DCAF**) or CUL4–DDB1-associated WDR (**CDW**) proteins. These proteins contain the **WD40 domain** formed by four or more WD repeats that fold around a central axis into a propeller-like structure. Several DDB1-WD40 proteins have been identified using proteomic, bioinformatic, and structural analyses, and it has been suggested that they have a relatively conserved WDXR motif. Additionally, it is possible that other factors or PTMs of DCAFs may also be required for the recruitment and proper presentation of the substrate to the E2 enzyme[285-289].

CRL4 complexes (containing either both CUL4A and CUL4B or only one of them) can ubiquitinate different substrates, many of which are related to chromatin. They can regulate either monoubiquitination, for example in histones, or polyubiquitination. This last modification may target proteins to degradation, such as the WDR5 protein[284], Cdt1[290], and DDB2[291], but it can also regulate other functions; for instance, polyubiquitination of the repair factor XPC[292] enhances its binding to chromatin, and polyubiquitination of histones might alter the chromatin structure[293-295].

Given its importance in the context of our results, we will focus on two E3 ligase complexes, the **CRL4B** and the **UV-RING1B** complexes, both of which are involved in the ubiquitination of histone H2A in lysine 119 (Figure I21).

The **CRL4B complex** comprises **DDB1, RBX1,** and **Cul4B** and can associate either with PHF1, which recognizes H4R3me2, or with PRC2, which is important for regulating gene repression and promoting tumorigenesis through H2AK119ub[293,296]. In addition, CRL4B interacts with SUV39H1, HP1, and DNMT3, facilitating H3K9me3 and DNA methylation and thus epigenetic silencing[297].

The **UV-RING1B** complex is formed by the **RING1B** E3 ligase (instead of RBX1), **CUL4B,** and both the **DDB1** and **DDB2** proteins. This complex catalyzes H2AK119ub and is important early during nucleotide excision repair (NER)[294]. Once incorporated, it is recognized by ZRF1, which acts as a switch factor to recruit other E3 ligases essential for repairing the DNA lesions.

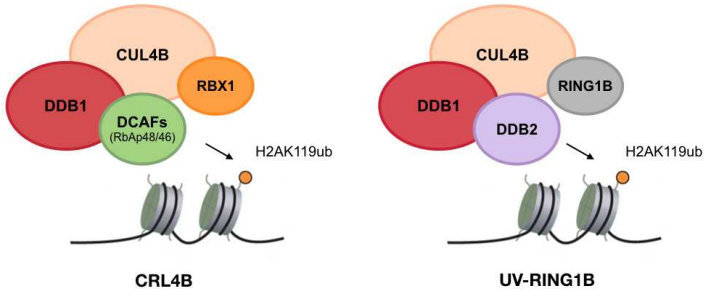

Figure I21. Cullin 4-RING E3 ubiquitin ligase (CRL4s) complexes involved in H2AK119ub. Schematic diagram of the two CRL4 complexes that ubiquitinate H2AK119, with their different subunits.

As previously mentioned, CRLs are also involved in cancer. They are overexpressed in several types of cancer and are important for regulating tumorigenesis through many different cellular mechanisms. They have been proposed as promising targets for cancer therapy, and recent studies have demonstrated that the genetic or pharmaceutical inactivation of CRLs can lead to cancer cell death[282].

7.2. H2AK119 ubiquitination

Ubiquitination of specific lysines on histone tails produces a large, bulky histone PTM as compared to others, such as methylation and acetylation. It consists of the conjugation of one or several ubiquitins, a 76-residue protein, which changes the overall conformation of the nucleosome. This PTM is reversible and can be eroded from target substrates by so-called de-ubiquitin enzymes (DUBs)[39,41].

Monoubiquitination of histone H2A is one of the most frequent type of nuclear proteins, and several complexes can catalyze it on different residues. K13 and K15 can be ubiquitinated by RNF8 and RNF168 during DNA damage. In contrast, BRCA-1 is involved in K127 and K129 ubiquitination, which is required for transcriptional silencing of pericentromeric DNA[298]. The most well-studied monoubiquitination of H2A is in the residue K119 (K118 in *Drosophila*, and not detected in yeast species)[299], and we will focus on this modification in this section.

Typically, **H2AK119ub** has been associated with the **PRC1** complex, formed by several subunits including the RING domain E3 ubiquitin ligases RING1B and RING1A. The PRC1 complex is recruited to chromatin downstream of H3K27me3 by PRC2, and it is involved in chromosome X inactivation and silencing of the *Hox* gene as well as of Polycomb-target genes[300-302].

However, depending on the context, other E3 enzymes can also mediate this H2AK119 ubiquitination[303]. Specifically, it can be mediated by: **CRL4B** and **UV-RING1B** complexes during tumorigenesis and NER, respectively; **LASU1** in testis[304]; **TRIM37** in association with PRC2 to silence genes in human cancer[305]; and the E3 ligase **2A-HUB**, which associates with the N-CoR/HDAC1/3 complex and works in the promoters of chemokine genes to repress their expression[306].

Since its identification, several studies have shown that H2AK119ub acts as a repressive histone modification. However, the underlying mechanism by which it exerts this silencing function remained unclear for a long time[303,307].

One possible mechanism is by preventing chromatin access to regulators of transcription. It has been described that H2AK119ub causes pausing of RNA PolII without affecting its initial recruitment, but by avoiding the recruitment of FACT (for “facilitates chromatin transcription”), consequently leading to the release of RNA Pol II at the early stage of elongation[306]. In addition, it has been proposed to inhibit MLL3-mediated H3K4me2/3, repressing transcription initiation but not elongation *in vitro*[308].

In response to photolesion-containing DNA, ubiquitination of H2A at Lys 119/Lys 120 is necessary for destabilization of nucleosomes and subsequent release of DDB1-DDB2-CUL4B, which allows the damaged DNA to be repaired[309].

Despite its role in transcriptional repression, H2AK119ub does not affect the intramolecular fiber folding of nucleosomal arrays *in vitro* at lower $MgCl_2$ concentrations, likely due to its position in the nucleosome[310]. Alternatively, it has been suggested to affect the higher-order chromatin structure that involves H1 and that occur with elevated salt concentrations. H2AK119ub enhances the binding of the linker histone H1 to reconstituted nucleosomes *in vitro* without affecting the positioning of the histone octamer[311]. In addition, mononucleosomes purified from K119R H2A lack histone H1, indicating that H2A deubiquitination might cause the dissociation of linker histones from the core nucleosomes[312].

OBJECTIVES

Oxidation of histone H3 by LOXL2 has been described to be important in TNBC cells for generating compacted heterochromatin regions. However, it is still unknown how this histone modification induces chromatin compaction, or how it can be maintained at high levels in cancer cells.

Thus, the general objective of this thesis is to further characterize which are the molecular mechanisms underlying LOXL2-dependent chromatin compaction.

To this aim, we focused on:

I. Identifying LOXL2 interactors and H3K4ox readers involved in the establishment and/or maintenance of heterochromatin;

II. Characterizing how these proteins regulate LOXL2 activity and changes in chromatin structure;

III. Assessing the biological relevance of LOXL2-dependent chromatin compaction through these proteins in TNBC cells.

RESULTS

1. LOXL2 interacts with RUVBL1, RUVBL2, BAF53A, and DMAP1

To characterize the molecular mechanisms involved in the induction of chromatin compaction by LOXL2 and H3K4ox, we first attempted to identify LOXL2 interactors that could contribute to this function. For this, we reanalyzed a tandem-affinity purification approach previously published by our laboratory (see Annex 1).

Analysis of the revisited list of putative interactors showed the presence of RUVBL1 and RUVBL2 (two members of the AAA+ family of ATPases), BAF53A/ACTL6A, and DMAP1 (Figure R1A).

All these proteins are components of both the SRCAP and TIP60 chromatin remodeling complexes (Figure R1B), which are known to regulate the exchange of the histone H2A for the histone variant H2A.Z[243]. Moreover, it has also been described that another subcomplex only formed by the subset of proteins found in this screening can also catalyzes the incorporation of H2A.Z *in vitro*[260].

Interestingly, this histone variant is known to regulate different conformational states and is important for the establishment of heterochromatin[121,279]. Hence, we hypothesize that LOXL2 could regulate chromatin structure through these partners and the deposition of the histone variant H2A.Z.

We confirmed LOXL2 interactions with RUVBL1, RUVBL2, BAF53A, and DMAP1 in HEK293T cells that ectopically expressed LOXL2-Flag. Specifically, co-immunoprecipitation assays showed that LOXL2-FLAG interacts with these endogenous proteins (Figure R1C).

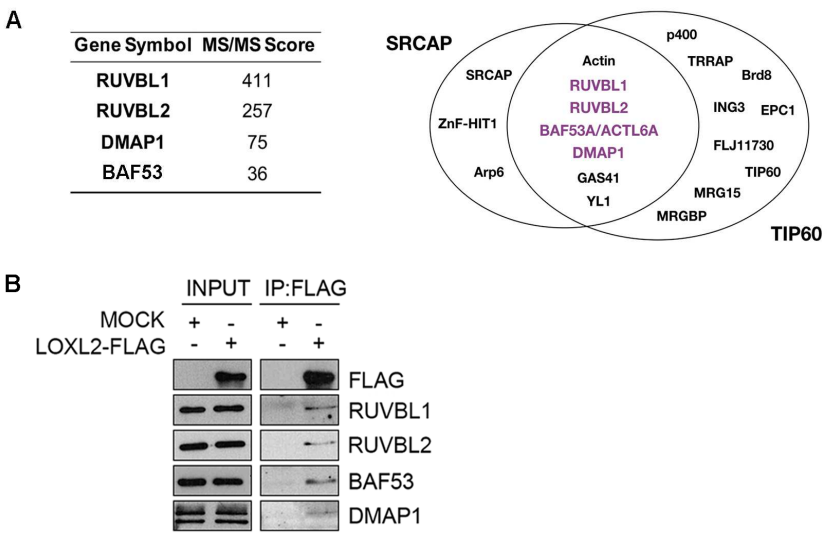

Figure R1. LOXL2 interacts with RUVBL1, RUVBL2, BAF53A, and DMAP1. A) Putative LOXL2 interactors identified in a previously published tandem-affinity purification approach and mass spectrometry (MS) analysis; MS score is shown (left panel). Schematic representation of SRCAP and TIP60 complexes with the identified LOXL2 partners in purple (right panel). **B)** Extracts from HEK293T cells transiently transfected with LOXL2-Flag or an empty vector were subjected to immunoprecipitation (IP) with Flag-M2 beads. Immunocomplexes were analyzed by Western blot using the indicated antibodies.

The RUVBL1 and RUVBL2 proteins are known to be essential for the proper assembly and functionality of some chromatin remodeling complexes[236,244]. However, as the presence of RUVBL2 is required to induce the conformational changes for ADP-ATP exchange[313], we performed loss- and gain-of-function experiments in the presence or absence of RUVBL2 to determine the relevance and contribution of this complex.

In fact, we observed that in HEK293T cells infected with a lentivirus carrying an irrelevant shRNA (shControl) or a shRNA for RUVBL2 (shRUVBL2), the complex was disrupted in the absence of RUVBL2, and that LOXL2 was no longer able to interact with these proteins (Figure 2B). Here it is important to mention that although the shRNA was specific for RUVBL2, RUVBL1 protein levels were also decreased in shRUVBL2 conditions, as it has been reported in other studies[314-316] (Figure R2A, R2B, left panel).

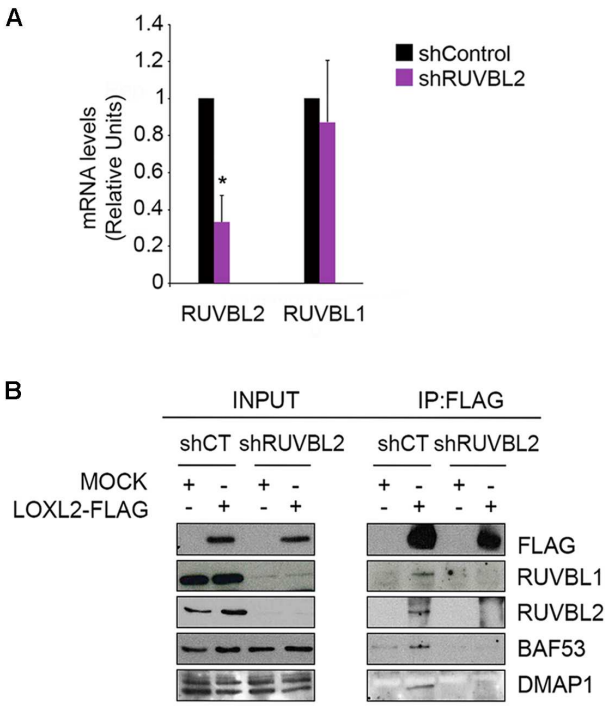

Figure R2. Knockdown of RUVBL2 disrupts the complex and interactions with LOXL2. A) mRNA levels of RUVBL1 and RUVBL2 analyzed by qRT-PCR in HEK293T cells with shControl or shRUVBL2. Gene expression was normalized to the *Pumilio* housekeeping gene and presented as the fold-change relative to the shControl cells, which was set as 1. Error bars indicate standard deviation in at least three experiments. *$p < 0.05$. **B)** HEK293T cells with shControl or shRUVBL2 were transiently transfected with LOXL2-Flag or an empty vector. Cell extracts were subjected to IP with Flag-M2 beads, and immunocomplexes were analyzed by Western blot using the indicated antibodies.

2. LOXL2 induction of chromatin compaction depends on RUVBL2 and H2A.Z

To investigate whether RUVBL2 is important for H3K4ox-mediated chromatin condensation, we analyzed the general chromatin status by micrococcal nuclease (MNase) digestion in HEK293T cells transfected with wild-type LOXL2 (LOXL2) or a LOXL2 mutant (LOXL2m) with compromised catalytic activity[147,202]. In this mutant, two histidine residues of the catalytic domain involved in copper binding were

changed to glutamine (H626Q, H628Q), and the tyrosine residue involved in the formation of lysyl tyrosylquinone cofactor, to phenylalanine (Y689F) (Figure R3A).

Analysis of MNase digestion patterns showed that in control conditions, when the active form of LOXL2 was overexpressed, cells were less sensitive to the enzyme, indicating increased chromatin compaction. In contrast, this increased compaction was not observed in the absence of RUVBL2, suggesting that this protein and the maintenance of the complex is necessary for LOXL2-mediated chromatin compaction (Figure R3B).

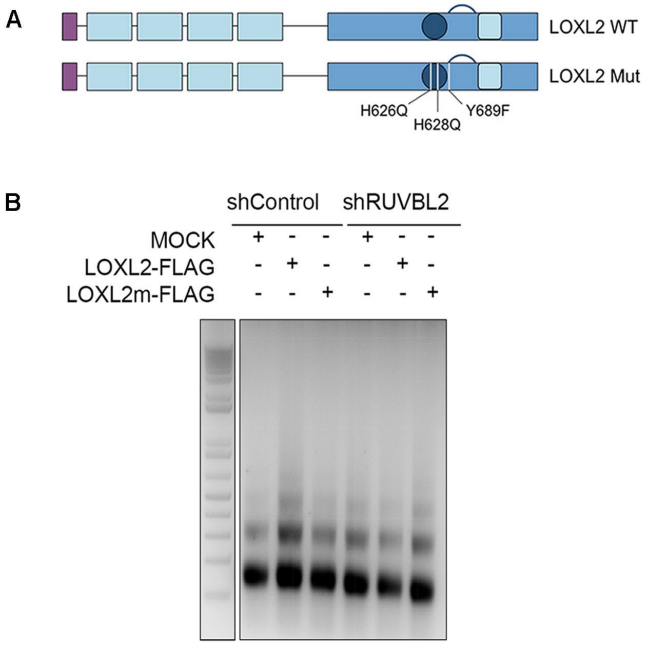

Figure R3. RUVBL2 is required for LOXL2-mediated chromatin compaction. A) Schematic representation of LOXL2 protein showing its main domains and point mutations in the mutant form. **B)** HEK293T with shControl or shRUVBL2 were transfected with wild-type LOXL2 (LOXL2), an inactive LOXL2 mutant (LOXL2m), or an empty vector (mock). Isolated nuclei were digested with micrococcal nuclease (MNase) for 2 min, and total genomic DNA was analyzed using agarose gel electrophoresis.

We then studied whether H2A.Z, the histone variant deposited by the RUVBL1/2 complex, was also required for this function. For this, we repeated the same experiment but down-regulated the H2A.Z.1 isoform (Figure R3A), as it is the one referred as “H2A.Z” in the studies that characterize its role in heterochromatin. MNase assays in shControl or shH2A.Z conditions showed that the induction of chromatin compaction after transfecting active LOXL2 was also blocked in the absence of H2A.Z (Figure R3B).

In summary, these results demonstrate that both RUVBL2 and the incorporation of H2A.Z are required for LOXL2 induction of chromatin compaction.

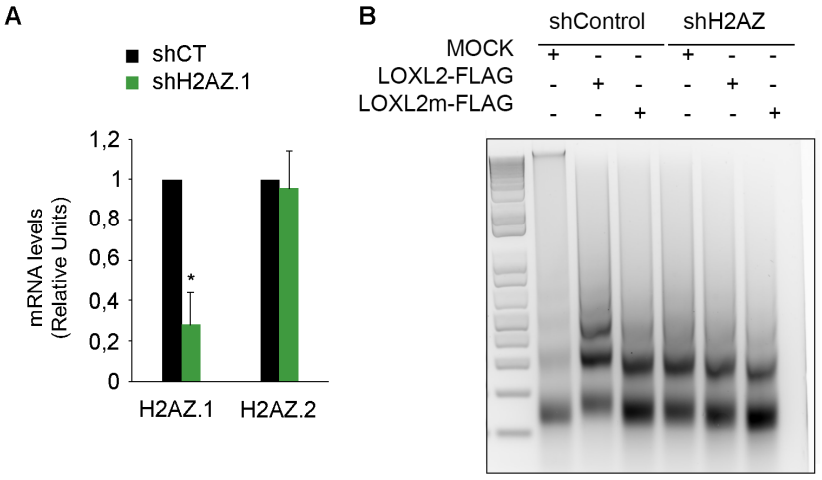

Figure R4. H2A.Z is equired for LOXL2-mediated chromatin compaction. A) mRNA levels of H2A.Z.1 and H2A.Z.2 analyzed by qRT-PCR in HEK293T cells with shControl or shH2A.Z.1. Gene expression was normalized to the *Pumilio* housekeeping gene and presented as the fold-change relative to the shControl cells, which was set as 1. Error bars indicate standard deviation in at least three experiments. *p < 0.05. **B)** HEK293T cells with shControl or shH2A.Z.1 were transfected with wild-type LOXL2 (LOXL2), inactive mutant LOXL2 (LOXL2m), or an empty vector (mock). Isolated nuclei were digested with micrococcal nuclease (MNase) for 2 min, and total genomic DNA was analyzed using agarose gel electrophoresis.

3. RUVBL2 and H2A.Z are required for maintaining LOXL2-dependent H3K4ox levels

At this point, we wondered if the presence of RUVBL2 is a requirement for allowing the oxidation reaction of H3K4 or its maintenance, and therefore for the induction of compacted chromatin. To address this, we performed *in vivo* and *in vitro* biochemical approaches.

HEK293T cells with control or RUVBL2 knocked-down were transfected with LOXL2 or LOXL2m, and the levels of H3K4ox were analyzed by Western blot. We observed that in the absence of RUVBL2, oxidation of histone H3 was blocked (Figure R5A). Furthermore, in agreement with the previous experiments, the presence of H2A.Z was also required for maintaining H3K4ox (Figure R5B). Here it is worth noting that, although loss-of-function experiments of H2A.Z were performed with a shRNA specific for the H2A.Z.1 isoform (Figure R4A), the antibody used for this histone variant recognizes both isoforms. Thus, a less strong decrease of H2A.Z was observed at protein level (Figure R5B) as well as in other antibody-based techniques performed in this study, such as ChIPs

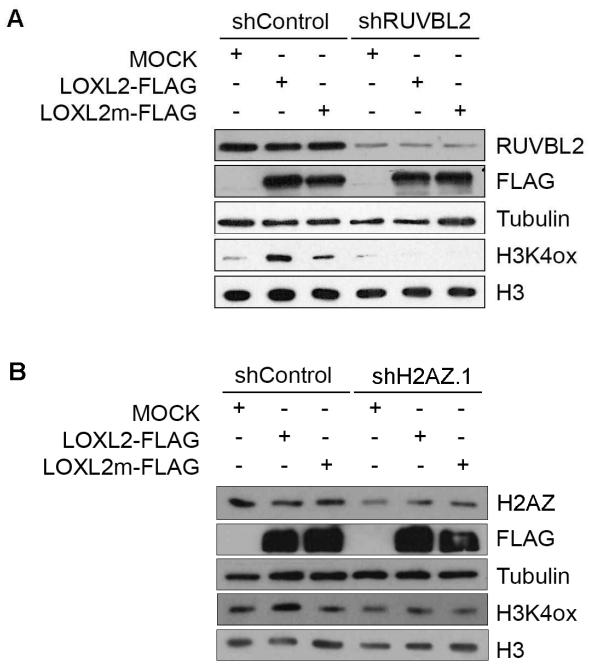

Figure R5. RUVBL2 and H2A.Z are required for LOXL2-mediated oxidation of histone H3. HEK293T cells with either shControl or shRUVBL2 **(A)** or shH2A.Z.1 **(B)** were transfected with wild-type LOXL2 (LOXL2), inactive mutant LOXL2 (LOXL2m), or an empty vector (mock). At 48 hr after transfection, total and histone extracts were obtained and analyzed by Western blot using the indicated antibodies.

In order to further confirm this result, and to elucidate whether the catalytic activity of RUVBL2 is required to maintain LOXL2-dependent oxidation, HEK293T cells were infected with shControl or shLOXL2 and transfected with an active RUVBL2 (RUVBL2) or the RUVBL2-D299N mutant (RUVBL2m). In this latter, a conserved aspartic acid residue in the Walker B motif was mutated to asparagine (D299N), resulting in deficient ATPase activity[317] (Figure R6A).

Western blot analyses showed that active RUVBL2 is needed for LOXL2-mediated oxidation of H3, and that its overexpression leads to increased levels of H3K4ox.

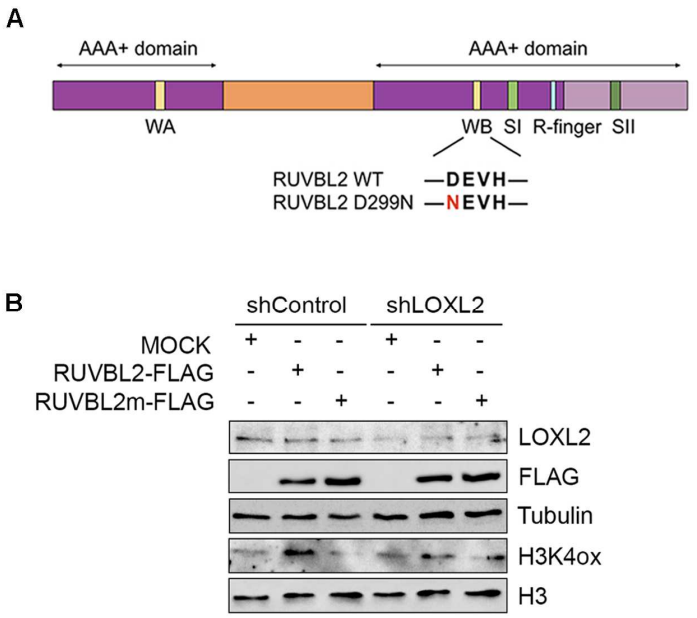

Figure R6. Active RUVBL2 is needed for LOXL2-mediated oxidation of histone H3. A) Schematic representation of the RUVBL2 protein, showing its main domains and the point mutation in the mutant form. **B)** HEK293T cells with shControl and shLOXL2 were transfected with wild-type RUVBL2 (RUVBL2), ATPase deficient mutant RUVBL2 (RUVBL2m), or empty vector (mock). At 48 hr after transfection, total and histone extracts were obtained and analyzed by Western blot using the indicated antibodies.

Based on the previous results, we wanted to understand why the presence and activity of RUVBL2 is needed for LOXL2-mediated H3K4 oxidation.

One possible explanation could be that RUVBL2 is required for LOXL2 enzymatic activity. In order to test this hypothesis, we performed *in vitro* reactions by incubating purified nucleosomes with the immunoprecipitated LOXL2-FLAG complex from HEK293T cells with shControl or shRUVBL2. We observed that LOXL2 was still able to oxidase nucleosomes in the absence of RUVBL2 (Figure R7A), indicating that this protein is not required for LOXL2 enzymatic activity. This result is consistent with previously published experiments in which recombinant LOXL2 could oxidize purified histones or nucleosomes *in vitro* without the presence of either RUVBL2 or ATP[147].

Alternatively, we speculated with the possibility that RUVBL2 was required to load LOXL2 into chromatin. Thus, LOXL2 levels in the chromatin fraction were analyzed by subcellular fractionation in shRUVBL2 and shH2A.Z conditions. To better study this effect, we used the TNBC cells MDA-MB-231 in this this experiment, which were previously characterized as expressing high levels of LOXL2 and H3K4ox[210]. Interestingly, in the absence of RUVBL2, reduced levels of LOXL2 in the chromatin fraction were detected, without affecting global levels of this protein (Figure R7B). In contrast, knockdown of H2A.Z did not affect the maintenance of LOXL2 in chromatin (Figure R7B), although it was also required for oxidation of histone H3 and chromatin compaction.

To further confirm this result, we attempted to perform ChIP experiments for LOXL2 in regions enriched with H3K4ox. However, the antibody did not work for this technique, and we were not able to successfully detect LOXL2 in chromatin.

Altogether, these results suggest that RUVBL2 regulates the maintenance of H3K4ox levels by affecting both LOXL2 recruitment into chromatin and changes in chromatin structure through the incorporation of the histone variant H2A.Z.

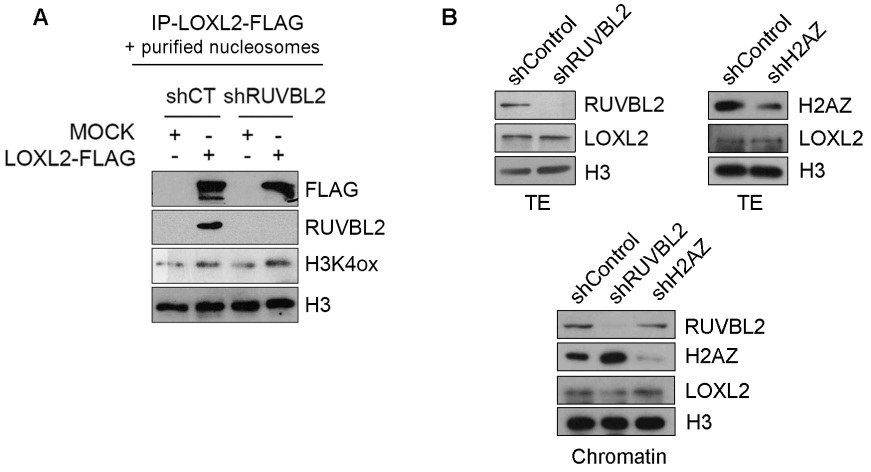

Figure R7. RUVBL2 is not required for LOXL2 enzymatic activity but affects LOXL2 recruitment into chromatin. A) HEK293T cells with shControl or shRUVBL2 were transfected with empty vector or LOXL2-FLAG. After 48 hr, co-immunoprecipitation assays with Flag-M2 were performed. Immunoprecipitated complexes were incubated with purified nucleosomes for 2 hr at 37ºC, and samples were analyzed by Western blot. **B)** Total extracts (upper panel) and **c**hromatin fraction obtained by subcellular fractionation assays (lower panel) of MDA-MB-231 cells with shControl, shRUVBL2, or shH2A.Z were analyzed by Western blot.

Finally, in order to study the dynamics of H3K4ox, we used SNAP-tag imaging to monitor the deposition of both newly synthesized H3.1 and H3.3 variants[318].

For this, we generated MDA-MB-231 cells stably expressing H3.1 or H3.3 fused to a SNAP polypeptide, which is an enzyme that covalently reacts with cell-permeable fluorescent substrates to enable the specific labelling of these proteins *in vivo*. Moreover, in this system, the pool of SNAP-tagged proteins can also be quenched by the non-fluorescent SNAP substrate bromothenylpteridine (BTP), allowing newly synthetized proteins after a given amount of time (chase).

First, we determined the conditions of this deposition assay. On the one hand, we performed a ‘‘pulse’’ with the red fluorescent substrate Tetramethylrhodamine (TMR) to label preexisting H3.1 and H3.3. On the other hand, we also included a quench-pulse control, labelling cells with TMR directly after the BTP treatment to ensure full quenching (Figure R8).

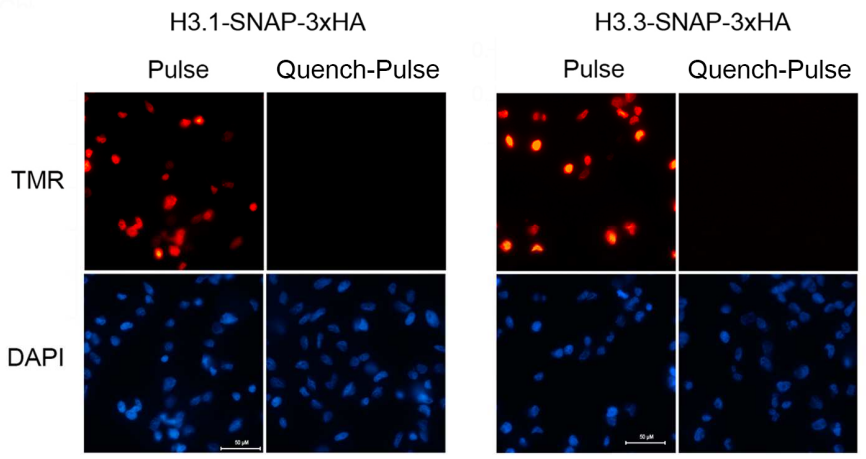

Figure R8. *In vivo* visualization assay for newly synthesized H3.1 and H3.3 deposition. Fluorescent microscopy visualization of MDA-MB-231 cells expressing H3.1/H3.3-SNAP after labeling assays with red fluorescent TMR-Star. The pulse labels pre-existing H3.1/3-SNAP, and the quench control ensures that treatment with a non-fluorescent block prevents the labeling with TMR-Star. Scale bars represent 50 µM.

Quench-chase-pulse assays were then performed in MDA-MB-231 cells stably expressing H3.1 or H3.3-SNAP in the absence of LOXL2 and RUVBL2. In these experiments, cells were treated with Triton X-100 before fixation to visualize only chromatin incorporated histones (Figure R9A). In addition, global levels of H3.1-SNAP and H3.3-SNAP were analyzed by Western blot to ensure that they were not affected in knockdown conditions (Figure R9B).

Notably, we observed a decrease in H3.1 and H3.3 deposition in the absence of RUVBL2 and LOXL2 (Figure R9C). These results suggest that H3 variants would be constantly exchanged when the levels of H3K4ox are high, and that LOXL2 would be actively reoxidizing histone H3.

To sum up, we demonstrated that LOXL2 interacts with RUVBL1, RUVBL2, DMAP1, and BAF53A in a RUVBL2-dependent manner, and that active RUVBL2 and H2A.Z incorporation are essential to maintain H3K4ox levels in chromatin and to induce LOXL2 mediated-chromatin condensation.

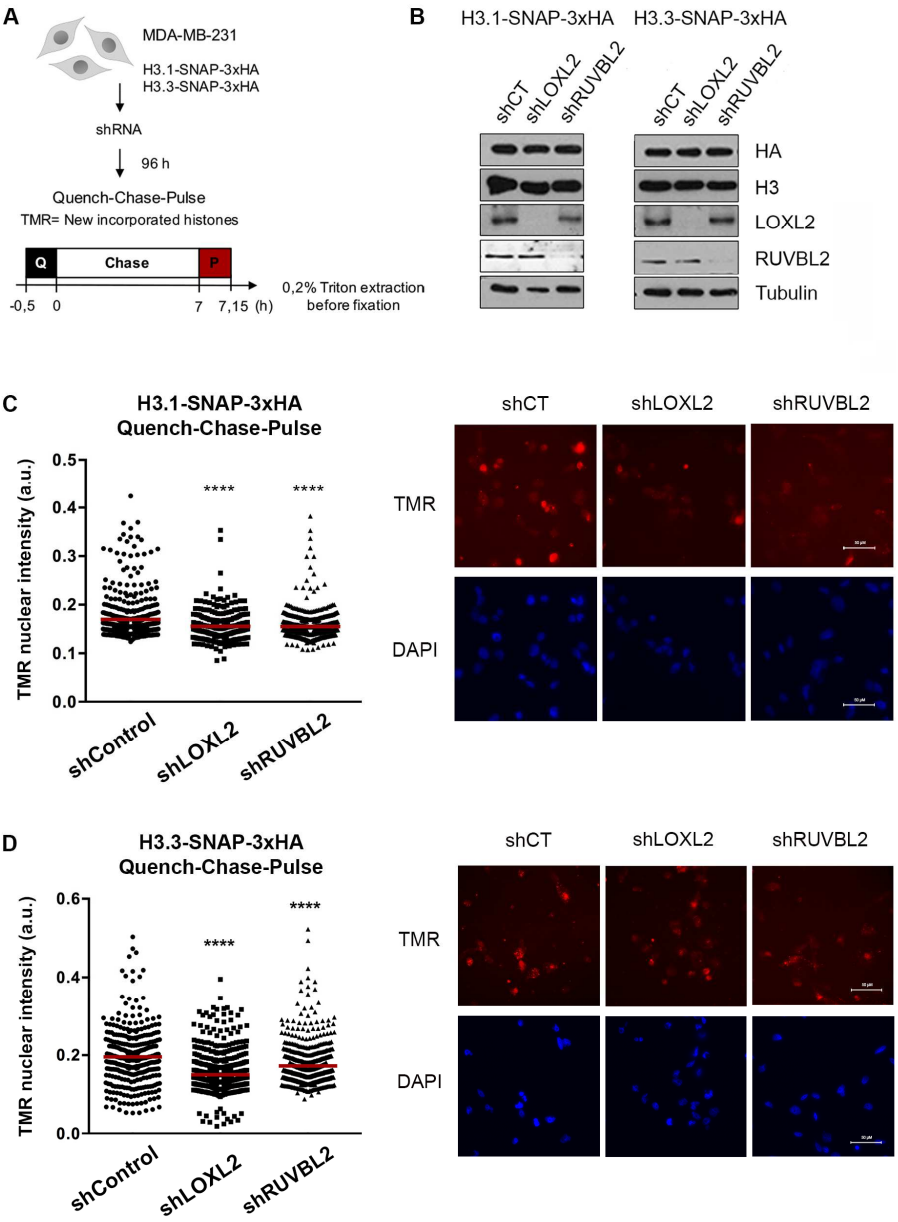
A
MDA-MB-231
H3.1-SNAP-3xHA
H3.3-SNAP-3xHA
shRNA
96 h
Quench-Chase-Pulse
TMR= New incorporated histones
Q
Chase
P
-0,5
0
7
7,15 (h)
0,2% Triton extraction
before fixation
B
H3.1-SNAP-3xHA
H3.3-SNAP-3xHA
shCT
shLOXL2
shRUVBL2
HA
H3
LOXL2
RUVBL2
Tubulin
C
H3.1-SNAP-3xHA
Quench-Chase-Pulse
TMR nuclear intensity (a.u.)
0.5
0.4
0.3
0.2
0.1
0.0
****
****
shControl
shLOXL2
shRUVBL2
shCT
shLOXL2
shRUVBL2
TMR
DAPI
D
H3.3-SNAP-3xHA
Quench-Chase-Pulse
TMR nuclear intensity (a.u.)
0.6
0.4
0.2
0.0
****
****
shControl
shLOXL2
shRUVBL2
shCT
shLOXL2
shRUVBL2
TMR
DAPI

Figure R9. RUVBL2 or LOXL2 knockdown affects H3 exchange. A) Experimental design for assaying histone incorporation in MDA-MB-231 cells stably expressing H3.1/3-SNAP. Cells were quenched with BTP, chased for 7 hr, and then pulsed with TMR-Star. **B)** Western blot analysis of whole-cell lysates of MDA-MB-231 stably expressing H3.1/3-SNAP at 96 hr after shRNA infection. **C)** High-throughput microscopy (HTM) analysis of quench-chase-pulse experiments for H3.1 and H3.3-SNAP. Quantification and images of one representative experiment are shown (at least 130 nuclei were analyzed). At least two independent experiments were performed. Scale bars represent 50 μM. Median is indicated in red. ***, $p < 0.001$; ****, $p < 0.0001$.

4. H3K4ox, RUVBL2, and H2A.Z are enriched in heterochromatin regions in TNBCs

Previous work in our laboratory showed that the TNBC cells MDA-MB-231 have high levels of LOXL2 and H3K4ox. Genome-wide experiments demonstrated that, in these cells, H3K4ox is enriched in heterochromatin regions and is important for regulating chromatin compaction[210].

The requirement of RUVBL2 and H2A.Z to maintain H3K4ox levels prompted us to investigate whether RUVBL2 and H2A.Z co-occupy the same chromatin regions as H3K4ox. To address this, ChIP-sequencing experiments for RUVBL2 and H2A.Z were performed in MDA-MB-231 cells.

In this study, genome-wide data of H2A.Z, RUVBL2 and H3K4ox (from *Cebrià-Costa et al.* [210]) was analyzed using multi-analysis alignment to include constitutive heterochromatin (repetitive sequences). Interestingly, we found that there is a strong overlap between H3K4ox and RUVBL2 (60% of total RUVBL2 peaks), and that 15% of these regions also contained H2A.Z (26% of total H2A.Z peaks) (Figure R10A). A total of 10,231 genomic regions showed co-occupancy of H3K4ox, RUVBL2, and H2A.Z. Additionally, as depicted in the heatmap, these regions were also enriched in H3K9me3 (ChIP from[319]; GSE85158), a distinctive histone modification of heterochromatin regions (Figure R10C, D). Gene ontology analysis showed that these common regions contain 2,267 genes involved in the regulation of calcium signaling, leukocyte differentiation, or nucleotide catabolism (Figure R10B).

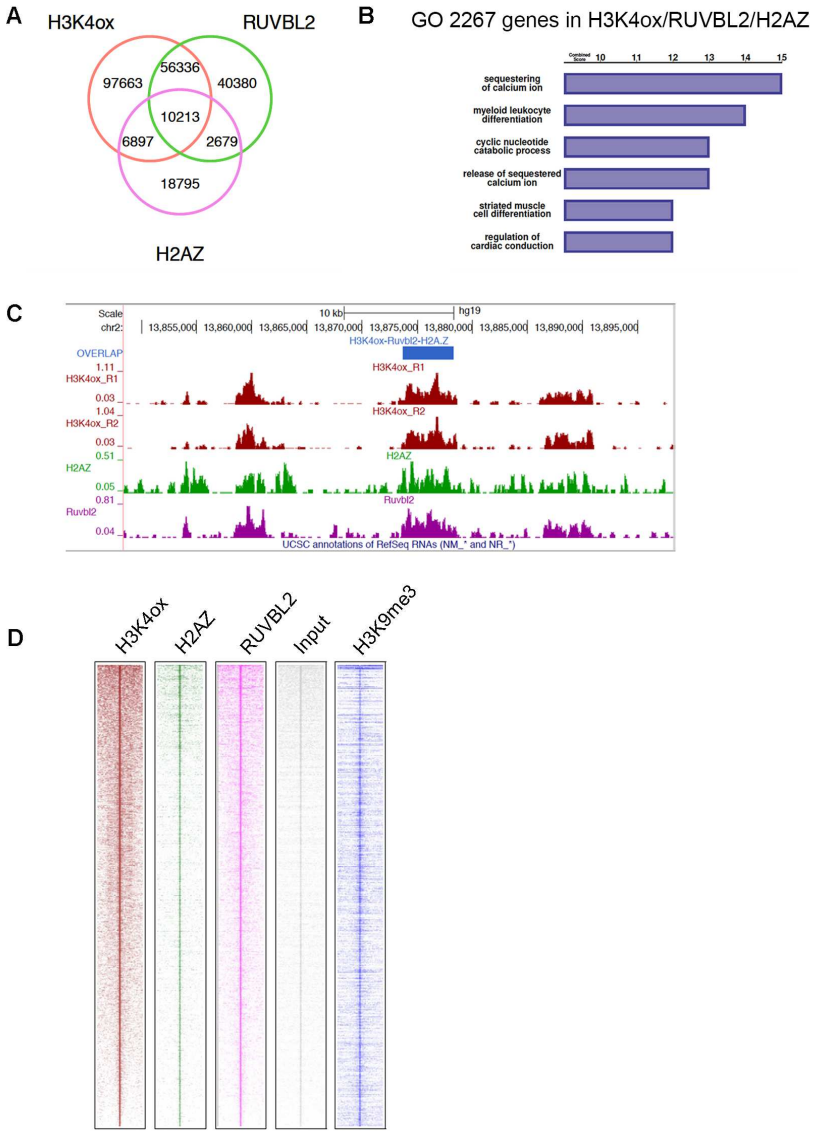

Figure R10. H3K4ox, RUVBL2, and H2A.Z localize in heterochromatin regions in MDA-231 cells. A) Venn diagram showing the overlap between H2A.Z, RUVBL2, and H3K4ox ChIP-seq peaks. **B)** Gene ontology analyses (biological process 2018) of 2,267 genes located in the common regions. **C)** UCSC Genome Browser overview of one region across chromosome 2 containing ChIP-seq profiles of H3K4ox (2 replicates, in red), H2A.Z (in green) and RUVBL2 (in purple). **D)** Heatmap of H3K4ox, H2A.Z, RUVBL2, input, and H3K9me3 in the 10,231 common genomic regions.

In addition, chromatin accessibility was analyzed by ATAC sequencing experiments in MDA-MB-231 cells with shControl or shRUVBL2.

In the absence of RUVBL2, an increase in ATAC signal was observed specifically in H3K4ox and H2A.Z peaks, further supporting the observation that RUVBL2 is important for regulating chromatin compaction (Figure R11). However, this tendency was not observed in the 10,231 common regions that contain H3K4ox, H2A.Z, and RUVBL2 (see Discussion). Interestingly, chromatin decorated with H3K27me3 and H3K9me3 was also more open in shRUVBL2 conditions, but no effect was observed after the knockdown in H3K4me3 peaks, which are open euchromatin regions with basal high ATAC signal.

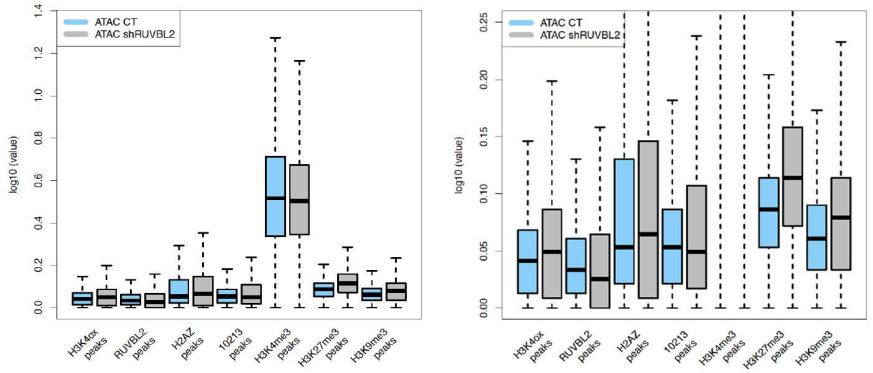

Figure R11. RUVBL2 regulates chromatin compaction in genomic regions enriched with H3K4ox, H2A.Z and selected chromatin marks. ATAC-sequencing signal on different set of ChIP-seq peaks in MDA-MB-231 cells shControl and shRUVBL2. From left to right: H3K4ox, RUVBL2, H2A.Z, 10213 peaks (common regions with H3K4ox, RUVBL2 and H2A.Z), H3K4me3, H3K27me3 and H3K9me3. Right panel is a zoom of the left one.

Transcriptome analysis done by RNA-seq revealed a considerable overlap between dysregulated genes in shLOXL2 and shRUVBL2, supporting the fact that they work together in chromatin. In particular, 37% and 22% of up- and downregulated genes in shLOXL2, respectively, were also up- or downregulated in shRUVBL2 (Figure R12A). Gene ontology analysis showed that common upregulated genes in shLOXL2 and shRUVBL2 were involved in positive regulation of macrophage migration and chemotaxis as well as apoptotic signaling pathways (Figure R12B). On the other hand, the common downregulated genes were related to G1/S transition of mitotic cell cycle, DNA replication and DNA checkpoints (Figure R12C). Some identified genes in the RNA-sequencing were validated by RT-qPCR (see Annex 3). However, these genes were not located in the common chromatin regions (Figure R12D), suggesting that H3K4ox maintenance through RUVBL2 and H2A.Z is not implicated directly in gene expression regulation, but it affects chromatin structure, consistent with ATAC-sequencing results.

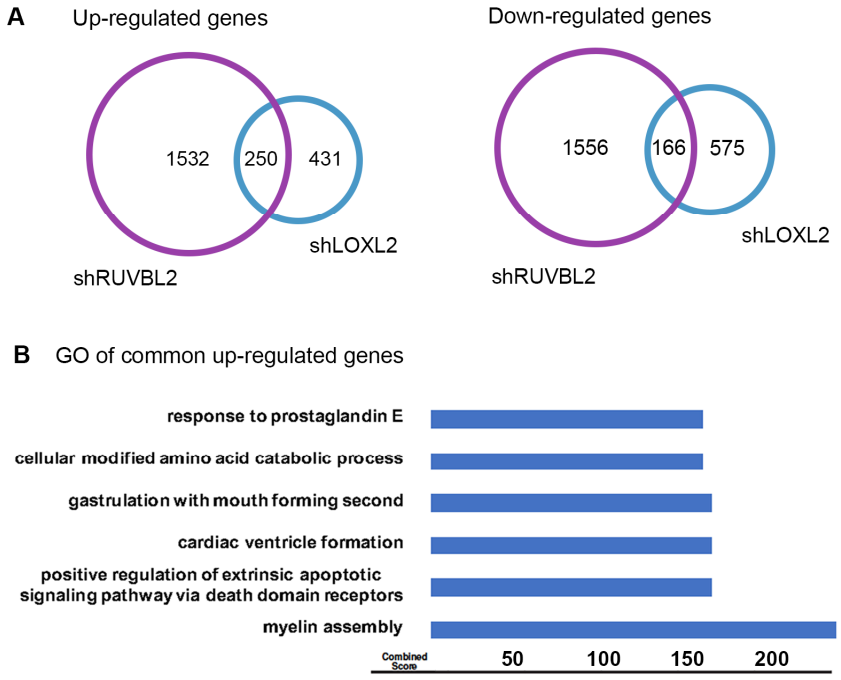

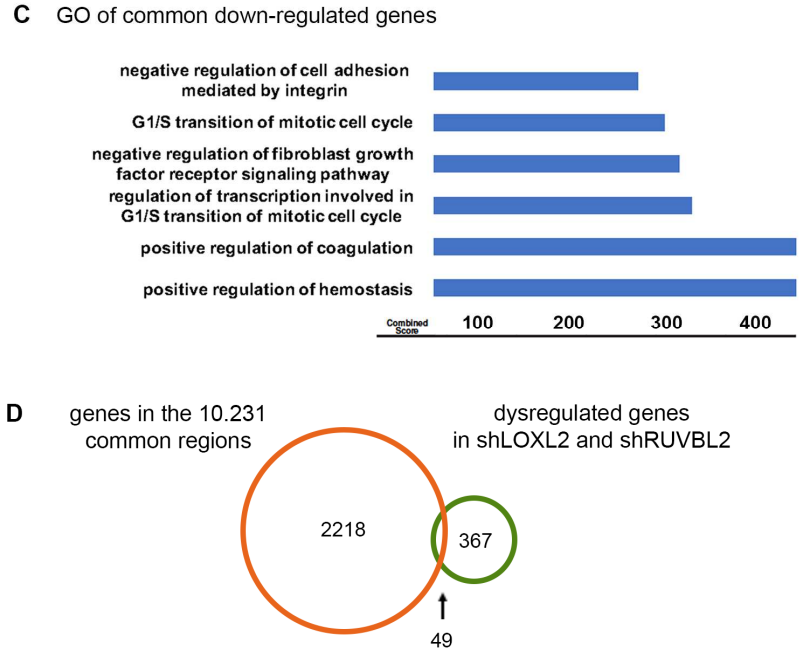

Figure R12. Common dysregulated genes in shRUVBL2 and shLOXL2. A) Venn diagram showing the overlap between up-regulated (left) and down-regulated (right) genes in MDA-MB-231 shRUVBL2 or shLOXL2. **B, C)** Gene ontology analysis (biological process 2018) of the common upregulated genes (B) and the common downregulated genes (C). **D)** Venn diagram showing the overlap between the 2.267 genes embedded in the 10,231 common genomic regions (orange) and common dysregulated genes (both up- and down-regulated) in MDA-MB-231 transfected with shRUVBL2 or shLOXL2 (green).

At this point, in order to both validate ChIP-sequencing analysis and better define how RUVBL2 and LOXL2 function in these heterochromatin regions, we performed ChIP-PCR experiments in the absence of these proteins. Thus, a set of primers named as hits were designed in the common regions with H3K4ox, H2A.Z, and RUVBL2.

As expected, in shLOXL2 conditions, the H3K4ox amount in chromatin was decreased. Concomitantly, we also observed less H2A.Z and RUVBL2 recruitment (Figure R13C); this latter result also was demonstrated by subcellular fractionation assays (Figure R13B). Moreover, global levels of RUVBL1/2 were not affected in the absence of LOXL2, further supporting this loss of binding (Figure R13A, B).

Similarly, downregulation of RUVBL2 did not affect the amount of LOXL2 protein and RNA, but decreased H2A.Z deposition and H3K4ox levels in heterochromatin regions (Figure R14, R7B). This result is consistent with the fact that, in the absence of RUVBL2, there is less LOXL2 recruitment in chromatin (R7B).

Furthermore, ChIP-PCR experiments in the absence of H2A.Z reinforced our previous results, demonstrating that this histone variant is required to maintain oxidation of histone H3 in these regions (Figure R15).

It is worth mentioning that Figures R12, R13, and R14 show the results of ChIP-PCR experiments expressed as a fold-change of the percent input in knockdown conditions as compared to shControl (set as 1). However, all of them were also performed with irrelevant immunoglobulins (IgGs) to demonstrate specific binding of the proteins in these genomic regions (see Annex 4 for representative examples of positive binding of these proteins in shControl conditions). In addition, a region of the RNA polymerase II (RNAPII) promoter was used as a negative control for ChIP-PCR experiments of H3K4ox and RUVBL2, but not for H2A.Z, since this histone variant can be located in this region. Despite showing a statistically significant difference after protein downregulation in some cases, the percentage of input in shControl conditions was very low and similar to the one for IgGs; thus, we do not consider positive binding of RUVBL2 and H3K4ox in this region.

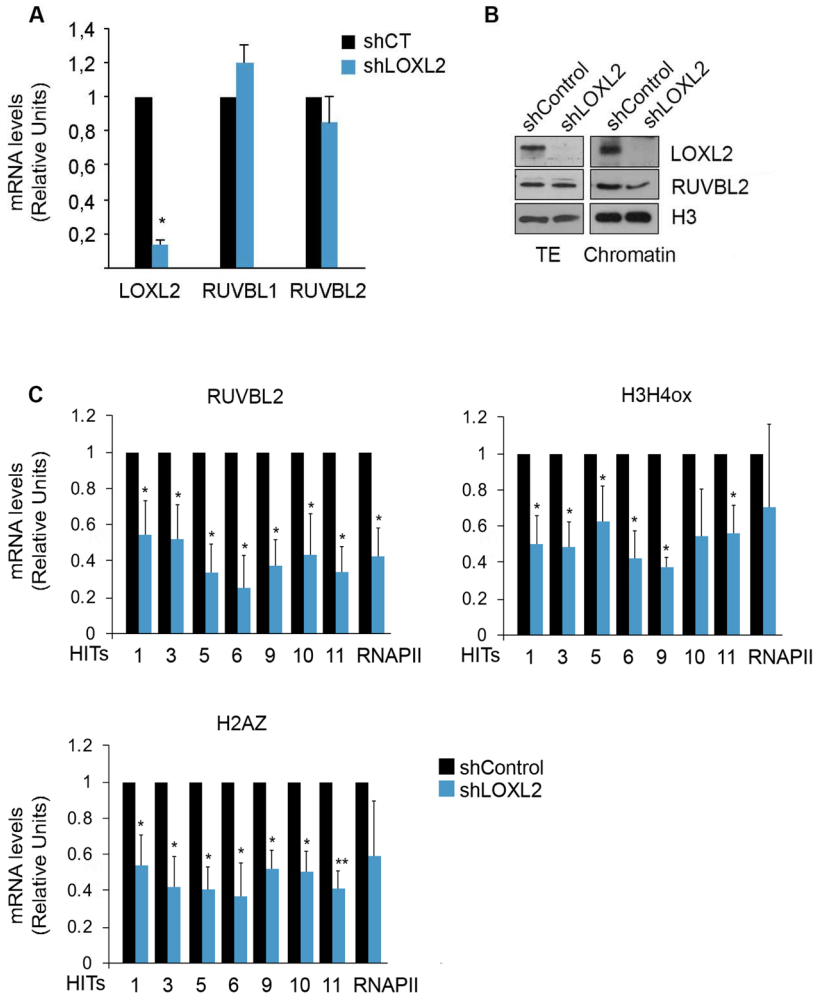

Figure R13. LOXL2 regulates H3K4ox, RUVBL2 and H2A.Z occupancy in heterochromatin regions of MDA-MB-231 cells. All the experiments were performed in MDA-MB-231 cells shControl and shLOXL2. **A)** mRNA levels of LOXL2, RUVBL1 and RUVBL2 were analyzed by qRT-PCR. Gene expression was normalized to the Pumilio housekeeping gene and presented as the fold-change relative to the shControl cells. **B)** Chromatin fraction obtained by subcellular fractionation assays (left panel) and total extracts (right panel) were analyzed by Western blot. **C)** ChIP-PCR experiments of RUVBL2, H3K4ox and H2A.Z in selected regions (hits) and in the RNAPII promoter, which was used as a negative control for H3K4ox and RUVBL2. Data of qPCR amplifications were normalized to the input and to total immunoprecipitated H3 for H3K4ox. Results are expressed as a fold-change relative to the data obtained in shControl. Error bars indicate SD in at least three experiments *$p < 0.05$, **$p \leq 0.01$.

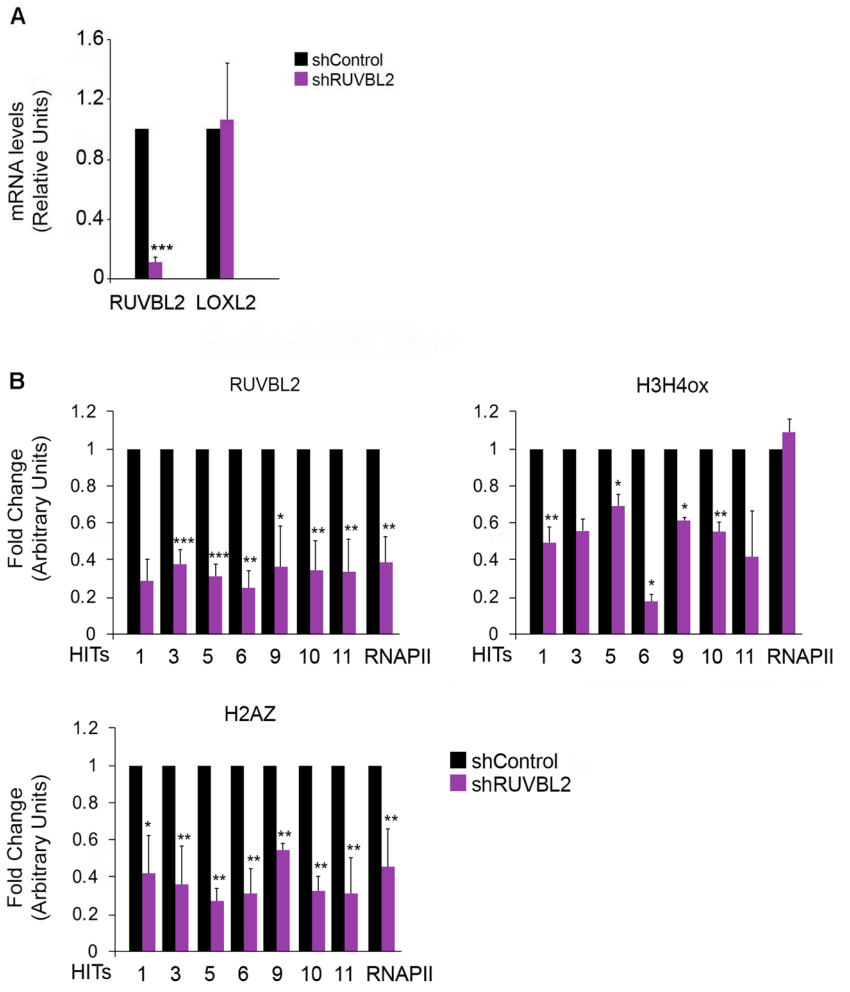

Figure R14. RUVBL2 regulates H3K4ox, RUVBL2 and H2A.Z occupancy in heterochromatin regions of MDA-MB-231 cells. Experiments were performed in MDA-MB-231 cells shControl and shRUVBL2. **A)** mRNA levels of LOXL2 and RUVBL2 were analyzed by qRT-PCR. Gene expression was normalized to the *HPRT* housekeeping gene and presented as the fold-change relative to the shControl cells. **B)** ChIP-PCR experiments of RUVBL2, H3K4ox and H2A.Z in selected regions (hits) and RNA pol II promoter (RNAPII), which was used as a negative control for H3K4ox and RUVBL2. Data of qPCR amplifications were normalized to the input and to total immunoprecipitated H3 for H3K4ox. Results are expressed as a fold change relative to the data obtained in shControl. Error bars indicate SD in at least three experiments *$p < 0.05$, **$p \leq 0.01$, ***$p \leq 0.001$.

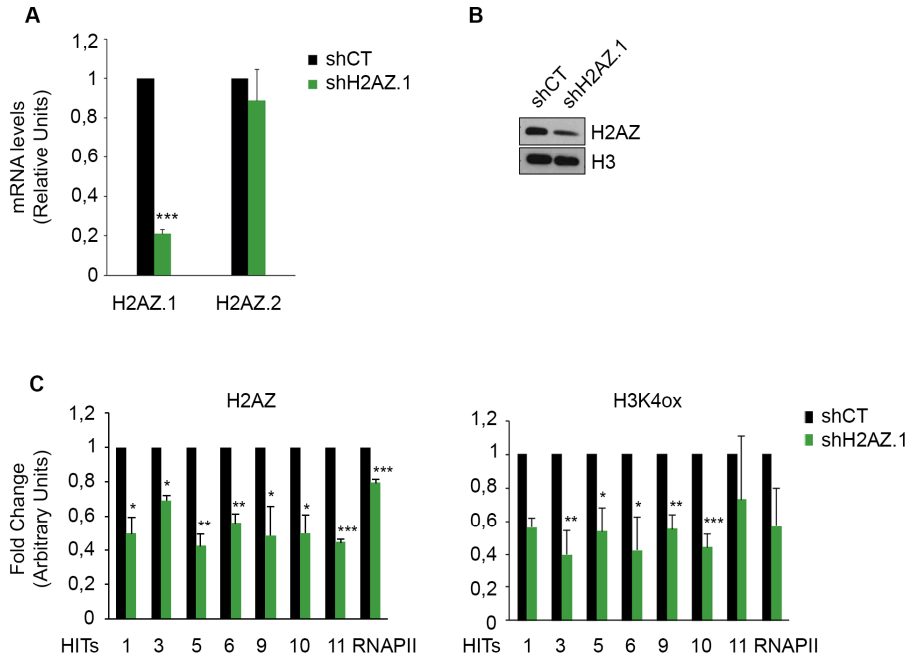

Figure R15. H2A.Z regulates H3K4ox occupancy in heterochromatin regions of MDA-MB-231 cells. Experiments were performed in MDA-MB-231 cells with shControl or shH2A.Z.1. **A)** mRNA levels of H2A.Z.1 and H2A.Z.2 were analyzed by qRT-PCR. Gene expression was normalized to the *Pumilio* housekeeping gene and is presented as the fold-change relative to shControl cells. **B)** Total extracts were analyzed by Western blot. **C)** ChIP-PCR experiments of H2A.Z and H3K4ox in selected regions (hits) and RNAPII promoter (RNAPII), which was used as a negative control for H3K4ox. Data of qPCR amplifications were normalized to the input and to total immunoprecipitated H3 for H3K4ox. Results are expressed as a fold change relative to the data obtained in shControl. Error bars indicate SD from at least three experiments. Note that although the shRNA specifically targeted H2A.Z.1, the antibody used for Western blot and ChIP-PCR experiments recognized both H2A.Z.1 and H2A.Z.2. *$p < 0.05$, **$p \leq 0.01$.

Finally, to further analyze the effect on H2A.Z incorporation, we monitored newly synthetized H2A.Z.1 and H2A.Z.2 in the absence of RUVBL2 and LOXL2, again using the SNAP-tag system (Figure R16A).

Surprisingly, quench-chase-pulse experiments showed that in the absence of RUVBL2, more H2A.Z.1 and H2A.Z.2 were incorporated into chromatin than under control condition (Figure R16B). In addition, the same tendency was observed in subcellular fractionation experiments analyzed by Western blot (Figure R16C). This effect was unexpected considering the previous ChIP-PCR experiments in heterochromatin regions, but suggests that in the absence of RUVBL2, the incorporation of this histone variant in chromatin becomes massively altered.

In contrast, only a slight increase or no significant differences were observed after H2A.Z.1 or H2A.Z.2 incorporation, respectively, after LOXL2 knockdown, suggesting that LOXL2 effect on H2A.Z is probably restricted to specific genomic regions.

In summary, results in this section reinforce the previous biochemical data and further demonstrate that in TNBC cells, LOXL2 and RUVBL2 work together in heterochromatin regions to regulate the deposition of H2A.Z and to maintain high levels of H3K4ox promoting chromatin compaction.

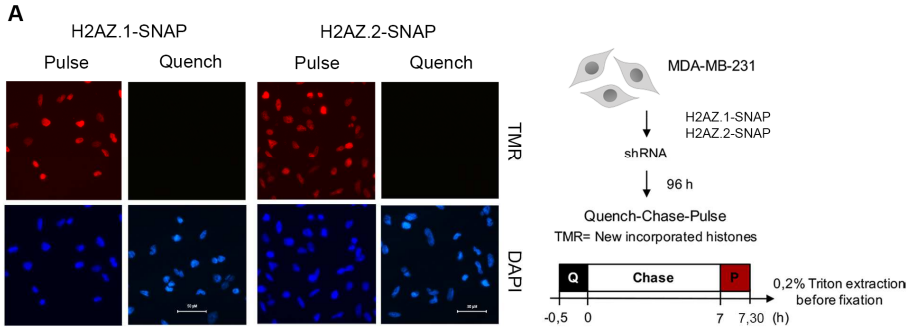

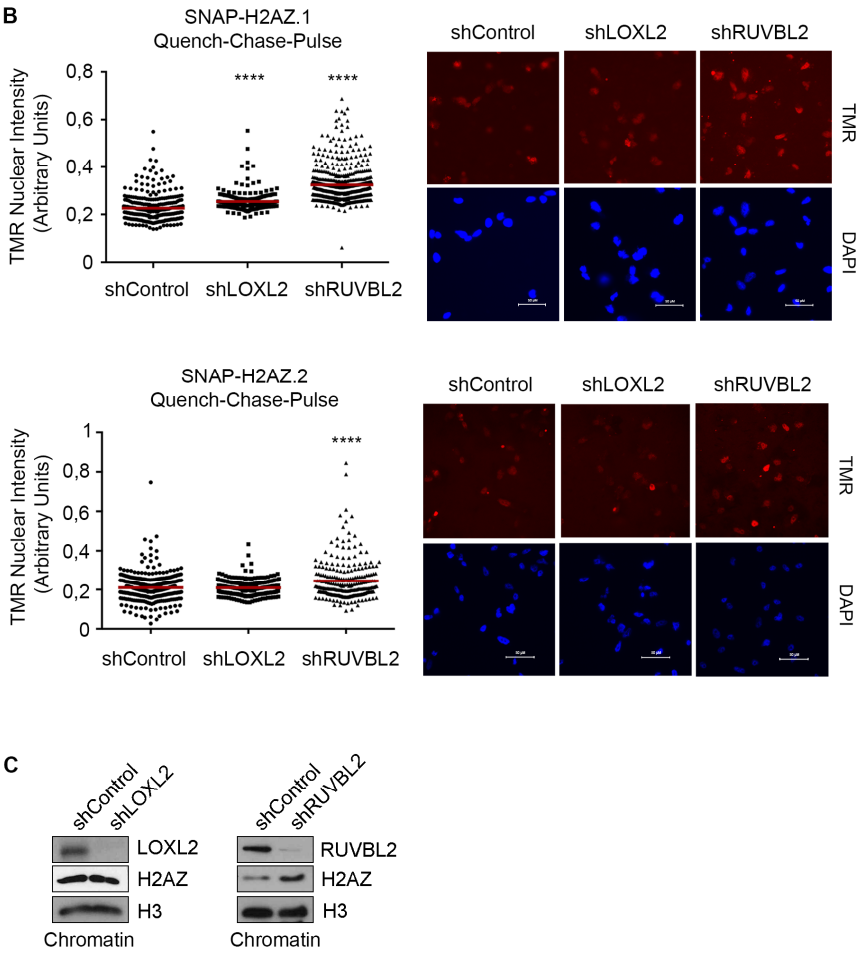

Figure R16. Knockdown of RUVBL2 massively affects the incorporation of H2A.Z. A) Experimental design for assaying histone incorporation in MDA-MB-231 cells stably expressing H2A.Z.1/2-SNAP. Cells were quenched with BTP, chased for 7 hr, and then pulsed with TMR-Star (right panel). Technical controls: pulse with TMR star to label pre-existing H2A.Z.1/2-SNAP and quench control to ensure fully quenching (left panel). **B)** High-throughput microscopy (HTM) analysis of quench-chase-pulse experiments for H2A.Z.1/2-SNAP. Quantification and images of one representative experiment are shown (at least 240 nuclei were analyzed). Scale bars represent 50 µM. At least two independent experiments were performed. Median is indicated in red. ****, $p < 0.0001$. **C)** Chromatin fraction obtained by subcellular fractionation assays was analyzed by Western blot.

5. DDB1 is a putative H3K4ox reader involved in the ubiquitination of histone H2A through RBX1

In order to better understand the molecular mechanism by which H3K4ox maintains chromatin in a compacted state, we performed pulldown experiments followed by mass-spectrometry to identify putative readers of H3K4ox.

As the aldehyde group generated in the histone H3 tail after LOXL2 oxidation is highly reactive, it is not possible to produce a H3 peptide with this modification[147,210]. Therefore, we synthetized a biotinylated-H3 peptide containing the artificial amino acid 6-hydroxy-norleucine in position 4, which resembles the intermediate alcohol oxidized during LOXL2 reaction (Figure R17B). As a control, we used an irrelevant biotinylated peptide.

Briefly, peptides were immobilized with streptavidin beads, washed and incubated with MDA-MB-231 nuclear extracts. Bound proteins were subjected to trypsin digestion and analyzed by liquid chromatography-tandem mass spectrometry (LC-MS/MS) (Figure R17A). Dot blot experiments were performed to ensure that the two peptides were equally recovered (Figure R17C).

We identified 77 putative readers of H3K4ox in MDA-MB-231 nuclear extracts (Figure R17C and Annex 2). Figure R17D depicts the peptide-pulldown interaction plot, showing the putative readers in the upper right part. Background proteins are clustered together around the origin of the plot.

Among the most enriched H3K4ox readers, we identified the DNA damage binding protein 1 (DDB1), a component of the cullin4 E3-ubiquitin ligase complexes (CRL4), together with CUL4A or CUL4B, WDR-domain–containing proteins (DCAFs) and a RING finger protein (RING1B or RBX1)[280,281]. Furthermore, many WDR-domain containing proteins were also found as putative readers. (Figure R17D).

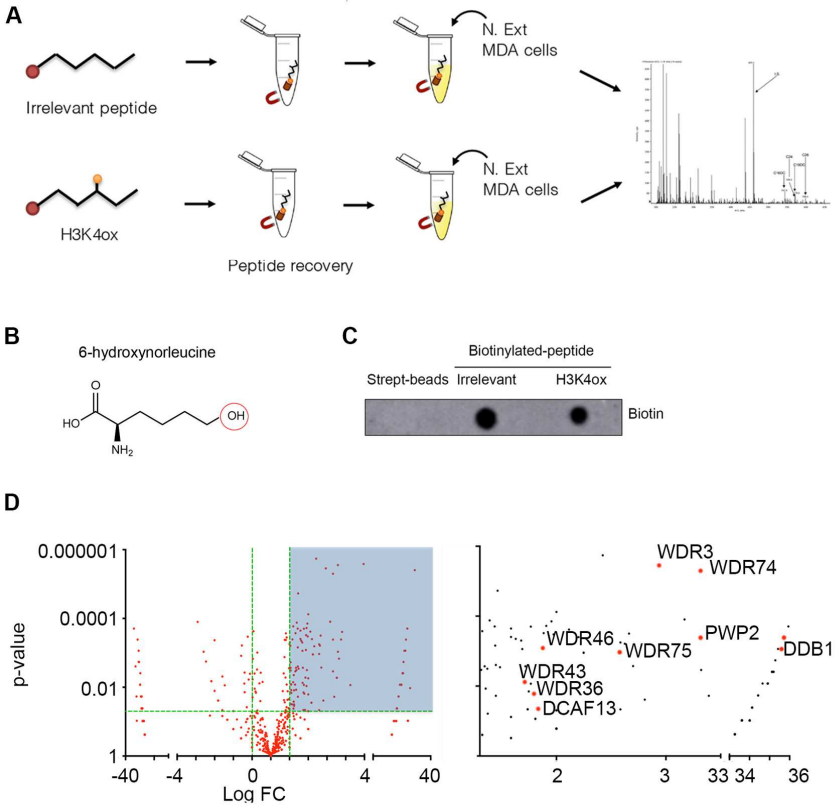

Figure R17. Identification of H3K4ox readers. A) Schematic representation of the experimental approach used to identify putative H3K4ox readers. **B)** Artificial amino acid 6-hydroxy-norleucine, the intermediate alcohol that is oxidized during LOXL2 reaction, which was added in the position 4 of the biotinylated H3 peptide. **C)** Control of biotinylated peptides recovery. **D)** Peptide pulldown interaction plot, showing the putative H3K4ox readers in the upper right part (right panel). The zoom of the highlighted graph area shows the identified proteins (left panel).

As explained in the Introduction, a huge number of CRL4 complexes have been identified so far, with specificity for many different substrates. Among them, the DDB1-CUL4B-RBX1 (CRL4B) and DDB1-CUL4B-RING1B (UV-RING1B) complexes were particularly interesting in this context, as they have been described to monoubiquitinate H2A[293,294]. This histone modification mediates transcriptional repression and

regulates chromatin accessibility during DNA repair in response to UV-induced DNA damage[303,307,309].

First, we studied if DDB1 recruitment into chromatin fraction depends on H3K4ox. Subcellular fractionation assays were performed both overexpressing LOXL2-FLAG in HEK293T cells and downregulating LOXL2 in MDA-231 cells, which leads to an increase or decrease of H3K4ox levels, respectively. We observed that DDB1 recruitment into chromatin fraction was totally associated with the levels of this histone modification supporting the role of DDB1 as a H3K4ox reader. In addition, global levels of DDB1 in these conditions did not showed such pronounced changes, reinforcing the fact that DDB1 recruitment to chromatin depends on H3K4ox (Figure R18A).

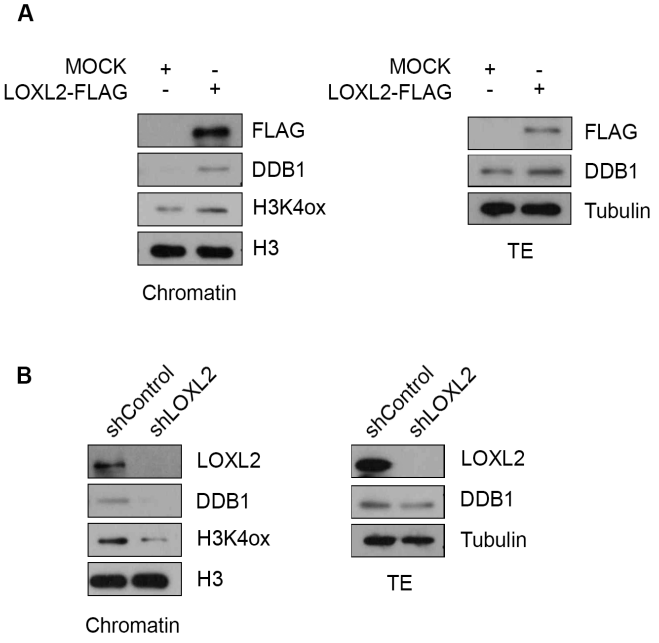

Figure R18. DDB1 recruitment into chromatin is associated with oxidation of histone H3. Western blot analysis of total extracts (right panels) and chromatin fraction obtained by subcellular fractionation assays (left panels). **A)** HEK293T cells were transfected with an empty vector or LOXL2-FLAG and cell extracts were obtained 48 hr later. **B)** MDA-MB-231 cells were infected with shControl and shLOXL2 and selected for 96 hr.

To strengthen our theory, co-immunoprecipitation experiments were performed in MDA-MB-231 cells. We observed that DDB1 interacts with H3K4ox in the presence or absence of ethidium bromide (EtBr) and therefore independently of DNA (Figure R19A, B).

Moreover, additional co-immunoprecipitation assays showed that oxidized H3 and DDB1 also interact with RING1B and RBX1, the two RING-domain proteins of the CRL4 complex. This association could be detected both pulling down DDB1 (Figure R19C) and H3K4ox (Figure R19D).

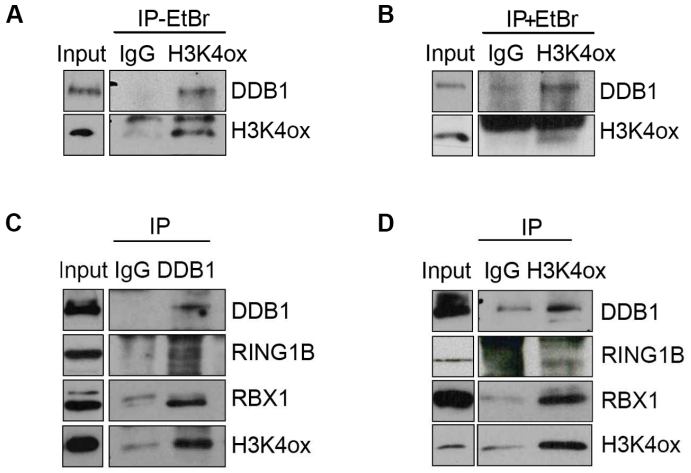

Figure R19. H3K4ox interacts with DDB1, RBX1 and RING1B. Co-immunoprecipitation assays with MDA-MB-231 nuclear extracts. H3K4ox interacts with DDB1 in the presence **(A)** or absence **(B)** of ethidium bromide. Additional experiments pulling down DDB1 **(C)** or H3K4ox **(D)** were performed. Immunocomplexes were analyzed by Western blot using the indicated antibodies.

Considering these data, we wanted to further study the recruitment of this complex in chromatin and its function after oxidation of histone H3. Thus, we performed chromatin association assays in HEK293T cells transfecting LOXL2 and obtaining crosslinked chromatin fractions at different time points. We observed that upon LOXL2 transfection, H3K4ox levels increased concomitant with DDB1, RUVBL2, and H2A.Z. In contrast, RING1B and RBX1 levels in chromatin remained constant during all the experiment. Interestingly, monoubiquitination of H2A (ubH2A) was also accumulated in chromatin fraction (Figure R20A). Subcellular fractionation experiments in non-crosslinked cells confirmed this result, showing an increase in ubH2A levels after LOXL2 overexpression (Figure R20B).

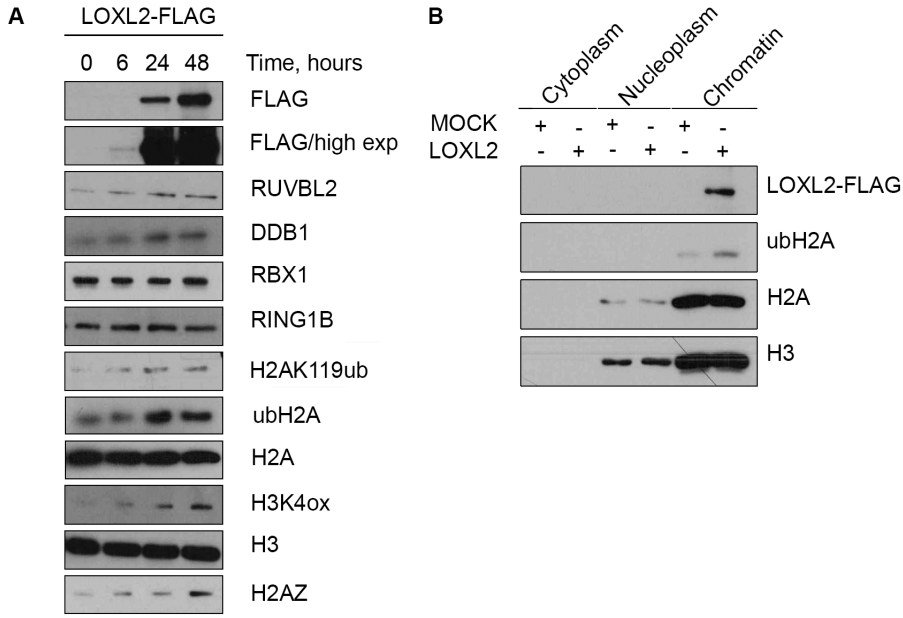

Figure R20. LOXL2 oxidation of histone H3 is linked to ubiquitination of H2A. **A)** HEK293T cells were transfected with LOXL2-FLAG and chromatin association assays were performed at 0, 6, 24, and 48 hr post-transfection. **B)** Subcellular fractionation assay 48 hr after transfecting HEK293T with LOXL2-FLAG or an empty vector. Protein levels were analyzed by Western blot using the indicated antibodies.

Finally, we asked which complex mediates the ubiquitination of H2A after LOXL2 oxidation of H3K4ox. We repeated these experiments in 293T cells infected either with RBX1 (shRBX1) or RING1B (shRING1B), the two RING finger proteins that differentiate CRL4B and UV-RING1B complexes, respectively. Chromatin association and subcellular fractionation experiments revealed that when RBX1 was knocked down, the increase in the levels of ubH2A after LOXL2-transfection was completely abrogated (Figure R21A). However, this LOXL2-mediated ubiquitination of H2A was RING1B independent (Figure R21B)

To further confirm this result, shRBX1 cells were transfected with ectopic RBX1, and the levels of ubH2A were analyzed by Western blot. Importantly, RBX1 was able to rescue ubH2A levels in the presence of LOXL2 in shRBX1 cells (Figure R21C).

In sum, we found that upon oxidation of H3 by LOXL2, the members of the CRL4B complex DDB1 and RBX1 are recruited to chromatin and regulate the ubiquitination of H2A.

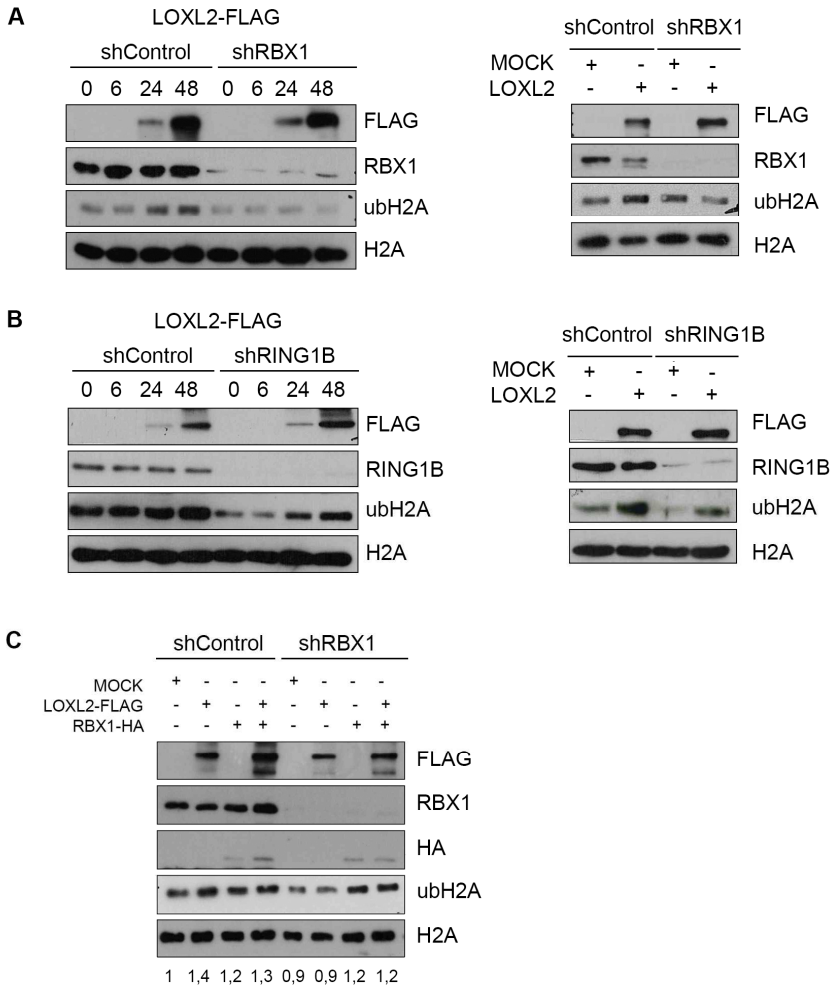

Figure R21. RBX1 regulates LOXL2-dependent ubiquitination of histone H2A. HEK293T cells shControl and shRBX1 **(A)** or shRING1B **(B)** were transfected with LOXL2-FLAG and chromatin association assays were performed at 0, 6, 24, and 48 hr post-transfection (left panels)**.** Additionally, cells were transfected with LOXL2-FLAG or an empty vector to do subcellular fractionation assays after 48 hr (right panels). **C)** Chromatin association assays in HEK293T cells with shControl or shRBX1 cells at 48 hr after transfection of the indicated vectors. Protein levels were analyzed by Western blot using the indicated antibodies. Numbers indicate quantification of ubH2A normalized to the total levels of H2A; values are presented as the fold-change relative to the shControl cells transfected to mock vector.

6. Ubiquitination of H2A is required for the maintenance of H3K4ox, H2A.Z and chromatin compaction

We next asked whether the maintenance of H3K4ox was dependent on the ubiquitination of H2A. Since previous experiments in the absence of RBX1 showed a reduction in LOXL2-dependent ubH2A, we analyzed the effect on H3K4ox levels in this condition. For this, HEK293T cells infected with shControl and shRBX1 were submitted to the same approach as in Figures R5 and R6.

Interestingly, we observed that in cells lacking RBX1, the levels of H3K4ox could not be maintained after transfecting active LOXL2 (Figure R22A). Moreover, when this experiment was performed in the absence of RING1B, a similar increase in H3K4ox was observed in shControl and shRING1B conditions, further reinforcing the idea that this protein does not participate in the described epigenetic mechanism (Figure R22B).

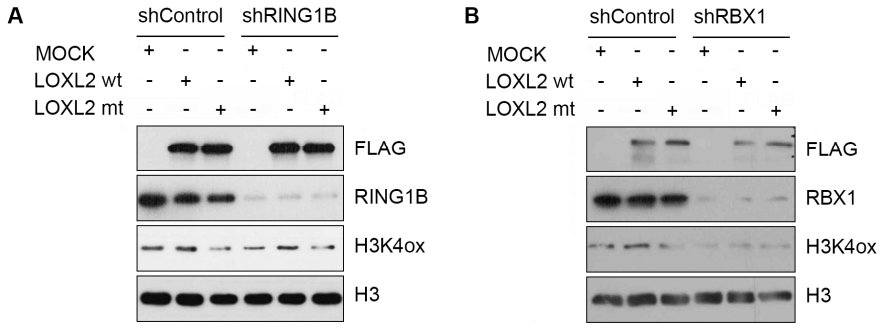

Figure R22. RBX1 is required for LOXL2-mediated oxidation of histone H3. HEK293T cells shControl and shRBX1 **(A)** or shRING1B **(B)** were transfected with LOXL2 wild type (LOXL2), inactive mutant (LOXL2m) or empty vector (mock). At 48 hr after transfection, histone and total extracts were analyzed by Western blot using the indicated antibodies.

To strengthen our theory, we also studied whether ubH2A is deposited in heterochromatin regions of TNBCs and is important for regulating the H3K4ox and H2A.Z present there. To this end, ChIP-PCR experiments in the selected genomic regions were performed in the absence of LOXL2 and RBX1.

As expected, both ubH2A occupancy in chromatin and global levels were dependent on RBX1. Moreover, knockdown of LOXL2 also reduced ubiquitination of H2A in heterochromatin regions but without affecting its global levels, further suggesting that ubH2A is incorporated after oxidation of histone H3 by LOXL2 (Figure R23 and Annex 4).

Notably, ChIP-PCR experiments showed that the decrease in ubH2A in these genomic regions was concomitant with a reduction of H3K4ox and H2A.Z. However, RUVBL2 recruitment was not altered in the absence of RBX1 (Figure R24A). In addition, knockdown of RBX1 did not affect LOXL2 recruitment in chromatin (Figure R24B), in agreement with the subcellular fractionation experiments in shH2A.Z conditions. These results suggest that changes in chromatin structure mediated by ubH2A and H2A.Z incorporation are crucial for the maintenance of H3K4ox in chromatin.

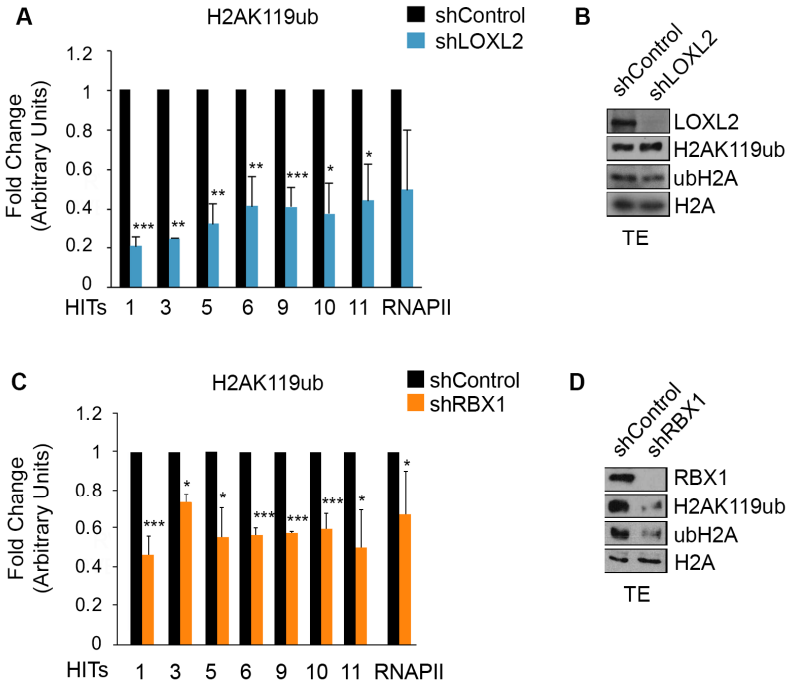

Figure R23. H2AK119ub in heterochromatin regions depends on LOXL2 and RBX1 in MDA-MB-231 cells. MDA-MB-231 cells were infected with shControl and shLOXL2 **(A, B)** or shRBX1 **(C, D). A, C)** ChIP-PCR experiments for H2AK119ub in selected regions (hits) and RNA pol II promoter (RNAPII), which was used as a negative control. Data of qPCR amplifications were normalized to the input and to total immunoprecipitated H2A. Results are expressed as a fold-change relative to data obtained from shControl. Error bars indicate SD of at least three experiments * $p < 0.05$, ** $p \leq 0.01$, *** $p \leq 0.001$**. B, D)**. Total extracts were analyzed by Western blot using the indicated antibodies.

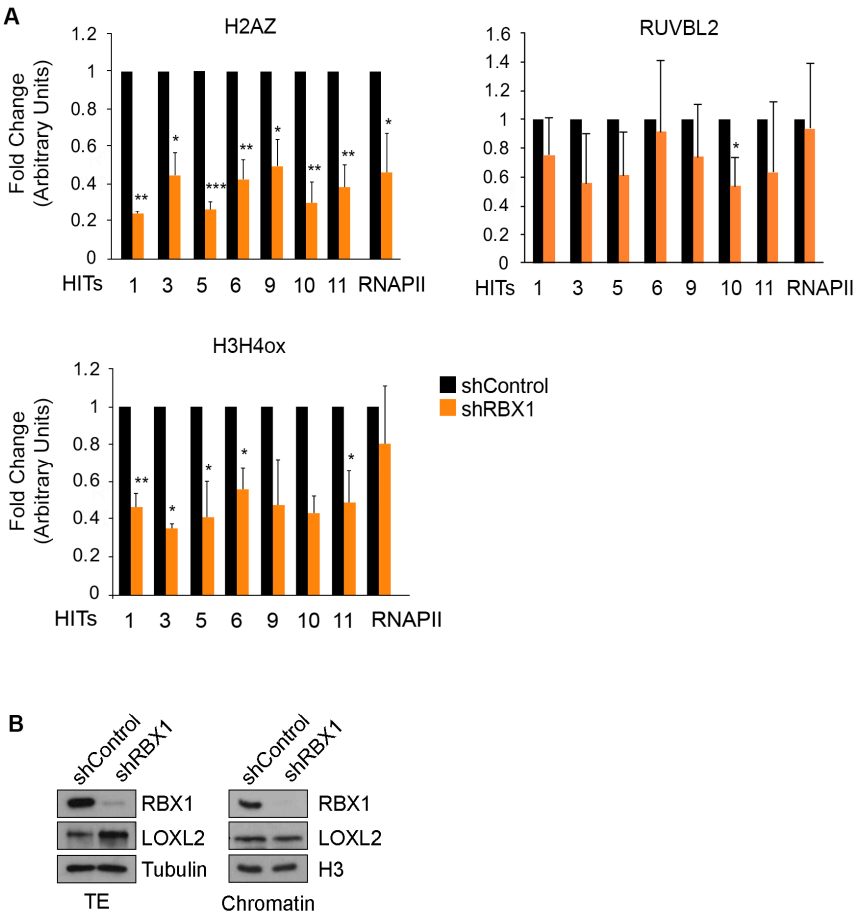

Figure R24. RBX1 regulates H3K4ox and H2A.Z incorporation in heterochromatin regions of MDA-MB-231 cells. Experiments were performed in MDA-MB-231 cells shControl and shRBX1. **A)** ChIP-PCR experiments of H2A.Z, RUVBL2 and H3K4ox in selected regions (hits) and RNA pol II promoter (RNAPII), which was used as a negative control for H3K4ox and RUVBL2. Data of qPCR amplifications were normalized to the input and to total immunoprecipitated H3 for H3K4ox. Results are expressed as a fold change relative to the data obtained in shControl. Error bars indicate SD in at least three experiments *$p < 0.05$, **$p \leq 0.01$, ***$p \leq 0.001$. **B)** Chromatin fraction obtained by subcellular fractionation assays (left panel) and total extracts (right panel) were analyzed by Western blot.

Finally, this effect on H3K4ox and H2A.Z prompted us to investigate if RBX1 was also required for LOXL2 induction of chromatin compaction. Indeed, MNase assays performed in 293T cells showed that in the absence of RBX1, the increase in chromatin compaction after transfecting LOXL2 was not observed (Figure R25).

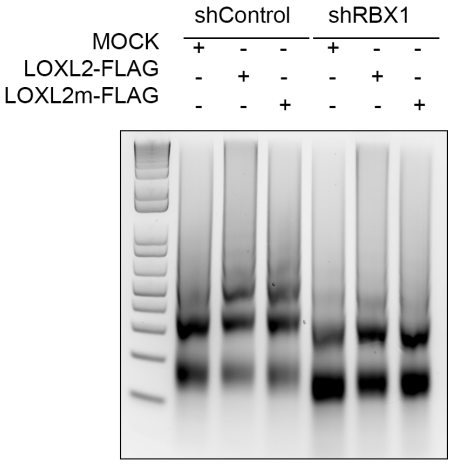

Figure R25. RBX1 is required for LOXL2 induction of chromatin compaction. HEK293T shControl and shRBX1 were transfected with LOXL2 wild-type (LOXL2), inactive mutant LOXL2 (LOXL2m), or an empty vector (mock). Isolated nuclei were digested with micrococcal nuclease (MNase) for 2 min, and total genomic DNA was analyzed using agarose gel electrophoresis.

Altogether, we found that after oxidation of histone H3 by LOXL2, H2A is ubiquitinated through the CRL4B complex, and that this is important for allowing H2A.Z deposition by RUVBL2 and consequently the establishment of compacted heterochromatin regions with maintained levels of H3K4ox.

7. H3K4ox is essential for maintaining heterochromatin integrity

Considering the key role of H3K4ox in regulating chromatin compaction, we wanted to investigate whether it is required for maintaining heterochromatin integrity. Thus, we analyzed histone modifications associated to heterochromatin in all the conditions that cause a decrease in H3K4ox levels.

MDA-MB-231 cells knocked down for LOXL2, RUVBL2, or RBX1 showed reduced levels of H3K9me3 both in total extracts and in the selected heterochromatin regions (Figure R26).

Additional ChIP-PCR experiments revealed that H3K9me2 levels were also decreased in these conditions. However, despite having enrichment of H3K27me3 in these genomic regions, no effect was observed in the levels of this histone modification after knocking down LOXL2, RUVBL2, or RBX1 (Figure R27 and Annex 4).

Therefore, these results demonstrate that the loss of H3K4ox compromises the proper maintenance of heterochromatin by affecting the levels of H3K9me2/3.

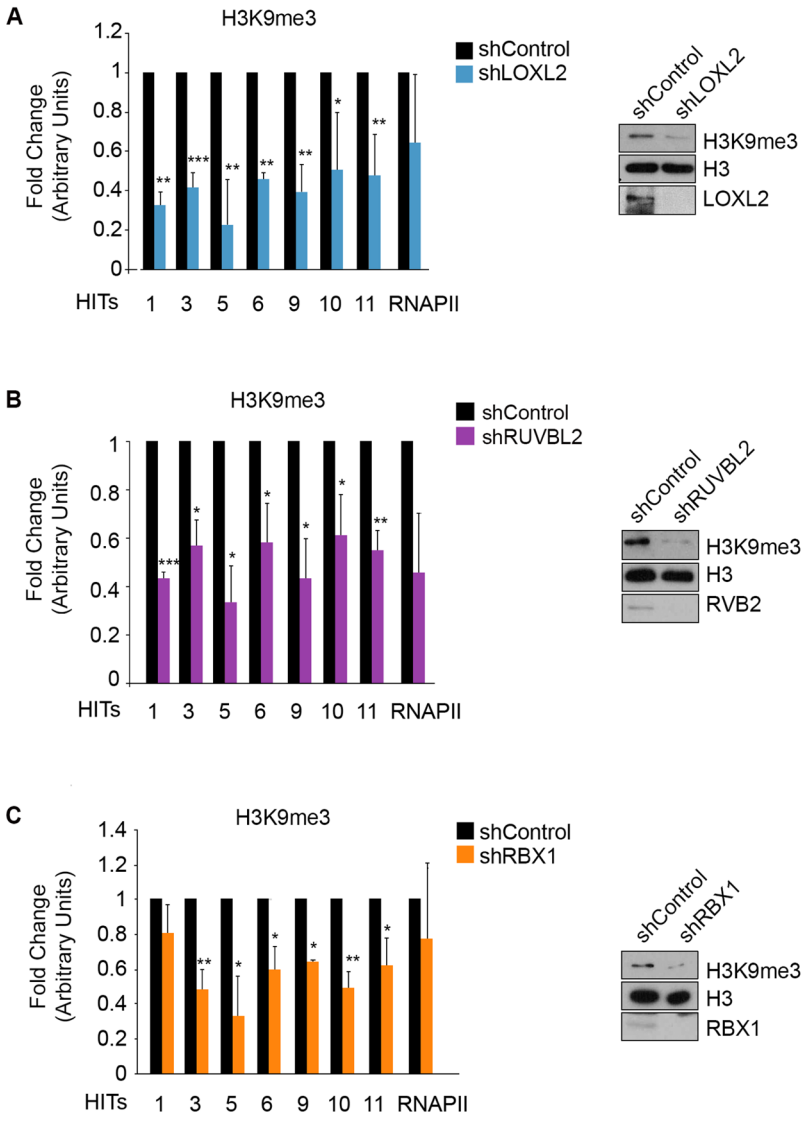

Figure R26. LOXL2, RUVBL2, and RBX1 regulate H3K9me3 levels in MDA-MB-231 cells. MDA cells were infected with shControl or shLOXL2 **(A)**, shRUVBL2 **(B),** or shRBX1 **(C)**. ChIP-PCR experiments of H3K9me3 were performed for the selected regions (hits) and for RNA pol II promoter (RNAPII), which was used as a negative control. Data of qPCR amplifications were normalized to the input and to total immunoprecipitated H3. Results are expressed as a fold-change relative to the data obtained from the shControl. Error bars indicate SD in at least three experiments *$p < 0.05$, **$p \leq 0.01$, ***$p \leq 0.001$. Total extracts were analyzed by Western blot using the indicated antibodies.

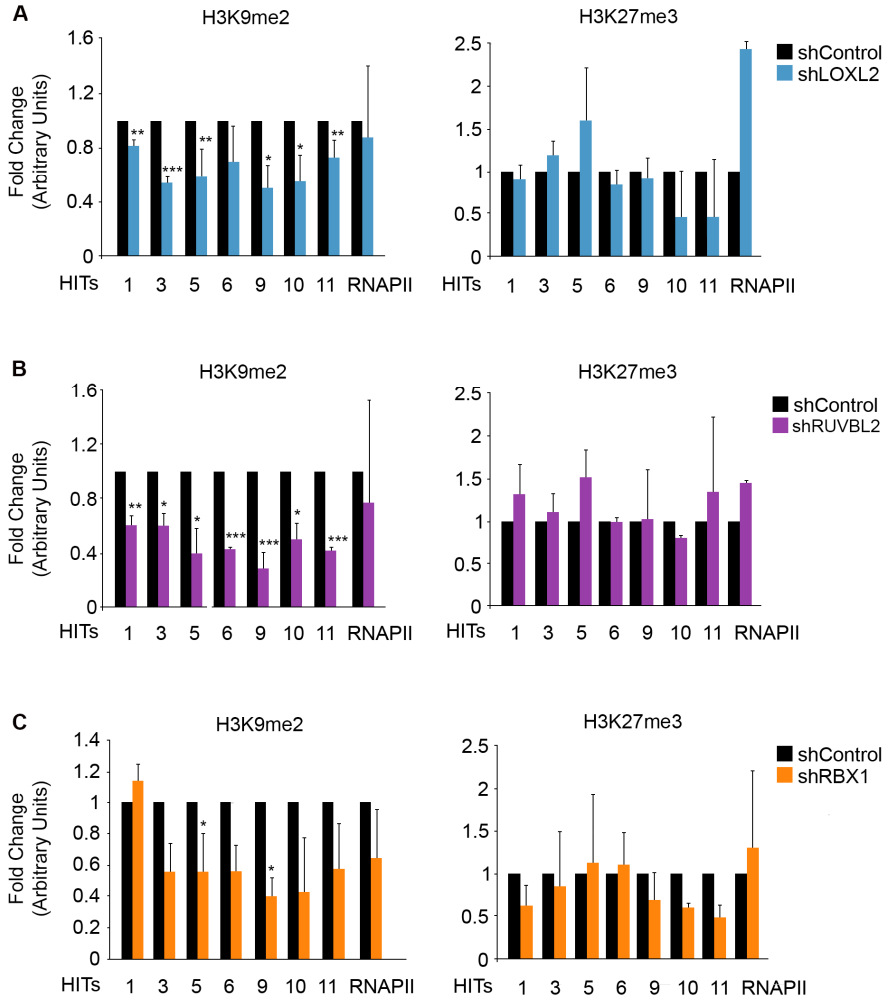

Figure R27. LOXL2, RUVBL2 and RBX1 regulate H3K9me2 levels but not H3K27me3 in MDA-MB-231 cells. MDA cells were infected with shControl and shLOXL2 **(A),** shRUVBL2 **(B)** or shRBX1 **(C)**. ChIP-PCR experiments of H3K9me2 and H3K27me3 were performed in the selected regions (hits) and RNA pol II promoter (RNAPII), which was used as a negative control. Data of qPCR amplifications were normalized to the input and to total immunoprecipitated H3. Results are expressed as a fold change relative to the data obtained in shControl. Error bars indicate SD in at least three experiments *$p < 0.05$, **$p \leq 0.01$, ***$p \leq 0.001$.

8. Heterochromatin alteration has an impact on the oncogenic properties of MDA-MB-231 breast cancer cells

Based on the crucial role of heterochromatin in cell fitness, we next investigated whether heterochromatin alterations affect the oncogenic properties of MDA-MB-231. For this purpose, MTT and colony formation assays were done in the absence of all the crucial members involved in the maintenance of H3K4ox, namely, LOXL2, RUVBL2, DDB1, RBX1, and H2A.Z. Intestingly, in all the knockdown conditions, both the proliferation rates and the number of colonies were decreased compared to that of the control cells (Figure R28 and R29).

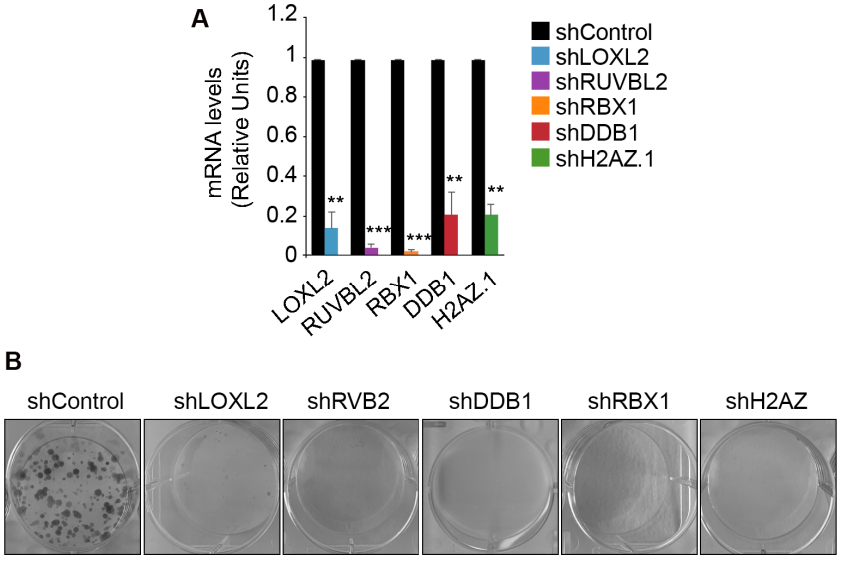

Figure R28. Knockdown of LOXL2, RUVBL2, DDB1, RBX1, or H2A.Z decreases the numbers of colonies formed in MDA-MB-231 cells. A) mRNA levels of the indicated genes were analyzed by qRT-PCR. Gene expression was normalized to the *Pumilio* housekeeping gene and presented as the fold-change relative to the shControl cells. **B)** Colony-survival assay in MDA-MB-231 cells shControl and the indicated knockdowns. Error bars indicate the SD from at least three independent experiments. *$p < 0.05$, **$p \leq 0.01$, ***$p \leq 0.001$.

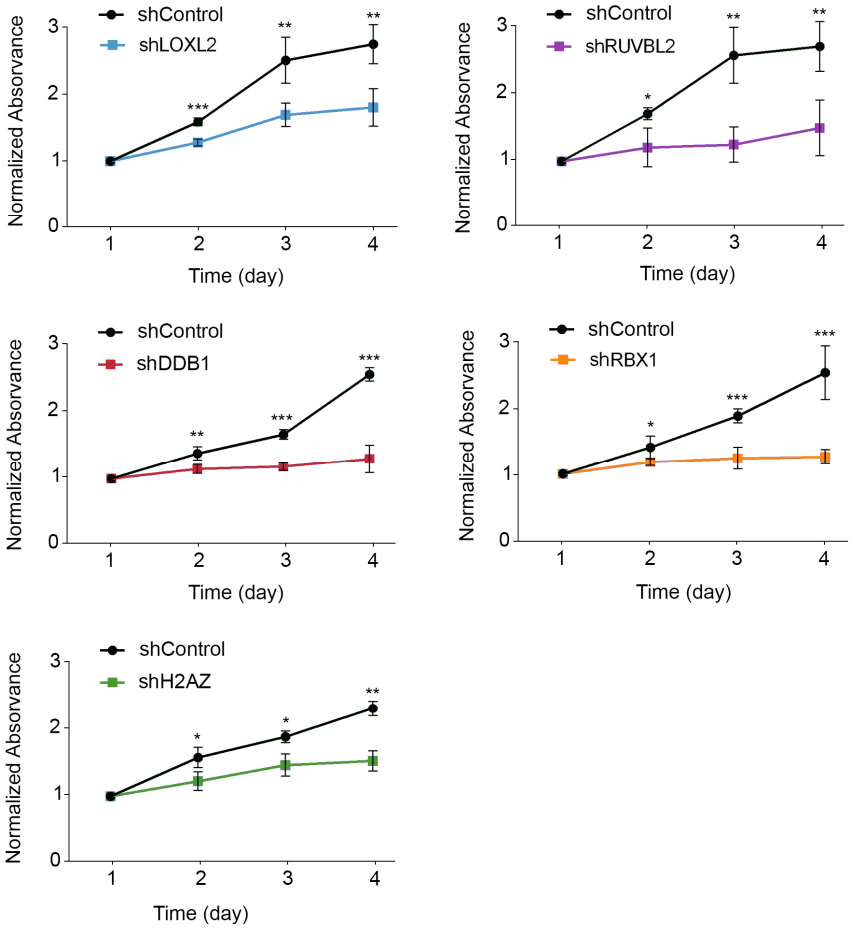

Figure R29. Knockdown of LOXL2, RUVBL2, DDB1, RBX1, or H2A.Z decreases the proliferation rates of MDA-MB-231 cells. MTT assays in MDA-MB-231 cells shControl and the indicated knockdowns. Measurements were obtained over four consecutive days after selection. Error bars indicate the SD from at least three independent experiments. *p < 0.05, **p ≤ 0.01, ***p ≤ 0.001.

In addition, migration and invasion assays were also performed in these conditions, and a reduction of this oncogenic capacity was also observed (Figure R30).

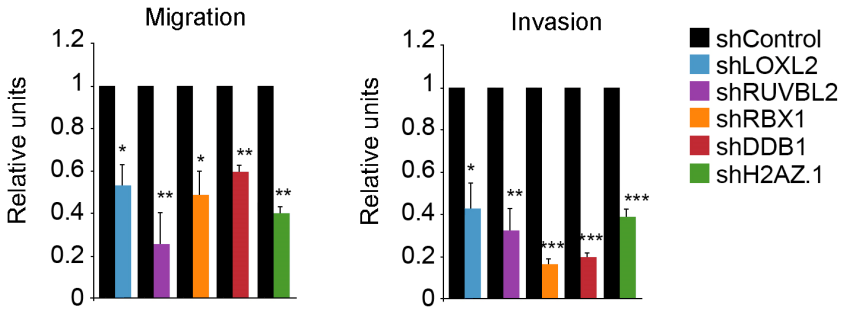

Figure R30. Knockdown of LOXL2, RUVBL2, DDB1, RBX1, or H2A.Z impairs the migration and invasion abilities of MDA-MB-231 cells. MDA-MB-231 cells were infected with the indicated shRNAs, and after 96 hr of selection, migration and invasion assays were performed. Results are presented as the fold-change relative to the shControl cells.

To gain insight into the extent to which changes in the heterochromatin state can affect oncogenic capacities of MDA-MB-231 cells, we analyzed whether the re-establishment of a normal heterochromatin state would also restore normal MDA-MB-231 cells behavior. To do so, SUV39H1[89,109], a methyltransferase that catalyzes the incorporation of H3K9me3 was reintroduced by retroviral infections in MDA-MB-231 cells knocked-down for LOXL2, RUVBL2 or RBX1. Importantly, at 48 hr after infection, both H3K9me3 levels and the migration capacity were partially restored (Figure 31).

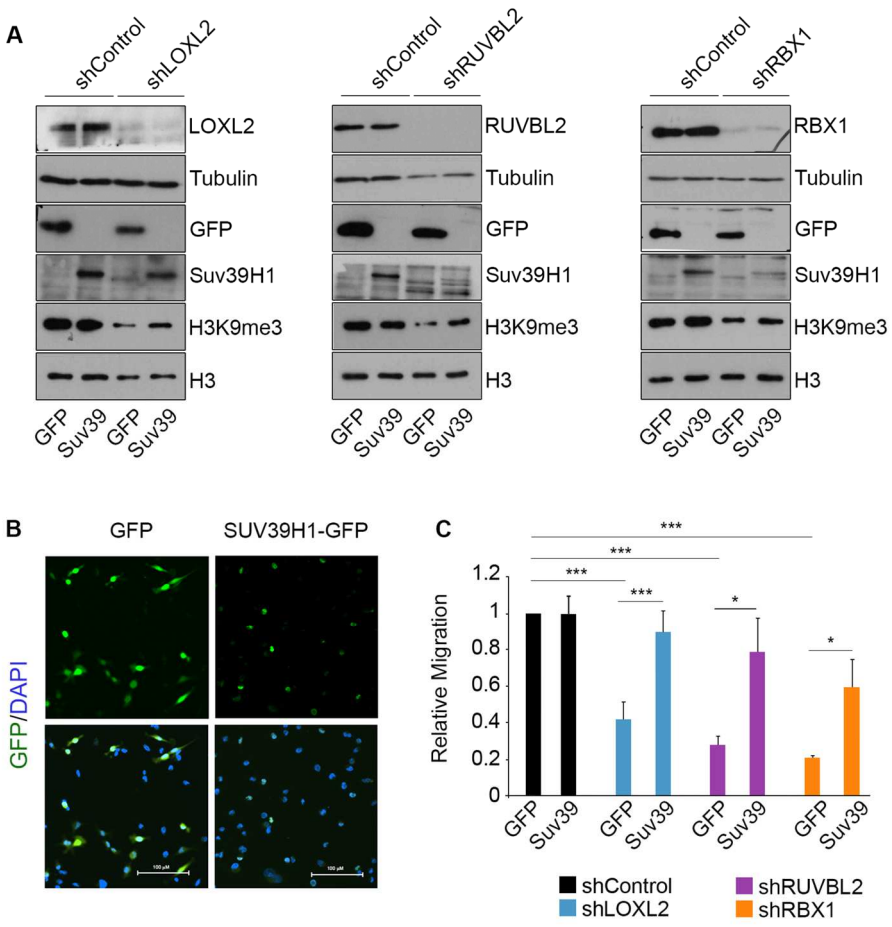

Figure 31. Re-establishment of normal heterochromatin state restores the migration ability of MDA-MB-231 cells. MDA-MB-231 cells were first infected with shControl, shLOXL2, shRUVBL2 or shRBX1. After puromycin selection, knocked-down cells were reinfected with GFP or SUV39H1-GFP and experiments were performed 48 hr later. **A)** Total extracts were analyzed by Western blot using the indicated antibodies. **B)** Representative images of MDA-MB-231 cells after retroviral infection with GFP and SUV39H1-GFP (specifically located in the nucleus). Scale bars indicate 100 µM. **C)** Migration assays presented as the fold-change relative to the shControl cells infected with GFP. Error bars indicate the SD from at least two independent experiments. *$p < 0.05$, **$p \leq 0.01$, ***$p \leq 0.001$.

In order to further demonstrate the relevance of this epigenetic mechanism in the acquisition of malignant traits, gain-of-function experiments were done by transfecting either active RUVBL2 or the ATPase-deficient mutant RUVBL2m. To better study this effect, we used CAL51 cells, a TNBC cell line previously characterized to have low levels of LOXL2 and H3K4ox^{210} (Figure 32). Interestingly, CAL51 cells transfected with active RUVBL2 showed a greater ability to migrate concomitantly with an increase in the levels of H3K4ox, reinforcing the idea that high levels of H3K4ox and chromatin compaction are linked to the acquisition of malignancy traits.

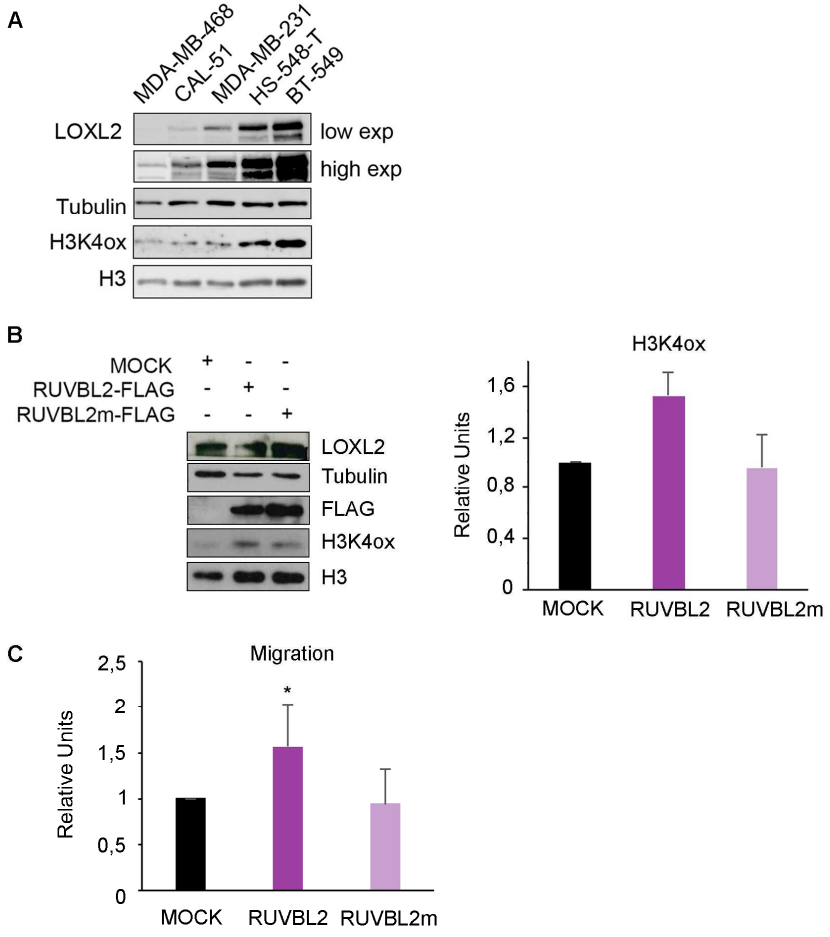

Figure 32. Active RUVBL2 transfection of CAL51 cells increase H3K4ox levels and their ability to migrate. A) Western blot for the indicated antibodies in a panel of TNBC cell lines (from *Cebrià-Costa et. al* [210]). **B** and **C)** CAL51 cells were transfected with RUVBL2 wild type (RUVBL2), ATPase deficient mutant (RUVBL2m) or an empty vector (MOCK) and 48 hr later experiments were performed. **B)** Total extracts were analyzed by Western blot using the indicated antibodies (left panel). Quantification of H3K4ox levels of three independent experiments is shown in the right panel. **C)** Migration assays presented as the fold-change relative to empty vector transfection. Error bars indicate the SD from at least two independent experiments. *$p < 0.05$.

Furthermore, we also considered the important role of heterochromatin in influencing the activation of the DNA damage repair pathway (DDR) in cancer cells. Previous work in the laboratory described that LOXL2- and H3K4ox-mediated changes in chromatin structure are important for preventing the aberrant activation of the DDR. Depletion of LOXL2 in MDA-MB-231 cells leads to an aberrant activation of the DDR and consequently to an increase in the number of γ-H2AX and 53BP1 foci[210]. Hence, we performed these quantifications in MDA-MB-231 cells shControl and shRUVBL2, and we observed the same effect in the knocked-down condition.

These results suggest that the roles of RUVBL2 and LOXL2 regulating H3K4ox levels in chromatin are crucial for avoiding the aberrant activation of DDR, which compromises the survival of tumor cells.

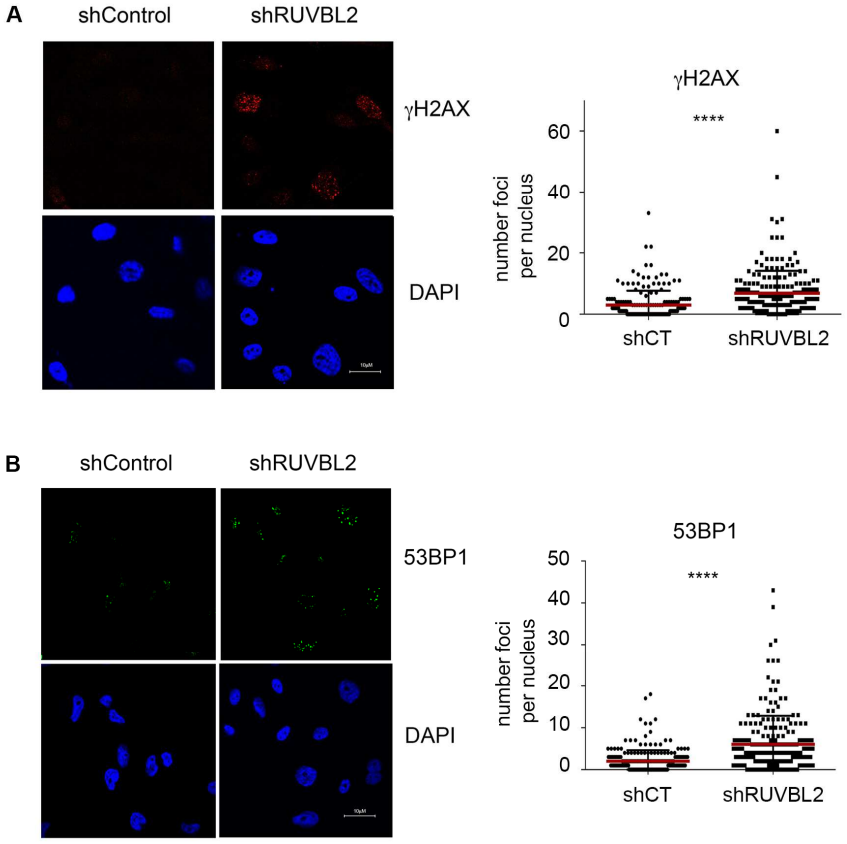

Figure 33. MDA-MB-231 cells lacking RUVBL2 showed increased DDR. MDA-MB-231 cells were infected with shControl or shRUVBL2. After 96 hr of selection, cells were fixed and stained for □-H2AX **(A)** and 53BP1 **(B)**. Representative images are shown; scale bars represent 10 μM. Graphs depict the quantification of □-H2AX and 53BP1 foci per nucleus; median is indicated in red. At least 195 nuclei were analyzed from two independent experiments. ****p ≤ 0.0001.

DISCUSSION

Since its identification as a new epigenetic writer, several studies have characterized LOXL2 oxidation on histone H3 to be linked to repressive environments[78,147,210]. Interestingly, this function and the maintenance of H3K4ox-enriched regions play important roles in cancer cells.

However, a lot of questions around LOXL2 and H3K4ox generation in chromatin were still unsolved, including: *How is LOXL2 recruitment to chromatin regulated? What is the dynamics of H3K4ox, and how is it maintained? How do LOXL2 and H3K4ox induce chromatin compaction?* and *How do they contribute to the oncogenic properties of cancer cells?*

In this thesis, we analyzed these issues in-depth. We studied LOXL2 partners and H3K4ox readers to better characterize the molecular mechanisms that regulate the generation of H3K4ox-enriched regions, its maintenance, and its effect on chromatin structure. Integrating all these data, we now have a more defined picture of how LOXL2 through oxidation of histone H3 acts in cancer cells, as well as its contribution to the oncogenic potential. We strongly believe that this information could be very useful for developing new therapeutic strategies to fight cancer disease.

LOXL2 and H3K4ox in chromatin: general questions

LOXL2 function as a histone modifying enzyme was first described in the E-cadherin promoter, where it deaminates H3K4me3 regulating the repression of this gene[147]. However, LOXL2 oxidation of histone H3 is not only restricted to H3K4me3-enriched regions, and there is also strong evidence that it plays important roles in heterochromatin. In this context, it regulates both pericentromeric heterochromatin transcription during the EMT[78] as well as the maintenance of compacted heterochromatin regions in TNBC cells[209]. Consistent with this information, unpublished data in our laboratory show that, despite having preference and specificity to deaminate H3K4me3, LOXL2 is also able to oxidize unmethylated H3K4, although to a lesser extent.

However, LOXL2 is not a transcription factor and does not recognize specific DNA sequences. Thus, its localization to specific chromatin regions probably involve interaction with other proteins that have this ability.

Considering several pieces of evidence and the above-mentioned scenarios, we speculate that LOXL2 recruitment to chromatin could depend on its interaction with the transcription factor Snail1, which is known to bind to the DNA sequences called E-boxes. First, it has been described that Snail1 works together with LOXL2 in the E-cadherin promoter during EMT. Second, ChIP-sequencing experiments for this transcription factor revealed that it also works in heterochromatin: more than 50% of Snail1-binding sites mapped to intergenic regions, including constitutive heterochromatin such as pericentromeric and centromeric regions [78]. In fact, Snail1 interaction with LOXL2 regulates heterochromatin transcription during EMT, and this is essential for the release of HP1α and chromatin reorganization during this process. Third, expression levels of Snail1, similar to LOXL2, are also increased in breast cancer cell lines, such as MDA-MB-231 and T47-D, as compared to normal mammary epithelial cells that do not express detectable levels of this transcription factor[320].

Moreover, our results suggest that LOXL2 maintenance in chromatin is also affected by its interaction with RUVBL1/2, as in the absence of these partners, LOXL2 levels in the chromatin fraction are decreased. Interestingly, despite not containing domains implicated in histone recognition, RUVBL1/2 are able to bind to the H3 tail as well as to naked DNA, independently of any identified consensus sequence[219]. Importantly, this interaction was much stronger with unmodified or methylated (both in K4 and K9) H3 peptides than with acetylated ones, fitting excellently with the contexts in which LOXL2 acts in chromatin[219].

Another interesting question to address is: what is the dynamics of H3K4ox in chromatin? Considering that the generation of a highly reactive aldehyde group may have an important impact biochemically, we think that H3K4ox is not a static modification. However, it is still not well known how H3K4ox is erased or how this lysine deamination can be reversed.

Unlike demethylation, deamination cannot be directly reversed by subsequent methylation, as the amino group is lost in this reaction. Thus, H3K4ox removal probably involves active mechanisms, such as histone exchange, clipping of histone tails[321], or the reaction of the generated aldehyde group with a histone aminotransferase enzyme that incorporates a new amino group. However, little is known about the regulation or the existence of enzymes with the last two functions, making it difficult to address their importance in our scenario.

Here, we studied the exchange of both H3.1 and H3.3 variants using SNAP-tag imaging. H3.1 is a replicative variant incorporated into chromatin coupled to DNA synthesis during replication and repair by the histone chaperone CAF-1. In contrast, H3.3 is a replacement variant deposited independently of DNA synthesis by HIRA in sites of naked DNA or by the DAXX-ATRX complex in heterochromatin, contributing to its proper establishment[322,323].

Interestingly, our experiments suggested that H3K4ox dynamics could depend on histone exchange. Thus, H3K4ox might be highly reactive or rapidly recognized as something “instable” or “unsuitable”, and a constant exchange of histone H3 could allow the reoxidation and the maintenance of high levels of this histone modification. Accordingly, we found that the putative LOXL2 interactors from the TAP approach included CHAF1B, the medium subunit of the CAF-1 complex and the histone chaperone involved in the H3.1 exchange.

Consistent with the hypothesis of a constant exchange of histone H3, we found that both H3 variants could contribute to this process. Thus, it could be possible to exchange histone H3 both during DNA synthesis and throughout the cell cycle. Moreover, even though LOXL2 oxidation of histone H3 has only been demonstrated with the canonical histone H3.1, we speculate that H3.3 could also be oxidized once it is incorporated into chromatin, as it contains the same lysine residue on position K4.

Importantly, the concomitant changes in chromatin structure mediated by LOXL2 partners and H3K4ox readers, such as the incorporation of ubH2A and H2A.Z, would also be crucial to maintaining this situation.

We observed that both in shLOXL2 and shRUVBL2 conditions, the levels of H3K4ox were decreased, and consequently there was less histone H3 exchange.

It should be noted that, with SNAP experiments, we analyzed H3 exchange globally, so that it would be important to know if the same effects are observed locally in chromatin regions with H3K4ox. However, RNA-sequencing analysis in shLOXL2 and shRUVBL2 showed a downregulation of DAXX and CHAF1B, so we cannot rule out that the observed effects on histone exchange were secondary to it. In addition, as H3.1 is a replicative variant, these effects could also be due to impaired DNA repair or alterations in the cell cycle.

Finally, it is also important to consider how LOXL2 oxidation of histone H3 affects chromatin structure. The generation of this peptidyl aldehyde in the histone tail alters the local macromolecular structure as well as the nature of any protein-protein or protein-nucleic acid interactions, creating a new specific chromatin environment. In particular, there is now strong evidence that LOXL2-mediated H3K4ox regulates chromatin compaction, both detected by changes in MNase-digestion patterns and ATAC-sequencing experiments.

However, we think that oxidation in histone tails does not have the same effects as in the extracellular matrix, where the aldehyde groups display high reactivity and become instantly crosslinked. Indeed, we have described here a molecular mechanism that explains how H3K4ox mediates chromatin compaction, and how high levels of this histone modification can be maintained. Specifically, these mechanisms involve RUVBL2 and DDB1-RBX1 as well as the incorporation of ubH2A and H2A.Z.

Contribution of RUVBL1/2 complex and H2A.Z in LOXL2 function

Using unbiased proteomic assays, we identified that LOXL2 interacts with a complex containing RUVBL1, RUVBL2, BAF53A, and DMAP1. These proteins are members of both the SRCAP and the TIP60 chromatin remodeling complexes, but none of the core and distinctive

subunits of these big complexes (SRCAP, KAT5/TIP60, EP400, TRRAP) were identified in the tandem affinity purification approach. However, it is highly likely that this was due to a technical limitation. Namely, identification of the putative LOXL2 interactors was performed by mass spectrometry after separation on NuPAGE 4-12% Bis-Tris gel; as these proteins have a high molecular weight, they would have been excluded in this experiment.

SRCAP and TIP60 complexes are involved in the deposition of the histone variant H2A.Z but so far, it is unclear if they are functionally redundant[324] or act independently in specific chromatin regions and cellular processes[246]. In addition, it is still not known which one is involved in H2A.Z incorporation in heterochromatin. However, as TIP60-dependent H2A.Z is linked to its acetylation function, gain of chromatin accessibility, and transcriptional regulation[174,325], we speculate that the SRCAP complex is probably responsible for this histone variant deposition in H3K4ox-enriched regions.

Alternatively, it has also been described that a small complex that only contains the subset of identified proteins RUVBL1/2, BAF53, DMAP1, and actin, but lacks the catalytic subunits p400 and SRCAP, can catalyze its incorporation *in vitro*[260]. Interestingly, RUVBL1 and RUVBL2 via their ATPase activity are the catalytic subunits in this small complex, and it is more dependent on ATP hydrolysis than the TIP60 for incorporating H2A.Z[260]. Here it is important to consider that *in vitro* incorporation of H2A.Z by this small complex is facilitated by acetylation, and that this would not fit much with heterochromatin regions. Nevertheless, we think that it could still be plausible in our scenario, as it also takes place without acetylation and its activity *in vivo* has not been studied yet; nonetheless, it could involve a completely different context.

Therefore, although it is clear that LOXL2 interacts with a complex involved in H2A.Z exchange, and that RUVBL2 is required for its formation, it remains to be defined whether it is one of the two big complexes (SRCAP or TIP60) or the small one. In order to elucidate this, loss-of-function experiments with specific shRNAs for SRCAP and/or p400 subunits as well as additional coimmunoprecipitation and gel filtration chromatography assays should be performed.

Importantly, we demonstrated that active RUVBL2 is essential for the maintenance of H3K4ox and the induction of chromatin compaction. In addition, this effect is not explained by the requirement of RUVBL2 for LOXL2 enzymatic activity, but it is linked to the recruitment of LOXL2 into chromatin as well as the incorporation of H2A.Z.

Here it is important to point out that the downregulation of RUVBL2 had a striking effect on H2A.Z distribution. We observed an unexpected increase in chromatin fraction and TMR signal in SNAP experiments, despite detecting a decrease in H3K4ox enriched heterochromatin regions by ChIP-PCR. Thus, we suggest that RUVBL2 knockdown massively alters the H2A.Z pattern, affecting the balance between H2A.Z deposition in euchromatin and heterochromatin. This result could be explained, because in shRUVBL2 conditions heterochromatin is altered, and it has been reported that in this situation the timing and the extent of H2A.Z deposition could be affected[326]. Alternatively, this accumulation could be due to the alteration of the INO80 complex, which removes H2A.Z from chromatin. In this complex, RUVBL1/2 are required for the proper incorporation of Arp5, an essential protein for its chromatin-remodeling activity[236]. In fact, although controversial with other studies, deletion of *ARP5* in yeast has been described to lead to global H2A.Z accumulation, mainly around the promoters[327].

Furthermore, we also found that the RUVBL2 effect on H3K4ox relies on the ATPase activity of RUVBL2. Interestingly, *in vitro*, the H2A.Z exchange is reduced in the absence of ATP hydrolysis[260]. Thus, it is probable that with the ATPase-deficient mutant of RUVBL2, H2A.Z deposition would also be affected, further reinforcing that RUVBL2's effect on H3K4ox is through the deposition of this histone variant.

On the other hand, we also found that LOXL2 regulates RUVBL2 recruitment and H2A.Z deposition. Hence, both proteins have a synergic effect cooperating to maintain stably their function as a writer and chromatin remodeler, allowing the consequent changes in chromatin structure. However, LOXL2's effect on H2A.Z seems to be only restricted to specific regions where LOXL2 acts, as it was only observed by ChIP-PCR but not by SNAP quench-chase-pulse experiments in which global incorporation is detected.

The histone variant H2A.Z characteristically contains an extended acidic patch as compared to the canonical histone H2A. Interestingly, this unique feature leads to an altered nucleosome surface, and several pieces of evidence support that this is linked to chromatin compaction. H2A.Z co-exists in the same nucleosome with HP1α (but not with HP1β or HP1γ) and H3K9me3, and it promotes HP1α-mediated intramolecular folding of nucleosomal arrays, being associated with gene repression[267-269]. In addition, it has also been proposed to work as a functional substitute for H3K9me3, as it is able to enhance the binding of HP1α similar to this histone modification[117]. Thus, we propose that its incorporation would be essential to mediate changes in chromatin structure, favor chromatin compaction and maintain H3K4ox levels. However, whether the H2A.Z effect on regulating chromatin compaction also involves HP1α in our context is still unknown. Moreover, we only studied the contribution of the H2A.Z.1 isoform, but it could be possible that H2A.Z.2 also contributes to the maintenance of H3K4ox.

Consistent with this information, several studies have also demonstrated that H2A.Z is required for both constitutive and facultative heterochromatin formation and gene silencing in different organisms and cell types. It is necessary for centromere formation and function as well as located in pericentromeric heterochromatin of mouse cells colocalizing with HP1α from the early embryo[274,275,279,326].

In addition, it has been reported that PTMs of H2A.Z could regulate its distribution in different chromatin contexts. Acetylation of H2A.Z is found at the 5′ regions of active genes in yeast and vertebrates, whereas its monoubiquitylation distinguishes the fraction associated with facultative heterochromatin[264,265]. Despite being a plausible possibility, our unpublished data suggest that H2A.Z would not be monoubiquitinated in this context. In fact, this result is reasonable, as this modification depends on RING1B, and we have shown that the maintenance of H3K4ox levels did not depend on this E3 ligase. However, we cannot discard that other modifications could happen.

Finally, genome wide experiments in triple-negative breast cancer cells demonstrated that RUVBL2 and H2A.Z are located in heterochromatin

domains enriched in H3K4ox, previously defined in these cells and being linked to chromatin compaction and a more aggressive phenotype. Interestingly, this overlap was strongly increased when the analysis of ChIP-sequencing data was performed using multi-analysis alignment to include constitutive heterochromatin. In agreement, we found that the common regions with H3K4ox, H2A.Z and RUVBL2 were mainly located in intergenic regions and only contained few genes. Moreover, enrichment analysis of the genes embedded in these regions showed that they are found near peaks of H3K27me3, a histone modification that marks heterochromatin (Figure D1).

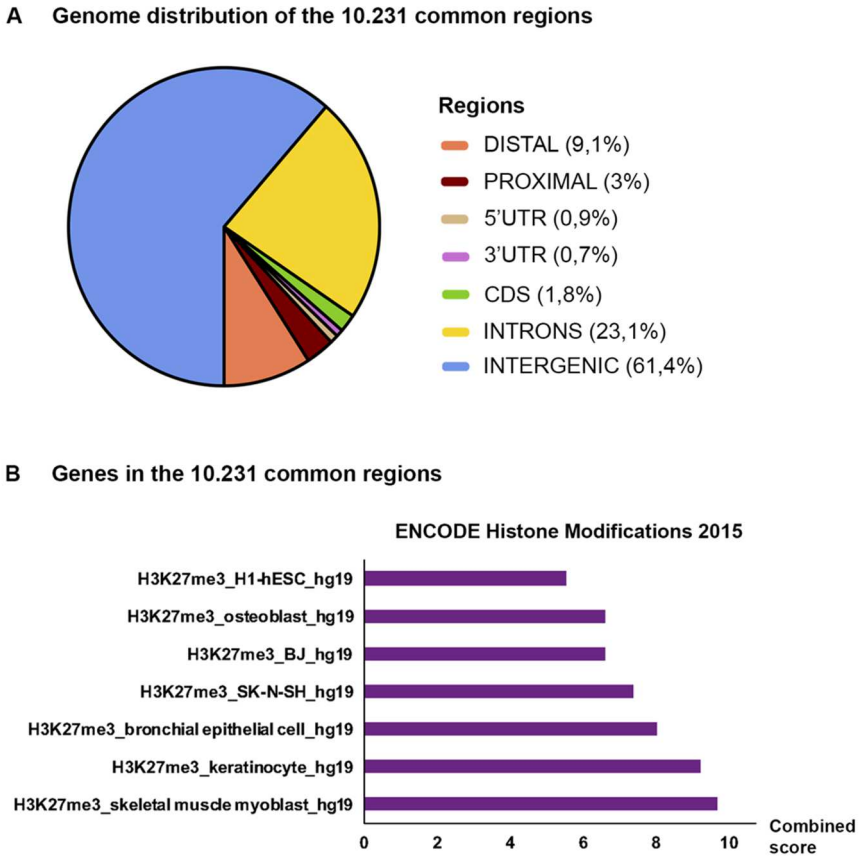

Figure D1. Distribution of common regions with H3K4ox, H2A.Z and RUVBL2. **A)** Plot generated by counting the number of ChIPseq peaks with H3K4ox, H2A.Z and RUVBL2 fitting on each class of region. DISTAL region is the region within 2.5 Kbp and 0.5 Kbp upstream of the TSS. PROXIMAL region is the region within 0.5 Kbp and the Transcription Start Site (TSS). UTR is UnTRanslated sequence. CDS is the protein CoDing Sequence. INTRONS are intronic regions. INTERGENIC is the rest of the genome. **B)** Enrichment analysis (histone modifications 2015) of the genes embedded in the 10.231 common regions.

ATAC-sequencing data in shCT and shRUVBL2 reinforced that in TNBC cells, RUVBL2 and H2A.Z function on H3K4ox maintenance is important for regulating chromatin compaction. Indeed, consistent with MNase experiments, a significant increase of ATAC signal was observed in the absence of RUVBL2 specifically in H3K4ox and H2A.Z peaks.

However, this tendency was not observed in the regions with the three H3K4ox, RUVBL2, and H2A.Z. This result might be explained because, despite being all repressive and compacted environments, the common regions have different characteristics in terms of histone modifications and possibly in higher-order chromatin structure (they include regions of constitutive heterochromatin and also genes enriched in H3K27me3). Hence, it could be possible that in the absence of RUVBL2, the effect on chromatin compaction could only (or strongly) be observed in a subset of regions, for instance the ones that contain higher levels of H3K9me3 or are involved in the formation of specific 3D structures. In this way, when considering the regions with the three marks, the increase in ATAC signal would not be as evident as it is when we study separately all the H3K4ox or H2A.Z regions.

This role of RUVBL1/2 in heterochromatin regions and chromatin compaction seems to be in contrast to the one proposed in liver cancer. In this context, it has been described that RUVBL1/2 function with E2F1 and the incorporation of H2A.Z are important for positively regulating gene expression in euchromatin, and are linked to an increase in chromatin accessibility[328]. Thus, we speculate that RUVBL1/2 distribution in the genome could be different depending on the type of cancer and their interaction with different partners. In this way, they

could mediate different cellular functions and contribute through different mechanisms to cancer malignancy.

As for H2A.Z, ChIP-sequencing experiments from other studies also demonstrated that this histone variant is present in intergenic heterochromatin regions[271,329], consistent with our results. However, in those studies, the relevance of having low amounts of H2A.Z in heterochromatin was not explained, and it was even proposed to be a mere consequence of the absence of transcription, which leads to its random accumulation. Thus, our results provide a biological context in which H2A.Z incorporation in heterochromatin regions is specifically regulated by RUVBL2 and LOXL2 and is crucial for shaping chromatin structure.

It is also important to note that we observed a higher overlap between H3K4ox and RUVBL2 than with H2A.Z. This result could be explained by their different patterns of distribution in chromatin: ChIP-sequencing binding profiles of H3K4ox and RUVBL2 are broader, whereas the one for H2A.Z is sharp with more well-defined peaks. Alternatively, it could be due to two technical limitations. First, during library preparation and ChIP-sequencing, regions with high amounts of H2A.Z could be overrepresented as compared to the ones that contain lower levels, such as in heterochromatin. Second, the resolution of ChIP sequencing experiments could be limiting; in that case, other techniques such as ChIP-exonuclease that are finer might provide a higher spatially mapping[330]. Indeed, we validated that H2A.Z binding is present in additional heterochromatin regions previously defined to contain H3K4ox[210], and that this presence was LOXL2- and RUVBL2-dependent as well. However, these regions were not detected as ChIP-sequencing peaks in the genome-wide analysis, supporting the fact that maybe some sensitivity was lost in this experiment and that the H2A.Z distribution in chromatin could be underrepresented. In addition, we also demonstrated by co-immunoprecipitation experiments that H2A.Z is able to interact with H3K4ox (data not shown), further reinforcing the fact that they can be found together in compacted regions.

Identification of H3K4ox readers: the role of two members of the CRL4B complex and ubH2A

In this study, we successfully identified H3K4ox readers in nuclear extracts of MDA-MB-231 cells using a synthetically modified and biotinylated H3 peptide resembling the intermediate alcohol of LOXL2 reaction. Although this is a fast reaction, we know from previous data that the intermediate alcohol is relatively stable and is maintained at least for two hours [210]. However, we cannot rule out that other proteins could also be readers of the lysine when it is completely oxidized. With this approach, we obtained consistent results that have been validated *in vitro* far better than with previous strategies in which nuclear extracts were incubated with either H3K4me3 peptide or this peptide after incubation with recombinant LOXL2; in that situation, complete oxidation of the H3K4me3 peptide could not be guaranteed, distorting the results and compromising their reliability.

Interestingly, we found that LOXL2 oxidation of histone H3 is associated with DDB1 recruitment to chromatin and the ubiquitination of H2A through the E3 ligase RBX1. In this context, we speculate that DDB1 and RBX1 probably form the CRL4B complex with the cullin protein CUL4B, as has been previously characterized in other studies. However, in co-immunoprecipitation assays, we only analyzed DDB1 and RBX1 but not CUL4B. Further biochemical experiments should be performed to study its presence.

As it was demonstrated that an alternative DDB1-CUL4B–containing complex formed by the E3 ligase protein RING1B can also mediate H2AK119ub[294], we wanted to distinguish which one was involved in our mechanism.

Loss-of-function experiments for RING1B and RBX1 confirmed that the incorporation of H2AK119ub upon LOXL2 oxidation of histone H3 depends on the DDB1 and RBX1, but not the UV-RING1B. In agreement, RING1B was found to be less strongly associated with H3K4ox than RBX1 by co-immunoprecipitation assays. This result is consistent with the fact that the UV-RING1B complex is only assembled and recruited to chromatin after UV-induced DNA damage and suggests

that H3K4ox represents a different signal in chromatin than the 6–4 photoproducts or the cyclobutane pyrimidine dimers (CPDs) arising after exposure to UV light[331]. Moreover, in the context of the UV-RING1B, DDB2 is the protein that recognizes the damage and recruits the complex. In contrast, we propose a scenario in which DDB1 would be the responsible for recognizing the chromatin signal, although we do not know if DDB2 is also part of the complex. Lastly, other studies have also demonstrated that in MDA-MB-231, RING1B does not exert its canonical function with PRC1 and has little effect on regulating the levels of H2AK119ub, but it is predominantly recruited to BRD4-containing enhancers regulating oncogenic transcriptional programs[332].

We also have to consider that our experiments do not demonstrate whether DDB1 directly interacts with H3K4ox or, in contrast, is recruited through another protein. *In vitro* experiments incubating H3K4ox peptide with the recombinant protein DDB1-GST should be performed to elucidate if DDB1 is the direct reader of H3K4ox and therefore the one that triggers the recruitment of the CRL4B complex to chromatin. Alternatively, other proteins could be involved in this function. For instance, in a similar scenario, PHF1 is a reader of symmetric dimethylation of H4R3 (H4R3me2s) catalyzed by PRMT5–WDR77 and interacts with DDB1 coordinating the recruitment of the CRL4B complex[296].

Another open question is if CRL4B complex contains an additional subunit that specifically recognizes the substrate to ubiquitinate, in this case the H2A. Considering the described composition of the complex, it could possibly be a WD40 protein. In fact, previous studies suggested that the WD40 proteins RbAp46/48 would be the ones in the CRL4B complex that recognize histone H2A. GST–RbAp48 can bind to H2A and H3 and the downregulation of this protein results in the decrease of H2AK119ub[293,333]. Interestingly, these two proteins were found as LOXL2 interactors in the TAP approach, suggesting that they could have this function in our context. Alternatively, other WD40 containing proteins could act similarly, as it has been described for DCAF8, the substrate receptor that recruits CRL4B complex and targets histone H3

for ubiquitination[295]. Notably, among the list of putative H3K4ox interactors there are many WD40 containing proteins.

We have also demonstrated that H2AK119ub is incorporated in heterochromatin regions of MDA-MB-231, and that this is crucial for maintaining H2A.Z in these regions. Previous reports suggest that PTMs in histone tails can affect the incorporation of the histone variant H2A.Z. For instance, acetylation of histones favors H2A.Z deposition both *in vitro* and *in vivo*[241,260]. Despite being very different modifications, ubiquitination could have a similar effect, as it involves the conjugation of a large PTM that produces a change in the overall conformation of the nucleosome. In fact, it has been suggested that after DNA damage H2A ubiquitination destabilize nucleosomes weakening the association of histones and allowing the repair of damaged chromatin[309]. We therefore speculate that H2AK119ub-mediated changes in chromatin structure could allow a proper incorporation of H2A.Z and/or avoid its elimination from chromatin.

Alternatively, another possibility would be that ubiquitination of H2AK119 could influence the association of RUVBL1/2 complex with histones, as has been reported for acetylation[260]. However, we think that this not the case, as ChIP-PCR experiments showed that RUVBL2 recruitment to chromatin is not affected after knocking down RBX1 and the consequent decrease in H2AK119ub.

Bearing the previous hypotheses in mind, ubiquitination of H2A could proceed or coexist with H2A.Z incorporation. The detection of both marks in heterochromatin regions could be explained because the experiments were performed with a pool of cells that might be asyncronic in this process, or because these epigenetic changes occur differentially in the two H2A histones of the histone core.

Finally, our results strongly demonstrate that DDB1 and RBX1 through H2AK119ub are required for maintaining H3K4ox in heterochromatin and chromatin compaction.

On the one hand, H2AK119ub has been linked to transcriptional repression and chromatin compaction. In contrast to H2A.Z, it does not

affect the intramolecular fiber folding of nucleosomal arrays *in vitro* at low $MgCl_2$ concentrations, likely for its position in the nucleosome[310]. However, it can regulate the recruitment of the linker histone H1 to affect higher-order chromatin structure[311]. Thus, H2A.Z and H2AK119ub could act synergistically to maintain high levels of H3K4ox and promote an inaccessible chromatin structure.

On the other hand, several studies demonstrated a crucial role of the CRL4B complex in repressive environments. It has been reported that CUL4B targets WDR5, a core subunit of the histone H3 lysine 4 (H3K4) methyltransferase complexes, for ubiquitination and degradation in the nucleus[284]. Furthermore, it interacts with PRC2 and SIN3A-HDAC complexes coordinating monoubiquitination of H2AK119 with H3K27me3 and histone deacetylation[334], two histone PTMs that also have repressive effects. Similarly, CRL4B is physically associated with SUV39H1, HP1, and DNMT3A, facilitating H3K9me3 and DNA methylation, and being important for maintaining these heterochromatin features[297].

In agreement with these functions, it has also been described that an orthologous complex of the human CRL4 in yeast, known as Cul4-Rik1, is required for heterochromatin formation and H3K9me3. This complex contains the RING-box protein Pip1, cullin Cul4 (or Pcu4) and Rik1, which shares 21% of identity with DDB1 and exerts its function as a linker instead of the yeast DDB1. In addition, this complex co-purifies with the two DCAF proteins Dos1 (Crl8 or Raf1) and Dos2 (or Crl7) as well as Crl4, the yeast orthologue of SUV39H1/2. However, the substrate of this CRL4Dos1/2 ubiquitin ligase in yeast is still unknown[335-337].

Interestingly, all the mentioned CRL4B contexts fit excellently with our scenario for several reasons. First, ChIP-PCR experiments in common heterochromatin regions with H2A.Z, H3K4ox and RUVBL2 were also enriched with H3K9me2/3 and H3K27me3. Second, the TAP approach revealed that LOXL2 also interacts with members of the above-mentioned CRL4B partners such as SIN3a/HDAC complex, NuRD, CHAF1B, and PRC2[147]. Interestingly, these interactions could be mediated through the WD40 domains that function as an adaptor in

protein or protein-DNA complexes[338,339]. Indeed, the LOXL2 interactors CHAF1B, RBBP4 (RbAp48), and RBBP7 (RbAp46), as well as many H3K4ox readers, contain this domain (Annex 1 and 2,[147]).

Altogether, we propose that LOXL2 and H3K4ox interact with other epigenetic writers and effectors to form a functional unit that induces further post-translational modifications. In this way, there is a functional interplay between a variety of epigenetic mechanisms including H3K4ox, H2A ubiquitination, the histone variant H2A.Z, and the heterochromatin marks H3K9me3 and H3K27me3, which is crucial for maintaining large stable environments with H3K4ox and chromatin compaction.

Generation of H3K4ox-enriched heterochromatin regions in TNBC cells

Here we propose that characteristically TNBC cells maintain specific heterochromatin domains with high levels of H3K4ox.

However, it is still not known whether these regions are conserved in different cancer cells with similar levels of LOXL2, or whether overexpressing exogenous LOXL2 in cells with low endogenous amounts of this protein would target LOXL2 to the same regions.

Interestingly, we observed by ChIP-PCR experiments that the selected common regions were enriched not only with H3K9me2/3, the hallmarks of constitutive heterochromatin, but also with H3K27me3, the prototypical histone modification of facultative heterochromatin. In agreement, common regions obtained by the analysis of the ChIP-sequencing data included both repetitive sequences and silenced genes enriched with H3K27me3 (Figure D1B).

These features suggest that heterochromatin regions might not exclusively show characteristics typically associated with constitutive or facultative heterochromatin, and that the classical distinction between these two compartments might be less strict than has been assumed[92-94]. In fact, several studies support this idea and show that these chromatin marks can co-localize and even cooperate in gene silencing

maintenance. It has been described that H3K27me3 can be found in regions typically defined as constitutive heterochromatin such as subtelomeric repeats and telomeres[340,341] as well as that H3K9me3 is present in some silenced promoters, with or without H3K27me3[93,342,343]. Moreover, further reinforcing the dynamism of constitutive heterochromatin, recent findings in *D. melanogaster* have indicated that even transcriptionally active genes can "live and work" properly within constitutive heterochromatin, being accessible to transcription and contributing to the phenotype[344].

Importantly, we also have shown that the described molecular mechanism is crucial for maintaining heterochromatin integrity. Specifically, alteration of LOXL2, RUVBL2, or RBX1 dramatically affects global levels of H3K9me3 as well as the incorporation of H3K9me2/3 in heterochromatin regions. This result could be explained because the CRL4B complex that reads H3K4ox interacts with SUV39H1[297], one of the methyltransferases that mediates the incorporation of H3K9me3. The levels of H3K4ox are decreased in the absence of all three proteins, and so these situations would lead to less recruitment of CRL4B and consequently of SUV39H1. Additionally, Snail1, a partner of LOXL2 that could bring it to heterochromatin, also interacts with SUV39H1 methyltransferase[145], further supporting the association between LOXL2 function and the maintenance of H3K9me3. Consistent with this hypothesis, we observed that SUV39H1 infection in cells knocked down for LOXL2, RUVBL2, and RBX1 rescued the levels of H3K9me3. However, as the levels were not fully rescued, we cannot rule out that other methyltransferases, such as G9a and SETB1, could also contribute to this function.

It is also worth mentioning that this effect on H3K9me3 levels was not observed in previous studies knocking down LOXL2 in pancreatic adenocarcinoma cells [147]. However, these cells express lower levels of LOXL2 than MDA-MB-231 cells, and the downregulation of this protein has a less strong phenotypic effect. Hence, TNBC cells that contain higher levels of LOXL2 and H3K4ox are more dependent on the described mechanism further reinforcing its importance for the viability and the malignancy of these cells.

Regarding H3K27me3, the levels of this histone modification were not affected by downregulating LOXL2, RUVBL2, or RBX1, contrary to what was expected. On the one hand, a reduction of this histone modification could be expected, as both LOXL2 and the CRL4B complex are able to interact with members of PRC2[147,297]. On the other hand, some studies show that when features of constitutive heterochromatin are disrupted (as in our situation), H3K27me3 is redistributed to this region[345-347]; thus, an increase of this histone modification could also be plausible.

Hence, our results suggest that the maintenance of H3K4ox enriched regions through the described epigenetic mechanism would have a stronger effect on the levels of H3K9me2/3 than H3K27me3. However, we have to consider that ChIP-PCR experiments were only performed in few selected regions as a representation of the ones that contain RUVBL2, H2A.Z, and H3K4ox, and that it could also be possible that the effect on H3K27me3 was better observed in other common regions that contain higher levels of this histone modification.

Contribution of H3K4ox maintenance and heterochromatin formation to oncogenic properties of cancer cells

Notably, we demonstrated that the maintenance of heterochromatin domains through LOXL2 function and high levels of H3K4ox is essential for the oncogenic properties of TNBC cells. Consistent with these results, LOXL2 has been found overexpressed in many cancers and to be related with the acquisition of cellular malignancy and tumor formation[206,212,216,348-350]. In breast cancer, its expression levels are higher in invasive and metastatic cell lines and patient-derived xenografs (PDXs)[207,208,210]; in addition, they are associated with poor outcome and lower survival rates of breast cancer patients[211].

LOXL2 nuclear function has also a crucial role in the context of the EMT. It could be possible that during tumor progression, some cancer cells undergo the EMT program and start to express LOXL2. The transcription factor Snail1, together with LOXL2, would participate in downregulating the CDH1 gene and heterochromatin transcripts, giving rise to transformation of cancer epithelial cells into mesenchymal

cells[78,213]. In fact, it has been described that overexpression of nuclear LOXL2 in MCF-7 cells, a luminal A noninvasive breast cancer cell, promotes a rapid transition to a mesenchymal phenotype[208].

In the last years, two different groups have suggested that EMT is dispensable for lung and pancreas metastasis, but that it contributes significantly to the formation of recurrent metastasis after chemotherapy[351,352]. Interestingly, it is now known that the EMT is involved in the pathogenesis of basal-like and triple-negative breast cancers, the most aggressive and resistant subtypes. In these breast cancers, some cells show mesenchymal phenotype and display gene-expression patterns consistent with this process[160,162]; importantly, some of them also show increased levels of LOXL2 and H3K4ox in heterochromatin [210].

Furthermore, both RUVBL2 and CRL4B complex are also known to play important roles in cancer biology[226,227,282] and in some contexts, the ATPase activity of RUVBL2 is also required for its effects on tumor cell growth and viability[317]. However, in PDXs expressing different protein levels of LOXL2, we did not observe any correlation between RUVBL2, RBX1, and LOXL2 (data not shown). Hence, as these proteins are part of many different complexes in cells, we speculate that their role in cancer would be more related to their partners rather than to the amount of protein expressed. In addition, our biochemical data and gain-of-function experiments suggest that the overexpression of only one of them could be sufficient for triggering this molecular mechanism despite having low or medium expression levels of LOXL2, allowing the accumulation of high levels of H3K4ox and thus of heterochromatin domains.

On the other hand, in agreement with our results, several studies have also demonstrated that cancer progression is associated with heterochromatin features. It has been reported that high levels of H3K9 trimethylation or other proteins involved in heterochromatin formation correlate with different types of cancer, poor prognosis, and tumor progression[172,353-355].

At this point, our findings raise a critical question: *how does the maintenance of these heterochromatin domains contribute to the acquisition of malignant traits in mesenchymal cells*?

To start with, the described mechanism does not seem to be implicated directly in gene expression regulation, as dysregulated genes in LOXL2 and RUVBL2 knockdown conditions were not located in chromatin regions with H3K4ox and RUVBL2. Accordingly, the expression of genes involved in cell proliferation and the acquisition of malignant traits were not strongly affected.

On the other hand, several studies have demonstrated that heterochromatin alteration leads to an upregulation of heterochromatin elements that are normally silenced and could compromise chromatin integrity[326,356,357]. In particular, previous work from our laboratory demonstrated that the LOXL2 function on oxidizing histone H3 was essential to maintain major satellite repression during the EMT[78]. In this context, our unpublished data demonstrated that both H2A.Z and RUVBL2 are found in pericentromeric heterochromatin and follow a similar kinetics than H3K4ox; in addition, RUVBL2 was also required for HP1α release. However, in contrast to what we expected from this evidence, it was not required for maintaining heterochromatin transcription. RNA-seq data from MDA-MB-231 cells shCT and shLOXL2 obtained considering the technical requirements for studying repetitive elements revealed that their expression was not altered in the absence of LOXL2[210]. In relation to these results, we have to consider that downregulation of heterochromatin transcripts through LOXL2 oxidation of histone H3 during the EMT occurs only in a specific time point, when chromatin is being reorganized; after that, the levels of heterochromatin transcription are recovered despite the presence of H3K4ox, suggesting that it might contribute with another function in mesenchymal cells.

Alternatively, it has also been described that aberrant heterochromatin silencing and conflicts between replication forks and transcription can facilitate the formation of R-loops, an important source of genomic

instability that can result in DNA damage. However, despite observing an increase in γH2AX and 53BP1 foci in the absence of LOXL2 and RUVBL2, no R-loop formation or replication fork stalling were detected in these conditions either[210], further discarding the possible role of H3K4ox in regulating heterochromatin transcription.

Therefore, we propose that alternatively these H3K4ox enriched chromatin domains would have more a structural role, being important for the maintenance of a proper balance between heterochromatin and euchromatin. Interestingly, this chromatin structure could be crucial for conferring other advantages to cancer cells independent of a direct effect on gene transcription regulation.

On the one hand, it could protect cells from the activation of the DNA damage response and the consequent cell cycle arrest or cell fate decisions such as apoptosis or senescence. Downregulation of both LOXL2 and RUVBL2 led to an increase in the number of γH2AX and 53BP1 foci concomitant with strong phenotypic effects that compromise the proliferation and survival of these cells. Consistently, transcriptome analysis showed that, as a result, in these situations, there was an upregulation of apoptotic signaling pathways and a downregulation of G1/S transition of mitotic cell cycle, DNA replication, and DNA checkpoints.

Currently, there is strong evidence that chromatin structure and accessibility plays a crucial role in the regulation of the DDR and the proper repair of the DNA damage[174-176]. Moreover, despite some controversy[185], it has been suggested that heterochromatin could be a barrier to the DDR affecting the accessibility[171,176-180] and allowing the accumulation of mutations[181,182] (see Introduction, Section 4.3).

Of particular interest, it has also been reported that oncogene-expressing transformed cells and human tumors that are constantly exposed to oncogene-induced DNA damage have high levels of heterochromatic markers as compared to the normal tissues. This feature is maintained upon inactivation of tumor suppressive barriers such as ATM or p53 and is crucial for inactivating DDR. In agreement with our results, alteration of heterochromatin components such as

SUV39H1, HP1α or treatment with inhibitors of HDACs in oncogene-expressing cells leads to an increase of the DDR signaling and consequently cell death by apoptosis.

Interestingly, as in this last study, the triple-negative MDA-MB-231 cells also have mutated p53, suggesting that they could represent a similar scenario in which cancer cells would be continually exposed to oncogene-induced DNA damage. Hence, in this context, the maintenance of H3K4ox enriched heterochromatin regions through LOXL2, RUVBL2, and CRL4B could be crucial for regulating the heterochromatin induction characteristic of oncogene-induced stress and bypass the activation of the DDR.

On the other hand, we also demonstrated that the maintenance of these increased heterochromatin status in mesenchymal cancer cells is required for their ability to migrate and invade. In agreement, several studies have shown that chromatin compaction plays a role in the migration process itself regulating the mechanical properties of the nucleus[358-362].

During migration, the physical link between chromatin and the cytoskeleton facilitates coordinated structural changes in these two components and nuclear reshaping. In this process, global condensation of chromatin contributes to decreased nuclear size, increased nuclear stiffness and better nuclear reshaping[359]. Thus, in response to migration signals, there is an increase in the levels of heterochromatin histone modifications, DNA methylation, resistance to DNase I digestion, and changes in the intranuclear mobility of chromatin architectural proteins[358,360].

Consistent with our results, overexpression of SUV39H1 activated migration in breast and colorectal cancer cells[362]. Indeed, the highly metastatic line MDA-MB-231 of breast cancer cells that contain higher levels of LOXL2 and H3K4ox and a more compacted chromatin showed higher transmigration capabilities than the poorly metastatic MCF7[361].

Accordingly, migration ability is strongly impaired after overexpressing a dominant negative form of histone H1 or SUV39H1 as well as

treatment with chemical compounds that promote an open chromatin state: HDAC inhibitors, the methylase inhibitor 5′-deoxy-5′-methylthioadenosine (MTA) or the specific inhibitor for SUV39H1 chaetocin[358,360,361].

Furthermore, this global chromatin condensation in response to migration signals seem to contribute to this process independently of gene transcription regulation[358,362], further supporting the observed phenotypic effects and our RNA-sequencing data.

Altogether, we propose that the maintenance of heterochromatin domains enriched in H3K4ox is crucial for the oncogenic potential of cancer cells through the regulation of chromatin structure and a proper balance between euchromatin and heterochromatin. In this way, it favors their ability to invade and migrate, as well as the bypass of the DDR activated by oncogene-induced stress, which could compromise the proliferation and survival of cancer cells.

Interestingly, this context would also allow cancer cells to accumulate DNA damage and thus heritable variation, which means the opportunity to acquire new properties that confer more malignancy. In addition, our results suggest that this gain of chromatin compaction and silent environments in cancer cells would not participate directly in transcriptional regulation and would be compatible with a proper expression of oncogenic gene programs.

Here it is important to mention that, considering the existing literature, our findings might seem contradictory to some studies that associate cancer progression with a gain in chromatin accessibility.

It has been reported that during the neoplasic process, the epigenome is reorganized from differentiated cells into cancer stem cells in a way that large heterochromatin domains, such as LOCKs and LADs, are erased, whereas euchromatin features, such as hypomethylated blocks, emerge. These changes would allow cancer stem cells to adopt more epigenetic and gene expression plasticity as well as facilitate the clustering of oncogenic super-enhancers and coordinate the expression of oncogenic pathway members[363,364]. In particular, during EMT, there

is a global reduction in the heterochromatin mark H3K9Me2 (specifically in LOCKs) and an increase in euchromatin marks H3K4Me3 and H3K36Me3, which is required for the acquisition of malignant traits and chemoresistance[365].

On the other hand, other studies have linked chromatin accessibility and metastasis. Tumors depleted for G9a, the histone modifying enzyme that incorporates H3K9me2, develop after a prolonged latency as compared to their wild-type counterparts, but are more aggressive, have a higher cancer progenitor pool, more genomic instability, and more frequent loss-of-function p53 mutations[185]. In addition, the transcription factor Nfib promotes metastasis increasing chromatin accessibility and allowing the opening of large number of distal regulatory elements across the genome[366].

Thus, different proteins and mechanisms that both increase and decrease the chromatin accessibility could be required depending on the cancer type or stage. In addition, we also have to distinguish between the ones involved in the transformation of cancer cells and acquisition of malignancy, such as during the EMT, and the ones that contribute to the function of metastatic cells, when they are in the mesenchymal stage and have already been transformed.

In addition, we speculate that the proposed molecular mechanism allows the formation of heterochromatin domains in cancer cells different from the previously described LOCKs and LADs, which are large repressive domains that robustly avoid the expression of clusters of genes. As previously discussed, the ones enriched in H3K4ox have features of both constitutive and facultative heterochromatin, and we think that they would probably involve a more dynamic and flexible regulation.

Maintenance of H3K4ox and heterochromatin as therapeutic targets

Our experiments revealed a direct link between the maintenance of H3K4ox, chromatin condensation, and tumorigenic capacities. Thus, these data provide novel therapeutic opportunities and suggest that any

of the components described could be a potential target for cancer therapy in TNBC tumors.

First, the development of LOXL2 inhibitors could be a promising success, and indeed, some of them have already been described[367,368]. However, considering the relevance and contribution of the described LOXL2 nuclear functions in cancer, it is crucial to find molecules capable of inhibiting the enzymatic activity of both extracellular and intracellular LOXL2.

Second, another possible therapeutic strategy could be the inhibition of RUVBL1/2 ATPase activity. So far, several efforts have been devoted to find compounds that efficiently and selectively inhibit this function. Importantly, some of them had promising results, affecting cancer cell proliferation and survival *in vitro* as well as tumor growth *in vivo*, without showing severe toxicity[228,369-371].

Third, although it is still at an early stage and needs further research, pharmaceutical inhibition of CRLs, CRLs-interacting factors, or the interactions between subunits of the complex such as CUL4B-DDB1 could also be feasible options[282,372]. Indeed, even targeting the WD40 domains to antagonize protein-protein interactions could be envisioned. As the WDR central pockets vary in shape and electrostatics, this strategy would offer several structures and degrees of chemical tractability. In addition, it would probably represent a bigger challenge for cancer cells to develop a resistant mechanism to this than to the inhibition of the catalytic activity of enzymes[338]. However, targeting these domains could also be risky, as it would perturb multiple protein complexes at the same time, resulting in either increased overall efficacy or unexpected phenotypic outcomes.

On the other hand, considering the link between chromatin compaction and cancer progression, the use of drugs that affect chromatin compaction and generates and open chromatin state could be an attractive strategy for targeting cancer cells by increasing DDR signalling and compromising their oncogenic potential and survival[172,210]. These compounds include histone deacetylase inhibitors such as trichostatin A (TSA)[373], methylase inhibitors such as 5′-deoxy-

5′-methylthioadenosine (MTA)[374] or specific inhibitors for the H3K9 methyltransferase SUV39H1 such as chaetocin[375]. Moreover, they could also be used as chemo- or radio-sensitizers to increase the effectiveness of conventional genotoxic treatments and overcome resistance to treatment[186,210].

However, some studies have also questioned the use of “chromatin-opening drugs”. In skin, tumors knocked out of G9a were linked to more cancer aggressiveness[185] and in gliomas, contrary to what we propose, the induction of chromatin compaction that limits the DDR could be a potential therapeutic tool to disrupt resistance to radiotherapy[178,376].

Therefore, when targeting epigenetic factors, each chromatin modifier should be studied individually. Further, we should consider the type of cancer, the mechanisms involved in its progression, and the response to treatment. In addition, possible long-term effects should also be addressed, as initial strong antitumor responses can be followed by a more aggressive disease due to the selection and expansion of aggressive tumor clones as a result of the newly imposed selection pressure[185].

Studying the chromatin and DDR status of tumors could be really helpful and even crucial before using chromatin-modifying drugs. Considering cancer heterogeneity in terms of features and therapeutic responses, it is possible that these drugs would only be useful to harm cancer cells characterized by high levels of heterochromatin, but would probably be less effective in cancers cells that do not present this feature[130].

CONCLUDING REMARKS

LOXL2 oxidation of histone H3 has been described to be important in TNBC cells to generate compacted heterochromatin regions. However, many questions around this function were still unsolved.

In this thesis, we identified LOXL2 partners and H3K4ox readers and characterized the molecular mechanisms that regulate the maintenance of H3K4ox enriched regions, how this histone modification induces chromatin compaction, and its relevance for the oncogenic potential of breast cancer cells.

First, we demonstrated that LOXL2 interacts with the RUVBL1, RUVBL2, DMAP1, and BAF53A proteins that form complexes involved in the exchange of the histone variant H2A.Z. Moreover, genome-wide experiments showed that, in triple-negative breast cancer cells, H2A.Z and RUVBL2 are located in heterochromatin regions enriched with H3K4ox. Interestingly, we found that LOXL2 and RUVBL2 cooperate to maintain their epigenetic functions as well as the consequent changes in chromatin structure. On the one hand, LOXL2 regulates RUVBL2 recruitment to chromatin and H2A.Z deposition. On the other hand, both active RUVBL2 and H2A.Z incorporation are essential for maintaining chromatin compaction and high levels of H3K4ox. However, RUVBL2 does not modulate LOXL2 enzymatic activity, but rather affects its recruitment into chromatin as well as the proper incorporation of H2A.Z.

Second, we successfully identified putative H3K4ox readers. We found that upon oxidation of H3 by LOXL2, the members of the CRL4B complex DDB1 and RBX1 are recruited to chromatin, regulating the ubiquitination of H2A. This histone modification is required for H2A.Z incorporation in heterochromatin regions, as well as the maintenance of H3K4ox and chromatin compaction.

Finally, we demonstrated that H3K4ox maintenance is crucial for heterochromatin integrity, and that this is linked to the oncogenic properties of triple-negative breast cancer cells. Loss of H3K4ox dramatically decreases the levels of H3K9me3 as well as the proliferation rates, colony formation and the migration and invasion capacities of cancer cells. Interestingly, these H3K4ox enriched heterochromatin domains do not seem to be implicated directly in gene

expression regulation. Alternatively, they would be important for chromatin structure and a proper balance between euchromatin and heterochromatin. Hence, the maintenance of chromatin compaction by the described epigenetic mechanism avoids the aberrant activation of the DDR that could compromise the proliferation and survival of cancer cells and favors their ability to invade and migrate.

Altogether, we propose that in TNBC cells LOXL2 and H3K4ox interact with RUVBL1, RUVBL2, DMAP1, and BAF53A, as well as the DDB1-RBX1 complex, to form a functional unit. In this way, there is an interplay between a variety of epigenetic mechanisms including H3K4ox, H2A ubiquitination, the histone variant H2A.Z, and the heterochromatin marks H3K9me3 and H3K27me3. This allows the maintenance of large stable environments with H3K4ox and sustained chromatin compaction, which are crucial for the tumorigenic capacities of breast cancer cells (Figure C1).

Our data revealed a direct link between H3K4ox, chromatin compaction, and oncogenic potential, and suggest novel therapeutic targets to fight TNBC tumors.

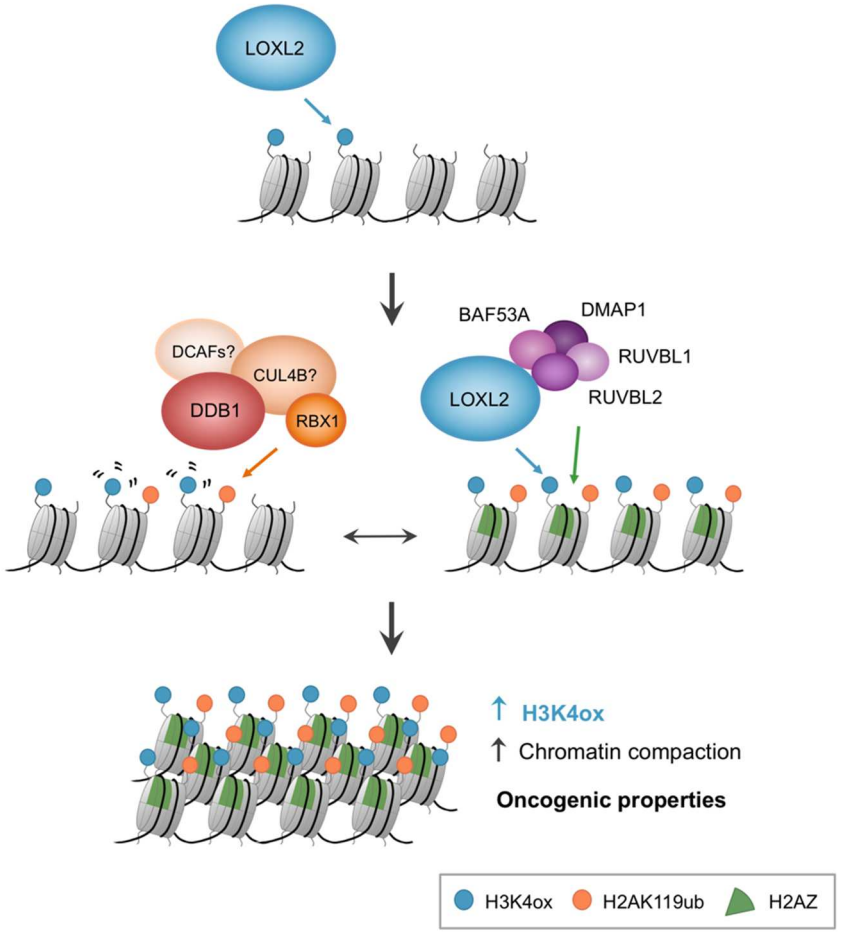

Figure C1. Representation of the working model. Upon LOXL2 oxidation of histone H3, DDB1 is recruited to chromatin regulating the ubiquitination of H2A (H2Aub) through RBX1. In addition, LOXL2 interacts with RUVBL1, RUVBL2, BAF53A and DMAP1, proteins involved in the exchange of the histone variant H2A.Z. The interplay between these series of events is required to maintain H3K4ox-enriched heterochromatin regions and sustained chromatin compaction, which are crucial for the tumorigenic capacities of breast cancer cells.

MATERIALS & METHODS

1. Cell lines and culture conditions

All cells were maintained in Dulbecco's modified Eagle's medium (Biowest; L0106-500) supplemented with 1% penicillin-streptomycin (Gibco; 15140122), 2 mM L-glutamine (Biowest; X0550-100) and 10% FBS (Gibco; 10270106) at 37ºC in 5% CO_2. Mycoplasma contamination was tested regularly using standard PCR with the primers:

F: 5′-GGCGAATGGGTGAGTAACACG-3′
R: 5'-CGGATAACGCTTGCGACCTATG-3′.

The following cell lines were used in this study:

- **HEK293T:** human embryonic kidney cells, used both for producing viruses and for experiments;
- **MDA-231:** human triple-negative breast cancer (TNBC) cells.
- **CAL-51**: human TNBC cells.

2. Transfection procedures

For overexpression assays, HEK293T and CAL-51 cells were seeded for 18–24 hr and transiently transfected with the indicated vectors by using either JetPrime reagent (Polyplus-transfection; 114-15) or Polyethylenimine polymer (Polysciences Inc; 23966-1) following manufacturer's instructions.

3. Virus production

3.1. Lentivirus production and infection

For lentiviral infections, HEK293T cells were used to produce viral particles. Cells were grown to 70% of confluency (day 0) and then transfected by adding dropwise a mixture of 150 mM NaCl, DNA (50% of the indicated shRNA vector, 10% pCMV-VSVG, 30% pMDLg/pRRE, and 10% pRSV rev) and polyethylenimine polymer (Polysciences Inc; 23966-1), which had been pre-incubated for 15 min at room temperature. The transfection medium was replaced with fresh medium after 24 hr (day 1). At days 2 and 3, cell-conditioned medium was filtered

with a 0.45 µm filter unit (Merk Millipore; 051338) and stored at 4ºC. Then, viral particles were concentrated with Lenti-X Concentrator product (Clonetech; 631232) following manufacturer's instructions, and virus aliquots were stored at –80ªC.

HEK293T and MDA-231 cells were infected with concentrated viral particles. After 16–18 hr, medium was changed for fresh medium with 2.7 µg/ml or 2.5 µg/ml puromycin, respectively, and cells were selected for 48 hr. At this point, cells were seeded, and 48 hr post-selection, experiments were performed. See Table MM1 for information about the shRNAs used.

Gene	TRC Code	Species	Sequence (5′–3′)
CT	SHC002V	Human	CCGGCAACAAGATGAAGAGC ACCAACTCGAGTTGGTGCTCT TCATCTTGTTGTTTTT
DDB1	TRCN0000082855	Human	CCGGCGACCGTAAGAAGGTG ACTTTCTCGAGAAAGTCACCT TCTTACGGTCGTTTTTG
H2AFZ	TRCN0000072587	Human	CCGGGTACTTGAACTGGCAG GAAATCTCGAGATTTCCTGCC AGTTCAAGTACTTTTTG
LOXL2	TRCN0000046196	Human	CCGGGAGAGGACATACAATA CCAAACTCGAGTTTGGTATTG TATGTCCTCTCTTTTTG
RBX1	TRCN0000022384	Human	CCGGCTTTCCCTGCTGTTACC TAATCTCGAGATTAGGTAACA GCAGGGAAAGTTTTT
RBX1 3'UTR	TRCN0000272586	Human	CCGGCTTTCCCTGCTGTTACC TAATCTCGAGATTAGGTAACA GCAGGGAAAGTTTTTG
RING1B	TRCN0000033697	Human	CCGGGCCAGGATCAACAAGC ACAATCTCGAGATTGTGCTTG TTGATCCTGGCTTTTTG
RUVBL2	TRCN0000051563	Human	CCGGCGAGAAAGACACGAAG CAGATCTCGAGATCTGCTTCG TGTCTTTCTCGTTTTTG

Table MM1. **shRNAs.** List of shRNAs used in this study, including their commercial information, species, and sequence. All shRNAs were purchased from Sigma-Aldrich MISSION shRNA Library.

3.2. Retrovirus production and infection

For retroviral infections, HEK293T cells were transfected with pCL-ampho packaging vector, and the indicated vectors using JetPrime reagent (Polyplus-transfection; 114-15) following manufacturer instructions (day 0). The transfection medium was replaced with fresh medium after 24 hr, and cell-conditioned medium at days 2 and 3 was filtered and used to infect MDA-231 cells twice. Target cells were seeded into a 6-well plate and infected by adding the filtered retroviral supernatant and spinning the plates at 32ºC for 2 hr at 1000 × g. After that, 1 ml of fresh complete medium was added and cells were incubated at 37ºC.

4. Cell extracts

In experiments for studying ubiquitination, the DUB inhibitor PR-619 (Tocris Bioscience; 4482) was added in lysis buffers (100 µM) to preserve maximum amounts of ubiquitinated proteins.

4.1. Total extracts

Cells were lysed in SDS lysis buffer. Samples were kept at room temperature to avoid SDS precipitation and syringed to homogenize them. Protein was quantified with the DC Protein Array kit (Lowry method; Bio-Rad) and Nanodrop analysis.

SDS lysis buffer: 2% SDS, 50 mM Tris-HCl pH [7.5], 10% glycerol

4.2. Histone isolation

Cells were harvested by centrifugation and washed with cold PBS. Pellets were resuspended by vortexing with lysis buffer and centrifuged at full speed for 15 seconds twice. The same procedure was repeated once with wash buffer. Then, 0.4 N H_2S0_4 was added to each pellet and left for 1 hr at 4ºC (finger flicking occasionally). After centrifuging at full speed for 5 min, supernatants were transferred to a new tube, and acetone was added (1:9). The mixture was left overnight at –20ºC and then centrifuged at full speed for 10 min. Pellets were air dried for 5 min and resuspended in 30–100 µl of sterile water. Protein was quantified

with the DC Protein Array kit (Lowry method; Bio-Rad) before sample preparation.

Lysis buffer: 10 mM Tris [pH 6.5], 50 mM sodium bisulfite, 1% Triton X-100, 10 mM $MgCl_2$, 8.6% sucrose, 10 mM sodium butyrate

Wash buffer: 10 mM Tris [pH 7.4], 13 mM EDTA

5. Western blot

Western blots were performed according to standard procedures. First, samples were mixed with 5× loading buffer and boiled at 95ºC for 5 min. Proteins were analyzed by sodium dodecyl sulfate polyacrylamide gel electrophoresis (SDS-PAGE) using different percentages of polyacrylamide concentration, ranging from 7.5% to 15%. Gels were run in Tris-glycine-SDS (TGS) buffer, and proteins were transferred to a nitrocellulose membrane (Amersham Protran 0.45 nitrocellulose, GE Healthcare) in Transfer Buffer for 60 to 120 min, depending on the molecular weight of the protein. Once completed, membranes were incubated with Ponceau staining solution to ensure that the protein was correctly transferred, which was removed with several washes with distilled water. Membranes were blocked with 5% non-fat milk or bovine serum albumin (BSA) in Tris-buffer saline-Tween (TBS-T) buffer for 1 hr. Primary antibodies were added in fresh blocking solution and incubated overnight at 4ºC. After three washes of 10 min with TBS-T, membranes were incubated with horseradish peroxidase (HRP)-combined secondary antibodies in fresh blocking solution for 1 hr at room temperature. After a new round of washes, membranes were developed by incubation with a substrate for HRP-enhanced chemiluminiscence (ECL) and exposure to autoradiography films. For proteins difficult to detect, more sensitive ECL and films were used.

5× loading buffer: 250 mM Tris-HCl [pH 6.8], 10% SDS, 0.02% Bromophenol blue, 50% glycerol, 20% β-mercaptoethanol

Tris-glycine-SDS (TGS) buffer: 25 mM Tris-OH [pH 8.3], 192 mM glycine, 5% SDS

Transfer buffer: 50 mM Tris-OH, 396 mM glycine, 0.1% SDS, 20% methanol

Tris-buffer saline-Tween (TBS-T): 25 mM Tris-HCl [pH 7.5], 137 mM NaCl, 0.1% Tween

Ponceau S: 0.5% Ponceau, 1% acetic acid

6. Co-immunoprecipitation (IP) assays

HEK293T were transfected with pcDNA3-hLOXL2wt-Flag or an empty pcDNA3. After 48 hr, co-immunoprecipitation assays were carried out as previously described[147] with the following modifications. Cells were washed with pre-warmed 37ºC 1× PBS and incubated with 1 mM DTBP solution for 30 min at 37ºC. The solution was then changed for cold 100 mM Tris-HCl (pH 7.4) and incubated for 5 min on ice. Cells were washed with cold PBS and lysed in high salt lysis buffer with protease inhibitors. After incubation for 30 min on ice, lysate was centrifuged at 13,000 rpm at 4ºC for 10 min. Balance buffer was added to the resulting supernatant to get a final NaCl concentration of 150 mM. Cell extracts were then incubated with Flag-M2 Affinity Agarose Gel (Sigma-Aldrich; A2220) for 4 hr at 4ºC and washed three times with wash buffer. Finally, precipitated complexes were eluted with 2× loading buffer.

For endogenous co-immunoprecipitation assays in MDA-231 cells, DTBP treatment was performed as described before, and then cells were lysed with soft lysis buffer supplemented with protease and phosphatase inhibitors. After incubation for 5 min on ice, lysates were centrifuged at 3,000 rpm at 4ºC for 15 min, and pellets were lysed with high-salt lysis buffer and balanced as explained before. Antibodies were added for 16–18h at 4ºC, followed by immunoprecipation of immunocomplexes with protein A agarose beads (Diagenode; C03020002), previously blocked with 0.5% BSA for 1 hr at 4ºC. Immunoprecipitated complexes were washed three times with wash buffer and eluted with 2× loading buffer. When used, ethidium bromide was added in lysis and washing buffers (100 µg/ml).

High-salt lysis buffer: 20 mM HEPES [pH 7.4], 10% glycerol, 350 mM NaCl, 1 mM $MgCl_2$, 0.5% Triton X-100, 1 mM dithiothreitol

Balance buffer: 20 mM HEPES [pH 7.4], 1 mM $MgCl_2$, 10 mM KCl

Wash buffer: 20 mM HEPES [pH 7.4], 1 mM $MgCl_2$, 150 mM NaCl, 10% glycerol, 0.5% Triton X-100

Soft lysis buffer: 50 mM Tris [pH 8], 10 mM EDTA, 0.1% NP-40, 10% glycerol

7. Nucleosome purification and oxidation assays with LOXL2-co-immunoprecipitated complexes

Nucleosomes were purified from HEK293T cells. After harvesting by centrifugation, cells were resuspended in buffer A supplemented with protease inhibitors and homogenized by ten strokes in a Dounce homogenizer. Cells were then centrifuged, and nuclei pellets were resuspended in buffer A with 10 mM $CaCl_2$. Four units of micrococcal nuclease were added for 30 min at room temperature, and the reaction was stopped by the addition of 50 mM EDTA. Purified nucleosomes were aliquoted and kept at –80ºC.

HEK293T cells were transfected with pcDNA3-hLOXL2wt-Flag or an empty pcDNA3. After 48 hr, co-immunoprecipitation assays were performed as described before but without DTBP treatment. After incubation with Flag-M2 Affinity Agarose Gel (Sigma-Aldrich; A2220), precipitated complexes were resuspended in oxidation buffer and incubated with 50 ng of purified nucleosomes for 2 hr at 37ºC. Then, 5× loading buffer was added to samples, and proteins were analyzed by SDS-PAGE and Western blotting.

Buffer A: 10 mM Tris buffer [pH 7.4], 10 mM NaCl, 3 mM $MgCl_2$, 300 mM sucrose, 0.2% NP-40

Oxidation buffer: 20 mM HEPES [pH 7.4], 100 mM NaCl, 1 mM $MgCl_2$, 0.1 mg/ml BSA, 1 mM DTT

8. Readers experiment

MDA-231 cells were lysed in soft lysis buffer supplemented with protease inhibitors for 5 min on ice and centrifuged at 3,000 rpm for 15 min. The supernatant was discarded, and the nuclear pellet was resuspended in high-salt lysis buffer for 30 min at 4°C. Samples were centrifuged at 13,000 rpm for 10 min and the NaCl concentration of the supernatant was reduced to 300 mM NaCl with balance buffer. To preclear the nuclear extracts, samples were incubated with streptavidin beads for 1-2 hr. Beads were separated, and nuclear extracts were incubated for 1.5 hr at 4ºC with 1 µg of H3K4ox or irrelevant peptide (see Table MM2) that had been previously recovered with streptavidin magnetic beads (Invitrogen; 65305) for 30 min at 4ºC. Finally, immunoprecipitated proteins were washed two times with wash buffer and once with high salt lysis buffer, and processed for mass spectrometry analysis.

Soft lysis buffer: 50 mM Tris [pH 8], 10 mM EDTA, 0.1% NP-40, 10% glycerol

High salt lysis buffer: 20 mM HEPES [pH 7.4], 10% glycerol, 350 mM NaCl, 1 mM $MgCl_2$, 0.5% Triton X-100, 1 mM dithiothreitol

Balance buffer: 20 mM HEPES [pH 7.4], 1 mM $MgCl_2$, 10 mM KCl

Wash buffer: 20 mM HEPES [pH 7.4], 1 mM $MgCl_2$, 150 mM NaCl, 10% glycerol, 0.5% Triton X-100

8.1. Peptides

Name	Description	Sequence
H3K4ox	Peptide of H3 tail with the intermediate alcohol of LOXL2 oxidation in lysine 4	ART-K(OH)-QTARKSTGGKAP-biotin
Irrelevant peptide	SpyTag was used, which is a short peptide that forms an isopeptide bond with its protein partner SpyCatcher	AHIVMVDAYKPTK-$NH(CH_2)_2NH$-biotin

Table MM2. Peptides. List of biotinylated peptides used in this study and their sequences.

9. Mass spectrometry (MS) analysis

9.1. Sample preparation

Beads used in immunoprecipitation were cleaned three times with 500 µl of 200 mM ammonium bicarbonate and 60 µl of 6 M urea / 200 mM ammonium bicarbonate were added. Samples were then reduced with dithiothreitol (30 nmol, 37 ºC, 60 min), alkylated in the dark with iodoacetamide (60 nmol, 25 ºC, 30 min) and diluted to 1 M urea with 200 mM ammonium bicarbonate for trypsin digestion (1 µg, 37ºC, 8 hr, Promega cat # V5113). After digestion, the peptide mix was acidified with formic acid and desalted with a MicroSpin C18 column (The Nest Group, Inc) prior to LC-MS/MS analysis.

9.2. Chromatographic and mass spectrometric analysis

Samples were analyzed using a LTQ-Orbitrap Velos Pro mass spectrometer (Thermo Fisher Scientific, San Jose, CA, USA) coupled to an EASY-nLC 1000 (Thermo Fisher Scientific (Proxeon), Odense, Denmark). Peptides were loaded onto the 2-cm Nano Trap column with an inner diameter of 100 µm packed with C18 particles of 5 µm particle size (Thermo Fisher Scientific) and were separated by reversed-phase chromatography using a 25-cm column with an inner diameter of 75 µm, packed with 1.9 µm C18 particles (Nikkyo Technos Co., Ltd. Japan).

Chromatographic gradients started at 93% buffer A and 7% buffer B with a flow rate of 250 nl/min for 5 min and gradually increased 65% buffer A and 35% buffer B in 60 min. After each analysis, the column was washed for 15 min with 10% buffer A and 90% buffer B. Buffer A: 0.1% formic acid in water. Buffer B: 0.1% formic acid in acetonitrile.

The mass spectrometer was operated in positive ionization mode with nanospray voltage set at 2.1 kV and source temperature at 300°C. Ultramark 1621 was used for external calibration of the FT mass analyzer prior the analyses and an internal calibration was performed using the background polysiloxane ion signal at m/z 445.1200. The acquisition was performed in data-dependent adquisition (DDA) mode and full MS scans with 1 micro scans at resolution of 60,000 were used over a mass range of m/z 350-2000 with detection in the Orbitrap. Auto gain control (AGC) was set to 1E6, dynamic exclusion (60 seconds) and charge state filtering disqualifying singly charged peptides was activated. In each cycle of DDA analysis, following each survey scan, the top twenty most intense ions with multiple charged ions above a threshold ion count of 5000 were selected for fragmentation. Fragment ion spectra were produced via collision-induced dissociation (CID) at normalized collision energy of 35% and they were acquired in the ion trap mass analyzer. AGC was set to 1E4, isolation window of 2.0 m/z, an activation time of 10 ms and a maximum injection time of 100 ms were used. All data were acquired with Xcalibur software v2.2. Digested bovine serum albumin (New england biolabs cat # P8108S) was analyzed between each sample to avoid sample carryover and to assure stability of the instrument; QCloud[377] was used to control instrument longitudinal performance during the project.

9.3. Proteomic Data Analysis

Acquired spectra were analyzed using the Proteome Discoverer software suite (v1.4, Thermo Fisher Scientific) and the Mascot search engine (v2.5 Matrix Science)[378]. The data was searched against a Swiss-Prot human database (as in April 2017, 20797 entries) plus a list of common contaminants and all the corresponding decoy entries[379]. For peptide identification, a precursor ion mass tolerance of 7 ppm was used for MS1 level, trypsin was chosen as enzyme, and up to three

missed cleavages were allowed. The fragment ion mass tolerance was set to 0.5 Da for MS2 spectra. Oxidation of methionine and N-terminal protein acetylation were used as variable modifications whereas carbamidomethylation on cysteines was set as a fixed modification. False discovery rate (FDR) in peptide identification was set to a maximum of 5%.

9.4. Interactome statistical analysis

The inferential statistical analysis was done using the open-source statistical package R. Files containing all spectral counts for each sample and its replicates were imported into the R software from the result tables of Proteome Discoverer (v1.4, Thermo Fisher Scientific). Data were assembled into a matrix of spectral counts, in which columns represented the different conditions and rows represented the identified proteins (5). An unsupervised exploratory data analysis (EDA) consisting of data normalizations, principal components analysis, and hierarchical clustering of the samples on the SpC matrix was first performed. The Generalized Linear Model based on the Poisson distribution was used as a significance test [380]. Finally, the Benjamini and Hochberg multitest correction was used to adjust the p-values to the control of the FDR. To identify statistically significant proteins, spectral count signal, fold change, and adjusted p-value were taken into account[380].

9.5. Dot blot assay

To check that the peptides were equally recovered, in parallel with the experiment, an additional microgram of H3K4ox or irrelevant peptides were incubated with streptavidin beads and eluted with 20 µl of SDS 1%. Then, 5× loading buffer was added and samples were boiled at 95ºC for 5 min. For dot blot assays, 2–10 µl of each peptide were applied to a nitrocellulose membrane freehand. The blot was blocked in 5% milk in TBS-T for 30 min to 1 hr at room temperature and incubated with anti-biotin overnight at 4ºC. Secondary antibody incubation and developing was performed as described for Western blots.

10. Chromatin association assay

Cells were crosslinked with 1% formaldehyde in PBS for 10 min at 24ºC, and pellets were resuspended in buffer A. After incubating 10 min on ice, samples were centrifuged and lysed in buffer B twice. The chromatin-containing pellets were resuspended in buffer C overnight at 4ºC. Samples were centrifuged 2 min at 16100 × g, and the supernatant was quantified and used for Western blotting.

Buffer A: 100 mM Tris, pH [7.5], 5 mM $MgCl_2$, 60 mM KCl, 125 mM NaCl, 300 mM sucrose, 1% NP-40, 0.5 mM DTT

Buffer B: 3 mM EDTA, 0.2 mM EGTA, 1 mM DTT

Buffer C: 1% SDS, 10 mM EDTA, 50 mM Tris [pH 8.0]

11. Subcellular fractionation assay

Subcellular fractionation assays were performed as previously described[381]. Cells were harvested in hypotonic buffer, incubated for 20 min on ice and disrupted by Dounce homogenization 10 times. Samples were centrifuged for 10 min at 3,600 rpm, and the supernatant was saved as the cytoplasmic fraction. Pellets were resuspended in extraction buffer, incubated for 30 min by rotating at 4ºC, and centrifuged at 13,200 rpm for 30 min. The supernatant was saved as the nuclear extract and the pellet, which was the chromatin fraction, was resuspended in SDS lysis buffer.

Hypotonic buffer: 10 mM Tris-HCl [pH 7.4], 10 mM KCl, 1.5 mM $MgCl_2$, 0.2 mM PMSF, 1 mM DTT, protease inhibitors

Extraction buffer: 15 mM Tris-HCl [pH 7.4], 0.4M NaCl, 1 mM $MgCl_2$, 1 mM EDTA, 10% glycerol, 0.2 mM PMSF, 1 mM DTT, plus protease inhibitors

SDS lysis buffer: 2% SDS, 50 mM Tris-HCl [pH 7.5], 10% glycerol)

12. Chromatin immunoprecipitation (ChIP)

Cells were crosslinked in 1% formaldehyde for 10 min at 37ºC and then glycine was added to a final concentration of 0.125 M for 2 min at room temperature to quench the crosslinking. Cells were scraped with cold soft lysis buffer supplemented with protease inhibitors and samples were centrifuged at 3000 rpm for 15 min. Nuclei pellets were lysed with SDS-lysis buffer supplemented with protease inhibitors and sonicated to generate 200–600 bp DNA fragments. After 20 min of incubation on ice, sonicated extracts were centrifuged 10 min at 13,000 rpm and supernatants were diluted 1:10 with dilution buffer.

Immunoprecipitation was done rotating overnight at 4ºC with primary antibody or irrelevant IgGs. Immunocomplexes were then captured with unblocked protein A agarose beads (Diagenode; C03020002), previously blocked with 0.5% BSA, incubating for 3 hr at 4ºC. Precipitated samples were sequentially washed three times with low salt buffer, three times with high salt buffer, and twice with LiCl buffer, and then incubated with elution buffer for 1 hr at 37 ºC and overnight at 65ºC with 200 mM NaCl to reverse formaldehyde crosslinking. Finally, samples were treated for 1 hr at 55ºC with proteinase K solution. DNA was purified with MinElute PCR purification kit (Qiagen; 28006) and eluted in MilliQ water (80 µl–100 µl). The amount of immunoprecipitated DNA was analyzed by quantitative PCR (qPCR) in duplicates or triplicates; in a final volume of 10 µl, 4 µl of the eluted DNA were mixed with forward and reverse primers (Sigma; 100-500 nM each) and 1× PerfeCTa® SYBR® Green FastMix (Quantabio; 95073-01). Thermocycling parameters used were: 95 °C 30 s; 40 cycles 95 °C 5 s, 60 °C 15 s, 72ºC 10s; melting curve. ChIP results were quantified relative to the input amount. The primers used for qPCR are indicated in Table MM6.

Soft lysis buffer: 50 mM Tris-HCl [pH 8], 10 mM EDTA, 0.1% NP-40, and 10% glycerol, supplemented with protease inhibitors

SDS lysis buffer: 50 mM Tris-HCl [pH 8], 1% SDS, 10 mM EDTA, supplemented with protease inhibitors

Dilution buffer: 0.01% SDS, 1.1% Triton X-100, 1.2 mM EDTA, 16.7 mM Tris-HCl [pH 8], 167 mM NaCl

Low salt buffer: 0.1% SDS, 1% Triton X-100, 2 mM EDTA, 20 mM Tris-HCl [pH 8], 150 mM NaCl

High salt buffer: 0.1% SDS, 1% Triton X-100, 2 mM EDTA, 20 mM Tris-HCl [pH 8], 500 mM NaCl

LiCl buffer: 250 mM LiCl, 1% Nonidet P-40, 1% sodium deoxycholate, 1 mM EDTA, 10 mM Tris-HCl [pH 8]

Elution buffer: 1% SDS, 100 mM Na_2CO_3

Proteinase K solution: 0.4 mg/mL proteinase K (Roche; 3115828001), 50 mM EDTA, 200 mM Tris [pH 6.5])

12.1. ChIP-seq

For ChIP sequencing (ChIP-seq) analysis, the NEBNext Ultra DNA library Prep Kit for Illumina was used to prepare the libraries, and samples were sequenced using Illumina HiSeq 2500 system.

12.2. Analysis of ChIP-seq data

ChIP-seq samples were mapped against the hg19 human genome assembly using BowTie with default parameters. In particular, the option –m must be off to allow for multi-locus reads that are mapped into more than one region[382]. MACS was run with the default parameters but with the shift-size adjusted to 100 bp to perform the peak calling against the corresponding Input sample[383]. To build the final set of 10213 H3K4ox regions with other features, we intersected first the peaks reported in common between both replicates of H3K4ox. Next, such segments were overlapped with the peaks previously reported for RUVBL2 and H2A.Z. The set of 2267 genes was retrieved by matching the 10213 peaks with the transcripts included into the RefSeq annotations[384]. Reports of functional enrichments of GO and other genomic libraries were generated using the EnrichR tool[385]. The heatmaps displaying the density of ChIP-seq reads around the summit of each ChIP-seq peak were generated by counting the number of reads in this region for each individual peak and normalizing this value with the total number of mapped reads of the sample. Peaks on each ChIP heatmap were

ranked by the logarithm of the average number of reads in the same genomic region. The UCSC genome browser was used to generate the screenshots of each group of experiments[386].

13. MNase assay

HEK293T cells that had been infected with indicated shRNAs and selected for 48 hr with puromycin were seeded and transfected with pcDNA3-empty or pcDNA3-hLOXL2wt/mut-Flag. 48 hr post-transfection cells were counted and $1.5x10^6$ cells per condition were used for the assay. Cell pellets were lysed in 500 µL of Buffer A supplemented with protease inhibitors for 10 min at 4ºC. Then, NP-40 was added to a final concentration of 0.2% (v/v) and incubated for 10 min at 4ºC. The lysate was centrifuged for 10 min at 1200 rpm at 4ºC and the resulted pellet was resuspended in 100 µl of buffer A containing $CaCl_2$ to a final concentration of 10 mM. MNase digestion was carried out with 0,004 units for 2 min at room temperature and the enzyme was inactivated with 50 mM EDTA. Finally, extracts were treated with RNase A for 2 min at room temperature and proteinase K for 10 min at 56ºC. DNA was purified using MinElute PCR purification kit (Qiagen; 28006) and digestion products were analyzed by 1.5% agarose gel electrophoresis using Gelred TM gel stain (Biotium; BT-41003) for DNA visualization.

Buffer A: 10mM Tris [pH 7.4], 10 mM NaCl, 3 mM $MgCl_2$ and 0.3 M sacarose.

14. ATAC sequencing

MDA-231 cells were infected with lentiviral particles for shControl and shRUVBL2 and 48 hr post selection ATAC experiment was performed as described[387]. 50,000 cells of each condition were treated with transposase Tn5 (Nextera DNA Library Preparation Kit, Illumina) and DNA was purified using MinElute PCR Purification Kit (Qiagen; 28006). Then, transposed DNA was amplified by PCR using NEBNextHigh-Fidelity 2× PCR Master Mix (New Englands Labs; M0541S) and primers containing a barcode (table MM3). The number of cycles for library amplification was calculated as described. Finally, DNA was again purified using MinElute PCR

Purification kit and samples were sequenced using Illumina HiSeq 2500 system.

Sample	Direction	Sequence
MDA-231 shCT	Forward	**Ad1_noMX:** AATGATACGGCGACCACCGAGATCTACACT CGTCGGCAGCGTCAGATGTG
	Reverse	**Ad2.1_TAAGGCGA:** CAAGCAGAAGACGGCATACGAGATTCGCC TTAGTCTCGTGGGCTCGGAGATGT
MDA-231 shRUVBL2	Forward	**Ad1_noMX:** AATGATACGGCGACCACCGAGATCTACACT CGTCGGCAGCGTCAGATGTG
	Reverse	**Ad2.2_CGTACTAG:** CAAGCAGAAGACGGCATACGAGATCTAGT ACGGTCTCGTGGGCTCGGAGATGT

Table MM3. Primers used for ATAC-sequencing. Sequences of the primers used for each sample are listed, in 5' to 3' direction.

14.1. Analysis of ATAC-seq data

ATAC-seq samples were mapped against the hg19 human genome assembly using Bowtie with the option –m 1 to discard those reads that could not be uniquely mapped to just one region, and with the option –X 2000 to define the maximum insert size for paired-end alignment[382]. Mitochondrial reads were removed from each resulting map and down-sampling was applied to obtain the same number of mapped fragments per sample. Boxplots showing the ATAC-seq level distribution for a particular ATAC-seq experiment on a set of ChIP-seq genomic peaks were calculated by determining the maximum value on this region at this sample, which was assigned afterwards to the corresponding peak.

15. RNA analysis

15.1. RNA extraction

Cells were washed three times with PBS and lysed with 800 µl of TRIzol® reagent (Invitrogen; 15596018). 200 µl of RNase-free chloroform were added, mixed and incubated at room temperature for 2 min. The solution was centrifuged at 12000 x g for 15 min at 4ºC and the upper aqueous phase was transferred to a new tube. 500 µl of RNase-free isopropanol were added and solution was incubated for 10 min at room temperature. Then, RNA was precipitated by centrifugation at 12000 x g for 10 min at 4ºC. Pellets were washed once with 1 ml of 75% RNase-free ethanol and centrifuged at 7500 x g for 5 min at 4ºC. Finally, RNA-pellets were air-dried for 5–10 min to eliminate ethanol traces, resuspended in DEPC water, and dissolved for 10 min at 60ºC. RNA was quantified with Nanodrop.

15.2. Quantitative RT-PCR

RNA was retrotranscribed using iScriptTM Reverse Transcription Supermix (Biorad; 1708841) following manufacturer's instructions. Quantitative determination of RNA levels was performed in duplicate or triplicate in a final volume of 10 µl with 15-–100 ng of cDNA, forward and reverse primers (Sigma; 100-500 nM each) and 1x PerfeCTa® SYBR® Green FastMix (Quantabio; 95073-01). Thermocycling parameters used were: 95 °C 30 s; 40 cycles 95 °C 5 s, 60 °C 15 s, 72ºC 10 s; melting curve. Values were normalized to the expression of housekeeping genes (*HPRT* or *Pumilio*). The primers used for quantitative RT-PCR are indicated in Table MM6.

15.3. RNA sequencing

MDA-231 cells were infected with lentiviral particles for shControl and shRUVBL2. At 48 hr post-selection, RNA was extracted with an RNeasy Mini Kit (Qiagen; 74104) following manufacturer's instructions. RNA-seq experiments were performed with two biological replicates of each condition and samples were sequenced using the Illumina HiSeq 2500 system.

15.4. Analysis of RNA-seq data

RNA-seq samples were mapped against the hg19 human genome assembly using TopHat[388]. Cufflinks[389] was run to quantify the expression in FPKMs of each annotated transcript in RefSeq and to identify the list of differentially expressed genes for each case (FDR ≤ 0.05 and log2 FC ≥ 0.58). Gene ontology analyses of the deregulated genes were generated using the EnrichR tool[385].

16. Immunofluorescence

Cells were grown on coverslips. At the indicated time point, cells were fixed with 4% PFA for 15 min at room temperature and permeabilized with 0.3% PBS-triton for 5 min at room temperature.

Cells were then blocked with 1% PBS-BSA for 1 hr at room temperature and incubated with primary antibodies 1 hr at 37ºC or overnight at 4ºC. After three washes with PBS, they were incubated for 1 hr at room temperature with the secondary antibody conjugated with a fluorescent dye (Alexa Fluor®). Cells were washed again with PBS, incubated 5 min with PBS-DAPI (0.25 µg/mL) for cell nuclei staining, and mounted with fluoromount.

16.1. Image acquisition

Fluorescent images were acquired with either Nikon C2+ Confocal Microscope and the NIS-Elements Advanced Research software or Leica TCS SPE confocal microscope with Leica DFC300 FX camera and Leica IM50 software.

16.2. Image analysis

Image analysis for γ-H2AX and 53BP1 immunostaining was performed using ImageJ software. Cell nuclei were defined with DAPI staining and maximal projection of the confocal images was performed. The average intensity of pixels in the reference channel (Alexa 488) and the number of dots within the defined nuclear region were measured. A threshold filter was used to define foci in all the conditions.

17. SNAP-based experiments

MDA-MB-231 cells stably expressing SNAP-tag histones H3.1 and H3.3 were generated by infection with retroviral particles with pBabe-H3.1-SNAP-3xHA and pBabe-H3.3-SNAP-3xHA and selection in medium containing 5 ug/ml blasticidin.

The MDA-MB-231 cells stably expressing SNAP-tag histones H2A.Z.1/2 were obtained transfecting with TransIT-X2® Dynamic Delivery System (Mirus) and selected with 800 µg/ml of G418.

These cells were then infected with the indicated shRNA, selected for 48 hr with puromycin, and seeded in Lab-Tek II Chamber slides (Labclinics). After 48 hr, SNAP labeling was performed as previously described[318], with modifications in compound concentration and treatment time.

For specific labeling of newly-synthetized histones (quench-chase-pulse experiments), pre-existing histones were first quenched by incubating cells with 5 µM SNAP-cell Block (New England Biolabs; S9106S) for 30 min at 37ºC. After two washes with medium, cells were incubated in medium for 30 min, washed again twice, and incubated in fresh medium at 37ºC for the chase period (6 to 7 h). The pulse step was performed with 2 µM SNAP-cell TMR Star (New England Biolabs, S9105S) for 15 min (for H3.1/3) or 30 min (for H2A.Z.1/1) followed by two washes with medium, incubation with fresh medium for 30 min and two more washes. At this point, cells were pre-extracted in 0.2% Triton X-100/PBS for 5 min on ice to remove the unbound chromatin fraction and fixed in 4% paraformaldehyde for 10 min at room temperature. Fixed cells were permeabilized with 0.2% Triton X-100/PBS for 10 min at room temperature and stained with DAPI.

High-throughput microscopy (HTM)-mediated quantification of the nuclear intensity of SNAP-H3.1/3 and SNAP-H2A.Z.1/2 was performed as described[390]. Forty-eight images per well were automatically acquired with a robotized fluorescence microscopy station (ScanR, Olympus) at 40× magnification. Signals were calculated with CellProfiler using DAPI staining to generate masks of cell nuclei. Uneven

background from fluorescence microscopy images and artifacts from autofluorescence were removed with ImageJ to ensure a proper quantification.

18. Clonogenic assay

Cells were plated in a 6-well plate at a clonogenic density (500, 750 and 1000 cells/well) with puromycin selection, replacing the media every 3 days. After 7–15 days, media was removed, and cells were washed with PBS and stained with a mixture of 6% glutaraldehyde and 0.5% crystal violet for at least 30 min. Plates were then washed immersing carefully the dishes in water and left to air dry at room temperature.

19. MTT assay

After infection and selection for 48 h with puromycin, 10,000 cells/well were seeded in 96-well plates with triplicates.

The following days, cells were incubated with MTT reagent 0.5 mg/ml 3-(4,5-dimethylthiazol-2-yl)-2,5-diphenyltetrazolium bromide (MTT; Sigma) in Dulbecco's modified Eagle's medium without FBS for 3 h at 37ºC. After incubation, dimethyl sulfoxide-isopropanol (1:4) was added; once the purple crystals were fully dissolved, the absorbance was measured at 570 nm.

20. Migration and invasion assays

For migration assays, 30,000 cells were resuspended in DMEM 0.1% FBS, 0.1% BSA, and reseeded on a transwell filter chamber (Corning; 3422). After 1 hr, when cells were attached, DMEM 10% FBS was added to the lower chamber as a chemoattractant and incubated for 6 to 8 hr. For invasion experiments, cells were placed in Matrigel-coated transwell (Corning; 354230) and incubated for 12 to 16 h after chemoattractant addition.

Non-migrating and non-invading cells were removed from the upper surface of the membrane, whereas cells adhered to the lower surface

were fixed with PFA 4% for 15 min and nuclei stained with PBS-DAPI (0.25 µg/ml). Images were acquired with InCell 2000 automated epifluorescence microscope and DAPI-stained nuclei were counted using ImageJ software.

21. Rescue experiments with SUV39H1-GFP

For SUV39H1-GFP rescue experiments, MDA-MB-231 cells were infected with the indicated shRNAs and selected with puromycin for 48 h. They were then seeded and infected twice with the retroviral particles expressing pBabe-SUV39H1-GFP or pBabe-GFP as described above. Migration experiments were performed 48 hr after the second infection, and GFP-positive cells were counted using ImageJ software.

22. Cloning procedures and plasmids

Information on the plasmids used is provided in Table MM4.

pBabe-GFP or pBabe-SUV-39H1 were generated by subcloning CGA-pCAGGS-Suv39H1-EGFP-IRES-Puro vector into pBabe-puro expression vector (Addgene #1764). First, SUV39H1-GFP or ATG-GFP sequences were amplified by PCR from CGA-pCAGGS-Suv39H1-EGFP-IRES-Puro vector. pBabe target vector was digested with BamHI and SalI and insert sequences were introduced using Gibson assembly.

Plasmid	Source
pcDNA3-hLOXL2wt -Flag	*Herranz N et al.,* 2016[147]; *Iturbide A et al.*, 2015[202]
pcDNA3-hLOXL2mutant-Flag	*Herranz N et al.*, 2016[147]; *Iturbide A et al.*, 2015[202]
Empty-pcDNA3	*Herranz N et al.*, 2016[147]; *Iturbide A et al.*, 2015[202]
pcDNA3-HA-RBX1	Addgene #19897
pc-DNA5-Flag-RUVBL2	Addgene #15358

Flag-RUVBL2 (D299N)	Gift from Jean Rosenbaum (from M. Cole)
H3.1/H3.3 SNAP-3xHA	Gift from Travis Straker
H2A.Z.1/2-SNAP	Gift from Sophie Polo
pBabe-GFP	Subcloned from CGA-pCAGGS-Suv39H1-EGFP-IRES-Puro (gift from Jenuwein) into pBabe-puro expression vector (Addgene #1764)
pBabe-SUV39H1	Subcloned from CGA-pCAGGS-Suv39H1-EGFP-IRES-Puro (gift from Jenuwein) into pBabe-puro expression vector (Addgene #1764)

Table MM4. Plasmids. List of plasmids used in this study and their source.

23. Antibodies

Protein	Specie	Provider	Reference	Assay and dilution or amount
ACTL6A	rb	Abcam	ab131272	WB: 1/1,000
Biotin	rb	Abcam	ab53494	WB: 1/1,000
DDB1	rb	Bethyl	A300-462A	WB: 1/1,000 IP: 3 ug
DMAP1	rb	Abcam	ab2848	WB: 1/1,000
Flag	rb	Sigma	F7425	WB: 1/2,000-5,000
GFP	rb	Abcam	ab6556	WB: 1/1,000
H2A	rb	Abcam	ab18255	WB: 1/5,000
H2AK119ub1	rb	Cell Signaling	8240S	WB: 1/10,000
H2A.Z	rb	Abcam	ab4174	WB: 1/1,000 ChIP: 3ug
H3	rb	Abcam	ab1791	WB: 1/10,000 ChIP: 2 ug
H3K27me3	rb	Diagenode	C15410069	ChIP: 2 ug
H3K4ox	rb	Handmade		WB: /500-1,000 ChIP: 3 ug IF: 1/500 IP: 3 ug

H3K9me2	ms	Abcam	ab1220	ChIP: 2 ug
H3K9me3	rb	Millipore	07-442	WB: 1/1,000
H3K9me3	rb	Abcam	ab8898	ChIP: 2 ug
HA	rb	Sigma	H6908	WB: 1/2,000-5,000
LOXL2	rb	Novus Biologicals	NBP1-32954	WB: 1/1,000
RBX1	rb	Abcam	ab133565	WB: 1/1,000
RING1B	rb	Handmade; gift from Luciano di Croce lab.		WB: 1/1,000
RUVBL1	rb	Abcam	ab109330	WB: 1/1,000
RUVBL2	rb	Abcam	ab36569	WB: 1/1,000 ChIP: 3 ug
α-Tubulin	ms	Sigma	T9026	WB: 1/10,000
53BP1	rb	Novus Biologicals	NB100-304	IF: 1/1,000
pH2A.X (Ser139)	ms	EMD Millipore	05-636	IF: 1/500

Table MM5. Antibodies. List of antibodies used in this study, their commercial information and dilution for use.

24. Primers

Target gene	Direction	Sequence (5'-3')	Specie	Use
CDC6	Forward	TGGATGTTTGCAGGAGAGCTA	Human	mRNA-qPCR
	Reverse	GCTCCTTCTTGGCTCAAGGT		
CHAF1B	Forward	CGGGTCCCTCCAGCATT	Human	mRNA-qPCR
	Reverse	TACACGGGCTCCTTGTTGTG		
CLSPN	Forward	CTCAACAGGTGAAGACAGGCT	Human	mRNA-qPCR
	Reverse	CTTAGACGATTCCTTTGCCG		
DDB1	Forward	CAAAAGGATAGCGCTGCC	Human	mRNA-qPCR
	Reverse	TGCATTACCAGAGAGCCGT		
H2A1A	Forward	CGCCAAGTCTAAGTCTCGC	Human	mRNA-qPCR
	Reverse	TCCGCTCTGCATAGTTTCC		
H2A.Z.1	Forward	CGGAATTCGAAATGGCTG	Human	mRNA-qPCR
	Reverse	TGTCGATGAATACGGCCC		
H2A.Z.2	Forward	GAACATGGCTGGAGGCAAA	Human	mRNA-qPCR
	Reverse	CAAGTGTCTGTGGATGCGG		
Hit 1_ overlap	Forward	GTCTCACTGTGTCCCCCAA	Human	ChIP-qPCR
	Reverse	ACCAGACTAGCCAACAAAGCA		

Hit 3_ overlap	Forward	TCCGTTTCTTCTGGACGAAC	Human	ChIP-qPCR
	Reverse	CTCCAGCGCGAACTTTGTA		
Hit 5_ overlap	Forward	GCCAGGCATGCTCTACTTT	Human	ChIP-qPCR
	Reverse	TATTAATCCAAGGCCGGG		
Hit 6_ overlap	Forward	AGTGAATGTTTCATTGAGTGCTTA	Human	ChIP-qPCR
	Reverse	CTTTCAAATGGGTTCTTGTGA		
Hit 9_ overlap	Forward	TCAGCCCCTGGAATAGCT	Human	ChIP-qPCR
	Reverse	TCCACCTGTACAGCCAGC		
Hit 10_ overlap	Forward	GGCTTGTGAAACCAAGTCCA	Human	ChIP-qPCR
	Reverse	CCGAAGCTGGCAGATCAC		
Hit 11_ overlap	Forward	GCACCCAACCAATATGTCTTC	Human	ChIP-qPCR
	Reverse	AGAGATACAACCAACACAGTGCA		
HPRT	Forward	CTGGCGTCGTGATTAGTGAT	Human	mRNA-qPCR
	Reverse	GGCTACAATGTGATGGCCT		
LEF1	Forward	CCCGTGAAGAGCAGGCTAAA	Human	mRNA-qPCR
	Reverse	TCGTTTTCCACCTGATGCAG		
LOXL2	Forward	CCCCCTGGAGACTACCTGTT	Human	mRNA-qPCR
	Reverse	TTCGCTGAAGGAACCACCTA		

NFIA	Forward	ATGTGAACGCAAGAAGCAG	Human	mRNA-qPCR
	Reverse	ATTCATCCTGGGTGAGACAG		
Pumilio	Forward	GACCAGCAGAATGAGATGGTTC	Human	mRNA-qPCR
	Reverse	CATAAGGATGTGTGGATAAGGCA		
RASD1	Forward	CCACCGCAAGTTCTACTCCA	Human	mRNA-qPCR
	Reverse	GGATGAAAACGTCTCCTGTGAG		
RBX1	Forward	CGACAGACCGTGTGTTTCC	Human	mRNA-qPCR
	Reverse	AGGGCTACTGCATTCCACTTT		
RHOB	Forward	GTGTGTCTGTTCGACTCCCC	Human	mRNA-qPCR
	Reverse	AGGGATATCAAGCTCCCGC		
RING1A	Forward	CTACGGAGCGGGAACAAGG	Human	mRNA-qPCR
	Reverse	AAGCACTCGGTCTTGATGGG		
RING1B	Forward	AGCACAATAATCAGCAAGCACT	Human	mRNA-qPCR
	Reverse	GCTCCACTACCATTTTCAATCTG		
RNA Pol II	Forward	CTGAGTCCGGATGAACTGGT	Human	ChIP-qPCR
	Reverse	ACCCATAAGCAGCGAGAAAG		
RP1L1	Forward	TAAGAACATGGACCCTCGCC	Human	mRNA-qPCR
	Reverse	CTGCAGCGAGTCCACCTTT		

RUVBL1	Forward	GCCCTGGAGTCTTCTATCGC	Human	mRNA-qPCR
	Reverse	CACTCGGTCCAGAAGGTCA		
RUVBL2	Forward	GATCATGGCCACCAACC	Human	mRNA-qPCR
	Reverse	CAGGTCTATGGGGATGCC		
TP53INP1	Forward	CGTCTGGGTACCTGAACGA	Human	mRNA-qPCR
	Reverse	AGAAGAGTCATTGTACGTGGGC		

Table MM6. Primers used for mRNA and ChIP analysis. List of primer sequences used in this study, shown in 5' to 3' direction.

25. Statistical analysis

Statistical significance was assessed using an unpaired two-tailed Student's t test. The symbols *, ** and *** indicate significant differences with different p-values: * $p < 0.05$, ** $p \leq 0.01$, *** $p \leq 0.001$ (see figure legends).

REFERENCES

1 Kornberg, R. D. Chromatin structure: a repeating unit of histones and DNA. *Science* **184**, 868-871, (1974).

2 Kornberg, R. D. & Lorch, Y. Twenty-five years of the nucleosome, fundamental particle of the eukaryote chromosome. *Cell* **98**, 285-294, (1999).

3 McGinty, R. K. & Tan, S. Nucleosome structure and function. *Chem Rev* **115**, 2255-2273, (2015).

4 McGinty, R. K. & Tan, S. in *Fundamentals of Chromatin* (eds Jerry L. Workman & Susan M. Abmayr) 1-28 (Springer New York, 2014).

5 Kalashnikova, A. A., Porter-Goff, M. E., Muthurajan, U. M., Luger, K. & Hansen, J. C. The role of the nucleosome acidic patch in modulating higher order chromatin structure. *J R Soc Interface* **10**, 20121022-20121022, (2013).

6 Bednar, J. *et al.* Structure and Dynamics of a 197 bp Nucleosome in Complex with Linker Histone H1. *Mol Cell* **66**, 384-397.e388, (2017).

7 Izzo, A. *et al.* The genomic landscape of the somatic linker histone subtypes H1.1 to H1.5 in human cells. *Cell Rep* **3**, 2142-2154, (2013).

8 Izzo, A., Kamieniarz, K. & Schneider, R. The histone H1 family: specific members, specific functions? *Biol Chem* **389**, 333-343, (2008).

9 Cutter, A. R. & Hayes, J. J. A brief review of nucleosome structure. *FEBS Lett* **589**, 2914-2922, (2015).

10 Hergeth, S. P. & Schneider, R. The H1 linker histones: multifunctional proteins beyond the nucleosomal core particle. *EMBO Rep* **16**, 1439-1453, (2015).

11 Szerlong, H. J. & Hansen, J. C. Nucleosome distribution and linker DNA: connecting nuclear function to dynamic chromatin structure. *Biochem Cell Biol* **89**, 24-34, (2011).

12 Olins, A. L. & Olins, D. E. Spheroid chromatin units (v bodies). *Science* **183**, 330-332, (1974).

13 Luger, K., Dechassa, M. L. & Tremethick, D. J. New insights into nucleosome and chromatin structure: an ordered state or a disordered affair? *Nat Rev Mol Cell Biol* **13**, 436-447, (2012).

14 Hubner, M. R., Eckersley-Maslin, M. A. & Spector, D. L. Chromatin organization and transcriptional regulation. *Curr Opin Genet Dev* **23**, 89-95, (2013).

15 Nishino, Y. *et al.* Human mitotic chromosomes consist predominantly of irregularly folded nucleosome fibres without a 30-nm chromatin structure. *Embo j* **31**, 1644-1653, (2012).

16 Maeshima, K., Hihara, S. & Eltsov, M. Chromatin structure: does the 30-nm fibre exist in vivo? *Curr Opin Cell Biol* **22**, 291-297, (2010).

17 Sanyal, A., Bau, D., Marti-Renom, M. A. & Dekker, J. Chromatin globules: a common motif of higher order chromosome structure? *Curr Opin Cell Biol* **23**, 325-331, (2011).

18 Cremer, T. & Cremer, M. Chromosome territories. *Cold Spring Harbor perspectives in biology* **2**, a003889-a003889, (2010).

19 Lieberman-Aiden, E. *et al.* Comprehensive mapping of long-range interactions reveals folding principles of the human genome. *Science* **326**, 289-293, (2009).

20 Dixon, J. R. *et al.* Topological domains in mammalian genomes identified by analysis of chromatin interactions. *Nature* **485**, 376-380, (2012).

21 Rao, S. S. *et al.* A 3D map of the human genome at kilobase resolution reveals principles of chromatin looping. *Cell* **159**, 1665-1680, (2014).

22 Taberlay, P. C. *et al.* Three-dimensional disorganization of the cancer genome occurs coincident with long-range genetic and epigenetic alterations. *Genome Res* **26**, 719-731, (2016).

23 Pascual-Reguant, L. *et al.* Lamin B1 mapping reveals the existence of dynamic and functional euchromatin lamin B1 domains. *Nat Commun* **9**, 3420, (2018).

24 Ea, V., Baudement, M. O., Lesne, A. & Forne, T. Contribution of Topological Domains and Loop Formation to 3D Chromatin Organization. *Genes (Basel)* **6**, 734-750, (2015).

25 Guelen, L. *et al.* Domain organization of human chromosomes revealed by mapping of nuclear lamina interactions. *Nature* **453**, 948-951, (2008).

26 Chakalova, L. & Fraser, P. Organization of transcription. *Cold Spring Harbor perspectives in biology* **2**, a000729-a000729, (2010).

27 Therizols, P. *et al.* Chromatin decondensation is sufficient to alter nuclear organization in embryonic stem cells. *Science* **346**, 1238-1242, (2014).

28 Kumaran, R. I. & Spector, D. L. A genetic locus targeted to the nuclear periphery in living cells maintains its transcriptional competence. *J Cell Biol* **180**, 51-65, (2008).

29 van Steensel, B. & Furlong, E. E. M. The role of transcription in shaping the spatial organization of the genome. *Nature Reviews Molecular Cell Biology* **20**, 327-337, (2019).

30 Bonasio, R., Tu, S. & Reinberg, D. Molecular signals of epigenetic states. *Science* **330**, 612-616, (2010).

31 Chen, Z., Li, S., Subramaniam, S., Shyy, J. Y. & Chien, S. Epigenetic Regulation: A New Frontier for Biomedical Engineers. *Annu Rev Biomed Eng* **19**, 195-219, (2017).

32 Koyama, M. & Kurumizaka, H. Structural diversity of the nucleosome. *J Biochem* **163**, 85-95, (2018).

33 Moore, L. D., Le, T. & Fan, G. DNA methylation and its basic function. *Neuropsychopharmacology* **38**, 23-38, (2013).

34 Bonev, B. & Cavalli, G. Organization and function of the 3D genome. *Nature Reviews Genetics* **17**, 661, (2016).

35 Narlikar, G. J., Sundaramoorthy, R. & Owen-Hughes, T. Mechanisms and functions of ATP-dependent chromatin-remodeling enzymes. *Cell* **154**, 490-503, (2013).

36 Peschansky, V. J. & Wahlestedt, C. Non-coding RNAs as direct and indirect modulators of epigenetic regulation. *Epigenetics* **9**, 3-12, (2014).

37 Arnaudo, A. M. & Garcia, B. A. Proteomic characterization of novel histone post-translational modifications. *Epigenetics Chromatin* **6**, 24, (2013).

38 Lawrence, M., Daujat, S. & Schneider, R. Lateral Thinking: How Histone Modifications Regulate Gene Expression. *Trends in Genetics* **32**, 42-56, (2016).

39 Bannister, A. J. & Kouzarides, T. Regulation of chromatin by histone modifications. *Cell research* **21**, 381-395, (2011).

40 Tollervey, J. R. & Lunyak, V. V. Epigenetics: judge, jury and executioner of stem cell fate. *Epigenetics* **7**, 823-840, (2012).

41 Tessarz, P. & Kouzarides, T. Histone core modifications regulating nucleosome structure and dynamics. *Nat Rev Mol Cell Biol* **15**, 703-708, (2014).

42 Yun, M., Wu, J., Workman, J. L. & Li, B. Readers of histone modifications. *Cell research* **21**, 564-578, (2011).

43 Zeng, L. & Zhou, M. M. Bromodomain: an acetyl-lysine binding domain. *FEBS Lett* **513**, 124-128, (2002).

44 Tajul-Arifin, K. *et al.* Identification and analysis of chromodomain-containing proteins encoded in the mouse transcriptome. *Genome Res* **13**, 1416-1429, (2003).

45 Musselman, C. A., Lalonde, M. E., Cote, J. & Kutateladze, T. G. Perceiving the epigenetic landscape through histone readers. *Nat Struct Mol Biol* **19**, 1218-1227, (2012).

46 Hyun, K., Jeon, J., Park, K. & Kim, J. Writing, erasing and reading histone lysine methylations. *Exp Mol Med* **49**, e324, (2017).

47 Zhang, T., Cooper, S. & Brockdorff, N. The interplay of histone modifications - writers that read. *EMBO Rep* **16**, 1467-1481, (2015).

48 Falkenberg, K. J. & Johnstone, R. W. Histone deacetylases and their inhibitors in cancer, neurological diseases and immune disorders. *Nat Rev Drug Discov* **13**, 673-691, (2014).

49 Latham, J. A. & Dent, S. Y. Cross-regulation of histone modifications. *Nat Struct Mol Biol* **14**, 1017-1024, (2007).

50 Bartke, T. *et al.* Nucleosome-interacting proteins regulated by DNA and histone methylation. *Cell* **143**, 470-484, (2010).

51 Albig, W., Kioschis, P., Poustka, A., Meergans, K. & Doenecke, D. Human histone gene organization: nonregular arrangement within a large cluster. *Genomics* **40**, 314-322, (1997).

52 Buschbeck, M. & Hake, S. B. Variants of core histones and their roles in cell fate decisions, development and cancer. *Nat Rev Mol Cell Biol* **18**, 299-314, (2017).

53 Law, C. & Cheung, P. Histone variants and transcription regulation. *Subcell Biochem* **61**, 319-341, (2013).

54 Mattiroli, F., D'Arcy, S. & Luger, K. The right place at the right time: chaperoning core histone variants. *EMBO Rep* **16**, 1454-1466, (2015).

55 Eissenberg, J. C. & Reuter, G. Cellular mechanism for targeting heterochromatin formation in Drosophila. *Int Rev Cell Mol Biol* **273**, 1-47, (2009).

56 Roadmap Epigenomics, C. *et al.* Integrative analysis of 111 reference human epigenomes. *Nature* **518**, 317, (2015).

57 Filion, G. J. *et al.* Systematic protein location mapping reveals five principal chromatin types in Drosophila cells. *Cell* **143**, 212-224, (2010).

58 Sexton, T. *et al.* Three-Dimensional Folding and Functional Organization Principles of the Drosophila Genome. *Cell* **148**, 458-472, (2012).

59 The, E. P. C. *et al.* An integrated encyclopedia of DNA elements in the human genome. *Nature* **489**, 57, (2012).

60 Grewal, S. I. S. & Elgin, S. C. R. Transcription and RNA interference in the formation of heterochromatin. *Nature* **447**, 399-406, (2007).

61 Huisinga, K. L., Brower-Toland, B. & Elgin, S. C. The contradictory definitions of heterochromatin: transcription and silencing. *Chromosoma* **115**, 110-122, (2006).

62 Barski, A. *et al.* High-resolution profiling of histone methylations in the human genome. *Cell* **129**, 823-837, (2007).

63 Schubeler, D. *et al.* The histone modification pattern of active genes revealed through genome-wide chromatin analysis of a higher eukaryote. *Genes Dev* **18**, 1263-1271, (2004).

64 Myers, F. A., Evans, D. R., Clayton, A. L., Thorne, A. W. & Crane-Robinson, C. Targeted and extended acetylation of histones H4 and H3 at active and inactive genes in chicken embryo erythrocytes. *J Biol Chem* **276**, 20197-20205, (2001).

65 Batta, K., Zhang, Z., Yen, K., Goffman, D. B. & Pugh, B. F. Genome-wide function of H2B ubiquitylation in promoter and genic regions. *Genes Dev* **25**, 2254-2265, (2011).

66 Ng, H. H., Ciccone, D. N., Morshead, K. B., Oettinger, M. A. & Struhl, K. Lysine-79 of histone H3 is hypomethylated at silenced loci in yeast and mammalian cells: a potential mechanism for position-effect variegation. *Proc Natl Acad Sci U S A* **100**, 1820-1825, (2003).

67 Bannister, A. J. *et al.* Spatial distribution of di- and tri-methyl lysine 36 of histone H3 at active genes. *J Biol Chem* **280**, 17732-17736, (2005).

68 Creyghton, M. P. *et al.* Histone H3K27ac separates active from poised enhancers and predicts developmental state. *Proc Natl Acad Sci U S A* **107**, 21931-21936, (2010).

69 Hon, G. C., Hawkins, R. D. & Ren, B. Predictive chromatin signatures in the mammalian genome. *Hum Mol Genet* **18**, R195-201, (2009).

70 Grewal, S. I. & Elgin, S. C. Transcription and RNA interference in the formation of heterochromatin. *Nature* **447**, 399-406, (2007).

71 Bernard, P. *et al.* Requirement of heterochromatin for cohesion at centromeres. *Science* **294**, 2539-2542, (2001).

72 Pidoux, A. L. & Allshire, R. C. The role of heterochromatin in centromere function. *Philos Trans R Soc Lond B Biol Sci* **360**, 569-579, (2005).

73 Allshire, R. C. & Madhani, H. D. Ten principles of heterochromatin formation and function. *Nat Rev Mol Cell Biol* **19**, 229-244, (2018).

74 Jia, S., Yamada, T. & Grewal, S. I. Heterochromatin regulates cell type-specific long-range chromatin interactions essential for directed recombination. *Cell* **119**, 469-480, (2004).

75 The, E. P. C. *et al.* Identification and analysis of functional elements in 1% of the human genome by the ENCODE pilot project. *Nature* **447**, 799, (2007).

76 Holoch, D. & Moazed, D. RNA-mediated epigenetic regulation of gene expression. *Nat Rev Genet* **16**, 71-84, (2015).

77 Iglesias, N. & Moazed, D. Silencing repetitive DNA. *eLife* **6**, e29503, (2017).

78 Millanes-Romero, A. *et al.* Regulation of heterochromatin transcription by Snail1/LOXL2 during epithelial-to-mesenchymal transition. *Mol Cell* **52**, 746-757, (2013).

79 Velazquez Camacho, O. *et al.* Major satellite repeat RNA stabilize heterochromatin retention of Suv39h enzymes by RNA-nucleosome association and RNA:DNA hybrid formation. *Elife* **6**, (2017).

80 Johnson, W. L. *et al.* RNA-dependent stabilization of SUV39H1 at constitutive heterochromatin. *eLife* **6**, e25299, (2017).

81 Trojer, P. & Reinberg, D. Facultative Heterochromatin: Is There a Distinctive Molecular Signature? *Molecular Cell* **28**, 1-13, (2007).

82 Bernstein, E. *et al.* Mouse polycomb proteins bind differentially to methylated histone H3 and RNA and are enriched in facultative heterochromatin. *Mol Cell Biol* **26**, 2560-2569, (2006).

83 Wiles, E. T. & Selker, E. U. H3K27 methylation: a promiscuous repressive chromatin mark. *Curr Opin Genet Dev* **43**, 31-37, (2017).

84 Margueron, R. & Reinberg, D. The Polycomb complex PRC2 and its mark in life. *Nature* **469**, 343-349, (2011).

85 Breiling, A., Turner, B. M., Bianchi, M. E. & Orlando, V. General transcription factors bind promoters repressed by Polycomb group proteins. *Nature* **412**, 651-655, (2001).

86 Becker, J. S., Nicetto, D. & Zaret, K. S. H3K9me3-Dependent Heterochromatin: Barrier to Cell Fate Changes. *Trends Genet* **32**, 29-41, (2016).

87 Eskeland, R. *et al.* Ring1B Compacts Chromatin Structure and Represses Gene Expression Independent of Histone Ubiquitination. *Molecular Cell* **38**, 452-464, (2010).

88 Schultz, D. C., Ayyanathan, K., Negorev, D., Maul, G. G. & Rauscher, F. J., 3rd. SETDB1: a novel KAP-1-associated histone H3, lysine 9-specific methyltransferase that contributes to HP1-mediated silencing of euchromatic genes by KRAB zinc-finger proteins. *Genes Dev* **16**, 919-932, (2002).

89 Rea, S. *et al.* Regulation of chromatin structure by site-specific histone H3 methyltransferases. *Nature* **406**, 593-599, (2000).

90 Shinkai, Y. & Tachibana, M. H3K9 methyltransferase G9a and the related molecule GLP. *Genes Dev* **25**, 781-788, (2011).

91 Tachibana, M. *et al.* G9a histone methyltransferase plays a dominant role in euchromatic histone H3 lysine 9 methylation and is essential for early embryogenesis. *Genes Dev* **16**, 1779-1791, (2002).

92 Boros, J., Arnoult, N., Stroobant, V., Collet, J. F. & Decottignies, A. Polycomb repressive complex 2 and H3K27me3 cooperate with H3K9 methylation to maintain heterochromatin protein 1alpha at chromatin. *Mol Cell Biol* **34**, 3662-3674, (2014).

93 Derks, S. *et al.* Promoter CpG island hypermethylation- and H3K9me3 and H3K27me3-mediated epigenetic silencing targets the deleted in colon cancer (DCC) gene in colorectal carcinogenesis without affecting neighboring genes on chromosomal region 18q21. *Carcinogenesis* **30**, 1041-1048, (2009).

94 Mozzetta, C. *et al.* The histone H3 lysine 9 methyltransferases G9a and GLP regulate polycomb repressive complex 2-mediated gene silencing. *Mol Cell* **53**, 277-289, (2014).

95 Heard, E. Delving into the diversity of facultative heterochromatin: the epigenetics of the inactive X chromosome. *Curr Opin Genet Dev* **15**, 482-489, (2005).

96 Feil, R. & Berger, F. Convergent evolution of genomic imprinting in plants and mammals. *Trends Genet* **23**, 192-199, (2007).

97 Squazzo, S. L. *et al.* Suz12 binds to silenced regions of the genome in a cell-type-specific manner. *Genome Res* **16**, 890-900, (2006).

98 Wen, B., Wu, H., Shinkai, Y., Irizarry, R. A. & Feinberg, A. P. Large histone H3 lysine 9 dimethylated chromatin blocks distinguish differentiated from embryonic stem cells. *Nat Genet* **41**, 246-250, (2009).

99 Soufi, A., Donahue, G. & Zaret, K. S. Facilitators and impediments of the pluripotency reprogramming factors' initial engagement with the genome. *Cell* **151**, 994-1004, (2012).

100 Vogel, M. J. *et al.* Human heterochromatin proteins form large domains containing KRAB-ZNF genes. *Genome Res* **16**, 1493-1504, (2006).

101 van Steensel, B. & Belmont, A. S. Lamina-Associated Domains: Links with Chromosome Architecture, Heterochromatin, and Gene Repression. *Cell* **169**, 780-791, (2017).

102 Nielsen, S. J. *et al.* Rb targets histone H3 methylation and HP1 to promoters. *Nature* **412**, 561-565, (2001).

103 Roopra, A., Qazi, R., Schoenike, B., Daley, T. J. & Morrison, J. F. Localized domains of G9a-mediated histone methylation are required for silencing of neuronal genes. *Mol Cell* **14**, 727-738, (2004).

104 Voigt, P., Tee, W. W. & Reinberg, D. A double take on bivalent promoters. *Genes Dev* **27**, 1318-1338, (2013).

105 Mikkelsen, T. S. *et al.* Genome-wide maps of chromatin state in pluripotent and lineage-committed cells. *Nature* **448**, 553-560, (2007).

106 Eymery, A., Callanan, M. & Vourc'h, C. The secret message of heterochromatin: new insights into the mechanisms and function of centromeric and pericentric repeat sequence transcription. *Int J Dev Biol* **53**, 259-268, (2009).

107 Saksouk, N., Simboeck, E. & Dejardin, J. Constitutive heterochromatin formation and transcription in mammals. *Epigenetics Chromatin* **8**, 3, (2015).

108 O'Carroll, D. *et al.* Isolation and characterization of Suv39h2, a second histone H3 methyltransferase gene that displays testis-specific expression. *Mol Cell Biol* **20**, 9423-9433, (2000).

109 Peters, A. H. *et al.* Loss of the Suv39h histone methyltransferases impairs mammalian heterochromatin and genome stability. *Cell* **107**, 323-337, (2001).

110 Müller, M. M., Fierz, B., Bittova, L., Liszczak, G. & Muir, T. W. A two-state activation mechanism controls the histone methyltransferase Suv39h1. *Nature Chemical Biology* **12**, 188, (2016).

111 Zhang, K., Mosch, K., Fischle, W. & Grewal, S. I. Roles of the Clr4 methyltransferase complex in nucleation, spreading and maintenance of heterochromatin. *Nat Struct Mol Biol* **15**, 381-388, (2008).

112 Kwon, S. H. & Workman, J. L. The changing faces of HP1: From heterochromatin formation and gene silencing to euchromatic gene expression: HP1 acts as a positive regulator of transcription. *Bioessays* **33**, 280-289, (2011).

113 Grewal, S. I. & Jia, S. Heterochromatin revisited. *Nat Rev Genet* **8**, 35-46, (2007).

114 Maison, C. & Almouzni, G. HP1 and the dynamics of heterochromatin maintenance. *Nat Rev Mol Cell Biol* **5**, 296-304, (2004).

115 Bannister, A. J. *et al.* Selective recognition of methylated lysine 9 on histone H3 by the HP1 chromo domain. *Nature* **410**, 120-124, (2001).

116 Lomberk, G., Wallrath, L. & Urrutia, R. The Heterochromatin Protein 1 family. *Genome Biol* **7**, 228, (2006).

117 Ryan, D. P. & Tremethick, D. J. The interplay between H2A.Z and H3K9 methylation in regulating HP1alpha binding to linker histone-containing chromatin. *Nucleic Acids Res* **46**, 9353-9366, (2018).

118 Schotta, G. *et al.* A silencing pathway to induce H3-K9 and H4-K20 trimethylation at constitutive heterochromatin. *Genes Dev* **18**, 1251-1262, (2004).

119 Vaquero, A., Sternglanz, R. & Reinberg, D. NAD+-dependent deacetylation of H4 lysine 16 by class III HDACs. *Oncogene* **26**, 5505-5520, (2007).

120 Santenard, A. *et al.* Heterochromatin formation in the mouse embryo requires critical residues of the histone variant H3.3. *Nat Cell Biol* **12**, 853-862, (2010).

121 Rangasamy, D., Berven, L., Ridgway, P. & Tremethick, D. J. Pericentric heterochromatin becomes enriched with H2A.Z during early mammalian development. *EMBO J* **22**, 1599-1607, (2003).

122 Wang, J., Lawry, S. T., Cohen, A. L. & Jia, S. Chromosome boundary elements and regulation of heterochromatin spreading. *Cell Mol Life Sci* **71**, 4841-4852, (2014).

123 Talbert, P. B. & Henikoff, S. Spreading of silent chromatin: inaction at a distance. *Nature Reviews Genetics* **7**, 793-803, (2006).

124 Erdel, F. & Greene, E. C. Generalized nucleation and looping model for epigenetic memory of histone modifications. *Proc Natl Acad Sci U S A* **113**, E4180-4189, (2016).

125 Yamamoto, K. & Sonoda, M. Self-interaction of heterochromatin protein 1 is required for direct binding to histone methyltransferase, SUV39H1. *Biochem Biophys Res Commun* **301**, 287-292, (2003).

126 Baubec, T. & Schubeler, D. Genomic patterns and context specific interpretation of DNA methylation. *Curr Opin Genet Dev* **25**, 85-92, (2014).

127 Fuks, F., Hurd, P. J., Deplus, R. & Kouzarides, T. The DNA methyltransferases associate with HP1 and the SUV39H1 histone methyltransferase. *Nucleic acids research* **31**, 2305-2312, (2003).

128 Margueron, R. *et al.* Role of the polycomb protein EED in the propagation of repressive histone marks. *Nature* **461**, 762-767, (2009).

129 Schwartz, Y. B. & Pirrotta, V. Polycomb silencing mechanisms and the management of genomic programmes. *Nat Rev Genet* **8**, 9-22, (2007).

130 Mohammad, H. P., Barbash, O. & Creasy, C. L. Targeting epigenetic modifications in cancer therapy: erasing the roadmap to cancer. *Nature Medicine* **25**, 403-418, (2019).

131 Christiansen, J. J. & Rajasekaran, A. K. Reassessing epithelial to mesenchymal transition as a prerequisite for carcinoma invasion and metastasis. *Cancer Res* **66**, 8319-8326, (2006).

132 Hanahan, D. & Weinberg, R. A. Hallmarks of cancer: the next generation. *Cell* **144**, 646-674, (2011).

133 Dagogo-Jack, I. & Shaw, A. T. Tumour heterogeneity and resistance to cancer therapies. *Nat Rev Clin Oncol* **15**, 81-94, (2018).

134 Polyak, K. Breast cancer: origins and evolution. *J Clin Invest* **117**, 3155-3163, (2007).

135 Nowell, P. C. The clonal evolution of tumor cell populations. *Science* **194**, 23-28, (1976).

136 Chaffer, C. L. & Weinberg, R. A. A perspective on cancer cell metastasis. *Science* **331**, 1559-1564, (2011).

137 Valastyan, S. & Weinberg, R. A. Tumor metastasis: molecular insights and evolving paradigms. *Cell* **147**, 275-292, (2011).

138 Aaltonen, M., Lipponen, P., Kosma, V. M., Aaltomaa, S. & Syrjanen, K. Prognostic value of cathepsin-D expression in female breast cancer. *Anticancer Res* **15**, 1033-1037, (1995).

139 De Craene, B. & Berx, G. Regulatory networks defining EMT during cancer initiation and progression. *Nat Rev Cancer* **13**, 97-110, (2013).

140 Lu, W. & Kang, Y. Epithelial-Mesenchymal Plasticity in Cancer Progression and Metastasis. *Dev Cell* **49**, 361-374, (2019).

141 Nieto, M. A., Huang, R. Y., Jackson, R. A. & Thiery, J. P. EMT: 2016. *Cell* **166**, 21-45, (2016).

142 Peinado, H., Ballestar, E., Esteller, M. & Cano, A. Snail mediates E-cadherin repression by the recruitment of the Sin3A/histone deacetylase 1 (HDAC1)/HDAC2 complex. *Mol Cell Biol* **24**, 306-319, (2004).

143 Lin, T., Ponn, A., Hu, X., Law, B. K. & Lu, J. Requirement of the histone demethylase LSD1 in Snai1-mediated transcriptional repression during epithelial-mesenchymal transition. *Oncogene* **29**, 4896-4904, (2010).

144 Herranz, N. *et al.* Polycomb complex 2 is required for E-cadherin repression by the Snail1 transcription factor. *Mol Cell Biol* **28**, 4772-4781, (2008).

145 Dong, C. *et al.* Interaction with Suv39H1 is critical for Snail-mediated E-cadherin repression in breast cancer. *Oncogene* **32**, 1351-1362, (2013).

146 Dong, C. *et al.* G9a interacts with Snail and is critical for Snail-mediated E-cadherin repression in human breast cancer. *J Clin Invest* **122**, 1469-1486, (2012).

147 Herranz, N. *et al.* Lysyl oxidase-like 2 (LOXL2) oxidizes trimethylated lysine 4 in histone H3. *FEBS J* **283**, 4263-4273, (2016).

148 Thiery, J. P., Acloque, H., Huang, R. Y. & Nieto, M. A. Epithelial-mesenchymal transitions in development and disease. *Cell* **139**, 871-890, (2009).

149 Dongre, A. & Weinberg, R. A. New insights into the mechanisms of epithelial-mesenchymal transition and implications for cancer. *Nat Rev Mol Cell Biol* **20**, 69-84, (2019).

150 Chiorean, R., Braicu, C. & Berindan-Neagoe, I. Another review on triple-negative breast cancer. Are we on the right way towards the exit from the labyrinth? *Breast* **22**, 1026-1033, (2013).

151 Koren, S. & Bentires-Alj, M. Breast Tumor Heterogeneity: Source of Fitness, Hurdle for Therapy. *Mol Cell* **60**, 537-546, (2015).

152 Sims, A. H., Howell, A., Howell, S. J. & Clarke, R. B. Origins of breast cancer subtypes and therapeutic implications. *Nat Clin Pract Oncol* **4**, 516-525, (2007).

153 Eliyatkin, N., Yalcin, E., Zengel, B., Aktas, S. & Vardar, E. Molecular Classification of Breast Carcinoma: From Traditional, Old-Fashioned Way to A New Age, and A New Way. *J Breast Health* **11**, 59-66, (2015).

154 Sorlie, T. *et al.* Gene expression patterns of breast carcinomas distinguish tumor subclasses with clinical implications. *Proc Natl Acad Sci U S A* **98**, 10869-10874, (2001).

155 Perou, C. M. *et al.* Molecular portraits of human breast tumours. *Nature* **406**, 747-752, (2000).

156 Perou, C. M. Molecular stratification of triple-negative breast cancers. *Oncologist* **15 Suppl 5**, 39-48, (2010).

157 Foulkes, W. D., Smith, I. E. & Reis-Filho, J. S. Triple-negative breast cancer. *N Engl J Med* **363**, 1938-1948, (2010).

158 Holliday, D. L. & Speirs, V. Choosing the right cell line for breast cancer research. *Breast cancer research : BCR* **13**, 215, (2011).

159 Boyle, P. Triple-negative breast cancer: epidemiological considerations and recommendations. *Ann Oncol* **23 Suppl 6**, vi7-12, (2012).

160 Lehmann, B. D. *et al.* Identification of human triple-negative breast cancer subtypes and preclinical models for selection of targeted therapies. *The Journal of Clinical Investigation* **121**, 2750-2767, (2011).

161 Prat, A. *et al.* Phenotypic and molecular characterization of the claudin-low intrinsic subtype of breast cancer. *Breast Cancer Res* **12**, R68, (2010).

162 Sarrio, D. *et al.* Epithelial-mesenchymal transition in breast cancer relates to the basal-like phenotype. *Cancer Res* **68**, 989-997, (2008).

163 Kumar, P. & Aggarwal, R. An overview of triple-negative breast cancer. *Arch Gynecol Obstet* **293**, 247-269, (2016).

164 Negrini, S., Gorgoulis, V. G. & Halazonetis, T. D. Genomic instability--an evolving hallmark of cancer. *Nat Rev Mol Cell Biol* **11**, 220-228, (2010).

165 Kastan, M. B. & Bartek, J. Cell-cycle checkpoints and cancer. *Nature* **432**, 316-323, (2004).

166 Jackson, S. P. & Bartek, J. The DNA-damage response in human biology and disease. *Nature* **461**, 1071-1078, (2009).

167 Davis, J. D. & Lin, S. Y. DNA damage and breast cancer. *World J Clin Oncol* **2**, 329-338, (2011).

168 Stratton, M. R., Campbell, P. J. & Futreal, P. A. The cancer genome. *Nature* **458**, 719-724, (2009).

169 Levy-Lahad, E. & Friedman, E. Cancer risks among BRCA1 and BRCA2 mutation carriers. *Br J Cancer* **96**, 11-15, (2007).

170 Halazonetis, T. D., Gorgoulis, V. G. & Bartek, J. An oncogene-induced DNA damage model for cancer development. *Science* **319**, 1352-1355, (2008).

171 Bartkova, J. *et al.* Oncogene-induced senescence is part of the tumorigenesis barrier imposed by DNA damage checkpoints. *Nature* **444**, 633-637, (2006).

172 Di Micco, R. *et al.* Interplay between oncogene-induced DNA damage response and heterochromatin in senescence and cancer. *Nat Cell Biol* **13**, 292-302, (2011).

173 Hemann, M. T. & Narita, M. Oncogenes and senescence: breaking down in the fast lane. *Genes Dev* **21**, 1-5, (2007).

174 Gursoy-Yuzugullu, O., House, N. & Price, B. D. Patching Broken DNA: Nucleosome Dynamics and the Repair of DNA Breaks. *J Mol Biol* **428**, 1846-1860, (2016).

175 Soria, G., Polo, S. E. & Almouzni, G. Prime, repair, restore: the active role of chromatin in the DNA damage response. *Mol Cell* **46**, 722-734, (2012).

176 Ayrapetov, M. K., Gursoy-Yuzugullu, O., Xu, C., Xu, Y. & Price, B. D. DNA double-strand breaks promote methylation of histone H3 on lysine 9 and transient formation of repressive chromatin. *Proc Natl Acad Sci U S A* **111**, 9169-9174, (2014).

177 Kim, J. A., Kruhlak, M., Dotiwala, F., Nussenzweig, A. & Haber, J. E. Heterochromatin is refractory to gamma-H2AX modification in yeast and mammals. *J Cell Biol* **178**, 209-218, (2007).

178 Murga, M. *et al.* Global chromatin compaction limits the strength of the DNA damage response. *J Cell Biol* **178**, 1101-1108, (2007).

179 Goodarzi, A. A. *et al.* ATM signaling facilitates repair of DNA double-strand breaks associated with heterochromatin. *Mol Cell* **31**, 167-177, (2008).

180 Ziv, Y. *et al.* Chromatin relaxation in response to DNA double-strand breaks is modulated by a novel ATM- and KAP-1 dependent pathway. *Nat Cell Biol* **8**, 870-876, (2006).

181 Goodarzi, A. A., Jeggo, P. & Lobrich, M. The influence of heterochromatin on DNA double strand break repair: Getting the strong, silent type to relax. *DNA Repair (Amst)* **9**, 1273-1282, (2010).

182 Hodgkinson, A., Chen, Y. & Eyre-Walker, A. The large-scale distribution of somatic mutations in cancer genomes. *Hum Mutat* **33**, 136-143, (2012).

183 Schuster-Bockler, B. & Lehner, B. Chromatin organization is a major influence on regional mutation rates in human cancer cells. *Nature* **488**, 504-507, (2012).

184 Supek, F. & Lehner, B. Differential DNA mismatch repair underlies mutation rate variation across the human genome. *Nature* **521**, 81-84, (2015).

185 Avgustinova, A. *et al.* Loss of G9a preserves mutation patterns but increases chromatin accessibility, genomic instability and aggressiveness in skin tumours. *Nat Cell Biol* **20**, 1400-1409, (2018).

186 Minucci, S. & Pelicci, P. G. Histone deacetylase inhibitors and the promise of epigenetic (and more) treatments for cancer. *Nat Rev Cancer* **6**, 38-51, (2006).

187 Williamson, P. R. & Kagan, H. M. Reaction pathway of bovine aortic lysyl oxidase. *J Biol Chem* **261**, 9477-9482, (1986).

188 Lucero, H. A. & Kagan, H. M. Lysyl oxidase: an oxidative enzyme and effector of cell function. *Cell Mol Life Sci* **63**, 2304-2316, (2006).

189 Lopez, K. M. & Greenaway, F. T. Identification of the copper-binding ligands of lysyl oxidase. *J Neural Transm (Vienna)* **118**, 1101-1109, (2011).

190 Moon, H. J., Finney, J., Ronnebaum, T. & Mure, M. Human lysyl oxidase-like 2. *Bioorg Chem* **57**, 231-241, (2014).

191 Borel, A. *et al.* Lysyl oxidase-like protein from bovine aorta. Isolation and maturation to an active form by bone morphogenetic protein-1. *J Biol Chem* **276**, 48944-48949, (2001).

192 Uzel, M. I. *et al.* Multiple bone morphogenetic protein 1-related mammalian metalloproteinases process pro-lysyl oxidase at the correct physiological site and control lysyl oxidase activation in mouse embryo fibroblast cultures. *J Biol Chem* **276**, 22537-22543, (2001).

193 Barker, H. E., Cox, T. R. & Erler, J. T. The rationale for targeting the LOX family in cancer. *Nat Rev Cancer* **12**, 540-552, (2012).

194 Iturbide, A., Garcia de Herreros, A. & Peiro, S. A new role for LOX and LOXL2 proteins in transcription regulation. *FEBS J* **282**, 1768-1773, (2015).

195 Molnar, J. *et al.* Structural and functional diversity of lysyl oxidase and the LOX-like proteins. *Biochim Biophys Acta* **1647**, 220-224, (2003).

196 Siegel, R. C. Biosynthesis of collagen crosslinks: increased activity of purified lysyl oxidase with reconstituted collagen fibrils. *Proc Natl Acad Sci U S A* **71**, 4826-4830, (1974).

197 Cano, A., Santamaria, P. G. & Moreno-Bueno, G. LOXL2 in epithelial cell plasticity and tumor progression. *Future Oncol* **8**, 1095-1108, (2012).

198 Giampuzzi, M., Oleggini, R. & Di Donato, A. Demonstration of in vitro interaction between tumor suppressor lysyl oxidase and histones H1 and H2: definition of the regions involved. *Biochim Biophys Acta* **1647**, 245-251, (2003).

199 Kagan, H. M., Williams, M. A., Calaman, S. D. & Berkowitz, E. M. Histone H1 is a substrate for lysyl oxidase and contains endogenous sodium borotritide-reducible residues. *Biochem Biophys Res Commun* **115**, 186-192, (1983).

200 Li, W. *et al.* Lysyl oxidase oxidizes basic fibroblast growth factor and inactivates its mitogenic potential. *J Cell Biochem* **88**, 152-164, (2003).

201 Mello, M. L., Alvarenga, E. M., Vidal Bde, C. & Di Donato, A. Chromatin supraorganization, mitotic abnormalities and proliferation in cells with increased or down-regulated lox expression: Indirect evidence of a LOX-histone H1 interaction in vivo. *Micron* **42**, 8-16, (2011).

202 Iturbide, A. *et al.* LOXL2 Oxidizes Methylated TAF10 and Controls TFIID-Dependent Genes during Neural Progenitor Differentiation. *Mol Cell* **58**, 755-766, (2015).

203 Ma, L. *et al.* Lysyl Oxidase 3 Is a Dual-Specificity Enzyme Involved in STAT3 Deacetylation and Deacetylimination Modulation. *Mol Cell* **65**, 296-309, (2017).

204 Khakoo, A. *et al.* Congenital cutis laxa and lysyl oxidase deficiency. *Clin Genet* **51**, 109-114, (1997).

205 Bonnans, C., Chou, J. & Werb, Z. Remodelling the extracellular matrix in development and disease. *Nat Rev Mol Cell Biol* **15**, 786-801, (2014).

206 Wong, C. C. *et al.* Lysyl oxidase-like 2 is critical to tumor microenvironment and metastatic niche formation in hepatocellular carcinoma. *Hepatology* **60**, 1645-1658, (2014).

207 Kirschmann, D. A. *et al.* A molecular role for lysyl oxidase in breast cancer invasion. *Cancer Res* **62**, 4478-4483, (2002).

208 Hollosi, P., Yakushiji, J. K., Fong, K. S., Csiszar, K. & Fong, S. F. Lysyl oxidase-like 2 promotes migration in noninvasive breast cancer cells but not in normal breast epithelial cells. *Int J Cancer* **125**, 318-327, (2009).

209 Wang, Y. *et al.* Escin Ia suppresses the metastasis of triple-negative breast cancer by inhibiting epithelial-mesenchymal transition via down-regulating LOXL2 expression. *Oncotarget* **7**, 23684-23699, (2016).

210 Cebria-Costa, J. P. *et al.* LOXL2-mediated H3K4 oxidation reduces chromatin accessibility in triple-negative breast cancer cells. *Oncogene*, (2019).

211 Ahn, S. G. *et al.* LOXL2 expression is associated with invasiveness and negatively influences survival in breast cancer patients. *Breast Cancer Res Treat* **141**, 89-99, (2013).

212 Moreno-Bueno, G. *et al.* Lysyl oxidase-like 2 (LOXL2), a new regulator of cell polarity required for metastatic dissemination of basal-like breast carcinomas. *EMBO Mol Med* **3**, 528-544, (2011).

213 Peinado, H. *et al.* A molecular role for lysyl oxidase-like 2 enzyme in snail regulation and tumor progression. *EMBO J* **24**, 3446-3458, (2005).

214 Schietke, R. *et al.* The lysyl oxidases LOX and LOXL2 are necessary and sufficient to repress E-cadherin in hypoxia: insights into cellular transformation processes mediated by HIF-1. *The Journal of biological chemistry* **285**, 6658-6669, (2010).

215 Voloshenyuk, T. G., Landesman, E. S., Khoutorova, E., Hart, A. D. & Gardner, J. D. Induction of cardiac fibroblast lysyl oxidase by TGF-beta1 requires PI3K/Akt, Smad3, and MAPK signaling. *Cytokine* **55**, 90-97, (2011).

216 Martin, A. *et al.* Lysyl oxidase-like 2 represses Notch1 expression in the skin to promote squamous cell carcinoma progression. *EMBO J* **34**, 1090-1109, (2015).

217 Silva, S. T. N. *et al.* X-ray structure of full-length human RuvB-Like 2 - mechanistic insights into coupling between ATP binding and mechanical action. *Sci Rep* **8**, 13726, (2018).

218 Matias, P. M., Gorynia, S., Donner, P. & Carrondo, M. A. Crystal structure of the human AAA+ protein RuvBL1. *J Biol Chem* **281**, 38918-38929, (2006).

219 Nano, N. & Houry, W. A. Chaperone-like activity of the AAA+ proteins Rvb1 and Rvb2 in the assembly of various complexes. *Philos Trans R Soc Lond B Biol Sci* **368**, 20110399, (2013).

220 Queval, R., Papin, C., Dalvai, M., Bystricky, K. & Humbert, O. Reptin and Pontin oligomerization and activity are modulated through histone H3 N-terminal tail interaction. *J Biol Chem* **289**, 33999-34012, (2014).

221 Clarke, T. L. *et al.* PRMT5-Dependent Methylation of the TIP60 Coactivator RUVBL1 Is a Key Regulator of Homologous Recombination. *Mol Cell* **65**, 900-916 e907, (2017).

222 Kim, J. H. *et al.* Roles of sumoylation of a reptin chromatin-remodelling complex in cancer metastasis. *Nat Cell Biol* **8**, 631-639, (2006).

223 Diop, S. B. *et al.* Reptin and Pontin function antagonistically with PcG and TrxG complexes to mediate Hox gene control. *EMBO Rep* **9**, 260-266, (2008).

224 Jha, S. & Dutta, A. RVB1/RVB2: running rings around molecular biology. *Mol Cell* **34**, 521-533, (2009).

225 Magalska, A. *et al.* RuvB-like ATPases function in chromatin decondensation at the end of mitosis. *Dev Cell* **31**, 305-318, (2014).

226 Mao, Y. Q. & Houry, W. A. The Role of Pontin and Reptin in Cellular Physiology and Cancer Etiology. *Front Mol Biosci* **4**, 58, (2017).

227 Grigoletto, A., Lestienne, P. & Rosenbaum, J. The multifaceted proteins Reptin and Pontin as major players in cancer. *Biochim Biophys Acta* **1815**, 147-157, (2011).

228 Assimon, V. A. *et al.* CB-6644 Is a Selective Inhibitor of the RUVBL1/2 Complex with Anticancer Activity. *ACS Chem Biol* **14**, 236-244, (2019).

229 Clapier, C. R. & Cairns, B. R. The biology of chromatin remodeling complexes. *Annu Rev Biochem* **78**, 273-304, (2009).

230 Cai, Y. *et al.* Purification and assay of the human INO80 and SRCAP chromatin remodeling complexes. *Methods* **40**, 312-317, (2006).

231 Ruhl, D. D. *et al.* Purification of a human SRCAP complex that remodels chromatin by incorporating the histone variant H2A.Z into nucleosomes. *Biochemistry* **45**, 5671-5677, (2006).

232 Papamichos-Chronakis, M., Watanabe, S., Rando, O. J. & Peterson, C. L. Global regulation of H2A.Z localization by the INO80 chromatin-remodeling enzyme is essential for genome integrity. *Cell* **144**, 200-213, (2011).

233 Vassileva, I., Yanakieva, I., Peycheva, M., Gospodinov, A. & Anachkova, B. The mammalian INO80 chromatin remodeling complex is required for replication stress recovery. *Nucleic Acids Res* **42**, 9074-9086, (2014).

234 Morrison, A. J. & Shen, X. Chromatin remodelling beyond transcription: the INO80 and SWR1 complexes. *Nat Rev Mol Cell Biol* **10**, 373-384, (2009).

235 Gerhold, C. B., Hauer, M. H. & Gasser, S. M. INO80-C and SWR-C: guardians of the genome. *J Mol Biol* **427**, 637-651, (2015).

236 Jonsson, Z. O., Jha, S., Wohlschlegel, J. A. & Dutta, A. Rvb1p/Rvb2p recruit Arp5p and assemble a functional Ino80 chromatin remodeling complex. *Mol Cell* **16**, 465-477, (2004).

237 Mizuguchi, G. *et al.* ATP-driven exchange of histone H2A.Z variant catalyzed by SWR1 chromatin remodeling complex. *Science* **303**, 343-348, (2004).

238 Hong, J. *et al.* The catalytic subunit of the SWR1 remodeler is a histone chaperone for the H2A.Z-H2B dimer. *Mol Cell* **53**, 498-505, (2014).

239 Singh, R. K. *et al.* Transient Kinetic Analysis of SWR1C-Catalyzed H2A.Z Deposition Unravels the Impact of Nucleosome Dynamics and the Asymmetry of Histone Exchange. *Cell Rep* **27**, 374-386 e374, (2019).

240 Wong, M. M., Cox, L. K. & Chrivia, J. C. The chromatin remodeling protein, SRCAP, is critical for deposition of the histone variant H2A.Z at promoters. *J Biol Chem* **282**, 26132-26139, (2007).

241 Raisner, R. M. *et al.* Histone variant H2A.Z marks the 5' ends of both active and inactive genes in euchromatin. *Cell* **123**, 233-248, (2005).

242 Watanabe, S., Radman-Livaja, M., Rando, O. J. & Peterson, C. L. A histone acetylation switch regulates H2A.Z deposition by the SWR-C remodeling enzyme. *Science* **340**, 195-199, (2013).

243 Lu, P. Y., Levesque, N. & Kobor, M. S. NuA4 and SWR1-C: two chromatin-modifying complexes with overlapping functions and components. *Biochem Cell Biol* **87**, 799-815, (2009).

244 Nguyen, V. Q. *et al.* Molecular architecture of the ATP-dependent chromatin-remodeling complex SWR1. *Cell* **154**, 1220-1231, (2013).

245 Auger, A. *et al.* Eaf1 is the platform for NuA4 molecular assembly that evolutionarily links chromatin acetylation to ATP-dependent exchange of histone H2A variants. *Mol Cell Biol* **28**, 2257-2270, (2008).

246 Gevry, N., Chan, H. M., Laflamme, L., Livingston, D. M. & Gaudreau, L. p21 transcription is regulated by differential localization of histone H2A.Z. *Genes Dev* **21**, 1869-1881, (2007).

247 Bao, Y. & Shen, X. SnapShot: chromatin remodeling complexes. *Cell* **129**, 632, (2007).

248 Durant, M. & Pugh, B. F. NuA4-directed chromatin transactions throughout the Saccharomyces cerevisiae genome. *Mol Cell Biol* **27**, 5327-5335, (2007).

249 Babiarz, J. E., Halley, J. E. & Rine, J. Telomeric heterochromatin boundaries require NuA4-dependent acetylation of histone variant H2A.Z in Saccharomyces cerevisiae. *Genes Dev* **20**, 700-710, (2006).

250 Keogh, M. C. *et al.* The Saccharomyces cerevisiae histone H2A variant Htz1 is acetylated by NuA4. *Genes Dev* **20**, 660-665, (2006).

251 Jha, S., Shibata, E. & Dutta, A. Human Rvb1/Tip49 is required for the histone acetyltransferase activity of Tip60/NuA4 and for the downregulation of phosphorylation on H2AX after DNA damage. *Mol Cell Biol* **28**, 2690-2700, (2008).

252 Jha, S., Gupta, A., Dar, A. & Dutta, A. RVBs are required for assembling a functional TIP60 complex. *Mol Cell Biol* **33**, 1164-1174, (2013).

253 Zlatanova, J. & Thakar, A. H2A.Z: view from the top. *Structure* **16**, 166-179, (2008).

254 Jackson, J. D. & Gorovsky, M. A. Histone H2A.Z has a conserved function that is distinct from that of the major H2A sequence variants. *Nucleic Acids Res* **28**, 3811-3816, (2000).

255 Vardabasso, C. *et al.* Histone variants: emerging players in cancer biology. *Cell Mol Life Sci* **71**, 379-404, (2014).

256 Matsuda, R. *et al.* Identification and characterization of the two isoforms of the vertebrate H2A.Z histone variant. *Nucleic Acids Res* **38**, 4263-4273, (2010).

257 Wratting, D., Thistlethwaite, A., Harris, M., Zeef, L. A. & Millar, C. B. A conserved function for the H2A.Z C terminus. *J Biol Chem* **287**, 19148-19157, (2012).

258 Bonisch, C. *et al.* H2A.Z.2.2 is an alternatively spliced histone H2A.Z variant that causes severe nucleosome destabilization. *Nucleic Acids Res* **40**, 5951-5964, (2012).

259 Obri, A. *et al.* ANP32E is a histone chaperone that removes H2A.Z from chromatin. *Nature* **505**, 648-653, (2014).

260 Choi, J., Heo, K. & An, W. Cooperative action of TIP48 and TIP49 in H2A.Z exchange catalyzed by acetylation of nucleosomal H2A. *Nucleic Acids Res* **37**, 5993-6007, (2009).

261 Weber, C. M., Henikoff, J. G. & Henikoff, S. H2A.Z nucleosomes enriched over active genes are homotypic. *Nat Struct Mol Biol* **17**, 1500-1507, (2010).

262 Nekrasov, M. *et al.* Histone H2A.Z inheritance during the cell cycle and its impact on promoter organization and dynamics. *Nat Struct Mol Biol* **19**, 1076-1083, (2012).

263 Luk, E. *et al.* Stepwise histone replacement by SWR1 requires dual activation with histone H2A.Z and canonical nucleosome. *Cell* **143**, 725-736, (2010).

264 Bruce, K. *et al.* The replacement histone H2A.Z in a hyperacetylated form is a feature of active genes in the chicken. *Nucleic Acids Res* **33**, 5633-5639, (2005).

265 Sarcinella, E., Zuzarte, P. C., Lau, P. N., Draker, R. & Cheung, P. Monoubiquitylation of H2A.Z distinguishes its association with euchromatin or facultative heterochromatin. *Mol Cell Biol* **27**, 6457-6468, (2007).

266 Bonisch, C. & Hake, S. B. Histone H2A variants in nucleosomes and chromatin: more or less stable? *Nucleic Acids Res* **40**, 10719-10741, (2012).

267 Zhou, J., Fan, J. Y., Rangasamy, D. & Tremethick, D. J. The nucleosome surface regulates chromatin compaction and couples it with transcriptional repression. *Nat Struct Mol Biol* **14**, 1070-1076, (2007).

268 Fan, J. Y., Rangasamy, D., Luger, K. & Tremethick, D. J. H2A.Z alters the nucleosome surface to promote HP1alpha-mediated chromatin fiber folding. *Mol Cell* **16**, 655-661, (2004).

269 Fan, J. Y., Gordon, F., Luger, K., Hansen, J. C. & Tremethick, D. J. The essential histone variant H2A.Z regulates the equilibrium between different chromatin conformational states. *Nat Struct Biol* **9**, 172-176, (2002).

270 Creyghton, M. P. *et al.* H2A.Z is enriched at polycomb complex target genes in ES cells and is necessary for lineage commitment. *Cell* **135**, 649-661, (2008).

271 Hardy, S. *et al.* The euchromatic and heterochromatic landscapes are shaped by antagonizing effects of transcription on H2A.Z deposition. *PLoS Genet* **5**, e1000687, (2009).

272 Santisteban, M. S., Hang, M. & Smith, M. M. Histone variant H2A.Z and RNA polymerase II transcription elongation. *Mol Cell Biol* **31**, 1848-1860, (2011).

273 Adam, M., Robert, F., Larochelle, M. & Gaudreau, L. H2A.Z is required for global chromatin integrity and for recruitment of RNA polymerase II under specific conditions. *Mol Cell Biol* **21**, 6270-6279, (2001).

274 Hou, H. *et al.* Histone variant H2A.Z regulates centromere silencing and chromosome segregation in fission yeast. *J Biol Chem* **285**, 1909-1918, (2010).

275 Greaves, I. K., Rangasamy, D., Ridgway, P. & Tremethick, D. J. H2A.Z contributes to the unique 3D structure of the centromere. *Proc Natl Acad Sci U S A* **104**, 525-530, (2007).

276 Zhou, B. O. *et al.* SWR1 complex poises heterochromatin boundaries for antisilencing activity propagation. *Mol Cell Biol* **30**, 2391-2400, (2010).

277 Buchanan, L. *et al.* The Schizosaccharomyces pombe JmjC-protein, Msc1, prevents H2A.Z localization in centromeric and subtelomeric chromatin domains. *PLoS Genet* **5**, e1000726, (2009).

278 Meneghini, M. D., Wu, M. & Madhani, H. D. Conserved histone variant H2A.Z protects euchromatin from the ectopic spread of silent heterochromatin. *Cell* **112**, 725-736, (2003).

279 Swaminathan, J., Baxter, E. M. & Corces, V. G. The role of histone H2Av variant replacement and histone H4 acetylation in the establishment of Drosophila heterochromatin. *Genes Dev* **19**, 65-76, (2005).

280 Dai, Q. & Wang, H. "Cullin 4 makes its mark on chromatin". *Cell Div* **1**, 14, (2006).

281 Jackson, S. & Xiong, Y. CRL4s: the CUL4-RING E3 ubiquitin ligases. *Trends Biochem Sci* **34**, 562-570, (2009).

282 Jang, S. M., Redon, C. E. & Aladjem, M. I. Chromatin-Bound Cullin-Ring Ligases: Regulatory Roles in DNA Replication and Potential Targeting for Cancer Therapy. *Front Mol Biosci* **5**, 19, (2018).

283 Zou, Y. *et al.* Characterization of nuclear localization signal in the N terminus of CUL4B and its essential role in cyclin E degradation and cell cycle progression. *J Biol Chem* **284**, 33320-33332, (2009).

284 Nakagawa, T. & Xiong, Y. X-linked mental retardation gene CUL4B targets ubiquitylation of H3K4 methyltransferase component WDR5 and regulates neuronal gene expression. *Mol Cell* **43**, 381-391, (2011).

285 Lee, J. & Zhou, P. DCAFs, the missing link of the CUL4-DDB1 ubiquitin ligase. *Mol Cell* **26**, 775-780, (2007).

286 Angers, S. *et al.* Molecular architecture and assembly of the DDB1-CUL4A ubiquitin ligase machinery. *Nature* **443**, 590-593, (2006).

287 Jin, J., Arias, E. E., Chen, J., Harper, J. W. & Walter, J. C. A family of diverse Cul4-Ddb1-interacting proteins includes Cdt2, which is required for S phase destruction of the replication factor Cdt1. *Mol Cell* **23**, 709-721, (2006).

288 He, Y. J., McCall, C. M., Hu, J., Zeng, Y. & Xiong, Y. DDB1 functions as a linker to recruit receptor WD40 proteins to CUL4-ROC1 ubiquitin ligases. *Genes Dev* **20**, 2949-2954, (2006).

289 Higa, L. A. *et al.* CUL4-DDB1 ubiquitin ligase interacts with multiple WD40-repeat proteins and regulates histone methylation. *Nat Cell Biol* **8**, 1277-1283, (2006).

290 Hu, J., McCall, C. M., Ohta, T. & Xiong, Y. Targeted ubiquitination of CDT1 by the DDB1-CUL4A-ROC1 ligase in response to DNA damage. *Nat Cell Biol* **6**, 1003-1009, (2004).

291 Nag, A., Bondar, T., Shiv, S. & Raychaudhuri, P. The xeroderma pigmentosum group E gene product DDB2 is a specific target of cullin 4A in mammalian cells. *Mol Cell Biol* **21**, 6738-6747, (2001).

292 El-Mahdy, M. A. *et al.* Cullin 4A-mediated proteolysis of DDB2 protein at DNA damage sites regulates in vivo lesion recognition by XPC. *J Biol Chem* **281**, 13404-13411, (2006).

293 Hu, H. *et al.* CRL4B catalyzes H2AK119 monoubiquitination and coordinates with PRC2 to promote tumorigenesis. *Cancer Cell* **22**, 781-795, (2012).

294 Gracheva, E. *et al.* ZRF1 mediates remodeling of E3 ligases at DNA lesion sites during nucleotide excision repair. *J Cell Biol* **213**, 185-200, (2016).

295 Li, G. *et al.* CRL4(DCAF8) Ubiquitin Ligase Targets Histone H3K79 and Promotes H3K9 Methylation in the Liver. *Cell Rep* **18**, 1499-1511, (2017).

296 Liu, R. *et al.* PHD finger protein 1 (PHF1) is a novel reader for histone H4R3 symmetric dimethylation and coordinates with PRMT5-WDR77/CRL4B complex to promote tumorigenesis. *Nucleic Acids Res* **46**, 6608-6626, (2018).

297 Yang, Y. *et al.* CRL4B promotes tumorigenesis by coordinating with SUV39H1/HP1/DNMT3A in DNA methylation-based epigenetic silencing. *Oncogene* **34**, 104-118, (2015).

298 Kalb, R., Mallery, D. L., Larkin, C., Huang, J. T. & Hiom, K. BRCA1 is a histone-H2A-specific ubiquitin ligase. *Cell Rep* **8**, 999-1005, (2014).

299 Osley, M. A. Regulation of histone H2A and H2B ubiquitylation. *Brief Funct Genomic Proteomic* **5**, 179-189, (2006).

300 Cao, R., Tsukada, Y. & Zhang, Y. Role of Bmi-1 and Ring1A in H2A ubiquitylation and Hox gene silencing. *Mol Cell* **20**, 845-854, (2005).

301 de Napoles, M. *et al.* Polycomb group proteins Ring1A/B link ubiquitylation of histone H2A to heritable gene silencing and X inactivation. *Dev Cell* **7**, 663-676, (2004).

302 Wang, H. *et al.* Role of histone H2A ubiquitination in Polycomb silencing. *Nature* **431**, 873-878, (2004).

303 Marsh, D. J. & Dickson, K. A. Writing Histone Monoubiquitination in Human Malignancy-The Role of RING Finger E3 Ubiquitin Ligases. *Genes (Basel)* **10**, (2019).

304 Liu, Z., Oughtred, R. & Wing, S. S. Characterization of E3Histone, a novel testis ubiquitin protein ligase which ubiquitinates histones. *Mol Cell Biol* **25**, 2819-2831, (2005).

305 Bhatnagar, S. *et al.* TRIM37 is a new histone H2A ubiquitin ligase and breast cancer oncoprotein. *Nature* **516**, 116-120, (2014).

306 Zhou, W. *et al.* Histone H2A monoubiquitination represses transcription by inhibiting RNA polymerase II transcriptional elongation. *Mol Cell* **29**, 69-80, (2008).

307 Braun, S. & Madhani, H. D. Shaping the landscape: mechanistic consequences of ubiquitin modification of chromatin. *EMBO Rep* **13**, 619-630, (2012).

308 Nakagawa, T. *et al.* Deubiquitylation of histone H2A activates transcriptional initiation via trans-histone cross-talk with H3K4 di- and trimethylation. *Genes Dev* **22**, 37-49, (2008).

309 Lan, L. *et al.* Monoubiquitinated histone H2A destabilizes photolesion-containing nucleosomes with concomitant release of UV-damaged DNA-binding protein E3 ligase. *J Biol Chem* **287**, 12036-12049, (2012).

310 Jason, L. J., Moore, S. C., Ausio, J. & Lindsey, G. Magnesium-dependent association and folding of oligonucleosomes reconstituted with ubiquitinated H2A. *J Biol Chem* **276**, 14597-14601, (2001).

311 Jason, L. J., Finn, R. M., Lindsey, G. & Ausio, J. Histone H2A ubiquitination does not preclude histone H1 binding, but it facilitates its association with the nucleosome. *J Biol Chem* **280**, 4975-4982, (2005).

312 Zhu, P. *et al.* A histone H2A deubiquitinase complex coordinating histone acetylation and H1 dissociation in transcriptional regulation. *Mol Cell* **27**, 609-621, (2007).

313 Cheung, K. L., Huen, J., Houry, W. A. & Ortega, J. Comparison of the multiple oligomeric structures observed for the Rvb1 and Rvb2 proteins. *Biochem Cell Biol* **88**, 77-88, (2010).

314 Venteicher, A. S., Meng, Z., Mason, P. J., Veenstra, T. D. & Artandi, S. E. Identification of ATPases pontin and reptin as telomerase components essential for holoenzyme assembly. *Cell* **132**, 945-957, (2008).

315 Morwitzer, M. J. *et al.* Identification of RUVBL1 and RUVBL2 as Novel Cellular Interactors of the Ebola Virus Nucleoprotein. *Viruses* **11**, (2019).

316 Izumi, N. *et al.* AAA+ proteins RUVBL1 and RUVBL2 coordinate PIKK activity and function in nonsense-mediated mRNA decay. *Sci Signal* **3**, ra27, (2010).

317 Grigoletto, A., Neaud, V., Allain-Courtois, N., Lestienne, P. & Rosenbaum, J. The ATPase activity of reptin is required for its effects on tumor cell growth and viability in hepatocellular carcinoma. *Mol Cancer Res* **11**, 133-139, (2013).

318 Bodor, D. L., Rodriguez, M. G., Moreno, N. & Jansen, L. E. Analysis of protein turnover by quantitative SNAP-based pulse-chase imaging. *Curr Protoc Cell Biol* **Chapter 8**, Unit8 8, (2012).

319 Xi, Y. *et al.* Histone modification profiling in breast cancer cell lines highlights commonalities and differences among subtypes. *BMC Genomics* **19**, 150, (2018).

320 Smith, B. N. *et al.* Snail promotes epithelial mesenchymal transition in breast cancer cells in part via activation of nuclear ERK2. *PloS one* **9**, e104987, (2014).

321 Azad, G. K. & Tomar, R. S. Proteolytic clipping of histone tails: the emerging role of histone proteases in regulation of various biological processes. *Mol Biol Rep* **41**, 2717-2730, (2014).

322 Filipescu, D., Szenker, E. & Almouzni, G. Developmental roles of histone H3 variants and their chaperones. *Trends Genet* **29**, 630-640, (2013).

323 Skene, P. J. & Henikoff, S. Histone variants in pluripotency and disease. *Development* **140**, 2513-2524, (2013).

324 Hsu, C. C. *et al.* Recognition of histone acetylation by the GAS41 YEATS domain promotes H2A.Z deposition in non-small cell lung cancer. *Genes Dev* **32**, 58-69, (2018).

325 Rispal, J. *et al.* The H2A.Z histone variant integrates Wnt signaling in intestinal epithelial homeostasis. *Nat Commun* **10**, 1827, (2019).

326 Boyarchuk, E., Filipescu, D., Vassias, I., Cantaloube, S. & Almouzni, G. The histone variant composition of centromeres is controlled by the pericentric heterochromatin state during the cell cycle. *J Cell Sci* **127**, 3347-3359, (2014).

327 Yen, K., Vinayachandran, V. & Pugh, B. F. SWR-C and INO80 chromatin remodelers recognize nucleosome-free regions near +1 nucleosomes. *Cell* **154**, 1246-1256, (2013).

328 Tarangelo, A. *et al.* Recruitment of Pontin/Reptin by E2f1 amplifies E2f transcriptional response during cancer progression. *Nat Commun* **6**, 10028, (2015).

329 Zanton, S. J. & Pugh, B. F. Full and partial genome-wide assembly and disassembly of the yeast transcription machinery in response to heat shock. *Genes Dev* **20**, 2250-2265, (2006).

330 McHaourab, Z. F., Perreault, A. A. & Venters, B. J. ChIP-seq and ChIP-exo profiling of Pol II, H2A.Z, and H3K4me3 in human K562 cells. *Sci Data* **5**, 180030, (2018).

331 de Laat, W. L., Jaspers, N. G. & Hoeijmakers, J. H. Molecular mechanism of nucleotide excision repair. *Genes Dev* **13**, 768-785, (1999).

332 Chan, H. L. *et al.* Polycomb complexes associate with enhancers and promote oncogenic transcriptional programs in cancer through multiple mechanisms. *Nat Commun* **9**, 3377, (2018).

333 Yoon, H. G. *et al.* Purification and functional characterization of the human N-CoR complex: the roles of HDAC3, TBL1 and TBLR1. *Embo j* **22**, 1336-1346, (2003).

334 Ji, Q. *et al.* CRL4B interacts with and coordinates the SIN3A-HDAC complex to repress CDKN1A and drive cell cycle progression. *J Cell Sci* **127**, 4679-4691, (2014).

335 Jia, S., Kobayashi, R. & Grewal, S. I. Ubiquitin ligase component Cul4 associates with Clr4 histone methyltransferase to assemble heterochromatin. *Nat Cell Biol* **7**, 1007-1013, (2005).

336 Li, F. *et al.* Two novel proteins, dos1 and dos2, interact with rik1 to regulate heterochromatic RNA interference and histone modification. *Curr Biol* **15**, 1448-1457, (2005).

337 Thon, G. *et al.* The Clr7 and Clr8 directionality factors and the Pcu4 cullin mediate heterochromatin formation in the fission yeast Schizosaccharomyces pombe. *Genetics* **171**, 1583-1595, (2005).

338 Schapira, M., Tyers, M., Torrent, M. & Arrowsmith, C. H. WD40 repeat domain proteins: a novel target class? *Nat Rev Drug Discov* **16**, 773-786, (2017).

339 Xu, C. & Min, J. Structure and function of WD40 domain proteins. *Protein Cell* **2**, 202-214, (2011).

340 Rosenfeld, J. A. *et al.* Determination of enriched histone modifications in non-genic portions of the human genome. *BMC Genomics* **10**, 143, (2009).

341 Arnoult, N., Van Beneden, A. & Decottignies, A. Telomere length regulates TERRA levels through increased trimethylation of telomeric H3K9 and HP1alpha. *Nat Struct Mol Biol* **19**, 948-956, (2012).

342 Bilodeau, S., Kagey, M. H., Frampton, G. M., Rahl, P. B. & Young, R. A. SetDB1 contributes to repression of genes encoding developmental regulators and maintenance of ES cell state. *Genes Dev* **23**, 2484-2489, (2009).

343 Hawkins, R. D. *et al.* Distinct epigenomic landscapes of pluripotent and lineage-committed human cells. *Cell Stem Cell* **6**, 479-491, (2010).

344 Marsano, R. M., Giordano, E., Messina, G. & Dimitri, P. A New Portrait of Constitutive Heterochromatin: Lessons from Drosophila melanogaster. *Trends Genet* **35**, 615-631, (2019).

345 Peters, A. H. *et al.* Partitioning and plasticity of repressive histone methylation states in mammalian chromatin. *Mol Cell* **12**, 1577-1589, (2003).

346 Jamieson, K. *et al.* Loss of HP1 causes depletion of H3K27me3 from facultative heterochromatin and gain of H3K27me2 at constitutive heterochromatin. *Genome Res* **26**, 97-107, (2016).

347 Basenko, E. Y. *et al.* Genome-wide redistribution of H3K27me3 is linked to genotoxic stress and defective growth. *Proc Natl Acad Sci U S A* **112**, E6339-6348, (2015).

348 Peinado, H. *et al.* Lysyl oxidase-like 2 as a new poor prognosis marker of squamous cell carcinomas. *Cancer Res* **68**, 4541-4550, (2008).

349 Fong, S. F. *et al.* Lysyl oxidase-like 2 expression is increased in colon and esophageal tumors and associated with less differentiated colon tumors. *Genes Chromosomes Cancer* **46**, 644-655, (2007).

350 Torres, S. *et al.* LOXL2 Is Highly Expressed in Cancer-Associated Fibroblasts and Associates to Poor Colon Cancer Survival. *Clin Cancer Res* **21**, 4892-4902, (2015).

351 Fischer, K. R. *et al.* Epithelial-to-mesenchymal transition is not required for lung metastasis but contributes to chemoresistance. *Nature* **527**, 472-476, (2015).

352 Zheng, X. *et al.* Epithelial-to-mesenchymal transition is dispensable for metastasis but induces chemoresistance in pancreatic cancer. *Nature* **527**, 525-530, (2015).

353 Park, Y. S. *et al.* The global histone modification pattern correlates with cancer recurrence and overall survival in gastric adenocarcinoma. *Ann Surg Oncol* **15**, 1968-1976, (2008).

354 Nguyen, C. T. *et al.* Histone H3-lysine 9 methylation is associated with aberrant gene silencing in cancer cells and is rapidly reversed by 5-aza-2'-deoxycytidine. *Cancer Res* **62**, 6456-6461, (2002).

355 Nakazawa, T. *et al.* Global histone modification of histone H3 in colorectal cancer and its precursor lesions. *Hum Pathol* **43**, 834-842, (2012).

356 Vujatovic, O. *et al.* Drosophila melanogaster linker histone dH1 is required for transposon silencing and to preserve genome integrity. *Nucleic Acids Res* **40**, 5402-5414, (2012).

357 Postepska-Igielska, A. *et al.* The chromatin remodelling complex NoRC safeguards genome stability by heterochromatin formation at telomeres and centromeres. *EMBO Rep* **14**, 704-710, (2013).

358 Gerlitz, G. & Bustin, M. Efficient cell migration requires global chromatin condensation. *Journal of Cell Science* **123**, 2207-2217, (2010).

359 Gerlitz, G. & Bustin, M. The role of chromatin structure in cell migration. *Trends Cell Biol* **21**, 6-11, (2011).

360 Gerlitz, G. *et al.* Migration cues induce chromatin alterations. *Traffic* **8**, 1521-1529, (2007).

361 Fu, Y., Chin, L. K., Bourouina, T., Liu, A. Q. & VanDongen, A. M. Nuclear deformation during breast cancer cell transmigration. *Lab Chip* **12**, 3774-3778, (2012).

362 Yokoyama, Y. *et al.* Cancer-associated upregulation of histone H3 lysine 9 trimethylation promotes cell motility in vitro and drives tumor formation in vivo. *Cancer Sci* **104**, 889-895, (2013).

363 Feinberg, A. P., Koldobskiy, M. A. & Gondor, A. Epigenetic modulators, modifiers and mediators in cancer aetiology and progression. *Nat Rev Genet* **17**, 284-299, (2016).

364 Timp, W. & Feinberg, A. P. Cancer as a dysregulated epigenome allowing cellular growth advantage at the expense of the host. *Nat Rev Cancer* **13**, 497-510, (2013).

365 McDonald, O. G., Wu, H., Timp, W., Doi, A. & Feinberg, A. P. Genome-scale epigenetic reprogramming during epithelial-to-mesenchymal transition. *Nat Struct Mol Biol* **18**, 867-874, (2011).

366 Denny, S. K. *et al.* Nfib Promotes Metastasis through a Widespread Increase in Chromatin Accessibility. *Cell* **166**, 328-342, (2016).

367 Chang, J. *et al.* Pre-clinical evaluation of small molecule LOXL2 inhibitors in breast cancer. *Oncotarget* **8**, 26066-26078, (2017).

368 Hutchinson, J. H. *et al.* Small Molecule Lysyl Oxidase-like 2 (LOXL2) Inhibitors: The Identification of an Inhibitor Selective for LOXL2 over LOX. *ACS Med Chem Lett* **8**, 423-427, (2017).

369 Elkaim, J. *et al.* First identification of small-molecule inhibitors of Pontin by combining virtual screening and enzymatic assay. *Biochem J* **443**, 549-559, (2012).

370 Matias, P. M. *et al.* The AAA+ proteins Pontin and Reptin enter adult age: from understanding their basic biology to the identification of selective inhibitors. *Front Mol Biosci* **2**, 17, (2015).

371 Elkaim, J. *et al.* Design, synthesis and biological evaluation of Pontin ATPase inhibitors through a molecular docking approach. *Bioorg Med Chem Lett* **24**, 2512-2516, (2014).

372 Chen, Z. *et al.* MicroRNA-300 Regulates the Ubiquitination of PTEN through the CRL4B(DCAF13) E3 Ligase in Osteosarcoma Cells. *Mol Ther Nucleic Acids* **10**, 254-268, (2018).

373 Yoshida, M., Kijima, M., Akita, M. & Beppu, T. Potent and specific inhibition of mammalian histone deacetylase both in vivo and in vitro by trichostatin A. *J Biol Chem* **265**, 17174-17179, (1990).

374 Williams-Ashman, H. G., Seidenfeld, J. & Galletti, P. Trends in the biochemical pharmacology of 5'-deoxy-5'-methylthioadenosine. *Biochem Pharmacol* **31**, 277-288, (1982).

375 Greiner, D., Bonaldi, T., Eskeland, R., Roemer, E. & Imhof, A. Identification of a specific inhibitor of the histone methyltransferase SU(VAR)3-9. *Nat Chem Biol* **1**, 143-145, (2005).

376 Bao, S. *et al.* Glioma stem cells promote radioresistance by preferential activation of the DNA damage response. *Nature* **444**, 756-760, (2006).

377 Chiva, C. *et al.* QCloud: A cloud-based quality control system for mass spectrometry-based proteomics laboratories. *PloS one* **13**, e0189209, (2018).

378 Perkins, D. N., Pappin, D. J., Creasy, D. M. & Cottrell, J. S. Probability-based protein identification by searching sequence databases using mass spectrometry data. *Electrophoresis* **20**, 3551-3567, (1999).

379 Beer, L. A., Liu, P., Ky, B., Barnhart, K. T. & Speicher, D. W. Efficient Quantitative Comparisons of Plasma Proteomes Using Label-Free Analysis with MaxQuant. *Methods Mol Biol* **1619**, 339-352, (2017).

380 Gregori, J., Villarreal, L., Sanchez, A., Baselga, J. & Villanueva, J. An effect size filter improves the reproducibility in spectral counting-based comparative proteomics. *J Proteomics* **95**, 55-65, (2013).

381 Wang, H. *et al.* Histone H3 and H4 ubiquitylation by the CUL4-DDB-ROC1 ubiquitin ligase facilitates cellular response to DNA damage. *Mol Cell* **22**, 383-394, (2006).

382 Langmead, B., Trapnell, C., Pop, M. & Salzberg, S. L. Ultrafast and memory-efficient alignment of short DNA sequences to the human genome. *Genome Biol* **10**, R25, (2009).

383 Zhang, Y. *et al.* Model-based analysis of ChIP-Seq (MACS). *Genome Biol* **9**, R137, (2008).

384 O'Leary, N. A. *et al.* Reference sequence (RefSeq) database at NCBI: current status, taxonomic expansion, and functional annotation. *Nucleic Acids Res* **44**, D733-745, (2016).

385 Kuleshov, M. V. *et al.* Enrichr: a comprehensive gene set enrichment analysis web server 2016 update. *Nucleic Acids Res* **44**, W90-97, (2016).

386 Kent, W. J. *et al.* The human genome browser at UCSC. *Genome Res* **12**, 996-1006, (2002).

387 Buenrostro, J. D., Giresi, P. G., Zaba, L. C., Chang, H. Y. & Greenleaf, W. J. Transposition of native chromatin for fast and sensitive epigenomic profiling of open chromatin, DNA-binding proteins and nucleosome position. *Nat Methods* **10**, 1213-1218, (2013).

388 Trapnell, C., Pachter, L. & Salzberg, S. L. TopHat: discovering splice junctions with RNA-Seq. *Bioinformatics* **25**, 1105-1111, (2009).

389 Trapnell, C. *et al.* Differential gene and transcript expression analysis of RNA-seq experiments with TopHat and Cufflinks. *Nat Protoc* **7**, 562-578, (2012).

390 Lee, S. B. *et al.* Tousled-like kinases stabilize replication forks and show synthetic lethality with checkpoint and PARP inhibitors. *Sci Adv* **4**, eaat4985, (2018).

ANNEX

1. New list of putative LOXL2 interactors

Gene symbol	MS/MS score
LOXL2	**1934**
HSPA5	1561
HSPA1A	1439
EEF1A1	868
HSPA8	559
RUVBL1	**411**
Filaggrin	305
RUVBL2	**257**
MYLK2	226
KIF5B	204
HIST2H2BE	**155**
SPRR2E	150
UBB;RPS27A;UBC	150
DOCK7 I	108
SAMD1	98
BAT2D1	90
DMAP1	**75**
MATR3	74
SERPINB3	73
CHAF1B	72
MEN1	71
INF2	64
KLC2	59
SMARCE1	58
SPRR1B	57
GLT8D3	56
ACTA2	55

CAMK2D	53
HIST2H3A;HIST2H3C HIST2H3D	**49**
TFRC	47
PFKL	47
NSUN5	45
DCD	45
LGALS3	44
MTA1	42
BYSL	40
MTA2	39
PTBP1	38
ACTL6A	**36**
CASP14	36
WDR20	35
HIST1H2AH	34
GATAD2A	33
CAMK2G	32
TNC	30
RBBP7	30
TCP1	30
COL6A3	29
DSG1	29
MRPL43	28
ABCA12	28
LTF	28
LRMP	27
KIF14	27
BAT2L	26
CEP55	26
DDX5	26

DBF4B	26
ACOT8	25
ELAVL3	24
OPRM1	24
PALM3	23
TRIP13	23

Table A1. New list of putative LOXL2 interactors. List of putative LOXL2 interactors identified in a tandem-affinity purification approach and mass spectrometry analysis. Gene symbols and MS scores are shown.

2. Putative H3K4ox readers

Gene	Prot. nm	T	C	LogFC	P.value	Adj p	
NOL11	**NOL11**	12.3	0	37	3.17E-05	3.67E-03	T
NUCL	**NCL**	8	0	36.17	3.61E-02	0.0007327	T
HNRL1	**HNRNPUL1**	5.7	0	35.82	0.0002448	0.003614	T
NIP7	**NIP7**	5	0	35.77	0.000268	0.003818	T
BAF	**BANF1**	4.3	0	35.69	0.0004804	0.006142	T
RRP7A	**RRP7A**	5.7	0	35.46	0.0008638	0.009742	T
LACTB	**LACTB**	4.3	0	35.37	0.001791	0.01634	T
DDB1	**DDB1**	3.3	0	35.32	0.001876	0.01692	T
PNO1	**PNO1**	4	0	35.17	0.001633	0.01542	T
PK1IP	**PAK1IP1**	3.7	0	35.03	0.00374	0.02839	T
SRFB1	**SRFBP1**	3.7	0	34.95	0.006841	0.04553	T
RBM19	**RBM19**	3.7	0	34.95	0.006841	0.04553	T
AKAP8	**AKAP8**	3.7	0	34.87	0.006525	0.04452	T
EXOS6	**EXOSC6**	3	0	34.87	0.007173	0.04697	T
RRP36	**RRP36**	4	0	34.87	0.007173	0.04697	T
UTP15	**UTP15**	15.3	0.5	4.715	3.02E-05	3.67E-03	T
RL35A	**RPL35A**	9.3	0.5	3.989	4.35E-02	0.000861	T
NLE1	**NLE1**	6.7	0.5	3.56	0.0007656	0.008986	T
PHIP	**PHIP**	15	1	3.547	2.18E-03	0.0001265	T
RLA0	**RPLP0**	14.3	1	3.501	3.62E-03	0.0001727	T
XRN2	**XRN2**	12.3	1	3.385	1.15E-02	0.0003448	T
REXO4	**REXO4**	12	1	3.333	1.90E-02	0.0004811	T

DDX31	**DDX31**	5.3	0.5	3.318	0.002642	0.02227	T
RS5	**RPS5**	12	1	3.274	3.24E-02	0.0006928	T
RLA0L	**RPLP0P6**	11.3	1	3.264	3.49E-05	0.0007267	T
DHX30	**DHX30**	10	1	3.155	9.09E-02	0.001639	T
NEP1	**EMG1**	5.3	0.5	3.088	0.00746	0.04808	T
WDR74	**WDR74**	19.3	2	3.064	1.16E-04	8.55E-03	T
PWP2	**PWP2**	14.7	1.5	3.064	4.44E-03	0.0001801	T
HEAT1	**HEATR1**	20	2.5	2.959	2.07E-05	3.35E-03	T
RL9	**RPL9**	9	1	2.918	0.0005109	0.00621	T
WDR3	**WDR3**	23.7	3	2.681	1.12E-04	8.55E-03	T
TBL3	**TBL3**	24.7	4	2.535	1.72E-05	3.35E-03	T
DDX52	**DDX52**	5	1	2.444	0.007399	0.04807	T
EXOSX	**EXOSC10**	10	1.5	2.399	0.001388	0.01342	T
CIR1A	**CIRH1A**	18	3	2.368	9.20E-03	0.0003113	T
WDR75	**WDR75**	19	3	2.333	1.42E-02	0.0003839	T
HNRL2	**HNRNPUL2**	10	1.5	2.33	0.002178	0.01902	T
K0020	**KIAA0020**	30.3	5.5	2.175	9.88E-05	8.55E-03	T
ILF3	**ILF3**	10	2	2.07	0.002661	0.02227	T
PABP4	**PABPC4**	9	2	1.999	0.004173	0.03137	T
IMP4	**IMP4**	9.7	2	1.975	0.004685	0.0349	T
MAK16	**MAK16**	10.3	2.5	1.945	0.001999	0.01783	T
RBM28	**RBM28**	47.3	10.5	1.873	1.69E-06	4.59E-04	T
UTP6	**UTP6**	13.7	3	1.872	0.001316	0.01291	T
RL5	**RPL5**	31.7	7.5	1.743	3.56E-03	0.0001727	T

RBM34	**RBM34**	28	7	1.719	1.10E-02	0.0003442	T
DHX9	**DHX9**	14.7	4	1.7	0.001052	0.0111	T
RRP5	**PDCD11**	34	8	1.651	8.09E-03	0.0002906	T
BRX1	**BRIX1**	28	8	1.638	1.02E-02	0.0003321	T
WDR46	**WDR46**	27	7.5	1.618	2.53E-02	0.0005875	T
RL7	**RPL7**	32.7	9.5	1.583	4.02E-06	0.0001733	T
DCA13	**DCAF13**	20	5.5	1.576	0.0004916	0.006142	T
WDR36	**WDR36**	24.3	6.5	1.532	0.0002527	0.003664	T
NOC4L	**NOC4L**	18	5	1.516	0.001558	0.01488	T
DDX56	**DDX56**	22.3	7	1.498	0.0002267	0.003409	T
WDR43	**WDR43**	27.3	8	1.45	0.0001539	0.002551	T
HP1B3	**HP1BP3**	14.3	4.5	1.439	0.00493	0.03615	T
NOL6	**NOL6**	15.3	5	1.438	0.003095	0.02565	T
NKRF	**NKRF**	17	5.5	1.359	0.003691	0.02828	T
KRR1	**KRR1**	19.7	6.5	1.333	0.002113	0.01865	T
RL18A	**RPL18A**	18	6	1.327	0.00328	0.02637	T
RL3	**RPL3**	53	18.5	1.209	4.06E-03	0.0001733	T
UT14A	**UTP14A**	29.7	11	1.195	0.0004597	0.00602	T
U3IP2	**RRP9**	21.3	8.5	1.185	0.00231	0.01995	T
RL28	**RPL28**	19	7	1.18	0.005844	0.04126	T
NOP2	**NOP2**	46	18.5	1.138	1.83E-02	0.0004791	T
UTP18	**UTP18**	28	11	1.113	0.001272	0.01275	T
DDX50	**DDX50**	25	10	1.064	0.003614	0.02795	T
RRS1	**RRS1**	38.7	16.5	1.052	0.0002236	0.003409	T

RL6	**RPL6**	35.3	15	0.9857	0.001118	0.01161	F
DDX21	**DDX21**	46.7	19	0.98	0.0002742	0.003839	F
CEBPZ	**CEBPZ**	34.7	15.5	0.9599	0.00132	0.01291	F
KI67	**MKI67**	31	13.5	0.9415	0.003375	0.02687	F
EBP2	**EBNA1BP2**	31	13	0.9034	0.006125	0.04288	F
HNRPM	**HNRNPM**	74.7	41.5	0.5466	0.005309	0.03815	F

Table A2. Putative H3K4ox readers. List of putative H3K4ox readers identified by mass spectrometry. Gene symbol and MS score are shown.

3. RNA-sequencing analysis validation in MDA-MB-231 shRUVBL2 and shLOXL2

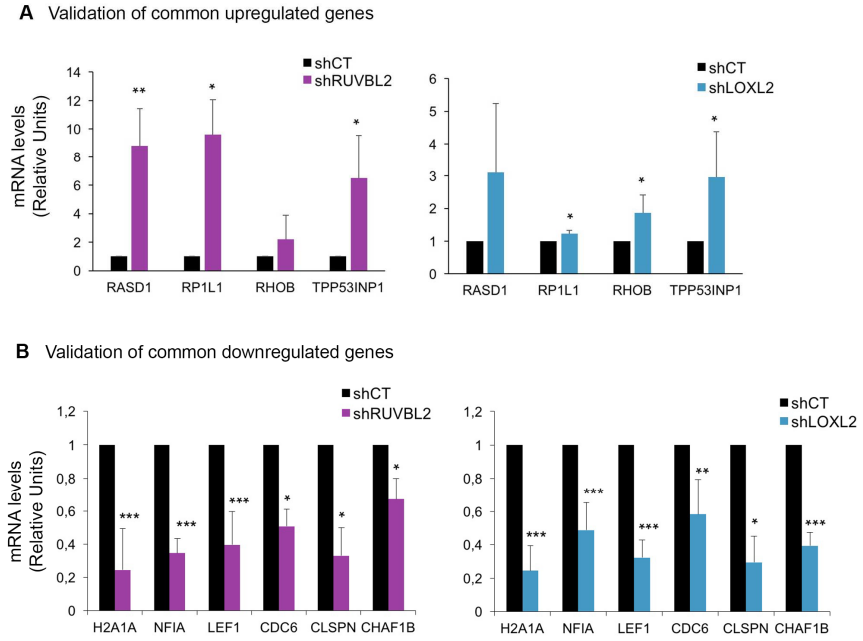

Figure A1. Validation of RNA-sequencing analysis. Common up- and down-regulated genes in shLOXL2 and shRUVBL2. mRNA levels of common up-(a) or down-(B) regulated genes in MDA-MB-231 cells shLOXL2 and shRUVBL2 were analyzed by qRT-PCR. Gene expression was normalized to the *Pumilio* housekeeping gene and presented as the fold-change relative to the shControl cells, which was set as 1. Error bars indicate standard deviation in at least three experiments. *p < 0.05, **p ≤ 0.01, ***p ≤ 0.001.

4. ChIPs in selected genomic regions of MDA-MB-231 shControl

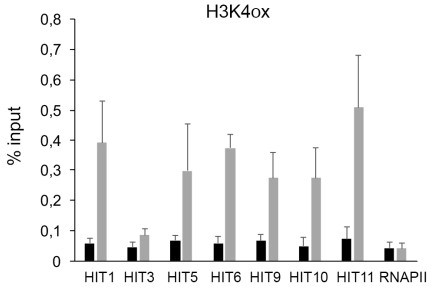

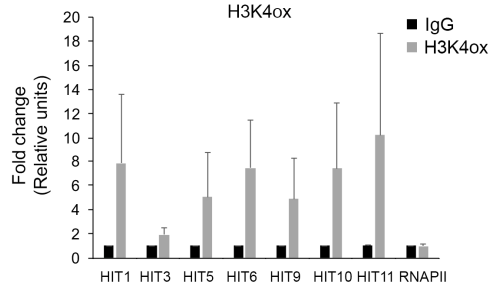

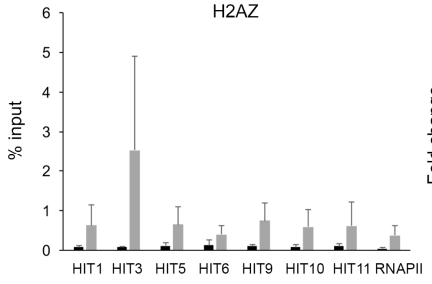

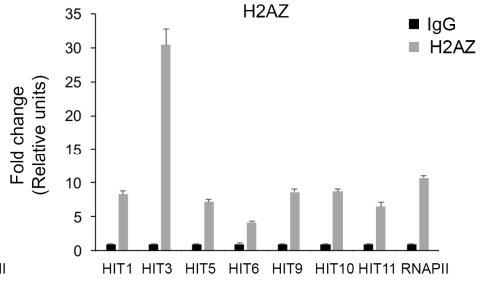

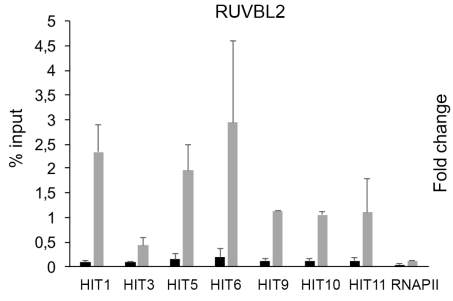

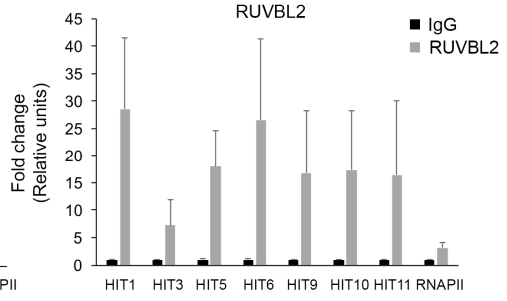

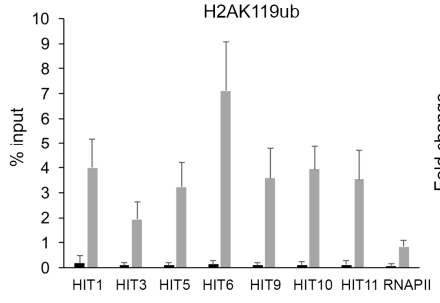

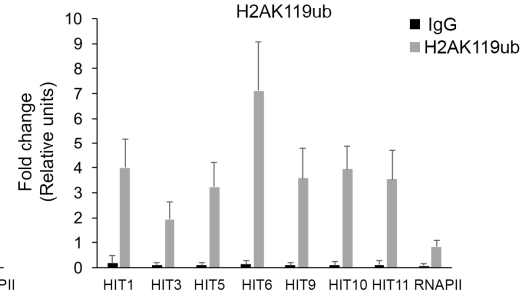

Figure A2. Representative examples of H3K4ox, H2A.Z, RUVBL2 and H2AK119ub ChIPs in selected genomic regions of MDA-MB-231 shControl. ChIP-PCR experiments of RUVBL2, H3K4ox, H2A.Z and H2AK119ub in selected regions (hits) and RNAPII promoter, which was used as a negative control for H3K4ox, RUVBL2 and H2AK119ub. Data of qPCR amplifications were normalized to the input and to total immunoprecipitated H3 or H2A for H3K4ox and H2AK119ub, respectively. Results are expressed as percentage of input or fold-change relative to IgG binding. Error bars indicate SD from at least three experiments.

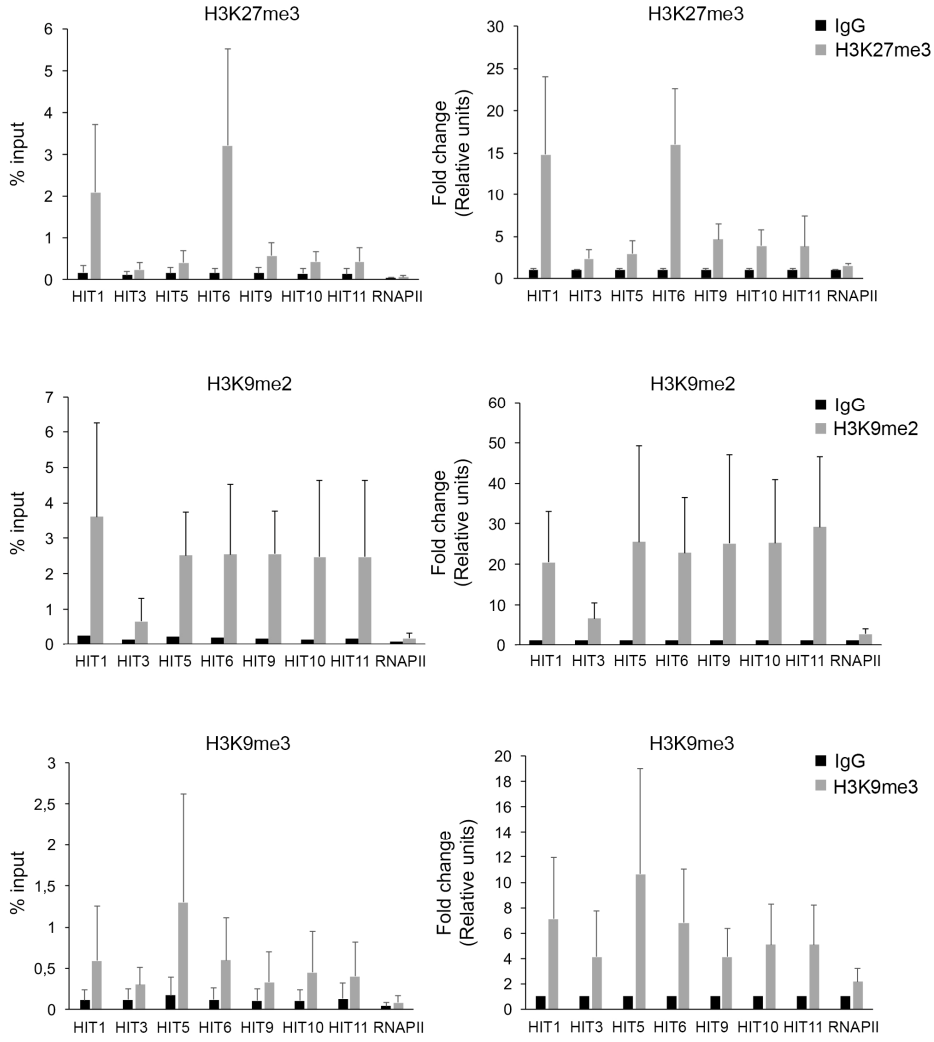

Figure A3. Representative examples of H3K27me3, H3K9me2 and H3K9me3 ChIPs in selected genomic regions of MDA-MB-231 shControl. ChIP-PCR experiments of H3K27me3, H3K9me2 and H3K9me3 in selected regions (hits) and RNAPII promoter, which was used as a negative control. Data of qPCR amplifications were normalized to the input and to total immunoprecipitated H3 or H2A for H3K4ox and H2AK119ub, respectively. Results are expressed as percentage of input or fold-change relative to IgG binding. Error bars indicate SD in at least three experiments.

RESEARCH ARTICLES

Research article resulting from this thesis:

Serra-Bardenys G, Querol J, Pascual-Reguant L, Blanco E, Cigliano RA, Millanes-Romero A, Jerónimo C, Villanueva J, di Croce L, Peiró S. Maintenance of oxidized histone H3 in chromatin and chromatin compaction requires RUVBL2, DDB1-RBX1 H2A ubiquitination and H2A.Z deposition. *In preparation*.

Collaboration with other projects:

Pascual-Reguant L, Blanco E, Galan S, Le Dily F, Cuartero Y, **Serra-Bardenys G**, Di Carlo V, Iturbide A, Cebrià-Costa JP, Nonell L, de Herreros AG, Di Croce L, Marti-Renom MA, Peiró S. Lamin B1 mapping reveals the existence of dynamic and functional euchromatin lamin B1 domains. Nat Commun, 2018, 9(1):3420.

Cebrià-Costa JP, Pascual-Reguant L, Gonzalez-Perez A, **Serra-Bardenys G**, Querol J, Cosín M, Verde G, Cigliano RA, Sanseverino W, Segura-Bayona S, Iturbide A, Andreu D, Nuciforo P, Bernado-Morales C, Rodilla V, Arribas J, Yelamos J, de Herreros AG, Stracker TH, Peiró S. LOXL2-mediated H3K4 oxidation reduces chromatin accessibility in triple-negative breast cancer cells. Oncogene. 2019. doi: 10.1038/s41388-019-0969-1.

ACKNOWLEDGEMENTS

Semblava molt lluny, però ja he arribat al final d'aquesta etapa. I si miro enrere i en faig balanç, estic molt contenta. Me n'adono que han estat uns anys intensos, amb moments de tot. Èpoques dures que sembla que tot està encallat i on fins i tot "t'enfades" amb la ciència; però també d'altres on la gaudeixes, superes les complicacions i tornes a casa satisfeta pensant que potser podrem aportar alguna cosa una mica rellevant. I, el més important de tot, me n'adono que he après tantíssimes coses! Crec que la paraula que millor defineix aquesta etapa és APRENENTATGE, tan a nivell professional com també moltíssim a nivell personal; en altres paraules, sento que m'he fet gran...

Però un doctorat no es fa sola. Aquests anys han estat una oportunitat per conèixer i aprendre de moltíssima gent i heu estat molts i moltes les que, d'una manera o altra, dins i fora del laboratori, m'heu acompanyat i ajudat a que això fos possible. Així doncs, vull donar-vos les gràcies perquè heu estat indispensables en aquest camí i, amb vosaltres, m'ho he passat molt bé.

Primer de tot gràcies a tu, Sandra. Sempre recordaré el primer dia que vàrem parlar; quina innocència! quan ho penso veig que era una nena, plena d'inseguretats i amb la sensació de saber molt poques coses... ara me n'adono de tot el que he après i en gran part és gràcies a tu. Gràcies per donar-me aquesta oportunitat. Per ensenyar-me a fer bona ciència, ser crítica i per fer-me espavilar i pensar per mi mateixa. Per confiar en mi (a vegades més que jo mateixa) i engrescar-me a fer i respondre preguntes. Per sempre ser positiva davant els experiments i no donar res per perdut, però alhora voler reconduir-ho quan no anàvem per la direcció correcta. Per motivar-te amb mi però també ajudar-me a buscar solucions quan les coses es complicaven. Per ser humana, propera i per valorar-nos. I, sobretot, per transmetre'm la teva passió per la ciència i sempre estar oberta a fer coses noves i afrontar reptes sense por; aquestes capacitats em van al·lucinar des del primer dia i crec que han fet i faran que *Chromatin Team* tingui un gran futur i moltes alegries!

I parlant de *Chromatin Team*, he tingut la sort de poder formar part d'un gran equip durant aquests 5 anys. Ane, coincidimos durante mi màster cuando aún estaba empezando pero muchas gracias por estar siempre dispuesta a ayudar y por todos los buenos consejos que me diste. Gaetano, gracias también por colaborar con este proyecto y las ganas de hacerlo bien. Joan Pau, a tu per fer que els dies al laboratori fossin molt divertits i sempre hi hagués una excusa per fer uns riures, fins i tot en els moments més difícils. Per la teva mania de fer-nos anar de vermell cada dimarts, per les anades d'olla a partir de les 7 a cultius, per posar-te amb els trabucs olotins i no acabaríem mai... gràcies per tots aquests bons moments i també pels consells i les xerrades de ciència. Laura, moltes gràcies per tot també. Ser mentora tot just començar el doctorat no és una feina gens fàcil però ho vas saber fer molt bé. Gràcies per posar-hi tantes ganes, per tenir paciència quan jo encara no sabia gairebé res i per transmetre'm les bones maneres de treballar i gaudir de la ciència. Crec que ets de qui més he après en el laboratori durant tot aquest temps i a molts nivells; molta sort en aquesta nova etapa, no tinc cap dubte que seguiràs tenint una gran carrera científica. Jess, ets una de les persones més generoses que he conegut. Gràcies per preocupar-te tant per nosaltres i per estar sempre disposada a ajudar-nos i buscar solucions; no sé què faríem sense tu... I també pels mesos que vam treballar juntes en aquest projecte, tot i les nostres negociacions amb la quantitat d'anticossos que blotariem entre tanta membrana...jajaja. I sobretot a tu, Marc, moltes i moltes gràcies per tot; has estat un gran suport. Gràcies per estar sempre amb un somriure i encomanar-lo (que regaaaaalo!!!); per ser crític però sempre veure la part bona de les coses; pels bons consells i per tot el que m'has ajudat tan a nivell científic com a nivell personal, sempre animant-me i estant disposat a fer un cafè quan ho necessitava. I a la Queralt, per encomanar-nos aquesta energia i motivació que et caracteritza; per ser atenta, propera i posar-ho fàcil des del primer minut. I per aportar tanta vida i bon rotllo al lab; gràcies per fer que els dies siguin intensos i divertits (i sovint un pèl dramàtics també...). Y a Carmen, la nueva incorporación; nos hemos coincidido poquito pero muchas gracias por los ánimos en mi recta final también. Tian, you are amazing! You are a great scientist and an even better person. You came to the laboratory

only a few months ago, but I have already learned so many things with you. Thank you very much for the good advice and for being always positive and willing to help us. But also for sharing great moments and lots of laughs (Mare de Déu...)!. It is a pleasure to work with you. I també volia donar les gràcies a la Carla i la Rita, les “meves” estudiants de practiques durant els estius. Va ser un plaer tenir-vos al laboratori. Moltes gràcies per venir amb il·lusió, energia, involucrar-vos amb el projecte i per tota la vostra ajuda. Espero que disfrutessiu de l’experiència i us servís per poder aprendre moltes coses noves. També a en Pep i la Laura, que heu fet estades al lab aportant bon ambient i il·lusió.

Però, a part de *Chromatin Team*, també vull donar les gràcies a moltes altres persones que he tingut a prop durant el meu dia a dia al laboratori.

Els primers anys de tesi vam estar al PRBB compartint espai amb *Snail Team*. Quina sort que vam tenir! Gràcies Àlex, Jelena, Lorena, Txell, Raul, David (A.K.A mi armah), Aida, Willy, Maria, Jordi, Ruben i Rumi; va ser una molt bona època i m’ho vaig passar molt bé. I també a l’Antonio, en Victor i en Jepi; gràcies pels bons consells científics, per ser crítics i per les vostres aportacions que eren de gran ajuda per millorar el projecte. I gràcies també a l’Antonio i en Víctor per donar-me la oportunitat de donar les pràctiques de la uni a la vostra assignatura. Víctor, ha estat un plaer compartir aquesta experiència; gràcies per posar-m’ho tan fàcil, per valorar-me i per deixar-me participar activament; i també per estar sempre disposat a ajudar-me.

I de l’IMIM gràcies també als PN’s, sobretot a la Judit i a en Joan. I al Bigas Lab, que sempre us guardaré un record especial per ser el primer lloc on vaig fer recerca. Anna i Lluís, gràcies per la oportunitat i per valorar-me. Cristina, per tot el que em vas ensenyar i per creure en mi. I Carlota, vam començar compartint unes practiques d’estiu i d’aquí n’ha sortit una bona amistat; gràcies per escoltar-me, animar-me, aconsellar-me i per tots els moments compartits; has estat molt important durant aquesta etapa.

I al mig de la tesi ens va tocar fer trasllat, pujar cap a la muntanya i començar nova etapa. No va ser fàcil haver d'emigrar al VHIO però tots i totes les que en formàveu part ens ho vàreu posar molt fàcil.

Primer de tot, als de la segona. Gràcies als Hector's per la vostra generositat i tot el que ens heu ajudat des que vàrem arribar (fins i tot per deixar-me fer westerns al vostre lab). Isa, ets encantadora i una gran científica; sempre estàs amb un somriure i disposada a ajudar i donar bons consells. Lorena, no saps la il·lusió que em va fer saber que treballaríem juntes i m'ha encantat; gràcies per posar-hi tantes ganes, pel que hem rigut i per voler fer les coses tan ben fetes. També a l'Oriol i a l'Albert. Gràcies per les xerrades, els ànims i totes les tardes a cultius (les fèieu tan més fàcils i entretingudes!). I, sobretot, pels moments "cintura"; vam començar odiant aquesta cançó entre placa i placa i ha acabat essent l'excusa per tenir bons records, fer uns riures assegurats i fins i tot algun bon audio. I ja ho diuen, "*de tal palo, tal astilla*"; l'Albert va marxar però va deixar una bona successora a cultius. Laia, què seria entrar-hi i que tu no hi fossis? Ja saps que em poso molt i molt trista si no hi ets.... Gràcies pel bon-rotllisme que desprens, pels riures i també per compartir drames de tant en tant. I també a la Mònica, per encomanar sempre tanta positivitat.

I a l'Ale. Illo, muchá grasia por tó! Llegar al VHIO y compartir lab con vosotros hizo las cosas muy muy fáciles. Gracias por tu apoyo, por los cafés, las bromas y tu alegria andaluza... Ah, y por los momentos niño corneta, que son lo más! Quin tàndem que feu amb en Marc... Gràcies per alegrar-me els dies, fer-me sentir sempre més capaç del que em penso i fins i tot frenar-me quan treballava massa. Estic molt contenta d'haver-vos conegut i compartit aquesta etapa amb vosaltres.

I en especial a tu Fani, milions de gràcies per tot!! Per conèixer gent com tu val molt la pena fer el doctorat. Gràcies per ser la meva confident en aquesta etapa. Per les aventures, les festes, les excursions, els riures, les posades al dia, els vins, les infusions de diumenge i una llista que no s'acaba. I per ser-hi absolutament sempre. Juntes hem rigut i ens hem motivat, però també ens hem emocionat i fins i tot plorat quan les coses no eren fàcils. Sé que d'aquí m'emporto una gran amistat i estic convençuda que estiguem on estiguem sempre ens tindrem. No

saps com m'emociona pensar que d'aquí molt poc les dues serem doctores i acabarem aquest camí juntes; prepara't, que ara bé l'ho bo!

Moltes gràcies també a la Garazi, a les *Violeta's*, al *Team Genòmica* i a la Cate i en Ramon. I a en Niko, pel bon rotllo, els consells científics i per alegrar-nos les birres i els cafès. També a en Toni, l'Isma i la Sandra, per compartir l'experiència d'organitzar el VHIOfinde, que va començar amb una broma entre birres i va acabar essent una realitat; gràcies per totes les anècdotes que vam compartir preparant-lo, m'ho vaig passar genial!. I als de la tercera i la quarta, per fer del VHIO una gran família.

També vull agrair l'ajuda de la Sandra Segura, l'Anna Lladó i l'Enrique Blanco; per la bona disposició, per ensenyar-me i per ajudar-me amb els experiments.

I, fora del laboratori, vull donar les gràcies a molta gent que també ha estat indispensable.

!Kungs, gràcies per tant! Marc, Neus, Maria, Laura, Lore, Gemma, Blanca, Anna i Moi, sembla ahir que començàvem a la uni... d'això ja n'han passat uns quants anys i com més temps passa més clar tinc que sou grans amics i amigues. Per tots els bons moments que hem compartit, per ajudar-nos en els no tan bons i per tenir-nos sempre. Necessito els nostres retrobaments i en aquesta etapa no sabeu com m'han ajudat a agafar forces. Espero no perdre-us mai.

A les nenes. Gràcies pels vespres de birres a passeig de Sant Joan i per totes les aventures. Per entendre'm (o intentar-ho jaja) tot i no tenir res a veure amb ciència i per fer-me desconnectar i somriure després de dies difícils al lab.

Als fisios (i no fisios), per acollir-me tan bé i regalar-me bons moments. I a tu Esquerrà, per compartir bons vins i viatges (que espero que en puguem fer molts més!). A l'Anna Barqué, que tot i estar molt lluny sempre et sento a prop. I a en Jordi, pels teus bons consells gràfics i la teva alegria.

Moltes gràcies a les *sushitas* també, pels sopars i les nostres escapades. Anna, Àstrid, Silvia, Núria, Paula i Miriam, sou un encant! I en especial a l'Àstrid; infinites gràcies per tot el suport, l'ajuda i per fer-me sentir capaç; per estar sempre disposada a donar-ho tot i fer-me disfrutar de cada moment.

I a les meves compis de pis. Ha estat una gran sort trobar-vos i compartir casa. Moltes gràcies per alegrar-me els dies fins i tot quan havien estat complicats, per recolzar-me tant i també per tenir molta paciència amb l'estrès dels últims mesos. Núria, ets única! No sé com t'ho fas però sempre m'acabes fent somriure. Marina, quin gran descobriment! Gràcies per arribar al pis amb tantes ganes, estar sempre amb tot i per l'energia positiva que encomanes. I també a la Silvia; pels ànims, per compartir emocions de doctoranda i per les bones xerrades que tant ens van unir.

I finalment, gràcies a la meva família. Als tiets i la Paqui, per estimar-nos tant i estar al nostre costat. I als avis, per tot el que ens heu donat i per sempre esperar-nos amb un somriure d'orella a orella.

A la mare i el pare. Gràcies per ser-hi en aquesta etapa, que us he sentit més a prop que mai, i per ser-hi SEMPRE. Per celebrar amb mi les coses bones, però també per fer-me costat en els moments complicats, quan les coses no eren gens fàcils. Per ensenyar-me a ser valenta i forta, a tenir clar el que vull i on vull arribar i a esforçar-me per aconseguir els meus objectius. Per tot això i molt més he pogut arribar fins aquí i de ben segur que sense vosaltres, no estaria on estic ara. Ja sé que vegades us agradaria tenir-me més a prop (o que almenys fes estades més llargues a Olot…), però espero que tingueu ben clar que sou indispensables i us estimo moltíssim.

Anna, i què dir de tu? Ets la germana petita, però ja t'has fet tan gran que a vegades ets més responsable que jo (i mira que ja és dir...). Moltes gràcies per tot també. Per escoltar-me, per fer-me costat, pels bons consells i per regalar-me grans moments i molts somriures (i algun bon bailoteo també, va, diguem-ho tot!). Tinc la sensació que constantment estic aprenent moltes coses de tu i amb tu, i sento que

encara que siguem diferents, estiguem lluny o a prop i hagi passat molt o poc temps, sempre notarem una connexió especial i ens tindrem l'una a l'altra pel que faci falta. *"Hermana",* t'estimo molt.

A tots i totes vosaltres, moltes gràcies!

Aquesta tesi ha estat impresa amb el suport del VHIO (Vall d'Hebron Institut d'Oncologia)